

Mass spectrometry based proteome profiling
to understand the effects of
Lipo-chito-oligosaccharide and Thuricin 17
in *Arabidopsis thaliana* and *Glycine max* under salt stress

By

Sowmyalakshmi Subramanian

Department of Plant Science
Macdonald Campus, McGill University
Montreal, Quebec

September 2013

A thesis submitted to McGill University in partial fulfillment
of the requirements of the degree of
Doctor of Philosophy

© Sowmyalakshmi Subramanian September 2013

TABLE OF CONTENTS

TABLE OF CONTENTS	i
LIST OF TABLES	v
LIST OF FIGURES	vi
LIST OF APPENDICES	viii
LIST OF ABBREVIATIONS	xi
ABSTRACT	xvi
RÉSUMÉ	xvii
ACKNOWLEDGEMENTS	xix
PREFACE AND CONTRIBUTIONS OF AUTHORS	xxi
CONTRIBUTIONS TO KNOWLEDGE	xxii
CHAPTER 1	1
INTRODUCTION	1
1.1 General Hypothesis	5
1.2 The Objectives	5
CONNECTING STATEMENT FOR CHAPTER 2	7
CHAPTER 2	7
GENERAL REVIEW OF LITERATURE	8
2.1 Abstract	8
2.2 Introduction to the phytomicrobiome	8
2.3 Proteomics as a part of integrative systems biology	12
2.4 <i>Arabidopsis thaliana</i> as a plant model system for proteomic studies	14
2.5 A proteomics approach to study soybean and its symbiont <i>Bradyrhizobium japonicum</i>	19
2.5.1 Biological nitrogen fixation	19
2.5.2 Soybean – the plant	20
2.5.3 <i>Bradyrhizobium japonicum</i>	22
2.5.4 Lipo-chitooligosaccharides (LCOs) from <i>Bradyrhizobium japonicum</i>	23
2.5.5 LCO signaling in other organisms	25
2.6. Analyses of soybean proteomics	26

2.6.1 Physiological and biological changes in the soybean proteome	26
2.6.1.1 Whole plant organs	26
2.6.1.2 Seeds	28
2.6.1.3 Roots, root hairs and nodules	29
2.7 Soybean proteomics under stress conditions	30
2.7.1 Flooding stress	31
2.7.2 Water stress – Drought	32
2.7.3 High temperature stress	33
2.7.4 Salt stress	34
2.7.5 Biotic stress	35
2.7.6 Other miscellaneous stress related reports	36
2.8 <i>Bradyrhizobium japonicum</i> and its proteomics/exoproteomics	37
2.9 Other dimensions to soybean-rhizobacteria interactions	40
CHAPTER 3	44
Lipo-chitooligosaccharide and Thuricin 17 regulate phytohormones differentially in <i>Arabidopsis thaliana</i> rosettes	44
CONNECTING STATEMENT FOR CHAPTER 3	45
3.1 Abstract	46
3.2 Introduction	46
3.3 Materials and methods	51
3.3.1 Plant material	51
3.3.2 Bacterial signal compounds	52
3.3.2.1 Extraction and purification of Lipo-chitooligosaccharides (LCOs)	52
3.3.2.2 Extraction of Thuricin 17 (Th17)	52
3.3.3 Effect of LCO and Th17 on the induction of phytohormone gene expression using GUS histo-chemical staining	53
3.3.4 Hormone analysis of <i>A. thaliana</i> rosettes	53
3.3.4.1 Extraction and purification	54
3.3.4.2 Hormone quantification by UPLC-ESI-MS/MS	55
3.4 Results	56
3.4.1 GUS assay	57

3.4.2 Phytohormone detection using UPLC ESI-MS/MS	57
3.5 Discussion	66
3.6 Conclusions	70
CHAPTER 4	71
Mass spectrometry based studies on the effects of Lipo-chito-oligosaccharide and Thuricin 17 on proteome regulation under unstressed and salt stressed conditions in <i>Arabidopsis thaliana</i> rosettes	71
CONNECTING STATEMENT TO CHAPTER 4	72
4.1 Abstract	74
4.2 Introduction	74
4.3 Materials and methods	78
4.3.1 Plant material and treatments	78
4.3.2 Extraction and purification of lipo-chitooligosaccharides (LCOs)	78
4.3.3 Extraction of Thuricin 17 (Th17)	78
4.3.4 Petri plate assay for screening for salt stress	79
4.3.5 Tray assay for assessing salt stress recovery of <i>A. thaliana</i>	79
4.3.6 Leaf proteomics using shotgun approach	80
4.3.6.1 Protein extraction	80
4.3.6.2 Protein profiling	81
4.3.7 Data analysis	81
4.4 Results	82
4.4.1 <i>A. thaliana</i> seed germination in Petri plates and trays under unstressed conditions and in the presence of salt stress screening, when treated with LCO and Th17	82
4.4.2 Protein profiling	86
4.5 Discussion	100
4.6 Conclusion	106
CHAPTER 5	107
A proteomic approach to Lipo-chitooligosaccharide and Thuricin 17 effects on soybean salt stress responses	107
CONNECTING STATEMENT TO CHAPTER 5	108
5.1 Abstract	109

5.2 Introduction	109
5.3 Materials and methods	113
5.3.1 Plant material	113
5.3.2 Extraction and purification of Lipo-chitooligosaccharides (LCO)	113
5.3.3 Extraction of Thuricin 17 (Th17)	114
5.3.4 Seed germination	114
5.3.5 Label free proteomics	115
5.3.5.1 Protein extraction	115
5.3.5.2 Proteome profiling	116
5.3.6 Data analysis	116
5.4 Results	117
5.4.1 Seed germination	117
5.4.2 Proteome profiling	119
5.5 Discussion	133
5.6 Conclusions	138
CHAPTER 6	140
SUMMARY, CONCLUSIONS AND SUGGESTIONS FOR FUTURE RESEARCH	140
6.1 General summary and conclusions	140
6.2 Suggestions for future research	142
LIST OF REFERENCES	145
APPENDICES	I, II and III

LIST OF TABLES

Table 2.1 Soybean production statistics (FAOSTAT 2011)	22
Table 2.2 Physicochemical properties of Thuricin 17 (based on Expasy results)	42
Table 3.1a UPLC-ESI/MS quantitation of ABA and ABA metabolites, Cytokinins, Auxins and Gibberellins detected in <i>Arabidopsis thaliana</i> rosettes 24h after treatment	65
Table 3.1b UPLC-ESI/MS quantitation of Salicylic acid and Jasmonic acid detected in <i>Arabidopsis thaliana</i> rosettes 24h after treatment	66
Table 4.1 Least square means of <i>A. thaliana</i> percentage germination - seeds treated with LCO and Th 17 under optimal conditions	83
Table 4.2a Grouping of proteins in <i>Arabidopsis thaliana</i> rosettes, that was significant in contrasts based on Fold change	88
Table 4.2b Grouping of proteins in <i>Arabidopsis thaliana</i> rosettes, that were significant in contrasts based on Fisher's Exact test	89
Table 4.5 Enzyme code distribution in un-stressed and salt stressed groups	92
Table 4.7 GO function categories amongst un-stressed and salt stressed groups in <i>Arabidopsis thaliana</i> rosettes	97
Table 5.2a Grouping of proteins that were significant in the contrasts based on Fold change	120
Table 5.2b Grouping of proteins that were significant based on Fisher's Exact test	121
Table 5.5 Enzyme code distribution in un-stressed and salt stress groups	125
Table 5.6 GO function categories amongst un-stressed and salt stressed groups	129

LIST OF FIGURES

Fig. 2.1 Lipo-chitooligosaccharide (LCO) produced by rhizobia is host specific and the host specificity is determined by 1) the number of β -1,4-linked <i>N</i> -acetyl-D-glucosamine in the backbone; 2) the type of fatty acyl side chain at the non-reducing end; 3) types of substituting groups such as R1, R2, R3	24
Fig. 2.2a Sequence of Thuricin 17	41
Fig. 2.2b Alpha helix structure of Thuricin 17 (based on Expasy results)	41
Fig. 2.2c Hydrophobicity plot for Thuricin 17 suggesting its hydrophilic nature	42
Fig. 3.1 GUS assay screening to understand the effect of LCO and Th17 on <i>Arabidopsis thaliana</i> phytohormones pattern of expression	58
Fig. 3.2 Auxin and auxin-conjugates identified in <i>Arabidopsis thaliana</i> rosettes 24 h after LCO and Th17 treatment (LCO = 10^{-6} M; Th17 = 10^{-9} M)	59
Fig. 3.3 Cytokinins identified in <i>Arabidopsis thaliana</i> rosettes 24 h after LCO and Th17 treatment (LCO = 10^{-6} M; Th17 = 10^{-9} M)	60
Fig. 3.4 Gibberellic acids identified in <i>Arabidopsis thaliana</i> rosettes 24 h after LCO and Th17 treatment (LCO = 10^{-6} M; Th17 = 10^{-9} M).	61
Fig. 3.5 Absciscic acid and its catabolites identified in <i>Arabidopsis thaliana</i> rosettes 24 h after LCO and Th17 treatment (LCO = 10^{-6} M; Th17 = 10^{-9} M)	62
Fig. 3.6 Free salicylic acid and jasmonic acid identified in <i>Arabidopsis thaliana</i> rosettes 24 h after LCO and Th17 treatment (LCO = 10^{-6} M; Th17 = 10^{-9} M)	63
Fig. 3.7 Hormones quantified using UPLC-ESI/MS. The graph represents the percentage increase or decrease of hormones identified in LCO and Th17 treated <i>Arabidopsis thaliana</i> rosettes 24h after treatment	64
Fig. 4.1 <i>Arabidopsis thaliana</i> germination at 22 °C in the presence of LCO and Th17	82
Fig. 4.2 Screening assay in petriplates for <i>Arabidopsis thaliana</i> response to 200 and 250 mM NaCl stress in the presence of LCO and Th17	84
Fig. 4.3 <i>Arabidopsis thaliana</i> response to different levels of salt stress in the presence of LCO and Th17, 15 days after imposition of salt stress	85
Fig. 4.4 Venn diagram for the output of differentially expressed proteins, unique peptides and unique spectra based on Scaffold	87

Fig. 4.5 Enzyme code distribution categorized based on main enzyme classes – <i>Arabidopsis thaliana</i>	92
Fig. 4.6a Pie chart representation of functional classification of GO distribution for molecular function in unstressed group and Signals + 250 mM NaCl stress in <i>Arabidopsis thaliana</i> rosettes	93
Fig. 4.6b Pie chart representation of functional classification of GO distribution for biological process in unstressed and signals + 250 mM NaCl stress in <i>Arabidopsis thaliana</i> rosettes	94
Fig. 4.6c Pie chart representation of functional classification of GO distribution for cellular components in unstressed and signals + 250 mM NaCl stress in <i>Arabidopsis thaliana</i> rosettes	95
Fig. 4.7 KEGG pathway depicting the role of photosystem I and II (KEGG Pathway)	96
Fig. 5.1a Soybean seed germination 48h post treatment (un-stressed) at 25 °C in dark, at 70 % relative humidity	117
Fig. 5.1b Soybean seed germination 48 h post treatment under 100 mM NaCl stress at 25 °C in dark, at 70 % relative humidity	118
Fig. 5.1c Bar chart representing soybean seed germination under optimal and 100 mM NaCl stress at 25 °C in dark, at 70 % relative humidity	118
Fig. 5.2 Venn diagram for the output of differentially expressed proteins, unique peptides and unique spectra based on Scaffold	122
Fig. 5.3 Enzyme code distribution categorized based on main enzyme classes in signals group and signals + salt group	125
Fig. 5.5a Pie chart representation of functional classification of the GO distribution for molecular function in the unstressed and salt stressed groups	126
Fig. 5.5b Pie chart representation of functional classification of the GO distribution for biological process in unstressed and salt stressed groups	127
Fig. 5.5c Pie chart representation of functional classification of the GO distribution for cellular components in unstressed and salt stressed groups	128
Fig. 5.6 Co-regulation of metabolic pathway components in soybean seeds after 48 h from the onset of germination, as reflected by label free proteomics data	132

LIST OF APPENDICES

Appendix I for Chapter 3

Table 3.1 Phytohormones and their catabolites/conjugates analyzed in three-week-old <i>Arabidopsis thaliana</i> rosette, 24 h after LCO and Th17 treatments (LCO - 10^{-6} M, Th17 - 10^{-9} M)	I 1
--	-----

Appendix II for Chapter 4

Table 4.3a Fold change of spectral count in <i>Arabidopsis thaliana</i> rosette Contrast 1 - Control Vs LCO	II 1
Table 4.3b Fold change of spectral count in <i>Arabidopsis thaliana</i> rosette Contrast 2 - Control Vs Th17	II 7
Table 4.3c Fold change of spectral count in <i>Arabidopsis thaliana</i> rosette Contrast 3 - LCO Vs Th17	II 11
Table 4.3d Fold change of spectral count in <i>Arabidopsis thaliana</i> rosette Contrast 4 - Control 250 mM NaCl Vs LCO + 250 mM NaCl	II 15
Table 4.3e Fold change of spectral count in <i>Arabidopsis thaliana</i> rosette Contrast 5 - Control 250 mM NaCl Vs Th17 + 250 mM NaCl	II 19
Table 4.3f Fold change of spectral count in <i>Arabidopsis thaliana</i> rosette Contrast 6 – LCO + 250 mM NaCl Vs Th17 + 250 mM NaCl	II 24
Table 4.4a Fisher's Exact test (P-value) (Spectral counts) for <i>Arabidopsis thaliana</i> rosette Contrast 1. Control Vs LCO	II 28
Table 4.4b Fisher Exact test (P-value) (Spectral counts) for <i>Arabidopsis thaliana</i> rosette Contrast 2 - Control Vs Th17	II 32
Table 4.4c Fisher's Exact test (P-value) (Spectral counts) for <i>Arabidopsis thaliana</i> rosette Contrast 3 - LCO Vs Th17	II 34
Table 4.4d Fisher Exact test (P-value) (Spectral counts) for Contrast 4. Control 250 mM NaCl Vs LCO + 250 mM NaCl	II 36
Table 4.4e Fisher Exact test (P-value) (Spectral counts) for <i>Arabidopsis thaliana</i> rosette Contrast 5. Control 250 mM NaCl Vs Th17 + 250 mM NaCl	II 38
Table 4.4f Fisher Exact test (P-value) (Spectral counts) for <i>Arabidopsis thaliana</i> rosette Contrast 6. LCO + 250 mM NaCl Vs Th17 + 250 mM NaCl	II 41

Appendix III for Chapter 5

Table 5.1 Least square means of germination by soybean seeds treated with lipo-chitooligosaccharide and thuricin 17 under optimal and salt stress conditions	III 1
Table 5.3a Fold change (Spectral counts) for Contrast 1. Control Vs LCO	III 3
Table 5.3b Fold change (Spectral counts) for Contrast 2. Control Vs LCO	III 6
Table 5.3c Fold change (Spectral counts) for Contrast 3. LCO Vs Th17	III 10
Table 5.3d Fold change (Spectral counts) for Contrast 4. Control 100 mM NaCl Vs LCO + 100 mM NaCl	III 11
Table 5.3e Fold change (Spectral counts) for Contrast 5. Control 100 mM NaCl Vs Th17 + 100 mM NaCl	III 12
Table 5.3f Fold change (Spectral counts) for Contrast 6. LCO + 100 mM NaCl Vs Th17 + 100 mM NaCl	III 14
Table 5.4a Fisher Exact test (P-value) (Spectral counts) for Contrast 1. Control Vs LCO	III 14
Table 5.4b Fisher Exact test (P-value) (Spectral counts) for Contrast 2. Control Vs Th17	III 19
Table 5.4c Fisher Exact test (P-value) (Spectral counts) for Contrast 3. LCO Vs Th17	III 24
Table 5.4d Fisher Exact test (P-value) (Spectral counts) for Contrast 4. Control 100 mM NaCl Vs LCO + 100 mM NaCl	III 25
Table 5.4e Fisher Exact test (P-value) (Spectral counts) for Contrast 5. Control 100 mM NaCl Vs Th17 + 100 mM NaCl	III 26
Table 5.4f Fisher Exact test (P-value) (Spectral counts) for Contrast 6. LCO + 100 mM NaCl Vs Th17 + 100 mM NaCl	III 28
Fig. 5.4a: Mean/Standard deviation scatterplot for Soybean Contrast 1. Control Vs LCO	III 30
Fig. 5.4b: Mean/Standard deviation scatterplot for Soybean Contrast 2. Control Vs Th17	III 30
Fig. 5.4c: Mean/Standard deviation scatterplot for Soybean Contrast 3. LCO Vs Th17	III 31
Fig. 5.4d: Mean/Standard deviation scatterplot for Soybean Contrast 4. 100 mM NaCl Vs LCO + 100 mM NaCl	III 31

Fig. 5.4e: Mean/Standard deviation scatterplot for Soybean Contrast
5. 100 mM NaCl Vs Th17 + 100 mM NaCl

III 32

Fig. 5.4f: Mean/Standard deviation scatterplot for Soybean Contrast
6. LCO + 100 mM NaCl Vs. Th17 + 100 mM NaCl

III 32

LIST OF ABBREVIATIONS

°C	Degree Celsius
µg	Micro gram
µL	Micro liter
µm	Micro meter
µM	Micro molar
1-D gel	One - dimensional gel
2-D gel	Two-Dimensional gel
2D-DIGE	2D Fluorescence Difference Gel Electrophoresis
2D-PAGE	Two-dimensional Poly Acrylamide Gel Electrophoresis
ABA	Abscisic acid
ABC1	Absence of bc1 Complex
ABRC	Arabidopsis Biological Resource Center
ABRE	Abscisic Acid Responsive Element
Absolute RR	Absolute Roundup Ready
ADP	Adenine Di Phosphate
Al	Aluminium
AlCl ₃	Aluminium Chloride
AM	Arbuscular Mycorrhiza
AON	Autoregulation of Nodulation
ATBH	<i>Arabidopsis thaliana</i> Homeobox Protein
ATP	Adenosine triphosphate
BLAST	Basic Linear Alignment Search Tool
BNF	Biological Nitrogen Fixation
BP	Brevipedicellus
Ca	Calcium
CaS	Calcium Sensing Receptor
Cd	Cadmium
CH	Chasmogamous
CID	Collision-induced measurement
Cl ⁻	Chlorine
CL	Cleistogamous

CO ₂	Carbon dioxide
COR	Cold Regulated
CSK	Chloroplast Sensor Kinase
Cu	Copper
cv.	Cultivar
DNA	Deoxyribonucleic acid
EC	Enzyme Code
ECe	Electrical Conductivity
<i>Enod</i> gene	Early <i>nodulin</i> gene
EPS	Exo Polysaccharide
ETH	Ethylene
FAO	Food and Agriculture Organization
FAOSTAT	Food and Agriculture Organization Statistics
FASTA	FAST All
FDR	False Discovery Rate
GA	Gibberellic acid
GDC	Glycine Decarboxylase Complex
GFP	Green Fluorescence Protein
GO	Gene Ontology
GST	Glutathione <i>S</i> -transferase
GTP	Guanidine Tri Phosphate
GUS	Gluc Uronidase
h	Hour
H ₂ O ₂	Hydrogen Peroxide
HPLC	High performance liquid chromatography
HR	Hypersensitive response
HSP	Heat shock protein
IAA	Indole-3-acetic acid
ICGR-CAAS	Institute of Crop Germplasm Resources-Chinese Academy of Agricultural Sciences
ISR	Induced Systemic Resistance
JA	Jasmonic acid

JAZ	Jasmonate ZIM Domain
K ⁺	Potassium ion
kDa	kilodalton
KEGG	Kyoto Encyclopedia of Genes and Genomes
L	Liter
LC	Liquid Chromatography
LCO	Lipo-chitooligosaccharides
LEA	Late Embryogenesis
LH	Light Harvesting
LHC	Light Harvesting Complex
LTRE	Low Temperature Response
LTQ	Linear ion Trap Quadrupole
LV	Lytic Vacuole
LysM	Lysine motif
m	Meter
M	Molar
m/z	mass to charge ratio
MALDI-TOF	Matrix-Assisted Lased Desorption/Ionization - Time of Flight
MBP	Mega Base Pairs
MeFuc	Methyl fucose
Mg	Magnesium
min	Minute
mm	millimeter
mM	millimolar
MRM	Multiple Reaction Monitoring
MS	Mass Spectrometry
MudPIT	Multidimensional Protein Identification Technology
MYB	Myeloblastosis
N ₂	Molecular nitrogen
N ₂ O	Nitrous oxide
Na ²⁺	Sodium ion
NaCl	Sodium Chloride

NAD	Nicotinamide Adenine Dinucleotide
PEG	Polyethylene glycol
NaOH	Sodium Hydroxide
NCBI	National Center for Biotechnology Information
NEB17	Non Endophytic Bacteria
Ng	nano gram
Ni	Nickel
NO	Nitric oxide
O ₃	Ozone
OAC	Ontario Agricultural College
P	Phosphorus
PAL	Phenylalanine Ammonia Lyase
PBM	Peribacteroid Membrane
PCR	Polymerase chain reaction
PEPC	Phosphoenolpyruvate carboxylase
pg	pico gram
PGPR	Plant Growth Promoting Rhizobacteria
pH	Hydrogen ion concentration
PIF	Phytochrome Interacting Factor
pMT	Plant Metallothionin
PNC	Peroxisomal Adenine Nucleotide Carrier
ppb	parts per billion
PPCK	Phosphoenolpyruvate Carboxylase Kinase
ppm	parts per million
PR	Pathogenesis-related
PSB	Phosphate Solubilizing Bacteria
PSV	Protein Storage Vacuole
PTS	Peroxisome-targeting Sequence
pVDAC	Peroxisomal Voltage Dependent Anionic Channel
PVPP	Polyvinyl Pyroviridone
QC	Quality Control
RAM	Root Apical Meristem

RBP	RNA Binding Protein
RNA	Ribonucleic acid
ROS	Reactive oxygen species
rpm	Revolutions per minute
rRNA	ribosomal ribonucleic acid
s	second
S	Svedberg sedimentation coefficient
SA	Salicylic acid
SAR	Systemic Acquired Resistance
SBMV	Soybean Mosaic Virus
SCF	Skp/Cullin/F-box
SEM	Standard Error of Mean
SIR	Salicylic Acid Independent
SNARE	Soluble N-ethylmaleimide-sensitive factor Attachment Protein Receptor
SO ₄	Sulfate
SON1	Suppressor of <i>nim1-1</i>
SP	Storage Protein
TCA	Tri Carboxylic Acid
TF	Transcription factor
TGG	Thioglucoside Glucohydrolase
Th17	Thuricin 17
TIC	Translocon at the Inner envelope membrane of Chloroplast
TTSS	Type III secretion system
UDP	Uridine Di Phosphate
UNEP	United Nations Environment Program
UPLC-ESI	Ultra Performance Liquid Chromatography- Electron Spray Ionization
USDA	United States Department of Agriculture
UV	Ultra-violet
v/v	volume/volume
VDAC	Voltage Dependent Anionic Channel
VSP	Vegetative storage protein
Zn	Zinc

ABSTRACT

Advances in chemical and bio-technology have helped boost modern agriculture with increased food productivity and consequently, impacted the environment leading to more saline and drought prone arable lands. Mandate of world food security heavily depends on crop improvement and developing strategies to increase abiotic stress tolerance. The use of rhizobacteria and their excreted compounds is a contextually safe and viable option.

Lipo-chito-oligosaccharide (LCO) from *Bradyrhizobium japonicum* 532C and Thuricin 17 (Th17) from *Bacillus thuringiensis* NEB17 are bacterial signal compounds promoting plant growth in legumes and non-legumes. The effect of these compounds at proteome level under unstressed and salt stressed conditions on *Arabidopsis thaliana* was studied using root drench method. The phytohormones in *Arabidopsis thaliana* rosettes were differential expressed at 24 h treatment. At the proteome level, > 2-fold changes in the activation of the carbon and energy metabolism pathway proteins in both LCO and Th17 were observed in comparison to control. At 250 mM NaCl stress, the control plants under osmotic-shock shut down most of the carbon-metabolism and up-regulated the energy-metabolism and antioxidant pathways, while the LCO and Th17 with salt stress retained some of the Light harvesting complex, Photosystem I and II proteins along with the up-regulation of energy and antioxidant pathways suggesting that the rosettes were able to amend the salt stress better when treated with LCO and Th17.

Soybean (Absolute RR) germination for salt tolerance suggested that LCO and Th17 helped seeds germinate the best at 100 mM NaCl. The proteome suggested efficient and speedier partitioning of storage proteins, up-regulation of carbon, nitrogen and energy metabolisms in LCO and Th17 seeds in comparison with controls both under optimal and salt stress.

These findings suggest that the *Arabidopsis* rosettes and the soybean germinating seeds alter their proteome based on bacterial signals and on stress. The specificity of this response plays a crucial role in the plants life cycle, and understanding this response is of importance in commercial application.

RÉSUMÉ

Les progrès de la chimie et de la biotechnologie ont contribué à stimuler l'agriculture moderne et la productivité accrue de nourriture. La conséquence en est l'impact sur l'environnement rendant les terres arables plus sujettes à la salinité et à la sécheresse. La sécurité alimentaire mondiale dépend fortement de l'amélioration des cultures et du développement de stratégies visant à accroître la tolérance aux stress abiotiques. L'utilisation de rhizobactéries et de leurs composés excrétés est dans ce contexte une option sécuritaire et viable.

Le lipo-chito-oligosaccharide (LCO) du *Bradyrhizobium japonicum* 532C et le Thuricin 17 (Th17) du *Bacillus thuringiensis* NEB17 sont des composés de signaux de bactéries favorisant la croissance des plantes dans les légumineuses et les non-légumineuses. L'effet de ces composés au niveau du protéome d'*Arabidopsis thaliana*, sans stress et avec le stress du sel, a été étudié en utilisant la méthode par trempage de racine. Les phyto-hormones dans les rosettes d'*Arabidopsis thaliana* ont été exprimées de manière différentielle lors du traitement de 24h. Au niveau du protéome, des changements 2 fois supérieurs en comparaison au témoin ont été observés dans l'activation des protéines de la voie métabolique énergétique du carbone, pour LCO et pour Th17. Sous un stress produit par 250 mM de NaCl, les plants témoins sous choc osmotique ont diminué la plupart du métabolisme du carbone, et régulé à la hausse les voies du métabolisme énergétique et antioxydant ; tandis que LCO et Th17 sous stress salin ont conservé une partie du complexe de capture de la lumière, les protéines de Photosystem I et II, et régulé positivement les voies énergétiques et antioxydants. Cela suggère que les rosettes furent en mesure de modifier positivement le stress salin lorsque traitées avec LCO et Th17.

La germination des graines de soja (Absolute RR) pour la tolérance au sel, a montré que LCO et Th17 aident les graines à germer de manière optimale avec 100 mM de NaCl. Pour les graines avec LCO et Th17 et par rapport aux témoins à la fois sous stress optimal et salin, le protéome suggère: une séparation des protéines de stockage efficace et plus rapide, et la régulation à la hausse des métabolismes du carbone, de l'azote et énergétiques.

Ces résultats démontrent que les rosettes d'*Arabidopsis* et les graines de soja en germination modifient leur protéome selon les signaux bactériens et le stress. La spécificité de cette réponse joue un rôle crucial dans le cycle de vie des plantes, et la compréhension de cette réponse est d'importance dans son application commerciale.

ACKNOWLEDGEMENTS

I wish to thank Prof. Donald Smith and my supervisory committee Prof. Jean Bennoit Charron and Prof. Lyle Whyte for their guidance and valuable suggestions during the progress of this research. I wish to thank Prof. Kushallapa, Prof. Danielle Donelly, Prof. Pierre Dutilleul, and Prof. Phillippe Seguin and all the faculty and staff of The Department of Plant Science, for constructive criticism and for all the support rendered.

Most part of this thesis was possible mainly from the support of Mr. Guy Rimmer who gave me enough growth chambers and germination chambers I required for conducting my experiments, especially at short notice. If not for this support, this project would have never taken the direction that it has taken now. I would also wish to thank Richard Smith, who was very helpful in the green house, during my teaching assistantships.

My thanks are due to Dr. Suzanne Abrams and her group at NRC-PBI, Saskatoon who helped with hormone analysis. I would specially wish to thank Dr. Denis Faubert and his group (Marguerite Boulos, Josee Champagne and Sylvain Tessier) from Institut de recherches cliniques de Montréal (IRCM) for all technical assistance in the proteomic studies.

The work of Emily Ricci who helped generate data for the soybean paper in this thesis is wholeheartedly appreciated. Emily especially was a great support during the summers of 2011 and 2012, and was my personal genie. My thanks are due to Dr. Xiaomin Zhou for all the help rendered both for general guidance and for all the travel for conferences through Green crop network. Dr. Alfred Souleimanov's help in obtaining enough bacterial signal compounds for testing and HPLC analysis is commendable.

I also wish to thank all my other lab members Dr. Fazli Mabood, Dr. Inna Teshler, Dr. Keomany Ker, Dr. Selvakumari Arunachalam, He, Nan, Tim, Rachel, Kaberi, Uttam, Shanta, Selina, Di, Uliana, Yoko, Martyna, Pratyusha, visiting scientists Dr. Jung, Dr. Marion, Dr. Mei, summer students Haomiao, Robert, Tessie, Winnie, Xuan, Tomona, and

Juian for all help, support and keeping the lab alive despite hectic schedules. And all those (the list is really long) who made the lunch room lively and kept me alive and sane with their humor.

I sincerely appreciate the support of Dr. Patricia Harney Fellowship from Nova Scotia Agriculture College, Truro, Nova Scotia, Canada, for the 1st three years of my PhD program.

And above all, support from my family and an understanding husband helped me complete this phase of research amicably. I owe this thesis to all of you.

Sowmyalakshmi Subramanian

PREFACE AND CONTRIBUTION OF AUTHORS

This thesis has been written in the form of manuscripts. This format has been approved by the Faculty of Graduate Studies, at McGill University, as described in “Guidelines for Thesis Preparation and Submission”. This research was designed by me in cooperation with Dr. Donald L. Smith, thesis supervisor and a co-author of all the manuscripts. I conducted all the laboratory work, analyzed the data, wrote the manuscripts, and the thesis under the supervision of Dr. Donald L. Smith. The current thesis is composed of six chapters. The first and second chapters are the Introduction and Literature Review respectively. The literature review is an amalgamation of two manuscripts one of which has been published and the other submitted for publication. Chapters 3, 4 and 5 represent the laboratory experiments and were written in form of manuscripts either published or submitted for publication. Chapter 6 represents Summary, Conclusions and suggestions for future research.

The first two manuscripts (Chapter 2) were co-authored by Dr. Donald L. Smith, who helped in organizing the thoughts, revised successive versions of the manuscripts and thesis, and provided valuable suggestions at all stages of this work.

The third manuscript (Chapter 3) and the fourth manuscript (Chapter 4) were co-authored by Dr. Alfred Souleimanov and Dr. Donald L. Smith. Dr. Alfred Souleimanov provided with the bacterial signal compounds lipo-chito-oligosaccharide and thuricin 17 for the experiments in Chapter 3 and 4. Contributions of Dr. Donald L. Smith were similar to the chapters mentioned above.

The fifth manuscript (Chapter 5) is co-authored by Emily Ricci, Dr. Alfred Souleimanov and Dr. Donald L. Smith. Emily Ricci helped carry out germination assays and initial protein extraction procedures for proteomic analysis of soybean. The contribution of Dr. Alfred Souleimanov and Dr. Donald L. Smith were similar to those described for Chapter 3 and 4.

CONTRIBUTIONS TO KNOWLEDGE

Based on the research conducted and interpreted, the following are original contributions to knowledge developed from the work contained in this thesis.

1. This was the first study to detail hormone analysis using UPLC-ESI/MS methods at 24 h after treatment of three-week-old *Arabidopsis thaliana* rosettes with the bacterial signals LCO and Th17. It is very clear from the study that at 24 h post treatment, the hormones and their catabolites are differentially regulated by LCO and Th17 in the signal treated rosettes. This early response of plants to LCO and Th17, in the form of hormonal regulation, might prepare the plants for enhanced growth and stress tolerance.
2. This is the first detailed functional proteome study of both LCO and Th17 treated *A. thaliana* plants under optimal conditions and under salt stressed conditions. The proteome, along with the metabolome, dictates the regulation of the transcriptome, hence the proteome profile is an important aspect of plant-microbe interaction studies.
3. In this study, we compared the effects of LCO and Th17 under unstressed and salt-stressed conditions; this was the first study conducted to determine the effects of chronic exposure effects to these signals, in combination with stressful levels of salt, on germinating soybean seeds. LCO is now commercially available as a wide range of products, such as Optimize marketed by Novozymes, and is known to enhance plant growth under field conditions. Comparisons between LCO and Th17 for seed germination effects, and understanding the effects on the proteome of the seeds under stressed and unstressed conditions, showed that these microbial-produced signal compounds enhance seed germination under stress conditions and that Th17, like LCO, has the potential for commercialization in this regard. In addition, the use of such growth promoting technologies potentially allows for decreased use of synthetic chemical inputs on agricultural land, and perhaps enhanced crop productivity on salinized soils around the world.

CHAPTER 1

INTRODUCTION

The use of modern technologies in agriculture, such as farm machinery and equipment, selection of new varieties and hybrids, and bio-engineering to create genetically modified crops, have all resulted in bettering the yield potentials of commercial crops worldwide. However, the need to increase food production has also resulted in use of synthetic chemicals as fertilizers, pesticides and herbicides that have contaminated the environment (Anderson, 2001). Concerns in this area have caused regulatory agencies to develop ever more stringent standards for chemical control methods, which has removed some previously allowed chemicals from practice and slowed the appearance of new chemical control methods. At the same time, plant pathogens have evolved resistance to some previously useful chemical control measures (Bender and Cooksey, 1986; Alexander et al., 1999).

This has led to the use of biocontrol compounds, which are becoming increasingly valued, in part because consumers have become uncomfortable with synthetic chemical control measures, and because pest organisms continue to evolve resistances to current chemical controls; hence in the current social context, biocontrol measures are more acceptable. Controlling plant diseases and pests using other organisms or their by-products is a centuries old agricultural practice, and includes development and improvement of biofertilizers and bioinoculants (Mabood et al., 2006). Similarly, the study of phytohormones as physiologically active substances is as old a practice, but development has been slow due to limited market potential, in part related to the complexity of these compounds and their effects, reliability in terms of stability and functionality outside of their natural environments, and the cost involved in their production for commercial application. In this context the use of signal compounds from microorganisms, both natural and their semi-synthetic analogues, has gained considerable industrial importance, as this technology constitutes another potentially important input to modern agriculture.

Bacteria and plants form an integral part of terrestrial ecosystems. The symbiotic and pathogenic relationships of bacteria and plants depend on the availability of resources for survival for the bacteria and the resistances from the plants they have to defend themselves from. Plant growth promoting rhizobacteria (PGPR) are free living bacteria that exist in the rhizosphere (the area immediately around the roots rich in plant exudates and microorganisms and the spaces between cells within the roots) and have beneficial effects in agriculture (Kloepper and Schroth, 1978). They are found not only in the rhizosphere, but also on and in the plant roots and also the cells of the nodules of legumes (Gray and Smith, 2005) and have been found to stimulate plant growth. The growth stimulation may be through direct mechanisms, as in biological nitrogen fixation, production of phytohormones and siderophores (Bloemberg and Lugtenger, 2001) and enhanced soil nutrient availability (Rodriguez and Fraga, 1999; Fasim et al., 2002); or indirect by disease suppression through antibiosis or improved plant resistance mechanisms (Layzell and Atkins, 1997; Whipps, 2001).

Some of the most widely used bacterial bio-fertilizers are based on nitrogen fixing rhizobia, such as members of the genera *Allorhizobium*, *Azorhizobium*, *Bradyrhizobium*, *Mesorhizobium*, *Rhizobium*, and *Sinorhizobium*, where the plants utilize the nodule-fixed nitrogen and provide photosynthetically fixed carbon to the rhizobia. The increased use of rhizobia-based commercial inoculants as biofertilizers (Vessey, 2003; Choudhary and Johri, 2009) has been in response to the use of fossil fuels in nitrogen fertilizer production, accompanied by a steep rise in fossil fuel prices over the recent years, plus the greenhouse gas emissions (particularly N₂O) associated with nitrogen fertilizer use; a significant expansion in the use of bio-fertilizers that is likely to continue over the long-term.

Signal exchanges are now recognized as a key first step in the establishment of rhizobia-legume N₂-fixing symbioses. Inside the established legume root nodules rhizobial cells are enclosed in plant cell membrane and both the rhizobial cell walls and metabolism are substantially modified so that the major activity of the resulting “symbiosome” is to supply nitrogen to the host plant (Provorov et al., 2012); the symbiosome has become an ephemeral organelle. Legume roots exude (iso)-flavonoids that act as a chemoattractant to rhizobia and induce the rhizobial *Nod* genes (Currier and

Strobel, 1976; Firmin et al., 1986). Lipo-chitooligosaccharides (LCOs), also known as Nod factors, are synthesized by rhizobia in response and excreted as host-specific rhizobia-to-plant signals (D'Haeze and Holsters, 2002). They are perceived by multiple receptors in host roots, triggering a cascade of signaling events essential for bacterial invasion of the host roots, leading to the formation of N₂-fixing root nodules (Hirsch and Oldroyd, 2009). Host plant responses upon exposure to LCOs are nodulation-related and non-nodulation-related. The former consists of four milestone events: 1) root hair curling and deformation, 2) electrophysiological responses including ion fluxes, 3) formation of infection threads and development of nodules, 4) activation of early *nodulin* (*enod*) genes in host plants, which encode proteins responsible for early nodule development (Kamst et al., 1998; Ramu et al., 2002). A little over a decade ago we discovered that the LCOs produced by rhizobia, to signal legume symbiotic partners, are also able to stimulate plant growth directly (Souleimanov et al., 2002c; Prithiviraj et al., 2003; Khan et al., 2008). This was subsequently confirmed for root growth in *Medicago truncatula* (Olah et al., 2005), accelerated flowering in tomato upon LCO spray (a typical response to stress), and increased yield (Chen et al., 2007). Enhanced germination and seedling growth, along with the mitogenic nature of LCOs, suggest accelerated meristem activity. LCO like molecules also stimulated early somatic embryo development in Norway spruce (Dyachok et al., 2002). A microarray study conducted on low temperature stressed soybean plants showed that the largest class of known soybean genes activated by an LCO spray was stress-response related (Wang et al., 2012). Products based on our LCO findings have been used to treat seeds sown into several million ha of crop land around the world in each of the last few years. The initial findings with LCOs have been widely repeated and several LCO technologies from our laboratory are now commercially available, of which the product Optimize marketed by Novozymes is notable.

(<http://bioag.novozymes.com/en/products/unitedstates/biofertility/Pages/default.aspx>).

The PGPR *Bacillus thuringiensis* NEB17, isolated from soybean nodules by our group, enhances nodulation when applied as a co-inoculant with *B. japonicum* 532C (Bai et al., 2003). This bacterium produces a novel antimicrobial peptide (bacteriocin), called thuricin17 (molecular weight 3.1 kDa), stable across a pH range of 1.0–9.25, highly heat

resistant and is inactivated by treatment with proteolytic enzymes. Thuricin 17 is non-toxic to *B. japonicum* 532C (Gray et al., 2006b) and is a class IId bacteriocin. The bacteriocins produced by *B. thuringiensis* strain NEB17 (Th17) and *B. thuringiensis* subsp. *kurstaki* BUPM4 (bacthuricin F4 - 3160.05 Da) have been reported to show functional similarities and anti-microbial activities (Jung et al., 2008a). In addition, Th17, applied as leaf spray and root drench, has positive effects on soybean and corn growth, as first reported from our laboratory (Lee et al., 2009); this constituted the first report of plant growth stimulation. However, Th17 has not been studied as much as LCO for its responses in plants; the mechanistic pathways for both of these compounds are still not clearly understood.

In terms of commercial exploitation, the production of Th17 from *Bacillus thuringiensis* NEB17 is comparatively easier, due to its fast growth in cultures (extractable cultures ready in 48 h, yielding about 300-500 $\mu\text{g L}^{-1}$ Th17), and therefore more economical, than LCO production from *Bradyrhizobium japonicum* 532C (extractable culture ready in 10 days, yielding not more than 150 $\mu\text{g L}^{-1}$ of LCO). Since the plant growth stimulation by Th17 is at the proof of concept stage and we do not yet understand the plant-growth related responses it triggers in plants, our general goal in this study was to evaluate the effects of both LCO and Th17 on plant proteome profiles, to add to previous knowledge about LCO based on microarray studies.

Of the various changes brought about by signal molecule interactions with plants, plant hormone changes and proteome responses are very interesting as they provide an actual representation of the plants responses at the systems level of functioning. Hence we have attempted to study the effects of LCO and Th17 on plant growth using a mass spectrometric approach of label free proteomics, and have also collected data on hormone profiles of the same plants. This study focuses on the comparison of the plants responses to these two bacterial compounds on the proteome level.

1.1 General Hypothesis:

Based on the previous findings of plant growth responses from our laboratory, we have attempted to extend our knowledge in this area by elucidating the mechanism of plant growth promotion in *Arabidopsis* under optimal and salt stressed conditions in response to the bacterial compounds LCO and Th17. Further, this is also investigated in soybean since it is a commercial crop of importance in Canada and in particular in the provinces of Eastern Canada.

Therefore, the following hypotheses are proposed:

1. Early hormonal responses of *A. thaliana* to the bacteria-to-plant signal compounds LCO and Th17 regulate responses related to plant growth and will cause increases in the level of hormones that control stress responses.
2. Proteome responses in *A. thaliana* plants will indicate increases in stress related proteins following treatment with LCO or Th17 under optimal and salt stressed conditions.
3. The proteome of soybean seeds will also indicate increases in stress related proteins following treatment with LCO and Th17 under optimal and salt stressed conditions that might have overall similarity to that of *Arabidopsis*.

Following from these hypotheses, several objectives were defined and executed.

1.2 The objectives

1. Screen GUS transgenes of *Arabidopsis thaliana* to study the pattern of hormonal regulation in response to LCO and Th17 treatments.
2. Study early responses [24 h post treatment response] of *A. thaliana* to various hormones, based on an UPLC-ESI approach, to quantify shifts in hormones and their catabolites, in response to LCO and Th17 treatments.
3. Study the proteome of *A. thaliana* to understand changes in the total protein profile of three-week-old *A. thaliana* rosettes in response to LCO and Th17 treatments, in the presence and absence of salt stress.

4. Study soybean seed germination under optimal and salt stressed conditions, with and without signal compound treatments
5. Elucidate the soybean proteome of 48 h germinated seeds in the presence of factorial combinations of salt stress and signal compounds.

Note: Not all the objectives were formulated at the onset of work. Some of the experiments were established based on findings from the initial aspects of the work.

CHAPTER 2

This chapter is an amalgamation of two review papers

1. Signalling in the Phytomicrobiome – Submitted to Cell - Trends in Plant Sciences

Sowmyalakshmi Subramanian, Donald L Smith

Department of Plant Science, Faculty of Agricultural and Environmental Sciences,
McGill University, Macdonald Campus, 21,111 Lakeshore Rd, Ste-Anne-de-Bellevue,
Quebec, Canada H9X 3V9

Corresponding author: Prof. Donald L Smith (donald.smith@mcgill.ca)

2. A proteomics approach to study soybean and its symbiont *Bradyrhizobium japonicum* –A review, A Comprehensive Survey of International Soybean Research - Genetics, Physiology, Agronomy and Nitrogen Relationships, Prof. James Board (Ed.), ISBN: 978-953-51-0876-4, InTech, DOI: 10.5772/53728. Available from: <http://www.intechopen.com/books/a-comprehensive-survey-of-international-soybean-research-genetics-physiology-agronomy-and-nitrogen-relationships/a-proteomics-approach-to-study-soybean-and-its-symbiont-bradyrhizobium-japonicum-a-review>

Sowmyalakshmi Subramanian and Donald L Smith

Department of Plant Science, Faculty of Agricultural and Environmental Sciences,
McGill University, Macdonald Campus, 21,111 Lakeshore Rd, Ste-Anne-de-Bellevue,
Quebec, Canada H9X 3V9

Corresponding author: Prof. Donald L Smith (donald.smith@mcgill.ca)

GENERAL REVIEW OF LITERATURE

2.1 Abstract:

Soil is a dynamic environment due to fluctuations in climatic conditions that affect pH, temperature, water and nutrient availability. These factors, along with agricultural management practices, affect the soil micro-flora health and the capacity for effective plant-microbe interactions. Despite these constant changes, soil constitutes one of the most productive of earth's ecospheres and is a hub for evolutionary and other adaptive activities. For the most part, energy enters terrestrial ecosystems at the green leaves of plants. The roots of plants exist in direct contact with soil and in a moist habitat, where there is little chance of escaping direct interactions with soil microflora. Those elements of the microflora able to co-exist closely with plants may have direct access to photosynthetically reduced carbon and so, preferential access to energy; they comprise the phytomicrobiome. At this juncture, we could compare the gut microbiome of the humans to the rhizosphere microbiome of plants, both being similar in function, as the microbiomes change with the age of the organism and play a pivotal role in governing the wellness of the organism throughout their life cycles.

2.2 Introduction to the phytomicrobiome:

Mammals are consistently associated with large bacterial populations, in their gut, lachrymal glands and skin, so that microbial genes outnumber the organism's, for example by one hundred to one in humans. Over the last decade, understanding of human genome has led to considerable attention to human microbiome, without which the understanding of the human genome is incomplete; a considerable amount of research has been focused on the gut microbiome (Scott et al., 2012; Culligan et al., 2012). The gastrointestinal tract is a hub of activity since the resident bacteria must adapt and establish successfully in environments with digestive acids, variable osmolarity, differences in nutrient and iron availability and a range of host immune factors. Metagenomics and bioinformatics studies have led to the understanding of novel salt tolerant loci in the gut microbiome and their importance therein. Microbial and mammalian partners have coexisted long enough to develop mutual dependencies. For

instance, the gene *murB* dictates bacterial peptidoglycan biosynthesis dictates host immunity stimulation, while *mazG* could delay programmed cell death to allow the bacteria to survive until a favorable nutrient environment is available (Culligan et al., 2012). Studies such as these broaden our understanding of these bacteria and their responses to stress conditions, information that is useful in developing bio-therapeutics and novel drugs.

It seems that there is a group of bacteria living consistently and closely with plant roots (Lugtenberg and Kamilova, 2009; Compant et al., 2010) similar to the gut microbiome of humans. We have been exploring aspects of signaling from members of the rhizosphere part of the “phytomicrobiome” with some interesting results. From the plant perspective, bacteria are found associated in the phyllosphere (as both epi- and endophytes, on and in leaves and stems), rhizosphere (as rhizobacteria) and reproductive structures such as flowers, fruits and seeds. In grape, for instance, *Pseudomonas* and *Bacillus* spp colonize the epidermis and xylem of the ovary and ovules, while some *Bacillus* spp colonize berries and seed cell walls (Lugtenberg and Kamilova, 2009; Compant et al., 2010; 2011). Similarly, in sugar cane, nitrogen fixing rhizobacteria associated with the plant reside in the roots (Pisa et al., 2011), but also well up into the stem (Velázquez et al., 2008). The sugarcane apoplast harbors *Acetobacter diazotrophicus*, a nitrogen fixing bacterium that survives in a non-nitrogen but high sucrose environment (Dong et al., 1994) and *Pantoea agglomerans* 33.1, which also is a PGPR (Loiret et al., 2004; Quecine et al., 2012). Other BNF bacteria such as *Azotobacter*, *Enterobacter*, *Bacillus*, *Klebsiella*, *Azospirillum*, *Herbaspirillum*, *Gluconacetobacter*, *Burkholderia* and *Azoarcus* are found in a wide range of grasses including rice and maize (Von Bulow and Dobereiner, 1975; Triplett, 1996; James, 2000; Baldani et al., 2002; Boddey et al., 2003; Santi et al., 2013).

Other than nitrogen fixation, PGPR employ a variety of mechanisms to promote plant growth and development. The more widely recognized mechanisms include: biofertilization (enhanced nutrient availability), including nitrogen fixation (Layzell and Atkins, 1997); suppression of diseases through a range of biocontrol mechanisms; induction of disease resistance in plants; production of phytohormones, and production of

signal compounds, including volatile forms (Whipps, 2001). Bio-fertilizers are substances that contain living microorganisms which, when applied to seeds, plant surfaces, or soil, colonize the rhizosphere or the interior of the plant and promote growth by increasing the availability of primary nutrients to the host plant (Vessey, 2003). Despite being abundant in soils phosphorus (P), one of the macronutrients required for plant growth and development, is often limiting because of its presence in conjugated and precipitated forms unavailable to plants. Phosphate solubilizing bacteria (PSB) mobilize phosphorus, making it substantially more available to plants (Kim et al., 1998; Rodriguez and Fraga, 1999). Microbial phosphate solubilisation can provide a solution, not only to compensate for the increasing fertilizer costs, but also as a way to increase efficiency of P fertilizers, by mobilizing insoluble forms of P in the soil. Some rhizobacteria produce siderophores that enhance iron availability to plants (Bloemberg and Lugtenberg, 2001), while others play an important role in the availability of other micronutrients to plants (Fasim et al., 2002).

However, the most widely used bacterial bio-fertilizers are the nitrogen fixing rhizobia largely in the genera *Allorhizobium*, *Azorhizobium*, *Bradyrhizobium*, *Mesorhizobium*, *Rhizobium*, and *Sinorhizobium*. Plants utilize nitrogen fixed inside the nodule and provide photosynthetically fixed carbon to the rhizobia. Increased use of rhizobia-based commercial inoculants as biofertilizers (Vessey, 2003; Choudhary and Johri, 2009) has been in response to the use of fossil fuels in nitrogen fertilizers production accompanied by a steep rise in fossil fuel prices over the recent years, and the greenhouse gas production associated with nitrogen fertilizer use (principally N₂O); a significant expansion in the use of bio-fertilizers is likely to continue over the long-term. Besides rhizobia, there are other rhizobacteria that live and fix nitrogen outside of formal symbioses, referred to as free-living or associative nitrogen-fixing bacteria, such as *Azospirillum*, *Acetobacter*, *Herbaspirillum*, *Azoarcus* and *Azotobacter* (Steenhoudt and Vanderleyden, 2000). These rhizobacteria, as biofertilizers, are interesting study models as they help provide nitrogen to non-legume plants (Boddey et al., 2003) and have potential use on marginal lands, as a low input nutrient provider to crop plants, and perhaps particularly in the production of biofuel feedstock crops, where energy balance is important.

Most bio-fertilizers are generally selected for both increased plant growth and increased stress resistance. Plants exhibit at least three known types of systemic resistance upon symbiotic and pathogen challenge, viz., systemic acquired resistance (SAR) via salicylic acid (SA) mediation (Malamy et al., 1990; Hammond-Kosack and Jones, 1996) induced systemic resistance (ISR) mediated by jasmonic acid (JA) and ethylene (ETH) (van Wees et al., 1997); and salicylic acid independent (SIR) (Kim and Delaney, 2002a); independent of SON1 protein regulation through the ubiquitin-proteasome pathway (Kim and Delaney, 2002b). Symbiotic bacteria often induce systemic resistance in plants they inhabit. ISR is similar to SAR but is also broad spectrum. The role of SA as a defence signal became apparent in the 1990s (Kessmann and Ryals, 1993). In SAR, plants attacked by some pathogens exhibit hypersensitive response (HR), which triggers broad spectrum disease resistance in uninfected parts of the plant, and accompanied by expression of PR1 proteins (Malamy et al., 1990; Hammond-Kosack and Jones, 1996); PR1 and PR5 are considered the most reliable markers for SAR detection. The regulatory gene *NPR1*, an important component of SA signalling (Delaney et al., 1995), interacts with the TGA2 transcription factor to regulate the expression of various pathogen related genes, including PR1, and promotes disease resistance (Kinkema et al., 2000; Fan and Dong, 2002; Cao et al., 1997). In ISR, the role of JA and ETH is evident from experiments on *jar1* (Staswick et al., 1992) and *etr1* mutants (Bleeker et al., 1988), in which *P. fluorescens* WCS417r failed to induce ISR (Pieterse et al., 2001). The biosynthesis of JA was reported by Vick and Zimmermann (1984), leading to the discovery of JA as a signal molecule in wounding, herbivory, biotic and abiotic stressor responses (Wasternack, 2007; Katsir et al., 2008). Pathogen-related proteins such as PR3, PR4, PR12 (PDF1.2) and PR13 (Thi2.1) are induced via the JA pathway (Penninckx et al., 1998). JA signalling is comprised of four components: a JA signal, Skp/Cullin/F-box (SCF) - type E3 ubiquitin ligase, jasmonate ZIM domain (JAZ) repressor protein and transcription factors (TF) such as WRKY70, MYC2, ERF1 and ORCA. JAZ repressors are targeted by SCFCOI1 for degradation by the ubiquitin/26S proteasome pathway (Dreher and Callis, 2007; Thines et al., 2007). Despite differences in the roles of signalling molecules, NPR1 is required for both SAR and ISR pathways (Pieterse et al., 2001). Other phytohormones such as abscisic acid (ABA), auxins (IAA), gibberellic acids

(GA), cytokinins and brassinosteroids are all seen to regulate plant responses to environmental cues, including biotic and abiotic stressors (Spoel and Dong, 2008; Ciesielska, 2012). At this juncture, the phytohormone regulation is very similar to that of the human immune system in that both their functions are protective to fluctuating environmental conditions.

2.3 Proteomics as a part of integrative systems biology

The “omics” approach to knowledge gain in biology has advanced considerably in the recent years. The triangulation approach of integrating transcriptomics, proteomics and metabolomics is being used currently to study interconnectivity of molecular level responses of crop plants to various conditions of stress tolerance and adaptation of plants, thus improving systems level understanding of plant biology (Sha Valli Khan et al., 2007; Nanjo et al., 2011).

While transcriptomics is an important tool for studying gene expression, proteomics actually portrays the functionality of the genes expressed. Several techniques are available for studying differential expression of protein profiles, and can be broadly classified as gel-based and MS-based quantification methods. The gel based approach uses conventional, two-dimensional (2-D) gel electrophoresis, and 2-D fluorescence difference gel electrophoresis (2D-DIGE), both based on separation of proteins according to isoelectric point, followed by separation by molecular mass. The separated protein spots are then isolated and subjected to MS analysis for identification. Major drawbacks of these techniques are laborious sample preparation and inability to identify low abundance, hydrophobic and basic proteins.

The MS based approach can be a label-based quantitation, where the plants or cells are grown in media containing ^{15}N metabolite label or using ^{15}N as the nitrogen source. Label-free quantitation, however, is easier and gaining popularity owing to the simple protein extraction procedures and low amounts of sample material required; and allows analysis of multiple and unlimited samples. This technique, also referred to as MudPIT (multidimensional protein identification technology), is a method used to study proteins from whole-cell lysate and/or a purified complex of proteins (Paoletti et al.,

2004; Delahunty and Yates, 2005). The total set of proteins or proteins from designated target sites are isolated and subjected to standard protease digestions (eg. such as tryptic digestion). In brief, flash frozen leaf samples are ground in liquid nitrogen and polyphenols; tannins and other interfering substances such as chlorophyll are removed. The processed tissue is resuspended in a chaotropic reagent to extract proteins in the upper phase, and the plant debris is discarded (Herbert et al., 1998; Molloy et al., 1998; Ferro et al., 2000; Cilia et al., 2009; Amalraj et al., 2010; Dawe et al., 2011; Koay and Gam, 2011). The total protein set, in the resulting solution, is further quantified using the Lowry method (Lowry et al., 1951). The protein samples (2 µg of total protein each), once digested with trypsin, can then be loaded onto a microcapillary column packed with reverse phase and strong cation exchange resins. The peptides get separated in the column, based on their charge and hydrophobicity. The columns are connected to a quaternary high-performance liquid chromatography pump and coupled with an ion trap mass spectrometer, to ionize the samples within the column and spray them directly into a tandem mass spectrometer. This allows for a very effective and high level of peptide separation within the mixture, and detects the eluting peptides to produce a mass spectrum (MS). The detected peptide ions, at measured mass-to-charge (m/z) ratios with sufficient intensity, are selected for collision-induced dissociation (CID). This procedure allows for the fragmenting of the peptides to produce a product ion spectrum, the MS/MS spectrum. In addition, the fragmentation occurs preferentially at the amide bonds, to generate N-terminal fragments (b ions) and C-terminal fragments (y ions) at specific m/z ratios, providing structural information about the amino acid sequence and sites of modification. The b ion and y ion patterns are matched to a peptide sequence in a translated genomic database to help identify the proteins present in the sample (Washburn et al., 2002; Aebersold and Mann, 2003; Lill, 2003; Liu et al., 2004). A variety of database searching and compiling algorithms are used to interpret the data obtained for structure and function of the identified proteins. Hence, studying the crop at the proteomics level, with a view to better crop management and productivity, is gaining importance in the post genomic era.

2.4 *Arabidopsis thaliana* as a plant model system for proteomic studies

Arabidopsis thaliana (L.) Heynh.

Arabidopsis thaliana is a model plant widely used in physiology and molecular biology studies and is one of the most researched plant species. *Arabidopsis thaliana* is a dicot that belongs to the family Brassicaceae (Cruciferae), native to temperate and tropical Asia, Europe and Africa. This plant is extensively used in plant research due to its small genome size (125 megabase pairs (MBP)), which codes for nearly 25,000 genes, a relatively short life cycle (4-6 weeks), prolific seed production and minimal requirements for growth. Nearly 750 ecotypes of *A. thaliana* are distributed worldwide (www.arabidopsis.org). It can be readily transformed using *Agrobacterium tumefaciens* for molecular biology studies (Meinke et al., 1998). A comparison of *A. thaliana* sequences to human genome sequences reveals a high percentage of conserved protein function and cellular processes despite the phylogenetic distance. Some of the proteins for human diseases such as Alzheimer's and Parkinson's, neurodegenerative disorders, are found in *Arabidopsis*, increasing the importance of this model plant in associating it with human diseases (Xu and Moller, 2011). The completion of the genome sequence in 2000 has facilitated a large volume of gene expression studies. However, transcription does not necessarily mean translation and protein function, and this has led to increased studies and related techniques the development of a proteomics platform as a complement to the transcriptomics.

Due to the complexity of the system and masking of relatively rare proteins due to high abundance ones, most of the *A. thaliana* proteomics work has been specifically targeted towards the cell organelles; many of the reports currently available are focused here.

Leaves - A comparison of MudPIT and 1-D gel-LC-MS/MS of the *Arabidopsis* leaf proteome revealed 2342 non-redundant proteins, most of which were similar to that encoded by the genome, based on GO ontology (Lee et al., 2007).

Cell wall and apoplast - Of the 93 proteins isolated using a calcium chloride salting method, 87 proteins seemed to have a signal peptide for interaction and 6 had cytoplasmic origin. Out of the 87 putative apoplastic proteins identified, 67 were found

to be basic (pH up to 8.9). Apoplast proteins extracted using PVPP, in order to minimize the secondary metabolite interference in mass spectrometric studies, revealed the presence of 44 secreted proteins, in liquid culture grown *Arabidopsis* seedlings (Charmont et al., 2005).

The cell wall proteins of *Arabidopsis* rosettes were similar to the cell wall proteins identified from proteome of *Arabidopsis* cell suspension culture (Boudart et al., 2005). About 1/4th the postulated cell wall proteins have been identified. The 400 proteins identified include enzymes that act on cell wall polysaccharides, proteases, hydrolytic enzymes and lipases involved in signal transduction, and many unknowns that might contribute to cell wall functioning in one way or another. The complexity of regulation in the cell wall is evident from the presence of many glycoside hydrolases and proteases (Jamet et al., 2008). During cell elongation, proteins from specific families such as xyloglucan endotransglucosylase-hydrolases, expansins, polygalacturonases, pectin methylesterases and peroxidases, play roles in the rearrangement of cell wall (Irshad et al., 2008, Albenne et al., 2013).

Plasma membrane – The plasma membrane is an interface for many biological processes and functions. *Arabidopsis* leaves, upon activation by the immune receptor RPS2, showed significant changes in proteins involved in calcium and lipid signaling, redox homeostasis and vesicle trafficking, membrane transport proteins for primary and secondary metabolites and protein phosphorylation, all of which were involved with plant immunity (Elmore et al., 2012).

The phosphorylated membrane tonoplast proteins identified so far include those from tonoplast anion transporters of the CLC family, potassium transporters of the KUP family, tonoplast sugar transporters and ABC transporters (Whiteman et al., 2008).

Chloroplast - A study of the stromal proteome of *Arabidopsis* chloroplasts found 10 % of the 241 proteins identified to be involved in chloroplast protein synthesis and biogenesis, 75 % to be oxidative pentose phosphate pathway, glycolysis and Calvin cycle proteins, 5 – 7 % to be nitrogen metabolism related and the rest to be associated with other biosynthetic pathways such as fatty acid metabolism, amino acid metabolism, nucleotides, vitamins B1 and 2, tetrapyrroles, lipoxygenase 2 and a carbonic anhydrase

(Peltier et al., 2006). About 80 - 200 proteins present in the thylakoid lumen are closely associated with the light harvesting complexes and the other proteins regulating photosynthesis. Following an 8 h light exposure, PsbP and PsbQ subunits of photosystem II were seen to increase along with a major plastocyanin and various proteins of unknown function. These photosystem II proteins also seem to be expressed at the transcription level (Granlund et al., 2009). Plants are exposed to varying levels of light in nature and they compensate for this by regulating their thylakoid membrane proteins. Exposure to light stress causes oxidative and nitrosative stresses and the proteins of photosystem I and II are affected differentially. The amino acid oxidation products are determined mostly in the photosystem II reaction center, and often lead to tyrosine and tryptophan oxidation or nitration (Galetskiy et al., 2011). The plastoglobule proteome of the chloroplast includes an M48 metallopeptidase, Absence of bc1 complex (ABC1) kinases and fibrillins, accounting for about 70 % of the plastoglobule protein biomass. The fibrillins present in other parts of the chloroplast are distributed, probably based on their isoelectric point and hydrophobicity. These proteins cater to specific functions such as chlorophyll degradation and senescence, plastid proteolysis, isoprenoid biosynthesis, redox and phosphoregulation of the electron flow, although most of the functions of the associated proteins are still unclear (Lundquist et al., 2012).

Carbonylation of proteins in organisms increases with age, a process that is irreversible and oxidative; leading to disfunctioning of modified proteins in the system. In Arabidopsis however, protein carbonylation increases as the plant grows but is seen to decrease drastically during the onset of bolting and flowering. Hsp70, ATP synthases, RUBISCO large subunit, proteins of the light harvesting complex and energy transfer proteins are all targets of this mechanism (Johansson et al., 2004).

Mitochondria - The last 6 years has seen rapid progress in proteome studies of the mitochondria due to refinement in organelle isolation and protein extraction procedures for LC-MS. To date 726 mitochondrial proteins have been detected, most of which participate in oxidative phosphorylation, pyruvate metabolism and TCA cycle, transport, protein folding and processing, processing of amino acids and other metabolites and a group of unknown proteins that still remains to be characterized (Lee et al., 2013).

Vacuoles - The two types of vacuoles found in younger plant tissues are lytic vacuole (LV) and protein storage vacuole (PSV), which is the main site of protein storage in seeds and roots. They merge into a single central vacuole retaining the parent vacuole's functions of degradation, storage of ions, metabolites and proteins, regulating pH, ion homeostasis and turgor pressure, toxic compound sequestration and harboring responsive elements to biotic and abiotic stresses, all of which contribute to signal transduction and overall plant growth and development (Surpin et al., 2003). Investigations of the vacuole proteome using Arabidopsis rosettes derived protoplasts subjected to MALDI-TOF and nano-LC MS/MS, revealed the presence of membrane proteins, vacuolar-ATPase subunits and tonoplast-localized soluble N-ethylmaleimide-sensitive factor attachment protein receptors (SNAREs) that are required for membrane fusion (Carter et al., 2004).

Cytoplasm - Plant cytosolic ribosomes are unique in comparison to other eukaryotic ribosomal proteins (Carroll, 2013). In Arabidopsis leaves, 2-6 paralogous genes code for about 79 different ribosomal proteins that are present in the cytoplasm as cytosolic ribosomes in the form of multi-subunit complexes. These proteins serve as vehicles in the transport of signals to and from the nucleus and regulate the translation process based on the signal perception (Hummel et al., 2012). Mutations of the cytoplasmic ribosomal proteins can lead to alterations in leaf growth such as pointed leaves, denticulation, reduction in size and number of palisade mesophyll cells and perturbations in leaf polarity (Horiguchi et al., 2011).

The peroxisomes contain a diverse group of peroxisome-targeting sequence (PTS1) tripeptide motifs that contain both basic and acidic residues, plus hydroxylated serine and threonine and hydrophobic alanine and valine residues, which are the predominant target enhancing residues (Chowdhary et al., 2012).

Proteasome pathway - The 20S proteasome pathway was seen to be up-regulated in both RNA and protein levels of cadmium stressed Arabidopsis leaves, suggesting that this proteasome pathway might help with degrading stress generated oxidized proteins (Polge et al., 2009). The 26 S proteasome of *A. thaliana* contains 26 unique proteins with at least 13 of them containing tryptophan residues, as identified using nanoflow liquid chromatography (Russel et al., 2013).

LEA proteins initially found in seeds are now reported to be present in other vegetative tissues and have a wide range of sequence diversity, intercellular localization and expression patterns, depending on environmental conditions. The majority of predicted LEA proteins are highly hydrophilic and found mostly in unfolded conditions, catering largely to cellular dehydration tolerance. In *Arabidopsis*, 9 distinct groups of LEA proteins encoded by 51 different LEA protein genes have been reported, most of which harbor abscisic acid response (ABRE) and/or low temperature response (LTRE) elements in their promoters (Hundertmark and Hinch, 2008).

In *Arabidopsis thaliana*, auxin-induced protein degradation is carried out by the ubiquitin proteasome pathway. This degradation mediates auxin effects on cellular and physiological processes, such as those associated with cytoskeleton structuring, intracellular signalling, chloroplast development and regulation of photosynthesis (Xing and Xue, 2012).

Ligands for metals such as cadmium (Cd), copper (Cu), nickel (Ni) and zinc (Zn) are seen in plant tissues and in the xylem sap. They form complexes with histidine and citrates in the xylem sap, moving from roots to leaves. The Cd binding complexes are found in both the cytosol and, predominantly, in the vacuole of the cell (Rauser, 1999).

Guard cell, stomata - The glucosinolates of Brassicales species are best known for their involvement in plant defense mechanisms using the glucosinolate-myrosinase pathway (Wittstocka and Burow 2010). The guard cell protoplast proteome has thioglucoside glucohydrolase 1 (TGG1) in abundance. TGG1 is a myrosinase that catalyses the conversion of glucosinolates to toxic isothiocyanates. This conversion system has been previously reported to be related to defense against biotic factors and is now recognized as is a requirement of guard cells, to function in association with ABA responses. In all probability, this system triggers defence responses during stomatal opening as a precaution during abiotic stress (Zhao et al., 2008). A dosage dependent gene mutation of isopropylmalate dehydrogenases caused gradual decreases in the leucine biosynthetic pathway creating an imbalance in amino acid homeostasis, changes in redox stress, increased protein production, decreased photosynthesis and thereby decreased plant growth. This also affected the glucosinolate pathway, resulting in the suppression

of protein degradation pathways leading to accumulation of toxic substances (He et al., 2013).

Pollen - Germinating pollen is rich in proteins and their regulation, providing for the rapid growth of the pollen tube. A shotgun proteomics study suggests close to 3500 proteins in the pollen, out of which 537 were new and not found based on earlier pollen genomic or transcriptomic studies. Interestingly, the pollen proteome was very similar to seed proteome, despite the differences in their developmental tissues (Grobei et al., 2009). It is important to note here that these two functional organs undergo a period of desiccation before they move into their next phases of development, a reason for which their proteomes might be similar.

2.5 A proteomics approach to study soybean and its symbiont *Bradyrhizobium japonicum*

Biological nitrogen fixation in legumes is arguably the second most important biological phenomenon, after photosynthesis, and is the most important natural source of nitrogen in the nitrogen cycle. It is an extremely effective symbiotic system, accounting for nearly $\frac{3}{4}$ of total biological nitrogen fixation (BNF). Soybean is one of the world's most important protein crops and also an important plant for the study of BNF. Soybean seed contains about 40 % protein and 20 % oil, which are of agriculture importance for livestock and human consumption, respectively. The N₂-fixation symbiosis between rhizobia and legumes is complex, requiring bacterium-to-plant recognition, and vice versa, for effective nodule formation. Effective nodulation translates into better crop development and yield. Recent proteomics studies have addressed research questions pertaining to soybean seed storage proteins, seedling growth, leaf and flower proteomics, seed filling strategies, abiotic stress responses (salt, drought, heat and flooding), biotic stress responses, nodulation and nodule function, and also the cellular proteins and exoproteins of rhizobia, the soybean-associated *Bradyrhizobium japonicum*.

2.5.1 Biological nitrogen fixation

Biological nitrogen fixation (BNF) is one of the most important phenomena occurring in nature, only exceeded by photosynthesis (Vance 1998; Graham and Vance

2000). One of the most common limiting factors in plant growth is the availability of nitrogen (Newbould, 1989). Although 4/5ths of earth's atmosphere is comprised of nitrogen, the ability to utilize atmospheric nitrogen is restricted to a few groups of prokaryotes that are able to convert atmospheric nitrogen to ammonia and, in the case of the legume symbiosis, make some of this available to plants. Predominantly, members of the plant family Leguminosae have evolved with nitrogen fixing bacteria from the family Rhizobiaceae. In summary, the plants excrete specific chemical signals to attract the nitrogen fixing bacteria towards their roots. They also give the bacteria access to their roots, allowing them to colonize and reside in the root nodules, where the modified bacteria (bacteroids) can perform nitrogen fixation (Sadowsky and Graham 1998; Vance, 1998; Graham and Vance, 2003). This process is of great interest to scientists in general, and agriculture specifically, since this highly complex recognition and elicitation is coordinated through gene expression and cellular differentiation, followed by plant growth and development; it has the potential to minimize the use of artificial nitrogen fertilizers and pesticides in crop management. This biological nitrogen fixation process is complex, but has been best examined in some detail in the context of soybean-*Bradyrhizobium* plant-microbe interactions.

2.5.2 Soybean – the plant

Soybean (*Glycine max* (L.) Merrill) is a globally important commercial crop, grown mainly for its protein, oil and nutraceutical contents. The seeds of this legume are 40 % protein and 20 % oil. Each year soybean provides more protein and vegetable oil than any other cultivated crop in the world.

Soybean originated in China, where it has been under cultivation for more than 5000 years (Cui et al., 1999). The annual wild soybean (*G. soja*) and the current cultivated soybean (*G. max*) can be found growing in China, Japan, Korea and the far east of Russia, with the richest diversity and broadest distribution in China, where extensive germplasm is available. The National Gene Bank at the Institute of Crop Germplasm Resources, part of Chinese Academy of Agriculture Sciences (ICGR-CAAS), Beijing, contains close to 24,000 soybean accessions, including wild soybean types. Soybean was introduced into North America during the 18th century, but intense cultivation started in

the 1940s – 1950s and now North America is the world's largest producer of soybean (Hymowitz and Harlan, 1983; Qui and Chang, 2010). Although grown worldwide for its protein and oil, high value added products such as plant functional nutraceuticals, including phospholipids, saponins, isoflavones, oligosaccharides and edible fibre, have gained importance in the last decade. Interestingly, while genistein and daidzein are signal molecules involved in the root nodulation process, the same compounds can attenuate osteoporosis in post-menopausal women. The other isoflavones have anti-cancer, anti-oxidant, positive cardiovascular and cerebrovascular effects (Lui, 2004). More recently soybean oil has also been used as an oil source for biodiesel (Mandal et al., 2002; Du et al., 2003; Mushrush et al., 2006; Huo et al., 2009; Pestana-Calsa et al., 2012). Table 2.1 provides the latest statistics on soybean cultivation and production as available at FAOSTAT (FAO, 2011).

Soybean is a well-known nitrogen fixer and has been a model plant for the study of BNF. Its importance in BNF led to the genome sequencing of soybean; details of the soybean genome are available at soybase.org (*G. max* and *G. soja* sequences are available at NCBI as well). The efficiency of BNF depends on climatic factors such as temperature and photoperiod (Shiraiwa et al., 2006); the effectiveness of a given soybean cultivar in fixing atmospheric nitrogen depends on the interaction between the cultivar's genome and conditions such as soil moisture and soil nutrient availability (Sridhara et al., 1995; Jung et al., 2008b) and the competitiveness of the bacterial strains available, relative to indigenous and less effective strains, plus the amount and type of inoculants applied, and interactions with other, possibly antagonistic, agrochemicals that are used in crop protection (Campo and Hungria, 2004). The most important criteria, however, is the selection of an appropriate strain of *B. japonicum* since specific strains can be very specific to soybean cultivar, and subject to influence by specific edaphic factors (Hughes and Herridge, 1989; Alves et al., 2003; Abaidoo et al., 2007). Under most conditions, soybean meets 50-60% of its nitrogen demand through BNF, but it can provide 100% from this source (Salvagiotti et al., 2008).

Table 2.1: Soybean production statistics (FAOSTAT 2011)

	World	Africa	Americas	Asia	Europe	Oceania	Canada
Area harvested (Ha)	102,386,923	1,090,708	78,811,779	19,713,738	2,739,398	31,300	1,476,800
Yield (Hg/Ha)	25,548	13,309	28,864	14,100	17,491	19,042	29,424
Production (Tonnes)	261,578,498	1,451,646	227,480,272	27,795,578	4,791,402	59,600	4,345,300
Seeds (Tonnes)	6,983,352	43,283	4,838,633	1,906,313	193,870	1,252	154,300
Soybean oil (Tonnes)	39,761,852	390,660	24,028,558	12,442,496	2,890,760	9,377	241,300

2.5.3 *Bradyrhizobium japonicum*:

B. japonicum, is a gram negative, rod shaped nitrogen fixing member of the rhizobia and is an N₂-fixing symbiont of soybean. *B. japonicum* strain USDA110, was originally isolated from soybean nodules in Florida, USA, in 1957 and has been widely used for the purpose of molecular genetics, physiology, and ecology, owing to its superior symbiotic nitrogen fixation activity with soybean, relative to other evaluated strains. The genome sequence of this strain has been determined; the bacterial genome is circular, 9.11 Million bp long and contains approximately 8373 predicted genes, with an average GC content of 64.1% (Kaneko et al., 2002a; 2002b).

Initially attached to the root-hair tips of soybean plants, rhizobia colonize within the roots and are eventually localized within symbiosomes, surrounded by plant membrane. This symbiotic relationship provides a safe niche and a constant carbon source for the bacteria while the plant derives the benefits of bacterial nitrogen fixation, which allows for the use of readily available nitrogen for plant growth. Inoculation of soybean with *B. japonicum* often increases seed yield (Ndakidemi et al., 2006).

Bradyrhizobium japonicum cells synthesize a wide array of carbohydrates, such as lipopolysaccharides, capsular polysaccharides, exopolysaccharides (EPS), nodule polysaccharides, lipo-chitin oligosaccharides, and cyclic glucans, all of which play a role in the BNF symbiosis. Bacteria produce polysaccharide degrading enzymes, such as polygalacturonase and carboxymethylcellulase, cleave glycosidic bonds of the host cell wall at areas where bacteria are concentrated, creating erosion pits in the epidermal layer of the roots, allowing the bacteria gain entry to the roots (Mateos et al., 2001). The energy source for *B. japonicum* is the sugar trehalose, which is taken up readily and converted to CO₂ (Salminen and Streeter, 1986; Müller et al., 2001; Streeter and Gomez, 2006; Sugawara et al., 2010). On the other hand UDP-glucose is taken up in large quantities but metabolized slowly, like sucrose and glucose. Promotion of plant growth causes more O₂ to be released and more CO₂ to be taken up (Kaneko et al., 2002a; Mateos et al., 2001).

2.5.4 Lipo-chitooligosaccharides (LCOs) from *Bradyrhizobium japonicum*:

As mentioned earlier, the process of nodulation in legumes begins with a complex signal exchange between host plants and rhizobia. The first step in rhizobial establishment in plant roots is production of isoflavonoids as plant-to-bacterial signals; the most common in the soybean-*B. japonicum* symbiosis being genestein and daidzein (Rao and Cooper, 1994), which trigger the *Nod* genes in the bacteria which, in turn, produce LCOs, or Nod factors, that act as return signals to the plants and start the process of root hair curling, leading to nodule formation. Some recent literature has shown that jasmonates can also cause *Nod* gene activation in *B. japonicum* although the strain specificities are very different from those of isoflavonoids such as genistein (Mabood et al., 2006a; 2006b; 2006c; Mabood and Smith, 2005). LCOs are oligosaccharides of β -1,4-linked N-acetyl-D-glucosamine coded for by a series of *Nod* genes and are rhizobia specific (Spaink et al., 1995). The nodDABCIJ genes, conserved in all nodulating rhizobia (Spaink et al., 1995; Kamst et al., 1998; Vazquez et al., 1993) are organized as a transcriptional unit and regulated by plant-to-rhizobia signals such isoflavanoids (Carlson et al., 1994; Schultze and Kondorosi 1996, 1998). Variations in LCO molecular structures such as (1) the length of the chitin oligomer backbone; (2) the type of fatty acyl

side chain on the non-reducing terminus and (3) the presence of additional groups on the reducing or non-reducing terminus of the LCO are the major determinants of host specificity (Fig. 1) (Schmidt et al. 1993; Spaink et al. 1995).

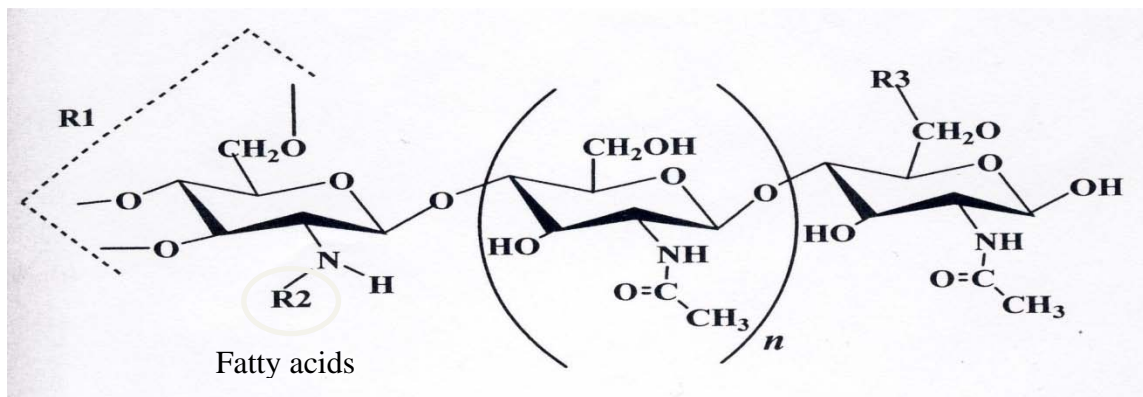


Fig. 2.1: Lipo-chitooligosaccharide (LCO) produced by rhizobia is host specific and the host specificity is determined by 1) the number of β -1,4-linked *N*-acetyl-D-glucosamine in the backbone; 2) the type of fatty acyl side chain at the non-reducing end; 3) types of substituting groups such as R1, R2, R3 (Spaink 2000).

Nodulation and subsequent nitrogen fixation are affected by environmental factors. It has been observed that, under sub-optimal root zone temperatures (for soybean 15-17 °C), pH stress and in the presence of nitrogen, isoflavanoid signal levels are reduced; while high temperature (39 °C) increases non-specific isoflavanoid production and reduces *nod* gene activation, thereby affecting nodulation (Bai et al., 2002a). Our laboratory has isolated and identified the major LCO molecule produced by *B. japonicum* 532C as Nod Bj V (C18:1; MeFuc) (Prithiviraj et al., 2000). This Nod factor contains a methyl-fucose group at the reducing end that is encoded by the host-specific *nodZ* gene (López-Lara et al., 1995), which is an essential component for soybean-rhizobia interactions.

LCOs also positively and directly affect plant growth and development in legumes and non-legumes. The potential role of LCOs in plant growth regulation was first reported by Denarie and Cullimore (1993). *Nod* genes A and B from *R. meliloti*, when introduced into tobacco, altered the phenotype by producing bifurcated leaves and stems, suggesting a role for *Nod* genes in plant morphogenesis (Schmidt et al., 1993). The development of somatic embryos of Norway spruce is enhanced by treatment with

purified Nod factor from *Rhizobium* sp. NGR234. It has been suggested that these Nod factors can substitute for auxin and cytokinin like activities in promoting embryo development, and that the chitin core of the Nod factor is an essential component for regulation of plant development (Dyachok et al., 2000; 2002). Some of the LCO induced *enod* genes in non-legumes seem to encode for defence related responses, such as chitinase and PR proteins (Schultz and Kondorosi, 1996; 1998), peroxidase (Cook et al., 1995) and enzymes of phenylpropanoid pathway, such as L-phenylalanine ammonia-lyase (PAL) (Inui et al., 1997). Seed germination and seedling establishment is enhanced in soybean, common bean, maize, rice, canola, apple and grapes, accompanied by increased photosynthetic rates (Zhang and Smith, 2001). Hydroponically grown maize showed an increase in root growth when LCO was applied to the hydroponic solution (Souleimanov et al., 2002a; 2002b; Khan, 2003) and foliar application to greenhouse grown maize resulted in increases in photosynthetic rate, leaf area and dry matter (Khan, 2003). Foliar application to tomato, during early and late flowering stages, increased flowering and fruiting and also fruit yield (Chen et al., 2007). An increase in mycorrhizal colonization (*Gigaspora margarita*) was observed in *Pinus abies* treated with LCO (Dyachok et al., 2002; Oláh et al., 2007). Recent research in our laboratory, on soybean leaves treated with LCOs under sub-optimal growth conditions, revealed the up-regulation of over 600 genes, many of which are defense and stress response related, or transcription factors; microarray results show that the transcriptome of the leaves is highly responsive to LCO treatment at 48 h post treatment (Wang et al., 2012). These results suggest the need to investigate more carefully the mechanisms by which microbe-to-plant signals help plants accommodate abiotic and biotic stress conditions. Products based on our LCO findings have been used to treat seeds sown into several million ha of crop land around the world in each of the last few years.

2.5.5 LCO signaling in other organisms

It is now well established that microbes signal amongst themselves, with the best example being quorum sensing, often involving compounds such as acyl-homoserine lactone. Other organisms, such as plant and animals have also been shown to respond to these signals in their complex microbiome (Ng and Bassler, 2009). An interesting and

now well established example of signaling between bacteria and animals involves light production by the symbiotic *Vibrio fischeri* in symbiosis with Hawaiian bobtail squid, comprising a lipid A and the peptidoglycan monomer signaling system (Mandel et al., 2012). The chitin produced by the squid assists the bacterial colonization and serves as the chemotactic signal and a trigger for luminescence as an antipredatory defense (Radar et al., 2012).

Recent experiments have shown that arbuscular mycorrhizal fungi produce a mixture of sulphated and non-sulphated LCOs. These fungal LCOs help stimulate the colonization of roots to form arbuscular mycorrhizae in plant families such as the fabaceae, asteraceae and umbelliferaceae (Maillet et al., 2011). The fungal LCOs are perceived in *Medicago truncatula* by LysM receptor kinase, like the Nod factor used in perception of the bacterial LCOs and required in activation of the calcium/calmodulin-dependent kinase Doesn't Make Infection3 pathway MtDMI3 (Czaja et al., 2012). The response to AM colonization is controlled by microRNA miR171h, which influences *NSP2*, by a negative feedback regulation (Lauressergues et al., 2012).

Since the protein quality of soybean plays an important role in overall agricultural and in nutraceutical production, it is imperative that we study the proteomics of soybean and its symbiont *B. japonicum*, not only for better understanding of the crop, but also for the betterment of agriculture practices and production of better high value added food products for human consumption.

2.6. Analyses of soybean proteomics

2.6.1 Physiological and biological changes in the soybean proteome

2.6.1.1 Whole plant organs –

The various tissues of soybean have specific groups of associated proteins at each developmental stage. While leaves at various developmental stages showed 26 differentially expressed proteins, the first trifoliolate stage manifested the greatest increase in protein types of the outer/inner envelope of chloroplast membrane and also of the protein transport machineries. Young leaves showed abundant chaperonin-60, while HSP

70 and TP-synthase b were present in all the tissues analyzed. Age dependent correlation was observed in net photosynthesis rate, chlorophyll content and carbon assimilation. During the flowering stage, flower tissue expressed 29 proteins that were exclusively involved in protein transport and assembly of mitochondria, secondary metabolism and pollen tube growth (Ahsan and Komatsu., 2009). Soybean peroxisomal adenine nucleotide carrier (GmPNC1) is associated with the peroxisomal membrane and facilitates ATP and ADP importing activities. The proteins At PNC1 and At PNC2 are Arabidopsis orthologs of Gm PNC1. Under constant darkness, Gm PNC1 increased in cotyledons up to 5 days post germination and the levels were rapidly reduced when the seedlings were exposed to light. RNA interference studies on Arabidopsis At PNC1 and At PNC2 suggests that PNC1 assists with transport of ATP/ADP in the peroxisomal fatty acid- β oxidation pathway post germination (Arai et al., 2008). This probably helps the seedling establish vigour for future growth.

In order to establish if xylem proteins and the apoplast conduit are involved in long distance signalling in autoregulation of nodulation (AON) in the soybean-*B. japonicum* symbiosis, xylem and apoplast fluids were collected from hypocotyl, epicotyl and stem tissues. In addition, proteins from imbibing seeds were evaluated to determine possible relationships of these proteins with the xylem and apoplast proteins, especially during the seed to seedling stage transition. The proteins secreted from imbibing seeds were different from the set of xylem-related proteins. Hypocotyl, epicotyl and stem xylem proteins were generally similar. Comparison of wild type and nts1007 plants showed no difference in xylem protein profiles, suggesting that xylem proteins were not involved in AON. However, a lipid transfer protein and Kunitz trypsin inhibitor, both known to have roles in plant signalling, were identified within the xylem proteins (Djordjevic et al., 2007).

Proteomic studies on chasmogamous (CH) CH cv. Toyosuzu and cleistogamous (CL) CL cv. Karafuto-1 flowerbuds using 2D gel revealed differential protein levels of β -galactosidase and protein disulfide isomerase. Cleistogamy occurs in plants under diverse stress conditions, such as drought and cold, and can also vary with temperature and light (Khan et al., 2009). Soybean cv Maverick was used to study proteomics during

seed filling stages, at 2, 3, 4, 5 and 6 weeks after flowering, using 2D and MALDI-TOF-MS. Storage proteins, proteins involved in metabolism and metabolite transport and defense related proteins were the most abundant, along with cysteine and methionine biosynthesis proteins, lipoxygenases and 14-3-3-like proteins (Hajduch et al., 2005; <http://www.oilseedproteomics.missouri.edu/soybean.php>).

Based on these findings, it is clear that the plant partitions its proteomics based on ontogeny and this specificity probably plays a crucial role in organ maturation and transition from one stage to another in the plants life cycle. Understanding this is of fundamental importance in agriculture, global food production, biofuel production and issues such as plant responses to climate change.

2.6.1.2 Seeds –

Both 2D gel and peptide mass fingerprinting techniques (MALDI-TOF-MS) were used to study the proteins of mature and dry soybean (cv. Jefferson) seeds. Sucrose binding proteins, alcohol dehydrogenase and seed maturation proteins were some of the key proteins identified (Mooney and Thelen, 2004). A comparison of four methods for protein isolation and purification from soybean seed was one of the first reports on soybean proteomics; thiourea/urea and TCA protocols were found to be the best. Proteins extracted with these two methods and further characterized by MALDI-TOF-MS and LC-MS helped identify proteins such as β -conglycinin, glycinin, Kunitz trypsin inhibitor, alcohol dehydrogenase, Gm Bd 28K allergen and sugar binding proteins in seeds (Natarajan et al., 2005). The two major soybean storage proteins are α -conglycinin and glycinin. While the α -conglycinin subunits separated well in the pH range 3.0-10.0, glycinin polypeptides could be separated in pH ranges 4.0-7.0 and 6.0 and 11.0. Apart from these major storage proteins, this combined proteomic approach (2D-PAGE and immobilized pH gradient strips) also identified 44 storage proteins in wild soybean (*G. soja*) and 34 additional storage proteins in its cultivated counterpart (*G. max*) (Natarajan et al., 2006). A comparative proteome analysis of soybean seed and seedling tissue suggested that there were dramatic changes in the protein profiles during seed germination and during seedling growth. The seed storage proteins β -conglycinin and glycinin were seen to degrade rapidly and their degradation products were either

accumulated or degraded further as the seeds germinated. This degradation of the storage proteins indicates that the proteolysis process provides amino acids and energy for the growing seedlings, and gives access to new detail regarding these processes (Kim et al., 2011).

Synthesis of soybean glycinin and conglycinin, was suppressed by RNA interference. The storage protein knockdown (SP2) seeds were very similar to the wild type during development and at maturity. Proteomic analysis of the SP2 soybean genotypes and next-generation transcript sequencing (RNA-Seq) suggested that the seeds could rebalance their transcriptome and metabolome in the face of at least some alterations. GFP quantification for glycinin allele mimics further revealed that glycinin was not involved in proteome rebalance and that seeds are capable of compensating through increases in other storage proteins, to maintain normal protein content, even if the major storage proteins were not available (Schmidt et al., 2011).

Transgenic soybean seeds have higher amounts of malondialdehyde, ascorbate peroxidase, glutathione reductase, and catalase (29.8, 30.6, 71.4, and 35.3 %, respectively) than non-transgenic seeds. Precursors of glycinin, allergen Gly m Bd 28k, actin and sucrose binding proteins were the other proteins identified (Brandao et al., 2010; Barbosa et al., 2012). High protein accessions of soybean (with 45 % or more protein in seeds) were compared with soybean cultivar Williams 82. 2-DE-MALDI-TOF-MS followed by Delta2D image analysis showed huge differences in 11S storage globulins amongst the accessions. In addition, the trait for high protein from PI407788A was moved to experimental line LG99-469 and was stable upon transformation (Krishnan, 2002; Krishnan and Nelson, 2011).

2.6.1.3 Roots, root hairs and nodules –

Since the root apical meristem (RAM) is responsible for the growth of the plant root system and root architecture plays an important role in determining the performance of crop plants, a proteome reference map of the soybean root apex and the differentiated root zone was established. The root apex samples were comprised of 1 mm of the root apex, encasing the RAM, the quiescent center and the root cap. The predominant proteins

in the root belonged to those of stress response, glycolysis, redox homeostasis and protein processing machinery. The root apex contained key proteins, such as those involved in redox homeostasis and flavonoid biosynthesis, but was underrepresented in glycolysis, stress response and TCA cycle related proteins (Mathesius et al., 2011). Analysis of the proteome of isolated soybean root hair cells using 2-D gel and shotgun proteomics approaches identified proteins involved in basic cell metabolism, those whose functions are specific to root hair cell activities, including water and nutrient uptake, vesicle trafficking, and hormone and secondary metabolism (Brechenmacher et al., 2009; Toorchi et al., 2009). Proteomic studies of soybean roots without and after *B. japonicum* inoculation explains the importance of initial plant-bacteria symbiotic interaction. A 2-D, MALDI-TOF, MS based approach shows that enzymes such as chitinase and phosphoenolpyruvate carboxylase are differentially expressed in root hairs. As well as peroxidase and phenylalanine-ammonia lyase, found to be expressed during rhizobial inoculation, other novel proteins such as phospholipase D and phosphoglucomutase were found to be expressed (Wan et al., 2005). Nodule cytosol proteins from soybean cv. Williams 82 were found to be 28% related to carbon metabolism, 12% related to nitrogen metabolism, 12 % related to reactive oxygen metabolism and 11 % related to vesicular trafficking proteins. The vesicular trafficking proteins could be involved in the exchange of micro- and macro-molecules during the process of nodulation, while carbon, nitrogen and reactive oxygen species are related to physiological functions during nitrogen fixation (Oerhle et al., 2008). The peribacteroid membrane (PBM) of the soybean symbiosome contains chaperonins such as HSP60, BiP (HSP70) and PDI, and serine and thiol protease, all of which are involved in protein translocation, folding, maturation and degradation of proteins related to the symbiosomes. Nodulin proteins 53b and 26B, associated with the PBM, were also present, although their function is not clear (Panter et al., 2000).

2.7 Soybean proteomics under stress conditions

Like all plants, soybean also encounters various stressors during its life cycle. Work related to flooding, drought, salt, heat, biotic stressors, metal toxicity, ozone, phosphorous deficiency and seed protein allergens are reviewed here.

2.7.1 Flooding stress –

Plasma membrane proteins from the root and hypocotyl of soybean seedlings were purified and subjected to 2-D gel electrophoresis, followed by MS and protein sequencing, and also using nanoliquid chromatography followed by nano-LC-MS/MS based proteomics. The two techniques were used to compare the proteins present, and this indicated that during flooding stress proteins typically found in the cell wall were up-regulated in the plasma membrane. Also, the anti-oxidative proteins were up-regulated to protect the cells from oxidative damage, heat shock proteins to protect protein degradation and signaling proteins to regulate ion homeostasis (Komatsu et al., 2009a). MS based proteomics applied to root tips of two-day-old seedlings flooded for 1 day showed increased levels of proteins involved in energy production. Proteins involved in cell structure maintenance and protein folding were negatively affected, as was their phosphorylation status (Nanjo et al., 2012).

Two-day-old germinated soybean seeds were subjected to water logging for 12 h and total RNA and proteins were analyzed from the root and hypocotyl. At the transcriptional level, the expression of genes for alcohol fermentation, ethylene biosynthesis, pathogen defense, and cell wall loosening were all significantly up-regulated, while scavengers and chaperons of reactive oxygen species were seen to change only at the translational level. Transcriptional and translational level changes were observed for hemoglobin, acid phosphatase, and Kunitz trypsin protease inhibitors. This adaptive strategy might be for both hypoxia and more direct damage of cells by excessive water (Komatsu et al., 2009b). Proteins from 2-day-old soybean seedlings flooded for 12 h were analyzed using 2-D gel MS, 2-D fluorescence difference gel electrophoresis, and nanoliquid chromatography. Early responses to flooding involved proteins related to glycolysis and fermentation, and inducers of heat shock proteins. Glucose degradation and sucrose accumulation increased due to activation of glycolysis and down-regulation of sucrose degrading enzymes, in addition the methylglyoxal pathway, a detoxification system linked to glycolysis, was up-regulated. 2-D gel based phosphoproteomic analysis showed that proteins involved in protein synthesis and folding were dephosphorylated under flooding conditions (Nanjo et al., 2010). Water logging

stress imposed on very early soybean seedlings (V2 stage) resulted in a gradual increase of lipid peroxidation and *in vivo* H₂O₂ production. Proteomic studies of the roots using 2-D gel, MALDI-TOF-MS or electrospray ionization tandem mass spectrometry (ESI-MS/MS) analysis, identified 14 up-regulated and 5 down-regulated proteins. Five newly discovered proteins were associated with water logging, a known anaerobic stress. The proteins included those associated with signal transduction, programmed cell death, RNA processing, redox homeostasis and energy metabolism. Increases in glycolysis and fermentation pathways associated proteins were indicative of adaptation of the plant to this alternate energy provision pathway. Other novel proteins, such as a translation initiation factor, apyrase, auxin-amidohydrolase and coproporphyrinogen oxidase, were also identified (Alam et al., 2010). Mitochondrial proteomics from 2-day-flooded 4-day-old soybean seedlings identified increases in the levels of proteins and metabolites associated with TCA cycle and the γ -amino butyrate shunt. Increases in NADH and NAD and a decrease in ATP during the stress suggest that the electron transport chain is disrupted, although NADH production increases through TCA cycle activity (Komatsu et al., 2011).

Soybean seeds germinated for 48 h were subjected to water logging stress for 6-48 h. In addition to general stress responses due to increases in reactive oxygen species scavengers, several glycolytic enzymes were up-regulated, suggesting changes in energy generation (Hashiguchi et al., 2009).

2.7.2 Water stress – Drought –

Soybean root activities are affected during water stress. The root-tip area can be partitioned into zones 1 (apical 4 mm zone) and 2 (4-8 mm zone), based on maximum elongation during well watered conditions. Soluble proteins from these regions, studied under both well-watered and water deficit stress conditions, revealed region-specific regulation of the phenylpropanoid pathway. Zone 1 of roots manifested increases in isoflavanoid biosynthesis related enzymes and proteins that contribute to growth and maintenance of the roots under water stress conditions. However, zone 2 of water stressed roots manifested up-regulation of caffeoyl-CoA *O*-methyltransferase (a protein involved in lignin biosynthesis), protective proteins related to oxidative damage, ferritin

proteins that sequester iron, and 20S proteasome α -subunit A. Increases in lignin accumulation and ferritin proteins preventing availability of free iron in this zone were suggested to be the factors affecting root growth during water stress (Yamaguchi et al., 2010). An investigation of the soybean plasma membrane proteome, under osmotic stress, was conducted using 2-day-old seedlings subjected to 10 % PEG for 2 days; both gel- and nano-LC MS/MS-based proteomics methods were utilized to analyze the samples. Out of the 86 proteins identified by nano-LC MS/MS approach, 11 were up-regulated and 75 proteins down-regulated under PEG mediated stress. Three homologues of plasma membrane transporter proteins H1-ATPase and calnexin were prominent (Nouri and Komatsu, 2010). Similarly, 3-day-old soybean seedlings were subjected to 10 % PEG treatment or water withdrawal and samples collected from roots, hypocotyl and leaves, 4-days after treatment, for proteome analysis. The root was the most responsive and affected organ for both drought stress induction methods. The leaves showed increases in metabolism-related proteins, while the energy production and protein synthesis machineries were negatively affected. HSP70, actin isoform B and ascorbate peroxidase were up-regulated in all the tissues analyzed. Importantly, methionine synthase, a drought response protein, decreased, suggesting negative effects of drought stress on these seedlings (Mohammadi et al., 2012).

2.7.3 High temperature stress –

Tissue specific proteomics under high temperature stress revealed 54, 35 and 61 differentially expressed proteins in the leaves, stems and roots, respectively. Heat shock proteins and those involved in antioxidant defense were up-regulated while proteins for photosynthesis, amino acid and protein synthesis and secondary metabolism were down-regulated. HSP70 and other low molecular weight HSPs were seen in all the tissues analyzed. ChsHSP and CPN-60 were tissue specific and the sHSPs were found only in tissues under heat stress, and were not induced by other stresses such as cold or hydrogen peroxide exposure (Ahsan et al., 2010).

2.7.4 Salt stress –

Salt stress is also an important abiotic stressor that affects crop growth and productivity. Of the 20 % of agricultural land available globally, 50 % is estimated by the United Nations Environment Program (The UNEP) to be salinized to the point of causing salt-stress to crops produced on them (Yan, 2008). As the plant grows under salt stresses conditions, depending on the severity of the stress, the plants can experience reduced photosynthesis, protein and energy production, and changes in lipid metabolism (Parida and Das, 2005; Sobhanian et al., 2011). As soil salinity increase, the effects on seed germination and germinating seedlings are profound. Responses to salinity and drought stress are similar; they affect the osmotic activity of the root system, thereby affecting the movement of water and nutrients into the plants. In Canadian soils, salinity varies between spring and fall and the most saline conditions are seen at the soil surface just after spring thaw. In the Canadian prairies, the dominant salts of saline seeps include calcium (Ca), magnesium (Mg) and sodium (Na) cations, and sulphate (SO_4^-) anions (Agri-Facts - <http://www1.agric.gov.ab.ca>). Soybean is very sensitive to Cl^- , but not greatly affected by Na^+ , because of its ability to restrict movement of Na^+ to leaves (Dabuxilatu and Ikeda, 2005).

This first report regarding soybean seedling proteomic responses to salt stress evaluated length and fresh weight of the hypocotyl and roots of soybean exposed to a series of NaCl concentrations. At 200 mM NaCl, the length and fresh weight of hypocotyl and roots were greatly reduced, with a simultaneous increase in proline content, suggesting activation of mechanisms for coping with salt stress. In addition, hypocotyl and root samples from 100 mM NaCl treated seedlings up-regulated seven key proteins, such as late embryogenesis-abundant protein, b-conglycinin, elicitor peptide three precursor, and basic/helix-loop-helix protein. The same treatment caused down-regulation of protease inhibitor, lectin, and stem 31-kDa glycoprotein precursor. This combination of up- and down-regulated proteins indicates a metabolic shift and could represent a strategy used by soybean seedlings to enhance tolerance of, or adapt to, salt stress (Aghaei et al., 2009).

Sobhanian et al. (2010; 2011) found that treatment of soybean seedlings with 80 mM NaCl arrests the growth and development of both hypocotyl and roots. This study assessed effects on leaf, hypocotyl and root proteomics of salt treated soybean seedlings and found that reduction of glyceraldehyde-3-phosphate dehydrogenase was indicative of reduction in ATP production, and down-regulation of calreticulin was associated with disruption in the calcium signalling pathway, both of which are associated with decreased plant growth. The levels of other proteins, such as kinesin motor protein, trypsin inhibitor, alcohol dehydrogenase and annexin, were also found to change, suggesting that these proteins might play different roles in soybean salt tolerance and adaptation (Shobanian et al., 2010; 2011).

Soybean cultivars Lee68 and N2899 are salt-tolerant and salt-sensitive respectively. The percentage germination was not affected when exposed to 100 mM NaCl, however, the mean germination time for Lee68 (0.3 days) and N2899 (1.0 day) was delayed, compared with control plants. Hormonal responses to salt stress differed between these cultivars. Both cultivars, increased abscisic acid levels and decreased gibberellic acid (GA 1, 3) and isopentyladenosine concentrations; auxin (IAA) increased in Lee68, but remained unchanged in N2899. 2-D gel electrophoresis, followed by MALDI-TOF-MS analysis, of the proteins from germinated seeds suggested increases in ferritin and the 20S proteasome subunit β -6 in both the cultivars. Glyceraldehyde 3-phosphate dehydrogenase, glutathione *S*-transferase (GST) 9, GST 10, and seed maturation protein PM36 were down-regulated in Lee68, but these proteins were naturally present in low concentrations in N2899 and were seen to up-regulate following exposure to salt stress (Xu et al., 2011).

2.7.5 Biotic stress –

The soybean-*Phytophthora sojae* plant-oomycete interaction is of agriculture and economic importance, as this oomycete causes soybean root and stem rot, translating to an annual global loss of \$1-2 billion US. Twenty-six proteins were significantly affected in a resistant soybean cultivar (Yudou25) and 20 in a sensitive one (NG6255), as determined by 2-D gel analysis, followed by MALDI-TOF-MS. The distribution pattern of the affected proteins were – 26 % energy regulation, 15 % protein destination and

storage, 11 % defense against disease, 11 % metabolism, 9 % protein synthesis, 4 % secondary metabolism, and 24 % unknown/hypothetical proteins (Zhang et al., 2011).

Soybean mosaic virus (SBMV) causes one of the most serious viral infections of soybean; leaves of infected plants were studied at a series of time points using 2-D gel electrophoresis, followed by MALDI-TOF-MS and tandem TOF/TOF-MS. Proteins expressed in the inoculated leaves were identified and were seen to be involved in protein degradation, defense signalling, coping with changes in the levels of reactive oxygen species, cell wall reinforcement, and energy and metabolism regulation. Quantitative real time PCR was used to focus on gene expression related to some of these proteins. Photosynthesis and metabolism related genes were down-regulated at all the time points, while most of the energy related genes (respiration in this case) were up-regulated for at least five of the six time points studied (Yang et. al., 2011). At the time of this writing, this report is the only one addressing the proteomic approach to molecular understanding of soybean-SBMV interaction.

2.7.6 Other miscellaneous stress related reports –

Aluminium toxicity is often observed in acidic soils and Baxi 10 (BX10) is an Al-resistant cultivar. One-week-old soybean seedlings treated with 50 mM AlCl₃ for 24, 48 and 72 h were studied for characterization of root proteins in response to Al; and 2-D gel electrophoresis followed by MS revealed 39 proteins expressed differentially following Al treatment. Of these 21 were up-regulated (such as heat shock proteins, glutathione S-transferase, chalcone related synthetase, GTP-binding protein, ABC transporters and ATP binding proteins). Five proteins were also down-regulated and 15 newly induced proteins were present following Al treatment (Zhena et al., 2007).

The process of nitrogen fixation demands large amounts of phosphorus (Vance, 2001). When soybean plants are starved of phosphorus, 44 phosphate starvation proteins are expressed in soybean nodules (Chen et al., 2011). Label free proteomics, coupled with multiple reaction monitoring (MRM) with synthetic isotope labelled peptides, was used to study 10 allergens from 20 non-genetically modified commercial varieties of soybean. The concentration of these allergens varied between 0.5-5.7 $\mu\text{g mg}^{-1}$ of soybean

protein. At the time of this writing, this is the only proteomic report on soybean allergens (Houston et al., 2011).

The responses of soybean plants exposed to 116 ppb O₃ involved significant changes to carbon metabolism, photosynthesis, amino acid, flavanoid and isoprenoid biosynthesis, signaling, homeostasis, anti-oxidant and redox pathways (Galant et al., 2012), as indicated by shifts in expression of the relevant proteins.

More information regarding soybean functional genomics and proteomics is available at the publicly accessible Soybean Knowledgebase (SoyKB) <http://soykb.org/> (Joshi et al., 2012).

2.8 *Bradyrhizobium japonicum* and its proteomics/exoproteomics

Culturing bacteria *in vitro* can cause changes in the bacterial physiology and genetics. In order to discriminate between types of these differences, *B. japonicum* cultivated in HM media and those isolated from root nodules were studied for their protein profile using 2-D PAGE and MALDI-TOF. The cultured cells showed greater levels of proteins related to fatty acid, nucleic acid and cell surface synthesis. While carbon metabolism proteins related to global protein synthesis, maturation and degradation and membrane transporters seemed to be similar in both cultured and nodule isolated bacteria, nitrogen metabolism was more pronounced in the bacteroids. Despite the quantitative differences in some proteins in the cultured and nodule isolated bacteria, it was observed that the various proteins in common between them performed similar functions (Sarma and Emerich, 2005). A high resolution 2-D gel electrophoresis analysis of these bacteroids revealed a number of proteins, of which about 180 spots could be identified using the *B. japonicum* database (<http://www.kazusa.or.jp/index.html>). The bacteroids showed a lack of defined fatty acid and nuclei acid metabolic pathways, but were rich in proteins related to protein synthesis, scaffolding and degradation. Other proteins with high expression levels were associated with cellular detoxification, stress regulation and signalling, all of which clearly establishes that differentiation into bacteroids results in a clear shift on metabolism and expression of metabolic pathways required by the bacteroids for their specialized activities (Sarma and Emerich, 2005).

Since competitiveness plays an important role in this symbiotic relationship, 2-D gel electrophoresis, image and data analysis, and in-gel digestion proteomic studies, were conducted on *B. japonicum* 4534, a strain with high competitiveness, and *B. japonicum* 4222, with low competitiveness, for nodulation. When treated with daidzein, both the strains showed up-regulation of proteins: 24 in *B. japonicum* 4534 and 10 in *B. japonicum* 4222. Upon treatment with daidzein and other extracellular materials such as extracellular enzymes and polysaccharides involved in nodulation of the strains tested, the numbers increased to 78 (43 up-regulated and 35 down-regulated) and 47 (25 up-regulated and 22 down-regulated) in these two strains. Proteins not related to nodulation were also present, and the higher number of proteins expressed by *B. japonicum* 4534 may be the reason for increased competitiveness during symbiosis (Jun et al., 2011). Comparative studies on whole cell extracts of genistein induced and non-induced cultures of a strain used in commercial inoculants in Brazil, *B. japonicum* CPAC 15 (=SEMIA 5079), and of two genetically related strains grown *in vitro* were conducted using 2-D gel electrophoresis followed by mass spectrometry. Some of the noteworthy proteins belonged to the cytoplasmic flagellar component FliG, periplasmic ABC transporters, proteins related to the biosynthesis of exopolysaccharides (ExoN), proteins that maintain redox state and the regulon $\text{PhyR}^{\sigma^{\text{EcfG}}}$, which is known to increase the competitiveness of *B. japonicum* and also help the bacteria under stress conditions, and several other hypothetical proteins (da Silva Batista and Hungaria, 2012).

B. japonicum utilizes the bacterial Type III secretion system (TTSS). In order for TTSS to be effective it requires a flavonoid inducer. The *tts* gene cluster of *B. japonicum* is regulated by the isoflavone genistein. In its presence NodD1 and NodW activate the *ttsI*, which is a two-component response regulator, necessary for expression of other genes in the *tts* cluster. In addition, the operons governing the TtsI regulon have a conserved motif in the *tts* box promoter region, which underscores the importance of regulation of TTSS in *B. japonicum*. Flagellin is a bulk protein synthesized by *B. japonicum* that plays an important role in TTSS. Mutant *B. japonicum* cells created by deleting the flagellin genes *bll6865* and *bll6866* were studied for their exoprotein profiles, in comparison with the non-mutated strains. Upon induction using genistein, it was observed that amongst the identifiable proteins, Blr1752 similar to NopP of *Rhizobium* sp.

strain NGR234, Blr1656 (GunA2) having endoglucanase activity and three other proteins having similarity to proteins of the flagellar apparatus were detected. However, none of these proteins were detected in the mutant exoproteome, suggesting that these proteins are the products of a highly conserved *tts* box motif containing genes that encode these secreted proteins (Suss et al., 2006 and references therein).

A study using 2-D gel electrophoresis combined with MALDI-TOF MS for the identification of *B. japonicum* strains 110, BJDΔ283 and BJD567 exoproteomes revealed a high frequency of substrate-binding proteins of the ABC transporter family. Addition of genistein to the cultures altered the exoproteome; three flagellar proteins and a nodulation outer protein, Pgl, were identified. Further shotgun mass spectrometry of the genistein induced exoproteome revealed the presence of nodulation outer proteins, NopB, NopH, NopT and type III-secreted protein GunA2. Addition of daidzein or coumestrol, instead of genistein, to the cell culture showed a reduction in the type III-secreted protein GunA2 (Hempel et al., 2009). *Bradyrhizobium japonicum* cell lines derived from strain SEMIA 566 are adapted to stressful environmental conditions in Brazil. They also vary in their capacity for symbiotic nitrogen fixation. A representational difference analysis study was conducted on the strains S 370 and S 516, derived from SEMIA 566. Strain S 370 produces the nodulation outer protein P gene, which is strongly associated with the TTSS, and is also the major determinant of effective nodulation (Barcellos et al., 2009).

B. japonicum strain CPAC 15 (5SEMIA 5079) is a strain used in commercial inoculants; it belongs to the same serogroup as strain USDA 123 and is used in Brazil on soybean. Both of these strains are known to be highly competitive and saprophytic. Apart from *B. japonicum* strain USDA 110, which has been sequenced (Kaneko et al., 2002a; 2002b), CPAC 15 is the only stain that has been partially sequenced in any significant measure (Godoy et al., 2008). CPAC 15 and two related strains, S 370 and S 516, were studied using whole-cell 2-D protein gel electrophoresis and spot profiles of selected proteins using MS. Cytoplasmic and periplasmic proteins found to occur in diverse metabolic pathways related to the saprophytic properties of CPAC 15; 26 hypothetical proteins were identified (Batista et al., 2010).

Bradyrhizobium japonicum strain USDA 110 from soybean plants cultivated in growth chambers were harvested at 21 days of symbiosis and subjected to transcriptomics studies and proteomics using gel LC-MS/MS. Through this integrated approach 27.8 % of the theoretical proteome and 43 % of the predicted genes and proteins were detected. Analysis of the biological and functional pathways highlighted proteins involved in carbon and nitrogen metabolism: several enzymes of the TCA cycle, gluconeogenesis and pentose phosphate pathway. Experiments with bacteroids obtained from soybean plants grown under field conditions showed identical results (Delmotte et al., 2010, and references therein).

2.9 Other dimensions to soybean-rhizobacteria interactions

Apart from *B. japonicum*, which produces LCOs, other rhizobacteria, such as *Bacillus thuringiensis* NEB17 reside in the rhizosphere of higher plants (Gray and Smith, 2005), forming a phyto-microbiome, much like the human microbiome now realized to be so important in human health (Kinross et al., 2008). *Bacillus thuringiensis* NEB17 is symbiotic with *B. japonicum*, produce bacteriocins. *Bacillus* species were first reported to produce bacteriocins in 1976. The low-molecular-weight bacteriocins of gram-positive bacteria have bactericidal activity, mainly against certain other gram-positive bacteria (Tagg et al., 1976). Bacteriocins are ribosomally produced peptides which affect the growth of related bacterial species. The most studied bacteriocin is colicin, produced by members of the Enterobacteriaceae (Pugsley, 1984). Due to their commercial importance as natural preservatives and as therapeutic agents against pathogenic bacteria, these antimicrobial peptides have been a major area of scientific research (Tagg et al., 1976; Jack et al., 1995).

Bacteriocins are grouped into four distinct classes based on the peptide characteristics such as post translational modifications, side chains, heat stability, N-terminal sequence homology and molecular weight (Klaenhammer, 1993). *Bacillus thuringiensis* NEB17 was isolated from soybean root nodules as putative endophytic bacteria in 1998 in our laboratory. When co-inoculated with *B. japonicum* under nitrogen free conditions this bacterium promoted soybean growth, nodulation and grain yield (Bai et al., 2002b, 2003). Subsequently, the causative agent of plant growth promotion, a

bacteriocin, was isolated from *B. thuringiensis* NEB17, and is now referred to as thuricin 17 (Gray et al., 2006b). Initially, its partial sequence was determined (Gray et al., 2006a), and its full sequence has been more recently reported (Lee et al., 2009). Thuricin 17 is a low molecular weight peptide of 3162 Da, stable across a pH range of 1.0–9.25, highly heat resistant and is inactivated by treatment with proteolytic enzymes (Fig. 2.2a,b,c).

```

.....10 .....20 .....30 .....40
      |       |       |       |
DWTCWSCLVC AACSVELLNL VTAATGASTA S

```

Fig. 2.2a: Sequence of Thuricin 17

SOPMA :

Alpha helix	(Hh) :	20 is	64.52%
3 ₁₀ helix	(Gg) :	0 is	0.00%
Pi helix	(Ii) :	0 is	0.00%
Beta bridge	(Bb) :	0 is	0.00%
Extended strand	(Ee) :	2 is	6.45%
Beta turn	(Tt) :	2 is	6.45%
Bend region	(Ss) :	0 is	0.00%
Random coil	(Cc) :	7 is	22.58%
Ambiguous states (?)	:	0 is	0.00%
Other states	:	0 is	0.00%

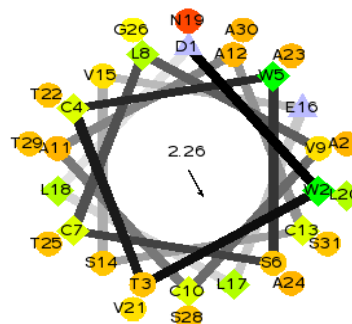


Fig. 2.2b: Alpha helix structure of Thuricin 17 (based on Expasy results - www.expasy.org).

Table 2.2: Physicochemical properties of Thuricin 17 (based on Expasy results - www.expasy.org)

Formula	C ₁₃₄ H ₂₁₂ N ₃₄ O ₄₅ S ₄	Polar residues	14
Absent amino acids	FHIKMPQRY	Aliphatic residues	7
Common amino acids	A	Tiny residues	11
Mass (Da)	3166.14	Boman Index	7.33
Net charge	-2	Hydropathy index	0.96
Isoelectric point	3.55	Aliphatic index	97.74
Basic residues	0	Instability index	35.15 (stable)
Acidic residues	2	Half life	Mammalian: 1.1 h Yeast: 3 min E. coli: > 10 h
Hydrophobic residues	15	Extinction Coefficient	11000 M ⁻¹ cm ⁻¹
Absorbance at 280 nm - 375			

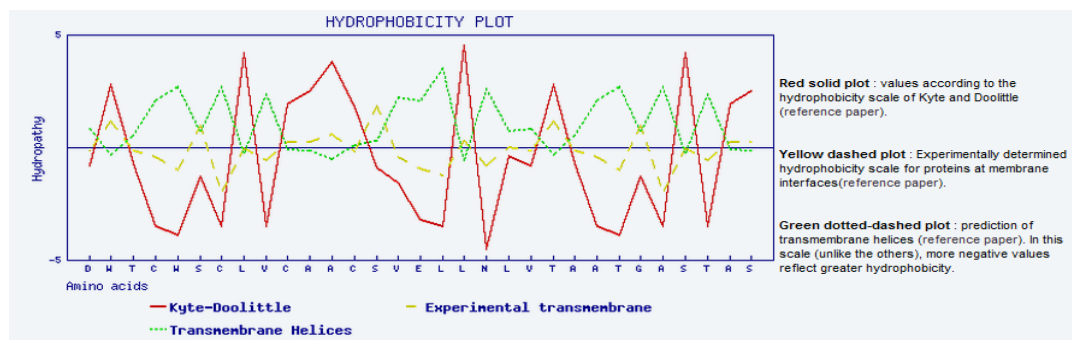


Fig. 2.2c: Hydrophobicity plot for Thuricin 17 suggesting its hydrophilic nature.

Based on its N-terminal sequence homology of thuricin 17 and that of the also newly isolated bacthuricin F4, a new class of bacteriocins, class IId was proposed (Gray et al., 2006b). The bacteriocins produced by *B. thuringiensis* strain NEB17 (Th17) and *B. thuringiensis* subsp. kurstaki BUPM4 (bacthuricin F4 - 3160.05 Da) have been reported to show functional similarities and anti-microbial activities (Jung et al., 2008a). In addition, thuricin 17, applied as leaf spray and root drench, has positive effects on soybean and corn growth, which was first reported from our laboratory (Lee et al., 2009); this constituted the first report of plant growth stimulation by a bacteriocin.

A plant growing in a field is not an individual entity; it is a well-structured and functional community that has evolved over a half billion years. It would seem that we are now beginning to elucidate the phytomicrobiome; considerable advancements in understanding are still needed, but the potential for increased crop production through novel, low-input technologies is also considerable. At a time when we are looking to crop plants to provide more food for an expanding population and also for fuel to replace fossil hydrocarbons, there is an urgency to move this work ahead. It would seem that we are beginning to elucidate the plant rhizobacterial community and its activities; considerable advancements in understanding are still needed, but the potential for increased crop production through novel technologies seems considerable.

CHAPTER 3

Lipo-chitooligosaccharide and Thuricin 17 regulate phytohormones differentially in *Arabidopsis thaliana* rosettes

Sowmyalakshmi Subramanian, Alfred Souleimanov, Donald. L. Smith^{*}

Department of Plant Sciences, Macdonald Campus, McGill University, 21111 Lakeshore Road, Sainte Anne de Bellevue, Quebec H9X3V9, Canada

*Corresponding author e-mail: donald.smith@mcgill.ca

CONNECTING STATEMENT TO CHAPTER 3

The content of Chapter 3 is derived from a recently submitted article (reformatted here to fit the thesis), co-authored by Sowmyalakshmi Subramanian, Alfred Souleimanov and Donald L. Smith titled “**Lipo-chitooligosaccharide and thuricin 17 regulate phytohormones differentially in *Arabidopsis thaliana* rosettes**”. The results of this study, in part, authored by myself and Donald L. Smith, were presented as a talk during the Green Crop Network Annual meeting, May 3-6, 2011, Montreal, Canada.

Existing literature shows that plant growth promoting rhizobacteria produce hormones that help boost plant growth, and the signal compounds produced by bacteria also trigger many innate plant responses during the plant’s life cycle (eg., Whipps, 2001; Vessey, 2003, Ryu et al., 2003; Choudhary and Johri, 2009). In this study, we investigated the response of *Arabidopsis thaliana* plants to the bacterial signal compounds LCO and Th17. From previous and separate studies reported from our laboratory, LCO and Th17 were found to promote plant growth (Prithiviraj et al., 2000; Souleimanov et al., 2002; Lee et al., 2009). In addition, microarray studies on soybean, in which LCO was applied as a root drench (Lindsay, 2007) and leaf spray on low temperature stressed soybean plants (Wang et al., 2012) suggests enhanced gene expression related to auxins, cytokinins, GA, salicylic acid and jasmonic acid. Hence we hypothesized that lipo-chitooligosaccharide and thuricin 17 might cause similar phytohormone profile changes in three-week-old *Arabidopsis thaliana* rosettes, within 24 h of treatment. Consequently, a GUS assay screening using transgenics from ABRC was conducted to establish this fact. Since gene expression does not always translate into actual presence of the compounds in the biological system, GUS assay was followed by quantification of the possible phytohormones using UPLC-ESI/MS method.

3.1 Abstract:

Lipo-chitooligosaccharide (from *Bradyrhizobium japonicum*) and Thuricin 17 (from *Bacillus thuringiensis*) are compounds secreted by bacteria living in the rhizosphere of soybean. These bacterial compounds have been reported to promote the growth of various legumes and non-legumes. However, the mechanisms by which they promote plant growth have remained unknown. As a first step to this understanding, we attempted to quantify phytohormone changes in *Arabidopsis thaliana* in response to treatment with these compounds; these phytohormones form an important component of the plant intracellular regulatory mechanisms. It was found that at 24 h after exposure to both these signal compounds, *A. thaliana* rosettes varied in their responses to the two signals. While LCO caused a decrease in total IAA, cytokinins, gibberellins and JA, and an increase in ABA and SA, Th17 treated rosettes on the other hand showed decreased levels of cytokinins, gibberellins, JA and ABA; and an increase in IAA and SA. However, both the signal compounds caused decreased JA levels. This, in part, suggests that these two compounds may not be inducing the classic induced systemic resistance (ISR) like responses in *A. thaliana*, and suggests a new concept of phytohormone network regulation in plant growth promotion.

3.2 Introduction:

The last two decades has seen a gamut of biobased products in the market place, generally in the forms of bioinoculants and biofertilizers, based on observations of increased plant growth and yield. This was followed by some research focused on physiological, morphological and molecular understanding of these bacteria and their responses to biotic and abiotic stresses. A somewhat greater amount of research has been focused on evaluating plant growth promotion effects, rather than delving deeply into the mechanisms that underlie this growth promotion and how it might be triggered. Plant-microbe interactions constitute a very dynamic system; the cross talk between elements of the system, and the responses generated, adds to the overall complexity of the system. With recent advances in instrumentation and techniques, it has become possible to understand some of these interactions in a more detailed manner, adding another potential dimension to understanding the mechanisms involved in these interactions.

The most widely used bacterial bio-fertilizers are the nitrogen fixing rhizobia, largely in the genera *Allorhizobium*, *Azorhizobium*, *Bradyrhizobium*, *Mesorhizobium*, *Rhizobium*, and *Sinorhizobium*. These rhizobacteria fix nitrogen inside legume root nodules; the legume plants provide photosynthetically fixed carbon to the rhizobia (Vessey, 2003; Choudhary and Johri, 2009). Recent interest in the relationship has been in response to the use of fossil fuels in nitrogen fertilizers production. Besides rhizobia, there are other rhizobacteria that live and fix nitrogen outside of formal symbioses, referred to as free-living or associative nitrogen-fixing bacteria, such as *Azospirillum*, *Acetobacter*, *Herbaspirillum*, *Azoarcus* and *Azotobacter* (Steenhoudt and Vanderleyden, 2000). These rhizobacteria help provide nitrogen to non-legume plants (Boddey et al., 2003), have potential use on marginal lands as a low input nutrient provider to crop plants, and in the production of biofuel feedstock crops, where energy balance is important.

Plant growth promoting rhizobacteria (PGPR) employ a variety of mechanisms to promote plant growth and development, such as enhanced nutrient availability (including nitrogen fixation) (Layzell and Atkins, 1997); suppression of diseases through a range of biocontrol mechanisms: induction of disease resistance in plants, production of phytohormones, and production of signal compounds, including volatile forms (Whipps, 2001). As bio-fertilizers (made with living microorganisms), they promote plant growth and make available essential nutrients from the environment that are otherwise unavailable to plants due to their conjugated or precipitated forms (Vessey, 2003). For example, phosphate solubilizing bacteria (PSB) mobilize phosphorus, making it substantially more available to plants (Kim et al., 1998; Rodriguez and Fraga, 1999). Some rhizobacteria produce siderophores that enhance iron availability to plants (Bloemberg and Lugtenberg, 2001), while others play an important role in the availability of other micronutrients to plants (Fasim et al., 2002). Rhizobacteria can increase plant tolerance to drought, salinity and metal toxicity (Dimkpa et al., 2009).

One of the central themes to plant growth and development is the cognition of intracellular regulatory mechanisms, of which phytohormones form an important component. For more than a century, phytohormone research has been revealing aspects of pathways, transport, perception and signal transduction, and adding to the complexity

in a plant's life cycle. In the last decade, the understanding of phytohormones has increased enormously. Not only do the hormones engage in extensive crosstalk, but also regulate plant growth by integration of these signals. Phytohormones are defined as low molecular weight compounds that have the ability to regulate basic physiological functions such as leaf and root growth and differentiation, stomatal activity, senescence, flower initiation and development, seed development and germination, all requiring very low levels of these compounds, in varying amounts at different stages. Apart for the five basic recognized hormone groups (auxins, cytokinins, gibberellins, abscisic acid and ethylene) brassinosteroids, salicylic acid, jasmonic acid, strigolactones and fusicoccins, have added to the complexity of the phytohormone network and plant-internal signalling dynamics. Phytohormones maintain and regulate more subtle processes such as the circadian rhythms, by adjusting the internal clock to environmental cues. While auxins regulate the amplitude and precision of the circadian clock, brassinosteroids and ABA regulate circadian periodicity and cytokinins delay the circadian phase using ARABIDOPSIS RESPONSE REGULATOR 4 and the photoreceptor phytochrome B (Hanano et al., 2006; Seung et al., 2012).

A large variety of developmental processes and adaptive responses to external environmental cues are also controlled by ABA. ABA in *A. thaliana* is encoded by at least 10 % of the protein-coding genes, making it by far the largest percentage of gene regulation among phytohormones. Transcription factors such as bZIP, AREB/ABFs are controlled in an ABA-responsive-element (ABRE) dependent manner during seed germination and in the vegetative stages during osmotic stress. While other transcription factors, such as AP2/ERF, MYB, NAC and HD-ZF, participate in ABA regulation based on circadian rhythms and light perception (Fujita et al., 2011). During abiotic stress responses, thiamine compounds (vitamin B1) and thiamine di-phosphate dependent enzymes are synthesized to overcome some of the oxidative stress effects. This biosynthetic mechanism is controlled by ABA (Rapala-Kozik et al., 2012). Cross talk between ABA and GA in endodermal cells of the roots restricts root growth under salinity stress. Quiescence is controlled by ABA and represses root growth (Duan et al., 2013).

Transcripts of hormonal metabolism, catabolism, perception and signalling are all regulated by the circadian clock, also referred to as gating. Changes in carbon and water

utilization also are governed by gating (Michael et al., 2008; Robertson et al., 2009). The BT2 gene of *A. thaliana* encodes a 41kD protein that activates telomerase expression in mature leaves, is controlled by gating and makes photosynthates available depending on the diurnal cycle (Mandadi et al., 2009).

During root growth, organ expansion and other aspects of plant development, auxins and gibberellic acids interact to regulate common targets. Genes encoding GA 20-oxidases, involved in GA biosynthesis, and GA 2-oxidases, for GA inactivation, are regulated in part by auxin/IAA and ARF proteins (Frigerio et al., 2006).

Plants lack the classical hormone receptors in the nucleus and thus have evolved proteins to perceive them in the nucleus (Lumba et al., 2010). Recent studies using Arabidopsis ABA mutant AtKu suggests that plant hormones modulate DNA repair proteins during genotoxic stress. This is a new insight into DNA repair and chromatin remodelling in plants that are under biotic (systemic acquired resistance inducing) stress where SA and JA participate in phytohormone balance. Other hormones such as GA and cytokinins also mediate such processes during seed germination and shoot meristem activities (Dona et al., 2013).

Hence it would be appropriate to say that plants mediate multiple mechanisms using hormones to speed up adaptive processes necessary during constant environmental challenges. An Arabidopsis hormone database (<http://ahd.cbi.pku.edu.cn>) has been created, and contains all the data from genetic and molecular work conducted so far (Peng et al., 2009).

Currently, two compounds secreted by rhizosphere bacteria of soybean, lipochitooligosaccharide (LCO) from *Bradyrhizobium japonicum* 532C, Nod Bj V (C18:1; MeFuc) (Prithiviraj et al., 2000); and thuricin 17 (Th17) from *Bacillus thuringiensis* NEB17 (Gray et al., 2006a, b), are under evaluation regarding mechanism(s) of action in plant growth promotion. LCOs are oligosaccharides of β -1,4-linked N-acetyl-D-glucosamine coded for by a series of *Nod* genes; they are rhizobia specific, and regulated by plant-rhizobia specific signals such as isoflavonoids (Spaink et al., 1995; Kamst et al., 1998; Vazquez et al., 1993; Carlson et al., 1994; Schultze and Kondorosi 1996, 1998). Nod Bj V (C18:1; MeFuc), the LCO most abundantly by *B. japonicum*, contains a methyl-fucose group at the reducing end that is encoded by the host-specific *nodZ* gene

(López-Lara et al., 1995), which is an essential component for successful soybean-rhizobia interactions. Nodulation and subsequent nitrogen fixation are affected by environmental factors, supported by the observations under sub-optimal root zone temperatures (for soybean 15-17 °C), pH stress and the presence of nitrogen, where isoflavanoid signal levels are reduced nodulation is delayed and/or reduced. Under high temperature (39 °C) there is an increase of non-specific isoflavanoid production and reduced *nod* gene activation, thereby affecting nodulation (Bai et al., 2002a). Apart from the nodulation process, LCO also positively affects plant growth and development in legumes and non-legumes. The potential role of LCOs in plant growth regulation was first reported by Denarie and Cullimore (1993). *Nod* genes A and B from *R. meliloti*, altered tobacco phenotype by producing bifurcated leaves and stems, suggesting a role for *nod* genes in plant morphogenesis (Schmidt et al., 1993); enhanced development of somatic embryos of Norway spruce following application of purified Nod factor from *Rhizobium* sp. NGR234 suggesting auxin and cytokinin like activities in promoting embryo development (Dyachok et al., 2000; 2002). Defense responses such as chitinase and PR proteins (Schultz and Kondorosi, 1996; 1998), peroxidase (Cook et al., 1995) and enzymes of phenylpropanoid pathway, L-phenylalanine ammonia-lyase (PAL) (Inui et al., 1997) and transient accumulation of salicylic acid in soybean leaves (Lindsay, 2007) have been reported upon LCO treatments. Seed germination and seedling establishment are enhanced in soybean, common bean, maize, rice, canola, apple and grapes, accompanied by increased photosynthetic rates (Zhang and Smith, 2001); an increase in root growth when LCO was applied to the hydroponic solution was observed in corn (Souleimanov et al., 2002a; 2002b; Khan, 2003), and foliar application to greenhouse grown corn resulted in increases in photosynthetic rate, leaf area and dry matter (Khan, 2003). Similarly, foliar application on tomato during early and late flowering stages, increased flowering, fruiting and fruit yield (Chen et al., 2007). *Pinus abies* treated with LCO increased its mycorrhizal colonization (*Gigaspora margarita*) (Dyachok et al., 2002; Oláh et al., 2005). Recent research in our laboratory, on soybean leaves treated with LCOs under sub-optimal growth conditions, revealed the up-regulation of over 600 genes, many of which are defense and stress response related, or transcription factors; microarray results show that the transcriptome of the leaves is highly responsive to LCO treatment at 48 h

post treatment (Wang et al., 2012). Products based on our LCO findings have been used to treat seeds sown into several million ha of crop land around the world in each of the last few years.

Bacillus thuringiensis NEB17, isolated from soybean root nodules as a putative endophytic bacteria in 1998 in our laboratory, when co-inoculated with *B. japonicum* under nitrogen free conditions promoted soybean growth, nodulation and grain yield (Bai et al., 2002b, 2003). The causative agent of plant growth promotion, now referred to as thuricin 17 (Gray et al., 2006b) has been shown to exhibit functional similarities and antimicrobial activities with bacthuricin F4 produced by *B. thuringiensis* subsp. *kurstaki* BUPM4 (Jung et al., 2008a). Th17, when applied as leaf spray and root drench, had positive effects on soybean and corn growth (Lee et al., 2009); this was the first report of plant growth stimulation by a bacteriocin.

The objective of this study was to investigate the role of bacterial signal compounds, LCO and Th17, on quantifiable phytohormones to suggest pathway(s) that might be involved in producing the observed plant growth responses and thus enhance our understanding of the effects of these two compounds on the plant model system *A. thaliana*.

3.3 Materials and methods

3.3.1 Plant material

Seeds of *Arabidopsis thaliana* Col-0 were purchased from Lehle Seeds (Round Rock, TX, USA). Transgenic seeds relating to different hormonal sensitivity were procured from the Arabidopsis Biological Resource Center (ABRC), Ohio State University, Columbus, Ohio, for the GUS assay [DR5 (Auxin), CS 25261 (Cytokinin), CS 57945 (Gibberellic acid), CS 6357 (PR1)].

The seeds of *A. thaliana* Col-0, were planted in peat pellets and grown in a growth chamber at $22\text{ }^{\circ}\text{C} \pm 2\text{ }^{\circ}\text{C}$ with a photoperiod of 16/8 h day/night cycle and under $100\text{--}120\text{ }\mu\text{mol quanta m}^{-2}\text{ s}^{-1}$, at 65 – 70 % relative humidity. Three-week-old plants were used for UPLC-ESI/MS hormone analyses. Treatment administration and sampling time for all

the experiments was always conducted between 8-8:30 am in order to be consistent with application within the circadian rhythm pattern of the plants. The experiments were structured following a completely randomized design.

3.3.2 Bacterial signal compounds

3.3.2.1 Extraction and purification of Lipo-chitooligosaccharides (LCOs)

The extraction and purification of LCOs followed the method of Souleimanov et al. (2002b). In brief, *B. japonicum* cultures were extracted with 40 % HPLC-grade 1-butanol. The culture supernatant was carefully removed and condensed in a low-pressure rotary evaporator system (Yamato RE500, Yamato, USA) at 50 °C, at a speed of 125 rpm, until dryness. The dried extract was resuspended in 4 mL of 18 % acetonitrile. The resuspended extract was loaded on to a C-18 column (PRESEP™ Fisher Scientific, Montreal, Canada) and eluted three times using 10 mL of 30 % acetonitrile and finally using, 60 % acetonitrile. The Nod factors were further isolated and purified by HPLC (Waters 501 pumps, a Waters 401 detector set at 214 nm and a WISP712 autosampler using a C18 reverse phase column (0.46 X 25 cm, 5 µm) - Vydac, CA, USA; catalogue # 218TP54). Chromatography was conducted for 45 min using a linear gradient of acetonitrile from 18 to 60 %, as described by Souleimanov et al. (2002b). Identification of Nod factors was conducted by comparing the retention time of isolated Nod factors with standard Nod factors, also from strain 532C and identified by mass spectrometry.

3.3.2.2 Extraction of Thuricin 17 (Th17)

Bacillus thuringiensis NEB17 was cultured in King's medium (King et al., 1954) as previously described (Gray et al., 2006a). In brief, the culture in King's B medium was incubated in an orbital shaker for 32 h after which this inoculum was subcultured into 4.0 L flasks containing 2.0 L medium and allowed to grow for 48 h. Th17 isolation and purification was carried out using High Performance Liquid Chromatography (HPLC) using the procedures of Gray et al. (2006b). The collected material was denoted partially purified Th17 and stored at 4 °C and diluted to required concentrations for all experiments.

In all experiments LCO concentrations of 10^{-6} M and Th17 concentrations of 10^{-9} M were used, the concentrations found to be the best in plant growth response studies (Prithiviraj et al., 2000; Souleimanov et al., 2002a; Lee et al., 2009).

3.3.3 Effect of LCO and Th17 on the induction of phytohormone gene expression using GUS histo-chemical staining

The effect of LCO and Th17 extracts on induction of phytohormones such as auxin, cytokinins, gibberellic acid and PR1, a marker gene for systemic acquired resistance, was tested with transgenic lines of *A. thaliana* carrying PR1::GUS reporter (Uknes et al., 1992, Shapiro and Zhang, 2001), DR5::GUS (Auxin) (Ulmasov et al., 1997), GA::GUS (Dora et al., 2000), CYT::GUS (To et al., 2004) plants were grown on solidified half strength Murashige and Skoog Basal (MS) Medium (Murashige and Skoog, 1962) supplemented with 1% sucrose. Seven-day-old seedlings were transferred to a twelve-well tissue culture plate containing 1 mL of liquid half strength MS medium for two days. After two days the MS medium was removed and replaced with 1 mL solution of 10^{-6} M LCO and 10^{-9} M Th17, placed on a gyratory shaker set at 90 rpm and a 16/8 h day/night cycle. Three plants per treatment were removed at 24, 48, 72 h after treatment and histochemical staining for localizing GUS activity was carried out following a published method (Jefferson et al., 1987). Briefly, the seedlings were fixed in cold 80 % acetone for 20 min and washed twice in 100 mM phosphate buffer containing Triton X-100, 0.5 mM potassium ferrocyanide and 0.5 mM potassium ferricyanide. The seedlings were then transferred to a GUS staining buffer (100 mM phosphate buffer, 2 mM 5-bromo-4-chloro-3-indolyl- β -D-glucuronide cyclohexylammonium salt (X-Gluc) and incubated overnight at 37 °C. The plants were then washed in several changes of buffer and chlorophyll was removed by incubating in a 50, 75 and 100 % ethanol series to visualize the staining. Three biological replicates of the experiment were conducted with each biological replicate comprised of three technical replicates for concordance.

3.3.4 Hormone analysis of *A. thaliana* rosettes

For the UPLC-ESI/MS analysis, *A. thaliana* plants were grown in trays. Two-and-half-week-old plants were treated with LCO (10^{-6} M) and Th17 (10^{-9} M). Twenty

four hours after the treatment, *A. thaliana* rosettes were sampled (each of the treatment replicates was a pool of 30 plants) and lyophilized by freeze drying to obtain about 1 g of lyophilized material for quantification (Savant Modulyo, Model VLP285 Valu pump, Savant Instruments Inc, NY, USA). Two biological replicates were analyzed by this method.

3.3.4.1 Extraction and purification

In brief, 100 μL aliquot containing all the internal standards, each at a concentration of $0.2 \text{ pg } \mu\text{L}^{-1}$, was added to approximately 50 mg of homogenized plant tissue; 3 mL of isopropanol:water:glacial acetic acid (80:19:1, v/v) was then added, and the samples were agitated in the dark for 24 h at 4°C . Samples were centrifuged and the supernatant isolated and dried on a Büchi Syncore Polyvap (Büchi, Switzerland). Samples were reconstituted in 100 μL acidified methanol, adjusted to 1 mL with acidified water, and then partitioned against 2 mL hexane. After 30 min, the aqueous layer was isolated and dried as above. Dry samples were reconstituted in 800 μL acidified methanol and adjusted to 1 mL with acidified water. The reconstituted samples were passed through equilibrated Sep-Pak C18 cartridges (Waters, Mississauga, ON, Canada), the eluate being dried on a LABCONCO centrivap concentrator (Labconco Corporation, Kansas City, MO, USA). An internal standard (blank) was prepared with 100 μL of the deuterated internal standards mixture. A QC (quality control) standard was prepared by adding 100 μL of a mixture containing all the analytes of interest, each at a concentration of $0.2 \text{ pg } \mu\text{L}^{-1}$, to 100 μL of the internal standard mix. Finally, samples, blanks, and QCs were reconstituted in a solution of 40 % methanol (v/v), containing 0.5 % acetic acid and $0.1 \text{ pg } \mu\text{L}^{-1}$ of each of the standards.

The analysis was performed on a UPLC/ESI-MS/MS utilizing a Waters ACQUITY UPLC system, equipped with a binary solvent delivery manager and a sample manager coupled to a Waters Micromass Quattro Premier XE quadrupole tandem mass spectrometer via a Z-spray interface. Samples were injected onto an ACQUITY UPLC® HSS C18 SB column (2.1 x 100 mm, $1.8 \mu\text{m}$) with an in-line filter and separated by a gradient elution of water containing 0.02% formic acid against an increasing percentage of a mixture of acetonitrile and methanol (volume ratio: 50:50).

For the SA/JA analysis the plant material was ground to a fine powder in liquid nitrogen with a mortar and pestle. Frozen plant material (approx. 500 mg) was extracted with a mixture of methanol:water:glacial acetic acid (3 mL, 90:9:1, v/v/v), to which the internal standards were added (100 L solution acetonitrile:water, 50:50 v/v, with 0.1% formic acid, containing 1 ng L⁻¹ of 3,4,5,6-*d*₄-2-hydroxybenzoic acid and 0.5 ng L⁻¹ of 2,2-*d*₂-jasmonic acid). Following sonication (5 min) and incubation on an orbital shaker (4 °C, 5 min), samples were centrifuged (4.4 k rpm, 10 min) to pellet the debris. The supernatant was transferred to a clean tube and the pellets were re-suspended in the extraction solution (2 mL), and the procedure repeated. The supernatant was combined with the initial extracted volume and the pellet was re-suspended in methanol (1 mL). The extraction step was repeated a third time. After the supernatants were combined, methanol was evaporated under reduced pressure. On ice, aqueous NaOH (1 mL, 0.3 N) was added to each sample, which was further extracted with dichloromethane (3 mL). The aqueous layer was transferred to a clean tub, while the organic layer was re-extracted with aqueous NaOH (2 mL). On ice, combined aqueous layers were acidified with 5 % aqueous HCl (1 mL), then they were extracted with a mixture of ethyl acetate:cyclohexane (1 mL, 1:1, v/v). The organic phase was collected and the aqueous phase was extracted a second time with the same mixture (0.5 mL). The organic fractions were pooled and the solvent was evaporated under a constant nitrogen stream. Prior to mass spectrometric analysis, the samples were reconstituted in a mixture of methanol:water (200 L, 30:70, v/v) containing 0.1 % formic acid, to which external standards were added (100 ng of 1,2,3,4,5,6-¹³C₆-2-hydroxybenzoic acid and 50 ng of 12,12,12-*d*₃-jasmonic acid).

3.3.4.2 Hormone quantification by UPLC-ESI-MS/MS

A detailed description of the procedure for quantification of multiple hormones and metabolites, including auxins (IAA, IAA-Asp and IAAGlu), abscisic acid and metabolites (ABA, PA, DPA, 7'-OH-ABA, neoPA and ABA-GE), cytokinins (2iP, iPA, Z, ZR, dhZ, dhZR and Z-O-Glu), and gibberellins (GAs 1, 3, 4, 7) is available in Chiwocha et al. (2003, 2005) (Please refer Appendix I, Table 3.1 for the types of hormones and their catabolites and/or conjugates studied in this experiment). Samples were injected onto an ACQUITY UPLC® HSS C18 SB column (2.1x100 mm, 1.8 µm)

with an in-line filter and separated by a gradient elution of water containing 0.02 % formic acid against an increasing percentage of a mixture of acetonitrile and methanol (volume ratio: 50:50).

For the SA/JA analysis the analytical UPLC column that was used was an ACQUITY UPLC® HSS C18 column (2.1 x 100 mm, 1.8 μ m). The compounds were eluted from the column with a mixture of solvents comprised of 1 % formic acid in HPLC-grade water (mobile phase A) and 1 % formic acid in HPLC-grade methanol (mobile phase B), using a gradient mode. Analytical procedures analogous to those reported in Ross et al. (2004) were employed to determine the quantities of phytohormones in the plant extracts. Briefly, the analysis utilizes the Multiple Reaction Monitoring (MRM) function of the MassLynx v4.1 (Waters Inc) control software. The resulting chromatographic traces are quantified off-line by the QuanLynx v4.1 software (Waters Inc) wherein each trace is integrated and the resulting ratio of signals (non-deuterated/internal standard) is compared with a previously constructed calibration curve to yield the amount of analyte present (ng per sample). Calibration curves were generated from the MRM signals obtained from standard solutions based on the ratio of the chromatographic peak area for each analyte to that of the corresponding internal standard, as described by Ross et al. (2004). The QC samples, internal standard blanks and solvent blanks were also prepared and analyzed along with each batch of tissue samples.

MassLynx™ and QuanLynx™ (Micromass, Manchester, UK) were used for data acquisition and data analysis. Results were expressed in ng g⁻¹ dry weight of the sample.

3.4 Results:

The identification, development and characterization of several mutants and transgenics have all been instrumental in understanding the role of these plant hormones in teasing apart the mechanisms involved in each of their signaling pathways, and in the general signal transduction pathways used by plants to respond to environmental conditions. Taking advantage of the repository of information available for *A. thaliana*, GUS transgenes available in ABRC stock were screened to study the phytohormone expression patterns of *A. thaliana* following treatment with LCO and Th17 signals, in this case, under optimal growth conditions.

3.4.1 GUS assay:

GUS assay screening revealed that auxin, cytokinins and GA were increased during the 24, 48 and 72 h exposures to LCO and Th17. Interestingly, the marker for salicylic acid - PR1 was not affected, suggesting that our compounds might be involving a PR1 independent pathway of salicylic acid expression (Fig 3.1). Many earlier reports have shown that higher gene expression need not necessarily matched with translation at the systems level. Hence, a quantification of available phytohormones, their conjugates and their catabolites were studied using the UPLC ESI-MS/MS method.

3.4.2 Phytohormone detection using UPLC ESI-MS/MS:

Auxin - Amongst the auxins, three auxin conjugates - IAA-Glu, IAA-Ala and IAA-Asp were identified. IAA-Glu was present in all samples and a 138 % increase was observed in Th17 treated samples. IAA-Ala and IAA-Asp were not identified in LCO treated samples while a 100 % increase in IAA-Ala was seen in Th17 treated samples. However, based on the percentage increase or decrease with reference to control plants, overall IAA levels decreased by approximately 49.68 % in LCO treated rosettes, while it increased by 85.39 % in Th17 treated rosettes (Fig 3.2; Fig 3.7; Table 3.1a).

Cytokinin - The cytokinins *cis*-ZOG, *cis*-and *Trans*-ZR and iPA were observed in all the samples but the overall levels were lower in LCO treated rosettes by 36.24 %, and in Th17 treated rosettes by 11.66 % (Fig 3.3; Fig 3.7; Table 3.1a).

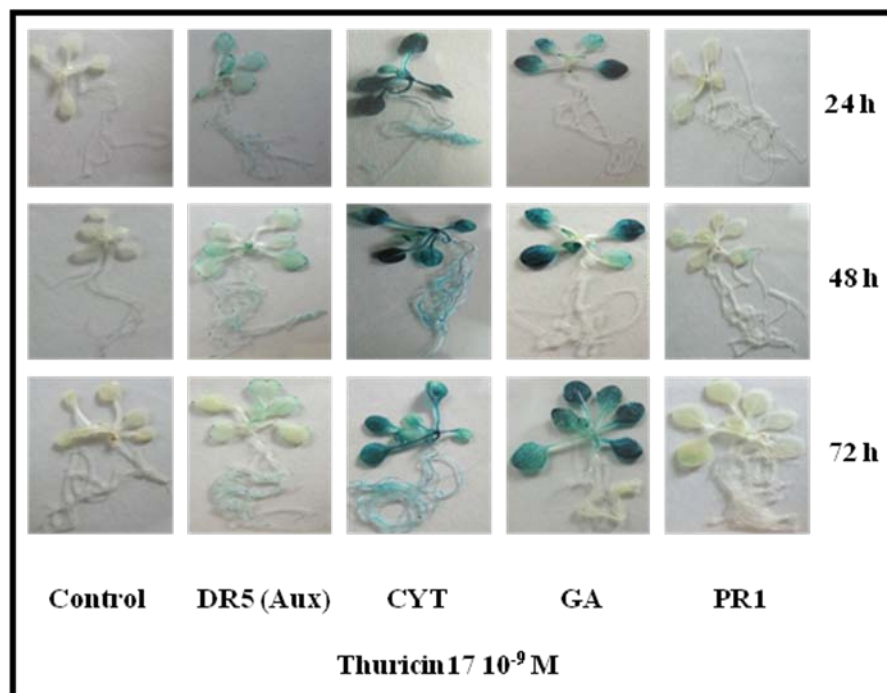
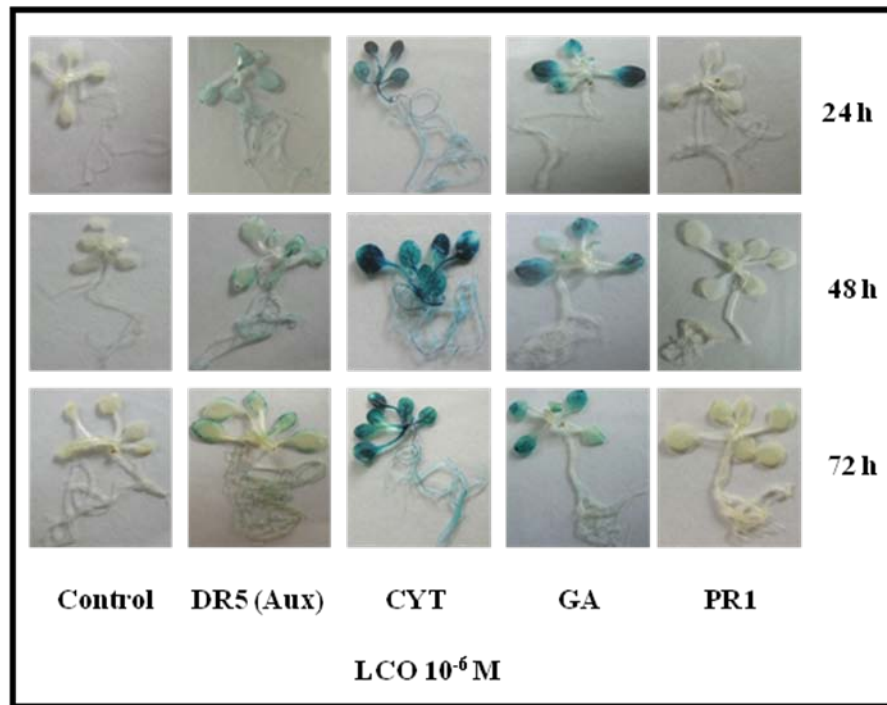
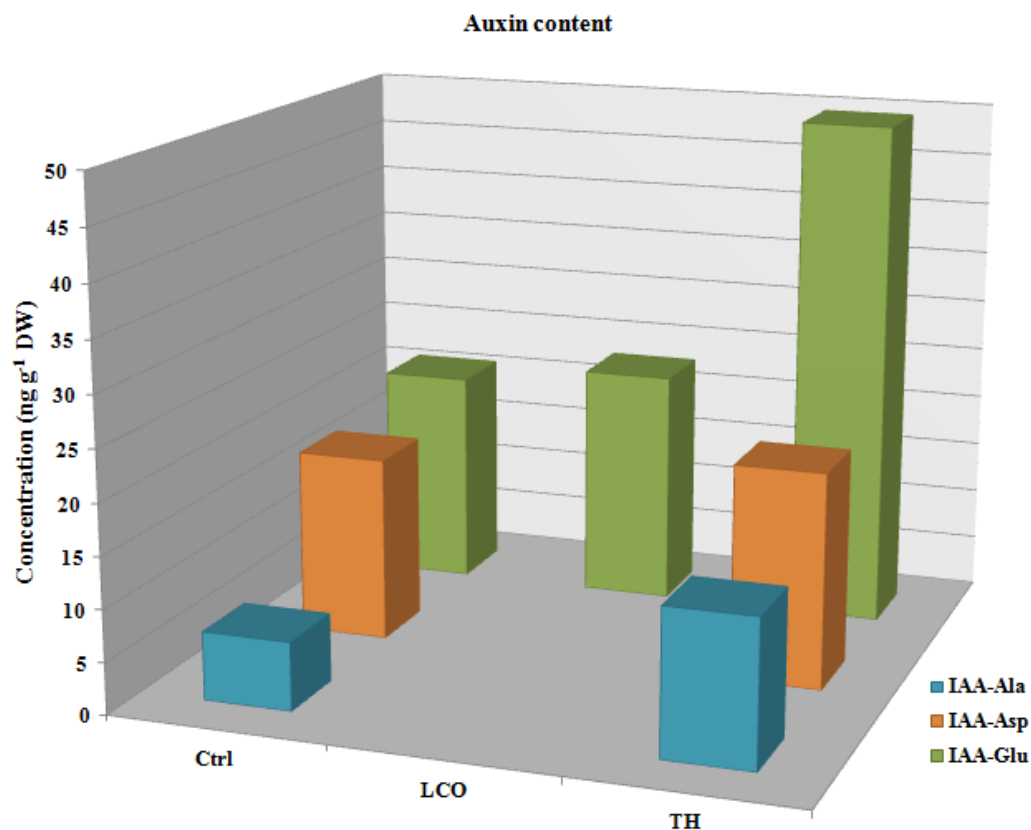
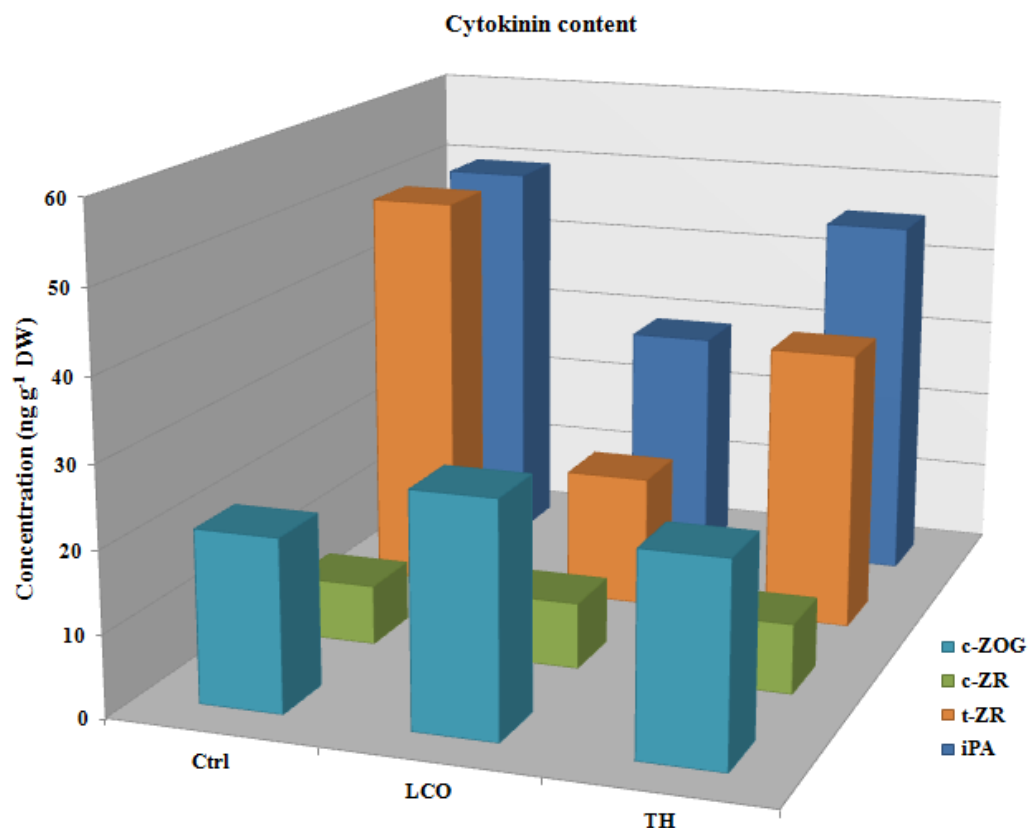


Fig. 3.1: GUS assay screening to understand the effect of LCO and Th17 on *Arabidopsis thaliana* phytohormones pattern of expression.



Treatments	IAA-Ala	IAA-Asp	IAA-Glu	Total
Ctrl	7	18	21	46
LCO	-	-	23 (9.5 % ↑)	23
TH	14 (100 % ↑)	21 (14.2 % ↑)	50 (138 % ↑)	85

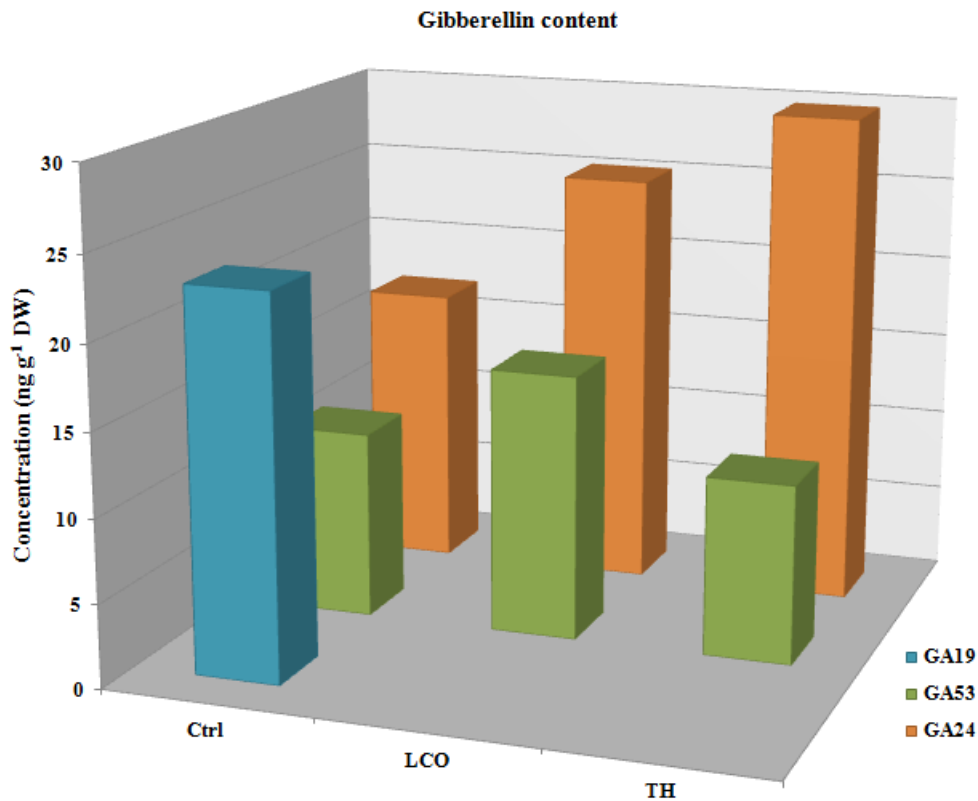
Fig. 3.2: Auxin and auxin-conjugates identified in *Arabidopsis thaliana* rosettes 24 h after LCO and Th17 treatment (LCO = 10^{-6} M; Th17 = 10^{-9} M). Numbers in brackets represent % increase or decrease with reference to the control; the arrows indicate direction of increase or decrease.



Treatments	c-ZOG	t-ZR	c-ZR	iPA	Total
Ctrl	21	50	7	49	128
LCO	28 (33.3 % ↑)	16 (68 % ↓)	8	29	82
TH	24 (14.28 % ↑)	35 (30 % ↓)	9	46	113

Fig. 3.3: Cytokinins identified in *Arabidopsis thaliana* rosettes 24 h after LCO and Th17 treatment (LCO = 10^{-6} M; Th17 = 10^{-9} M). Numbers in brackets represent % increase or decrease with reference to the control; the arrows indicate direction of increase or decrease.

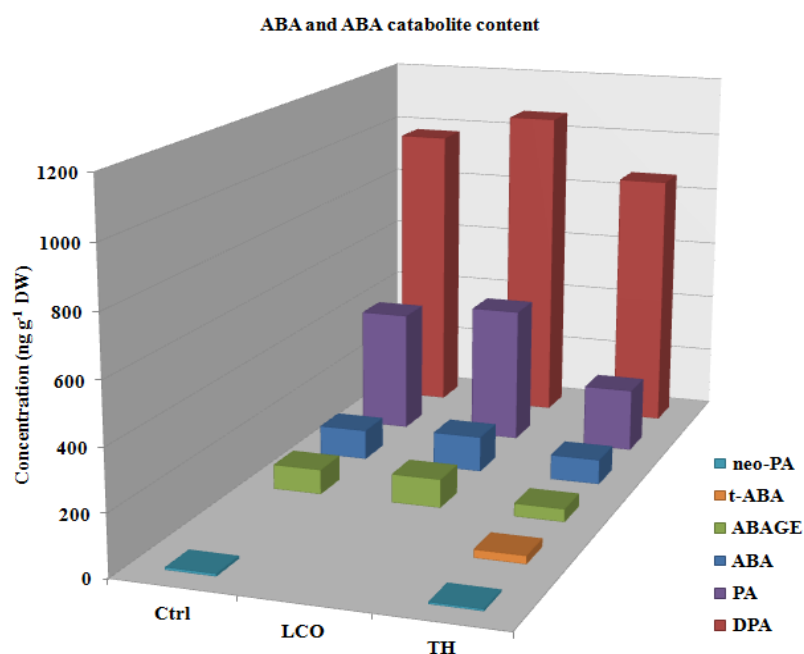
Gibberellins - Gibberellins were mainly represented by GA24 in all the samples. GA24 is produced by the non-13-hydroxylation pathway of GA metabolism. There was a 47 % increase of GA24 in LCO treated rosettes and a 76.4 % increase in Th17 treated rosettes. GA19 was identified only in control rosettes. The overall GA content in LCO and Th17 rosettes were lower by 19.41 % and 20.73 % respectively (Fig 3.4; Fig 3.7; Table 3.1a).



Treatments	GA19	GA24	GA53	Total
Ctrl	23	17	11	51
LCO	-	25 (47 %↑)	16	41
TH	-	30 (76.4 % ↑)	11	41

Fig. 3.4: Gibberellic acids identified in *Arabidopsis thaliana* rosettes 24 h after LCO and Th17 treatment (LCO = 10^{-6} M; Th17 = 10^{-9} M). Numbers in brackets represent % increase or decrease with reference to the control; the arrows indicate direction of increase or decrease.

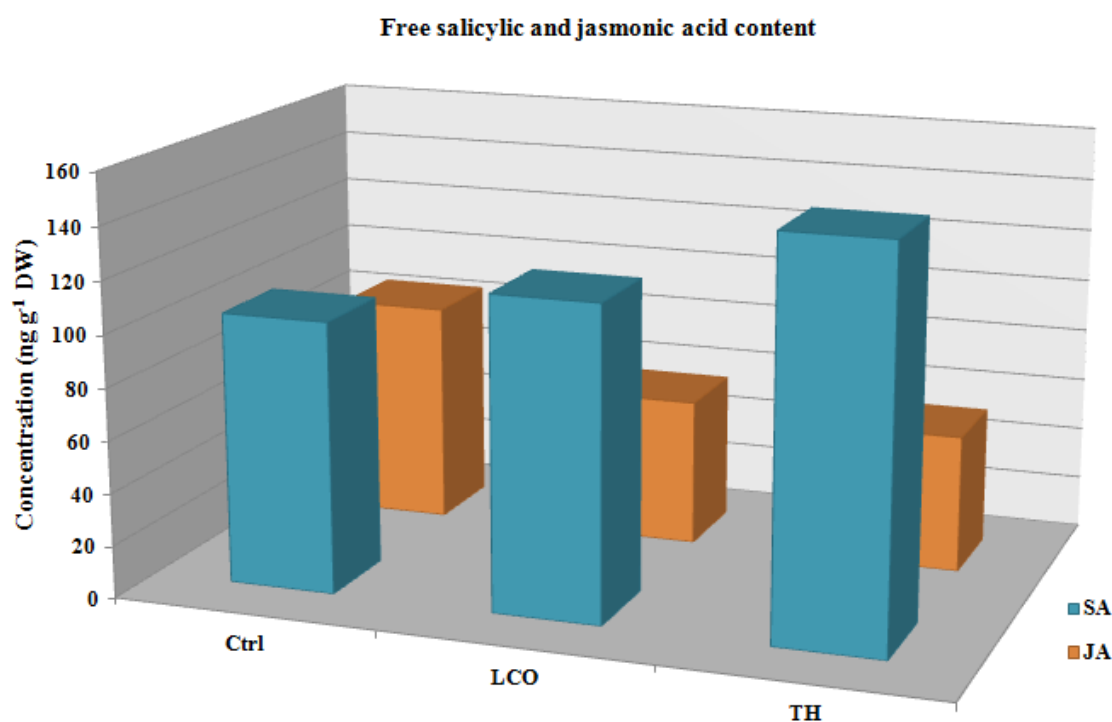
Absciscic acid - The lyophilized samples contained ABA and related metabolites in substantial amounts for all samples. The amount of ABA and the catabolites were consistently higher in the LCO treated rosette. Neo-PA and t-ABA were not identified in LCO treated rosettes. Neo-PA was observed in control treatments and t-ABA was exclusive to Th17 treated rosettes. There was a 10.18 % increase in overall ABA in LCO treated rosettes, while a decrease of 21.67 % ABA was observed in Th17 treated rosettes (Fig 3.5; Fig 3.7; Table 3.1a).



Treatments	ABA	DPA	ABAGE	PA	neo-PA	t-ABA	Total
Ctrl	99	977	82	407	8	-	1573
LCO	118 (19.9 % ↑)	1066 (9.10 % ↑)	94 (12.76 % ↑)	455 (10.54 % ↑)	-	-	1733
TH	82 (17.17 % ↓)	865 (11.46 % ↓)	42 (48.78 % ↓)	211 (48.15 % ↓)	6	26	1232

Fig. 3.5: Absciscic acid and its catabolites identified in *Arabidopsis thaliana* rosettes 24 h after LCO and Th17 treatment (LCO = 10^{-6} M; Th17 = 10^{-9} M). Numbers in brackets represent % increase or decrease with reference to the control; the arrows indicate direction of increase or decrease.

Free salicylic and jasmonic acid - Although GUS assay with PR1 did not show any PR1 dependent salicylic acid activity following LCO and Th17 treatments, the amount of free SA increased by 15 % in LCO treated rosettes and by 44.21 % in Th17 treated rosettes. The amount of free JA however decreased in both LCO and Th17 treated rosettes, by 33.66 % and 38.05 %, respectively (Fig 3.6; Fig 3.7; Table 3.1b).



Treatments	SA (ng/g DW)	JA (ng/g DW)
Ctrl	104	85
LCO	119 (15 % ↑)	56 (33.66 % ↓)
TH	149 (44.21 % ↑)	53 (38.05 % ↓)

Fig. 3.6: Free salicylic acid and jasmonic acid identified in *Arabidopsis thaliana* rosettes 24 h after LCO and Th17 treatment (LCO = 10^{-6} M; Th17 = 10^{-9} M). Numbers in brackets represent % increase or decrease with reference to control; the arrows indicate direction of increase or decrease.

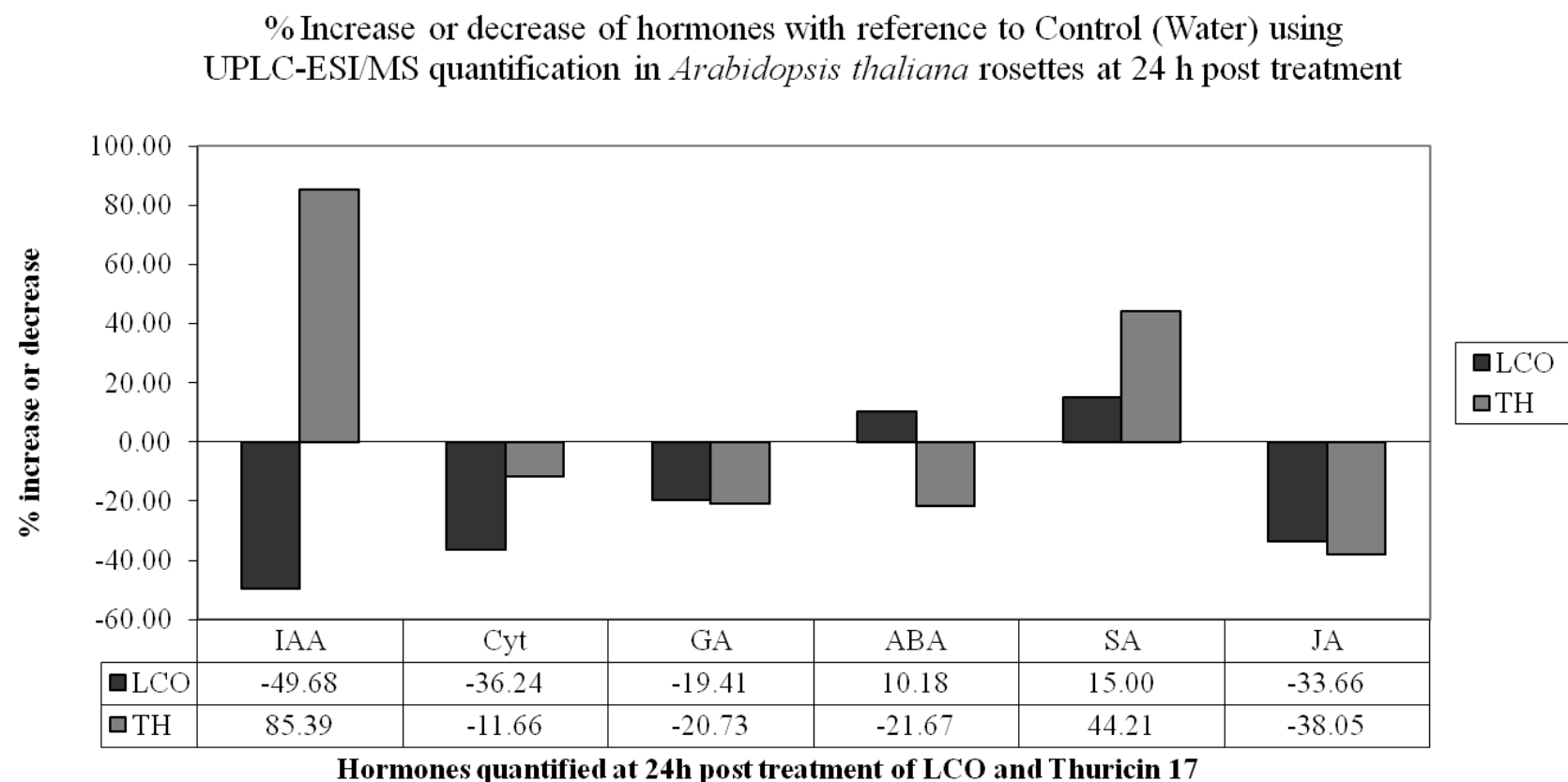


Fig. 3.7: Hormones quantified using UPLC-ESI/MS. The graph represents the percentage increase or decrease of hormones identified in LCO and Th17 treated *Arabidopsis thaliana* rosettes 24h after treatment. (LCO = 10^{-6} M; Th17 = 10^{-9} M).

Table 3.1a: UPLC-ESI/MS quantitation of ABA and ABA metabolites, Cytokinins, Auxins and Gibberellins detected in *Arabidopsis thaliana* rosettes 24h after treatment. (Control - Water, LCOA - 10^{-6} M, and THA - 10^{-9} M). (STDEV = Standard deviation; %RSD = Relative standard deviation expressed as percentage).

Sample Information		ABA and ABA metabolites (ng/g DW)						Cytokinins (ng/g DW)				Auxins (ng/g DW)			Gibberellins (ng/g DW)		
Sample	weight (mg)	ABA	DPA	ABAGE	PA	neo-PA	<i>t</i> -ABA	c-ZOG	t-ZR	c-ZR	iPA	IAA-Ala	IAA-Asp	IAA-Glu	GA19	GA24	GA53
Ctrl 1	51.6	84	943	65	266	6		21	62	7	51	7	18	21	23	18	10
Ctrl 2	51.0	114	1011	98	548	9		22	38	7	48			21		16	13
	average	99	977	82	407	8		21	50	7	49	7	18	21	23	17	11
	STDEV	21	48	23	200	2		1	18	0	2			0		1	2
	%RSD	21%	5%	29%	49%	30%		3%	35%	1%	4%			1%		6%	20%
LCOA 1	49.6	132	1268	122	586			25	21	8	36			10		29	16
LCOA 2	50.6	104	864	66	324			32	12	8	22			36		22	
	average	118	1066	94	455			28	16	8	29			23		25	16
	STDEV	20	285	40	185			5	6	0	10			19		5	
	%RSD	17%	27%	42%	41%			17%	40%	4%	36%			82%		19%	
THA 1	50.5	71	481	44	135	6	26	27	27	9	32	14	21	86		31	
THA 2	50.6	93	1249	41	286			22	42	8	59			14		29	11
	average	82	865	42	211	6	26	24	35	9	46	14	21	50		30	11
	STDEV	15	543	2	107			4	10	1	19			51		1	
	%RSD	19%	63%	5%	51%			15%	29%	8%	41%			103%		3%	

Table 3.1b: UPLC-ESI/MS quantitation of Salicylic acid and Jasmonic acid detected in *Arabidopsis thaliana* rosettes 24h after treatment. (Control - Water, LCOA - 10^{-6} M, and THA - 10^{-9} M). (STDEV = Standard deviation; %RSD = Relative standard deviation expressed as percentage).

Sample Information		SAJA (ng/g FW)	
Sample	weight (mg)	SA	JA
Ctrl 1	489.7	155	43
Ctrl 2	481.5	52	127
	average	104	85
	STDEV	72	59
	%RSD	70%	69%
LCO 1	562.5	127	16
LCO 2	530.4	111	96
	average	119	56
	STDEV	12	56
	%RSD	10%	100%
TH 1	485.7	70	21
TH 2	490.4	229	85
	average	149	53
	STDEV	112	45
	%RSD	75%	86%

3.5 Discussion:

Since previous studies have indicated increased plant growth upon exposure to LCO and Th17, the role of these compounds in triggering hormonal responses during plant growth and regulation was evaluated for the phytohormone categories auxins, cytokinins, gibberellins, abscisic acid, salicylic acid and jasmonic acid. The last century has seen several reports on plant hormones playing pivotal roles in diverse plant growth and developmental processes, including responses to abiotic and biotic stresses. In this study we show that LCO [Nod BjV(C18:1; MeFuc)] and Th17 provoke different phytohormone responses, 24 h after exposure to the treatments in three-week-old, root drenched *A. thaliana* rosettes. The role of phytohormones in plant growth and development is a crucial event tightly regulated by the circadian clock. A given hormone must be present in the right tissue at the right time to perform the right function. For this to happen, plants have devised a mechanism by which they can store the hormone as free forms or as conjugates or their inactive catabolites which, upon activation, can quickly

provide with the required dosage. A study on transcriptional effects of the hormones ABA, GA, auxin, ethylene, cytokinins, brassinosteroids and jasmonate using microarray data suggests that the hormones regulate specific protein families that, in turn, regulate the subsequent plant responses (Nemhauser et al. 2006).

Our experiment indicated that Th17 increased total auxin and SA in the rosettes, while LCO treatment did not. It is now becoming clearer that endogenous regulation of auxin is controlled by the circadian clock (Covington and Harmer, 2007; Covington et al., 2008; Hotta et al., 2007; Alabadi' and Bla'zquez, 2009). Auxins function in controlling cell division, lateral root development, gravitropism and nastic movements and in apical dominance. Although much has been studied about auxins, the mechanisms by which they modulate plant growth response are still elusive. Synthesized both by tryptophan dependent and independent pathways, auxins are transported between the cells through MULTIDRUG RESISTANCE/P-GLYCOPROTEIN transporters, PIN-FORMED efflux carriers and AUXIN 1/LIKE AUX 1 influx facilitators. Auxins also work via the 26S proteasome-dependent degradation pathway via an ubiquitin ligase complex, SCF^{TIR1}, inducing other auxin response transcription factors. *BREVIPEDICELLUS* (BP) belongs to a family of transcription factors that regulates meristem and organ initiation and patterning. BP controls the lignin biosynthetic pathway and binds to genes such as *ACID O-METHYLTRANSFERASE* and *CAFFEOYL-COA O-METHYLTRANSFERASE*, suggesting that auxin controls lignification (Sa'nchez-Rodri'guez et al., 2010). The interaction of auxin and cytokinins is also necessary to control root and shoot apical meristems, and also flower development (Su et al., 2011; Bielach et al., 2012; Sudre et al., 2013). Brassinosteroids, along with auxins, are known to control cell proliferation and differentiation during plant growth, while GA plays a role in cell wall pectin esterification and microtubule organization (Sa'nchez-Rodri'guez et al., 2010; and references therein). The auxin efflux carrier PIN1 is redirected to the vacuoles for degradation, by cytokinin receptors. This is another way of auxin-cytokinin modulation (Marhavy' et al., 2011). Light influences hormones and light influences are integrated in various pathways through signaling integrators such as PHYTOCHROMEINTERACTING FACTOR 3 (PIF3), PIF 4, PIF3-5like and LONG HYPOCOTYL 5 (HY5). Phytohormones such as gibberellins, auxins, cytokinins and abscisic acid use these integrators to regulate

photomorphogenesis of seedlings. Auxin-inducible gene IAA29 and ARABIDOPSIS THALIANA HOMEODOMAIN PROTEIN2 (ATH2) are expressed at their peak at dawn and are controlled by PIF4 and PIF5 (Lau and Deng, 2010; Kunihiro et al., 2011). Based on these earlier findings, it is probable that the increase in auxin levels following Th17 treatment suggests improved regulation of meristem initiation, organ differentiation and patterning.

IAA homeostasis is maintained by amino acid conjugates of IAA. While in excess, IAA is conjugated to amino acids such as Ala, Asp, Phe, Trp (Staswick et al., 2005). The conversion of active IAA to methyl-IAA (MeIAA) is catalyzed by indole-3-acetic acid (IAA)-methyltransferase-1 (IAMT1). IAMT1 plays an important role in leaf development, while MeIAA can also impart a range of responses, such as inducing lateral roots and inhibiting hypocotyl elongation (Li et al., 2008). In our study, most of the IAA conjugation was seen as IAA-Glu, probably suggesting another mechanism of IAA conjugation.

In both LCO and Th17 treated rosettes, levels of total cytokinins and total GA were decreased as compared to controls. In plants, isopentenyladenine and its hydroxylated derivative zeatin are the two known active cytokinins (Fre'bert et al., 2011). A MALDI-TOF/TOF MS analysis of cytokinin signalling indicated early effects of cytokinins in photosynthesis and nitrogen metabolism, light signalling and the CLAVATA pathway. Major phosphoproteomic effects were observed in the chloroplast suggesting that cytokinins might play a direct signalling role in chloroplast regulation and functioning (C'erny' et al., 2011). Of the nine histidine kinase receptors known in *A. thaliana*, many are now known to be associated with hormones. AhK3, AhK4 are found in the endoplasmic reticulum and interact with each other, and are associated with cytokinin perception and signalling (Caesar et al., 2011). Cytokinins negatively regulate salt and drought stress and the balance for this regulation is maintained through ABA metabolism and regulation (Nishiyama et al., 2011). The response of cytokinins in Arabidopsis leaves is necessary to determine the amplitude of the response a plant needs to reciprocate; this is conducted in concert with SA accumulation and defense gene activation in plant-oomycete pathogen interactions such as with *Hyaloperonospora arabidopsidis* isolate

Noco2 (Hpa Noco2) (Argueso et al., 2012). It is possible that increases in ABA in LCO treated rosettes might be involved in the decrease in cytokinin levels.

The signal compound treatments also had an influence on levels of the phytohormone ABA and ABA metabolite contents. The main ABA metabolism pathway is through 8'-hydroxylation, which results in phaseic acid (PA), a compound that is further reduced to de-oxy phaseic acid (DPA) and modified through secondary catabolism pathways, such as conjugation, resulting in the β -D glucopyranosyl ester of ABA (ABAGE), which is an endogenous conjugate of ABA. Studies in normal bean leaves suggested lower levels of ABA and ABAGE, both of which increased after 24 h of drought stress. However ABAGE was not the source of induced ABA under water stress and ABA is reported to be converted to PA or DPA (Niell et al., 2002). Traces of neoPA are also observed, which indicates occurrence of 9'-hydroxylation. NeoPA, as a 9'-hydroxylation product of ABA, is found in a number of plant tissues and also in drought stressed barley and *Brassica napus* seedlings, showing that 9'-hydroxylation is a general pathway for ABA catabolism. Also, the hydroxylated ABAs have hormonal activity, suggesting that the ABA catabolites play a role in ABA signalling, thus acting as a phytohormone (Zhou et al., 2004). The presence of ABA catabolites suggests that bioactive ABA was probably previously biosynthesized in the tissue and then rapidly metabolized following LCO or Th17 treatments. The presence of Trans-ABA, a product of isomerization of natural ABA under UV light, was observed in plants treated with Th17. We speculate that one of the ways Th17 modulates UV responses in plants might be by isomerization of natural ABA.

The patterns of SA and JA concentration in LCO and Th17 treated plants suggested an increase of SA for both the treatments, and a decrease of JA for both the treatments. Previous studies from our laboratory, on LCO treated nodulating and non-nodulating soybean cultivars, showed a transient increase of SA at 24 h after treatment (Lindsay, 2007). Our results are consistent with this pattern of SA expression, despite the fact that the PR1 marker for SA was not enhanced in the GUS assay. The soybean microarray data also suggested an up-regulation of stress, SA and nodulation related genes. The up-regulation of cinnamic acid 4-hydroxylase and not *PAL1* suggests the conversion of cinnamic acid to SA. In addition, the down-regulation of isochorismatase

hydrolase indicated that isochorismate is available for SA conversion using the isochorismate pathway as well (Lindsay, 2007). JA/SA antagonism is directed at the JA biosynthetic pathway (Leon-Reyes et al., 2010). A 2D-gel coupled with MS/MS proteomic approach to study SA/JA interaction was conducted by dipping 5-week-old *A. thaliana* rosettes in SA and JA (1 mM SA, 100 mM MeJA) and harvesting at 24 h after treatment. This experiment suggested that most of the biotic and abiotic stress related proteins are up-regulated by JA while only a few are induced by SA treatment (Proietti et al., 2013). AhK5 is an Arabidopsis histidine kinase which is required by the plant to integrate reactive oxygen species and hormones responses, so as to impart resistance to biotic stresses such as *Pseudomonas syringae* pv. *tomato* DC3000 (*Pst*DC3000) and the necrotrophic fungus *Botrytis cinerea*, by controlling SA and JA levels, as a negative regulator to salinity and for drought stress resistance responses via ABA and NO regulation (Pham and Desikan, 2012). With more information on SA/JA antagonism coming forth, it is not surprising that as SA increased in the LCO and Th17 treated plants, as there was a decrease of JA. An important consideration is that systemic resistance activated by ISR or SAR does not have any significant effects on the density and structure of the rhizobacterial community (Doornbos et al., 2011).

3.6 Conclusions:

Based on this phytohormone analysis, it is evident that LCO and Th17 trigger different patterns of phytohormone regulation at 24 h post treatment. The 24 h time point is also relevant to this study since plant growth and development control is most prevalent in plants at dawn and this dictates the day's growth progression. The differences in phytohormone levels in LCO and Th17 plants at 24 h are indicative of the early responses and the different pathways provoked by LCO and Th17 might impart for subsequent events in the plant developmental process. It is, however, necessary to study this pattern at other a broader range of time points and with more biological replicates because of the high variability in some of the hormones such as salicylic acid and jasmonic acid, to come to a clear understanding in changes to the pattern of phytohormone patterning following bacterial signal compound treatments.

CHAPTER 4

Mass spectrometry based studies on the effects of Lipo-chitooligosaccharide and Thuricin 17 on proteome regulation under unstressed and salt stressed conditions in *Arabidopsis thaliana* rosettes

Sowmyalakshmi Subramanian, Alfred Souleimanov, Donald. L. Smith^{*}

Department of Plant Sciences, Macdonald Campus, McGill University, 21111 Lakeshore Road, Sainte Anne de Bellevue, Quebec H9X3V9, Canada

*Corresponding author e-mail: donald.smith@mcgill.ca

CONNECTING STATEMENT FOR CHAPTER 4

The content of Chapter 4 is derived from an article recently submitted (reformatted here to fit the thesis), co-authored by Sowmyalakshmi Subramanian, Alfred Souleimanov and Donald L. Smith titled “Mass spectrometry based studies on the effects of Lipo-chitooligosaccharide and Thuricin 17 on proteome regulation under unstressed and salt stressed conditions in *Arabidopsis thaliana* rosettes.” The results of this study, in part, authored by myself, Alfred Souleimanov and Donald L. Smith were also presented as a talk at the Green Crop Network Annual Meeting, Montreal, Canada (May 3-6th, 2011).

Plant growth promotion to increase yield in agricultural systems is of primary importance. Existing literature indicates the use of many synthetic compounds that trigger plant growth promotion activities in plants; however, the use of natural compounds is of importance, in order to minimize the use of sometimes environmentally damaging synthetic chemicals. Lipo-chitooligosaccharide and thuricin 17 are two such compounds produced, by bacteria isolated from the soybean rhizosphere (Prithiviraj et al., 2000; Gray et al., 2006a, b); both have been reported to promote plant growth (Bai et al., 2002a; Souleimanov et al., 2002a; Lee et al., 2009). Microarray studies conducted on soybean under optimal conditions (Lindsay, 2007) and soybean under stressfully low temperature conditions (Wang et al., 2012), suggest that stress related genes are up-regulated under both these conditions. Our studies on phytohormone analysis of 24 h post treated rosettes suggests that LCO up-regulates ABA and SA, while Th17 increases levels of IAA and SA (Chapter 3).

Since proteins are key building blocks of life, dictated by an organism's genes, our approach to understanding their modulation in plant growth enhancement was conducted using LC-MS based proteomics. It was hypothesized that LCO and Th17 cause similar patterns of plant growth promotion, but through different pathways. Hence the objective of this study was to explore LC-MS based comprehensive proteome profiles under unstressed conditions on the rosettes of *Arabidopsis thaliana* 24 h after exposure to the bacterial signals LCO and Th17, in order to understand the pathways and mechanisms affected, in part to improve our understanding of the mechanisms that underlie the

observed plant growth benefits. The study was further extended to analyze the extent of salt tolerance imparted by these signals.

4.1 Abstract:

Plants, being sessile organisms, are exposed to widely varying environmental conditions throughout their life cycle, and compatible plant-microbe interactions are favourable for plant growth and development, helping the plants deal with environmental challenges. Microorganisms produce a diverse range of elicitor molecules to establish symbiotic relationships with the plants they associate with, in a given ecological niche. Lipo-chitooligosaccharide (LCO) and thuricin 17 (Th17) are two such compounds; they have been shown to positively influence plant growth of both legumes and non-legumes. *Arabidopsis thaliana* responded positively to treatment with the bacterial signal compounds LCO and Th17 in the presence of salt stress (up to 250 mM NaCl). Shotgun proteomics of unstressed and 250 mM NaCl stressed *A. thaliana* rosettes (7 days post stress) in combination with the LCO and Th17 revealed many known, putative, hypothetical and unknown proteins. Overall, carbon and energy metabolic pathways were affected under both unstressed and salt stressed conditions when treated with these signals. PEP carboxylase, Rubisco-oxygenase large subunit, pyruvate kinase, and proteins of photosystem I and II were some of the noteworthy proteins enhanced by the signals, along with other stress related proteins. These findings suggest that the proteome of *A. thaliana* rosettes is altered by the bacterial signals tested, and more so under salt stress, thereby imparting a positive effect on plant growth under high salt stress. The roles of the identified proteins are discussed here in relation to salt stress adaptation, which, when translated to field grown crops can be a crucial component and of significant importance in agriculture and global food production.

4.2 Introduction:

Microbes are a key component of all ecosystems on earth, playing major roles in the bio-geochemical cycles (Falkowski et al., 2008). Compounds secreted by the bacterial population of a rhizosphere are very species and environment dependent. Two bacterial signal compounds, LCO from *Bradyrhizobium japonicum* 532C and Th17, a bacteriocin from *Bacillus thuringiensis* NEB17, both isolated from bacteria that reside in the soybean rhizosphere, were successfully isolated and characterized, with regard to plant growth promotion, in our laboratory in 2000 and 2006 respectively (Prithiviraj et al.,

2000; Gray et al., 2006a,b). These two compounds are under evaluation for their capacity to promote plant growth and development in both legumes and non-legumes under laboratory and field conditions, and are being developed as low-input components of crop production systems for deployment under Canadian climatic conditions. While LCO technology is already in the market place for commercial application, in the form of products such as Optimize, marketed by Novozymes (now a part of BASF), Th17 is under evaluation for potential commercialization.

LCOs, also referred to as Nod factors, have been reported to positively and directly affect plant growth and development in legumes and non-legumes; as compounds they were first reported by Denarie and Cullimore (Denarie and Cullimore, 1993). Nod factors have since been reported to affect plant growth in diverse plant species. When introduced into tobacco *Nod* genes A and B from *R. meliloti* altered the phenotype by producing bifurcated leaves and stems, suggesting a role for *Nod* genes in plant morphogenesis (Schmidt et al., 1993). Purified Nod factor from *Rhizobium* sp. NGR234 enhanced development of somatic embryos of Norway spruce; auxin and cytokinin like properties were attributed to this promotional activity. The chitin core of the Nod factor is an essential component for regulation of plant development (Dyachok et al., 2000; 2002). The LCO induced *enod* genes in non-legumes code for defence related responses, such as chitinase and PR proteins (Schultz and Kondorosi, 1996; 1998), peroxidase (Cook et al., 1995, Lindsay, 2007; Wang et al., 2012) and enzymes of phenylpropanoid pathway, such as L-phenylalanine ammonia-lyase (PAL) (Inui et al., 1997). Seed germination and seedling establishment are enhanced in soybean, common bean, maize, rice, canola, apple and grapes, accompanied by increased photosynthetic rates (Zhang and Smith, 2001). Similar increases in photosynthetic rates were observed in LCO-treated, hydroponically-grown maize, as well as increased root growth (Souleimanov et al., 2002a; 2002b; Khan, 2003). Foliar application to greenhouse grown maize resulted in increases in photosynthetic rate, leaf area and dry matter (Khan, 2003). Foliar application to tomato, during early and late flowering stages, increased flowering and fruiting and also fruit yield (Chen et al., 2007). An increase in mycorrhizal colonization (*Gigaspora margarita*) was observed in *Pinus abies* treated with LCO (Dyachok et al., 2002; Oláh et al., 2007). Our first microarray study on soybean leaves sprayed with LCO also suggested the role of

stress related gene expression at 48 h, and a transient increase in SA at 24 h after LCO treatment for the sprayed leaves, using HPLC (Lindsay, 2007). More recent microarray data from our laboratory, on soybean leaves treated with LCOs under sub-optimal growth conditions, revealed the up-regulation of over 600 genes, many of which are defense and stress response related, or transcription factors; microarray results show that the transcriptome of the leaves is highly responsive to LCO treatment at 48 h post treatment (Wang et al., 2012). These results suggest the need to investigate more carefully the mechanisms by which microbe-to-plant signals help plants accommodate abiotic and biotic stress conditions.

Bacillus thuringiensis NEB17 was isolated from soybean root nodules as a putative endophytic bacterium in 1998, in our laboratory; when co-inoculated with *B. japonicum* under nitrogen free conditions, it promoted soybean growth, nodulation and grain yield (Bai et al., 2002b, 2003). Subsequently, the causative agent of plant growth promotion, a bacteriocin, was isolated from *B. thuringiensis* NEB17, and is now referred to as thuricin 17 (Gray et al., 2006b). Thuricin 17 (Th17), applied either as leaf spray or as root drench, has positive effects on soybean and corn growth. This report, from our laboratory, was the first to indicate plant growth stimulation by a bacteriocin (Lee et al., 2009). Th17 is now being tested under field conditions and DuPont Canada Crop Protection and Pioneer Canada have confirmed the stimulation of plant growth by Th17 (unpublished data).

Plants are sessile multi-cellular organisms that cope with various environmental stressors that play a major role in the growth and development of plants. Under field conditions they face a range of challenges, some of the most common being soil salinity, cold temperatures and drought. During the late 1990s and the early 2000s, intense gene expression and mutant studies were conducted to identify the probable signal transduction pathways, to understand the differences and commonalities between salt, drought and cold temperature stresses. Some of the key findings are summarized herein. These three abiotic stressors are physically different and yet elicit both specific and common gene responses. With nearly every aspect of plant physiology and metabolism being affected, a very complex network of signalling pathways exists, and helps plants respond to these

conditions (Zhu, 2001a, b). Salt stress creates both osmotic and ionic stress in plants; the ionic stress being very distinct and associated with high sodium (Na^+) and potassium (K^+) deficiency, and occurs a few days after the salt stress is perceived (Munns, 2002; Xiong et al., 2002). However, the osmotic stress component is common to all three mentioned abiotic stressors, thereby converging into the induction of common sets of genes (Shinozaki and Yamaguchi-Shinozaki, 1997; Zhu, 2001a, b). Excess salt in plants results in irregularities in ion homeostasis that are controlled by the cell via various ion transporters (*SOS1*, 2 and 3) that restrict Na^+ entry into the cytoplasm and regulate its accumulation in the vacuoles, and simultaneously selectively import K^+ ions (Hasegawa et al., 2000; Zhu, 2000). *SOS1* is now known to encode for the plasma membrane localized Na^+/H^+ antiporter which removes Na^+ from the cell to the outside; *SOS2* encodes for a serine/threonine protein kinase; *SOS3* encodes for a myristoylated calcium-binding protein and senses salt specific cytosolic Ca^{2+} concentration, interacts with *SOS2* using calcium as the second messenger and targets vegetative storage protein 2 (*VSP2*) to impart salt tolerance (Gong et al., 2001), simultaneously controlling the Na^+/H^+ antiporter system (Qui et al., 2002). About 5 % of *A. thaliana* genes are involved in ion regulation (Lehner et al., 2003). Differences in calcium concentration trigger protein phosphorylation cascades that provoke mitogen-activated protein-kinases, which in turn, regulate the stress response (Chinnusamy et al., 2004).

In our previous study, regarding phytohormone quantification, we observed that LCO treated *A. thaliana* rosettes had increased levels of ABA and free SA, while the rosettes showed increased levels of IAA and SA. Since ABA regulation is observed in abiotic stress tolerance and IAA regulates protein degradation using the ubiquitin proteasome pathway, which decreases the toxic effects of ROS, we wanted to assess the role of LCO and Th17 in regulation of the proteome for plant growth promotion both under optimal and salt stressed conditions.

4.3 Materials and methods

4.3.1 Plant material and treatments

Seeds of *Arabidopsis thaliana* Col-0 were procured from Lehle Seeds (Round Rock, TX, USA), the seeds were planted in peat pellets and the resulting plants grown in a growth chamber at 22 ± 2 °C, light intensity $100\text{-}120 \mu\text{mol quanta m}^{-1} \text{s}^{-1}$, with a photoperiod of 16/8 h day/night cycle and 60 - 70 % relative humidity. Three-week-old plants were sampled, after appropriate treatments, for proteomic patterns under unstressed conditions. Three-and-half-week-old plants were sampled for salt stress.

4.3.2 Extraction and purification of lipo-chitooligosaccharides (LCOs)

The extraction and purification of LCOs followed the method of Souleimanov et al., (2002b). In brief, *B. japonicum* cultures were extracted with 40 % HPLC-grade 1-butanol. The culture supernatant was carefully removed and condensed in a low-pressure rotary evaporator system (Yamato RE500, Yamato, USA) at 50 °C at a speed of 125 rpm, until dryness and the dried extract was resuspended in 4 mL of 18 % acetonitrile. The resuspended extract was loaded onto a C-18 column (PRESEP™ Fisher Scientific, Montreal, Canada) and eluted three times using 10 mL of 30 % acetonitrile, and finally using 60 % acetonitrile. The Nod factors were further isolated and purified by HPLC (Waters 501 pumps, a Waters 401 detector set at 214 nm and a WISP712 autosampler using a C18 reverse phase column (0.46 X 25 cm, 5 μm) - Vydac, CA, USA; catalogue # 218TP54). Chromatography was conducted for 45 min using a linear gradient of acetonitrile from 18 to 60 %, as described by Souleimanov et al. (2002b). Identification of Nod factors was conducted by comparing the retention time of standard Nod factors from strain 532C (identified by mass spectrometry).

4.3.3 Extraction of Thuricin 17 (Th17)

Bacillus thuringiensis NEB17 was cultured in King's B medium (King et al., 1954) as previously described (Gray et al., 2006a). In brief, the culture in King's B medium was incubated in an orbital shaker for 32 h after which this inoculum was subcultured into 4.0 L flasks containing 2.0 L medium and allowed to grow for 48 h.

Th17 isolation and purification was carried out using High Performance Liquid Chromatography (HPLC) using the procedures of Gray et al. (2006b). The collected material was denoted partially as purified Th17, stored at 4 °C and diluted to required concentrations for all the experiments.

In all the germination experiments LCO concentrations of 10^{-6} and 10^{-8} M (referred to as LCOA and LCOB, respectively), and Th17 concentrations 10^{-9} and 10^{-11} M (referred to as THA and THB, respectively) were used, the concentrations of which were found to be the best in plant growth response studies (Prithiviraj et al., 2000; Souleimanov et al., 2002a; Lee et al., 2009).

4.3.4 Petri plate assay for screening for salt stress

Seeds of *Arabidopsis thaliana* were surface sterilized in 90 % alcohol for 1 min and rinsed several times with sterile water. These seeds (25 per plate) were placed on agar plates comprised of control, 10^{-6} and 10^{-8} M LCO and 10^{-9} and 10^{-11} M Th17 treatments, to score for germination. To assess salt tolerance, the seeds (25 per plate) were placed on agar plates comprising 0, 100, 150, 200, 250 mM NaCl in combination with 10^{-6} and 10^{-8} M LCO and 10^{-9} and 10^{-11} M Th17. Control plates were comprised of only ½ MS medium with agar and the salt controls were 100, 150, 200, 250 mM NaCl. After 48 h of stratification, the seeds were allowed to germinate and the seedlings were allowed to grow for 20 days in a growth chamber at 22 ± 2 °C light intensity $100\text{-}120 \mu\text{mol quanta m}^{-1} \text{s}^{-1}$, with a photoperiod of 16/8 h day/night cycle and 60 - 70 % relative humidity, after which the samples from the plates were assessed for differences in growth. Since plants in Petri plate conditions are good for screening and not for long term growth, plants were grown in trays to assess salt stress tolerance and recovery and for label free proteomic studies.

4.3.5 Tray assay for assessing salt stress recovery of *A. thaliana*

Jiffy-peat pellets (Jiffy products, Plant Products Ltd, ON, Canada) were soaked in water to saturation and seeds of *A. thaliana* sown on them. The trays were covered and the seeds allowed to germinate. Two and half-week-old plants were subjected to 10^{-6} and 10^{-8} M LCO, or 10^{-9} and 10^{-11} M Th17 treatments, followed up by fulminant salt stress at

200, 250 and 300 mM NaCl, 48 h post bacterial signal treatments. All the plants were at the same stage of development when the bacterial signals and the subsequent salt treatment 48 h post bacterial treatment was given to the plants. The plants were watered regularly and allowed to grow for 15 days, after which the plants were assessed for visual symptoms of salt stress and loss of turgor. All plants were at the same developmental stage when sampled.

4.3.6 Leaf proteomics using shotgun approach

For the proteome analysis, the rosettes sampled at 24 h after treatment (from control, 10^{-6} M LCO and 10^{-9} M Th17) comprised the unstressed group. Plants from the 7 days of salt stress at 250 mM NaCl in combination with 10^{-6} M LCO and 10^{-9} M Th17 treatments were sampled as the salt stressed group. The samples were flash frozen in liquid nitrogen and stored in -80°C until protein extraction. Total proteins from the samples were extracted using a protein extraction kit (Sigma-Aldrich, PE-2305, St. Louis, MO, USA).

4.3.6.1 Protein extraction

In brief, the sampled (pool of 3 plants per replicate) rosettes were ground to a fine powder in liquid nitrogen. Approximately 100 mg of the fine powder was placed in sterile eppendorf tubes and 1 mL of ice cold methanol (Cat no. 15468-7, Sigma-Aldrich Co., St. Louis, MO, USA) was added, vortexed, incubated in -20°C for 20 min. and centrifuged (Micro12, Fisher Scientific, Denver Instrument Co., USA) at 13,000 rpm for 7 min. at 4°C . The supernatant was discarded and the procedure was repeated twice more, followed by similar incubation in acetone (Cat. no. 179124, Sigma-Aldrich, Co., St. Louis, MO, USA), both steps in order to remove phenolics and secondary metabolites that might otherwise interfere with LC-MS/MS analysis. The RW2 solution was added to the samples after removing acetone, vortexed for 30 s and incubated at room temperature (22°C) for 15 min. The samples were then centrifuged at 13,000 rpm for 10 min and the supernatant carefully collected in a fresh sterile tubes. The supernatant constituted total proteins from that sample. The proteins were then diluted and quantified using the Lowry method, and samples of 10 μg in 20 μL of 1 M urea were taken to the Institut de

recherches cliniques de Montréal (IRCM) for label free proteomic analysis using LC-MS/MS.

4.3.6.2 Protein profiling

The total protein extracts were then digested with trypsin and subjected to LC-MS/MS using LTQ-Velos Orbitrap (Thermo Fisher, MA, USA). Tandem mass spectra were extracted, charge state deconvoluted and deisotoped, and all MS/MS samples were analyzed using Mascot software (Matrix Science, London, UK; version 2.3.02). Mascot was set up to search the *Arabidopsis thaliana* database (unknown version, 80416 entries) assuming the digestion enzyme trypsin. Mascot was searched with a fragment ion mass tolerance of 0.60 Da and a parent ion tolerance of 15 ppm. Carbamidomethyl of cysteine was specified in Mascot as a fixed modification. Oxidation of methionine was specified in Mascot as a variable modification.

Criteria for protein identification - Scaffold (version Scaffold_3.4.7, Proteome Software Inc., Portland, OR), was used to validate MS/MS based peptide and protein identifications. Peptide identifications were accepted if they could be established at greater than 95.0 % probability, as specified by the Peptide Prophet algorithm (Keller et al., 2002). Protein identifications were accepted if they could be established at greater than 99.0 % probability and contained at least 2 identified peptides. Protein probabilities were assigned by the Protein Prophet algorithm (Nesvizhskii, 2003). Proteins that contained similar peptides and could not be differentiated based on MS/MS analysis alone were grouped to satisfy the principles of parsimony.

4.3.7 Data analysis

Experiments were structured following a completely randomized design. The SAS Statistical Package 9.3 (SAS Institute Inc., Cary, NC, USA) was used, and within this the Proc Mixed procedure and Tukey's multiple means comparison when there was significance at the 95 % confidence level. Data transformation was applied when necessary to meet the criteria for analysis of variance for seed germination.

Scaffold 3.4.6 was used for analyzing the proteomics data for fold change and Fisher exact test of the identified proteins after subjecting the quantitative value of the spectra to the embedded normalization. Scatter plots of the contrasts were also generated using this software, while the FASTA file generated was analyzed using Blast2GO-Pro V.2.6.6 (Conesa et al., 2005; Conesa and Götz, 2008; Götz et al., 2008, 2011), for the functional annotation and analysis of the protein sequences. Apart from these, Enzyme code (EC), KEGG maps and InterPro motifs were queried directly using the InterProScan web service.

4.4 Results:

4.4.1 *A. thaliana* seed germination in Petri plates and trays under unstressed conditions and in the presence of salt stress screening, when treated with LCO and Th17.

LCO and Th17 (LCO - 10^{-6} and 10^{-8} M; Th17 - 10^{-9} and 10^{-11} M) treatments generally had no effect on *A. thaliana* seed germination except at 30 h, when conditions were carefully maintained as optimal (Fig 4.1; Table 4.1).

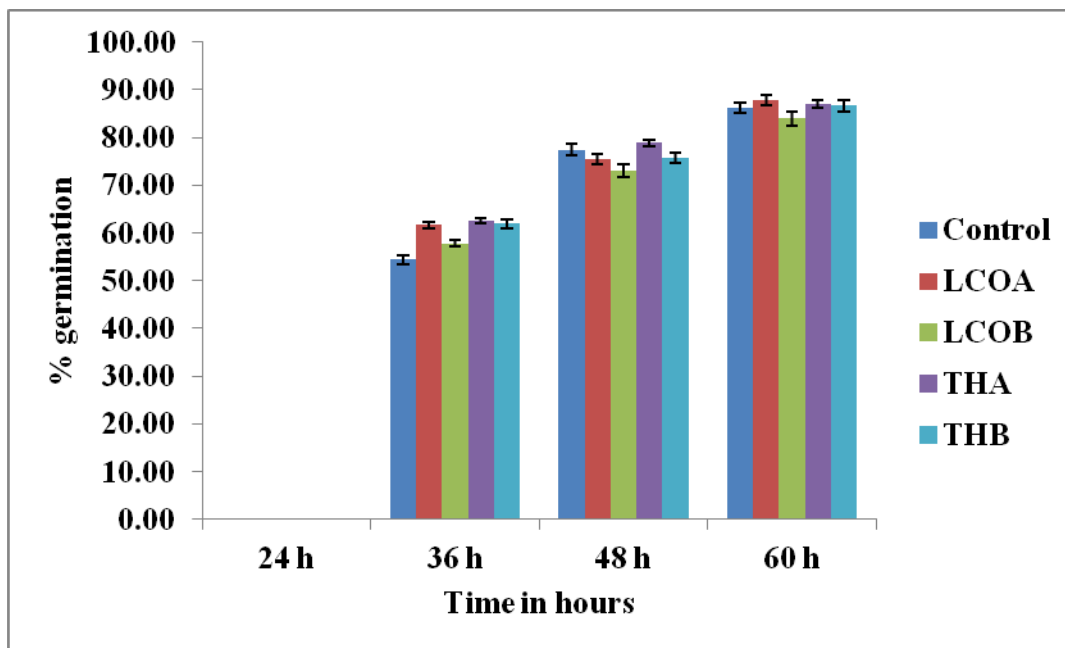


Fig. 4.1: *A. thaliana* germination at 22 °C in the presence of LCO and Th17 (Treatments - Control - $\frac{1}{2}$ MS, LCOA - 10^{-6} M, LCOB - 10^{-8} M, THA - 10^{-9} M, THB - 10^{-11} M).

Table 4.1: Least square means of *A. thaliana* percentage germination - seeds treated with LCO and Th 17 under optimal conditions. Means associated with the same letter are not significantly different at $p \leq 0.05$.

Treatments	24 h	± SEM	30 h	± SEM	36 h	± SEM	48 h	± SEM
P ≤ 0.05			0.1904		0.6972		0.8235	
Control	0.00	0.00	54.38^b	0.97	77.49^a	1.15	86.26^a	1.10
LCOA	0.00	0.00	61.69^{ab}	0.71	75.52^a	1.04	87.83^a	1.11
LCOB	0.00	0.00	57.77^{ab}	0.70	72.99^a	1.28	83.96^a	1.57
THA	0.00	0.00	62.66^a	0.53	78.87^a	0.77	87.12^a	0.76
THB	0.00	0.00	61.99^{ab}	0.97	75.81^a	1.10	86.67^a	1.12

Hence an evaluation of the effects of these signal compounds in the presence of salt stress was conducted; a NaCl dosage response screening was performed. This work suggested that, in the presence of signal compounds, the plants could withstand up to 200 mM NaCl in Petri plates where the plants showed signs of chlorophyll degradation, while the 250 mM NaCl stress completely inhibited root growth (Fig 4.2). However, the Petri plate assay is only good for early growth determinations as the seedlings are in an enclosed environment and this can induce other stresses. Hence, plants were grown in trays and two and half-week-old plants were screened with 200, 250 and 300 mM NaCl. After 48 h of treatment with LCO and Th17, the plants were treated with 200, 250 and 300 mM NaCl, allowed to recover from the shock and assessed for visual signs of stress 15 days after the NaCl stress was imposed. The plants could tolerate 250 mM NaCl while at 300 mM, the visible signs of stress were obvious as retarded plant growth and loss of turgor (Fig. 4.3). Hence, there were clear beneficial effects of LCO and Th17 for 250 mM NaCl treated plants at 7 d post exposure, and these conditions were selected for rosette proteomics.



Fig. 4.2: Screening assay in petriplates for *Arabidopsis thaliana* response to 200 and 250 mM NaCl stress in the presence of LCO and Th17, 20 days after imposition of salt stress. (Control - Water; LCOA - 10^{-6} M, LCOB - 10^{-8} M, THA - 10^{-9} M, THB - 10^{-11} M; 200 and 250 mM NaCl control).



Fig. 4.3: *Arabidopsis thaliana* response to different levels of salt stress in the presence of LCO and Th17, 15 days after imposition of salt stress. (Control - Water; LCOA - 10^{-6} M, LCOB - 10^{-8} M, THA - 10^{-9} M, THB - 10^{-11} M).

4.4.2 Protein profiling

To understand the effect of LCO and Th17 on unstressed and salt stressed *A. thailana* rosettes, total proteins were extracted from the samples and subjected to LC-MS based proteome profiling. Based on the quantitative value of the identified spectra, and at 99 % protein probability, with 2 minimum peptides and 95 % peptide probability, 688 proteins were identified at a 0.1 % protein FDR (False discovery rate) with 49285 spectra at 0.1% peptide FDR for the signals without stress. Similarly, for the signals with 250 mM NaCl group, 781 proteins were identified at 0.1 % protein FDR, with 54003 spectra at 0.4 % peptide FDR (Fig 4.4). The treatment contrasts were then analyzed for fold-change after normalization, and Fisher's Exact test was used to narrow down the up- and down-regulated proteins, to predict their probable functions at 24 h after signal compound treatment and 7 d after NaCl stress imposition. It is likely that we missed some of the relevant proteins due to very strict criteria for difference detection during data analysis; this level of stringency was utilized for ease of subsequent functional interpretation.

According to the fold-change patterns and Fisher's Exact test of the contrasts, the proteins were categorized as known proteins, putative proteins, hypothetical and unknown proteins (Table 4.2a, b).

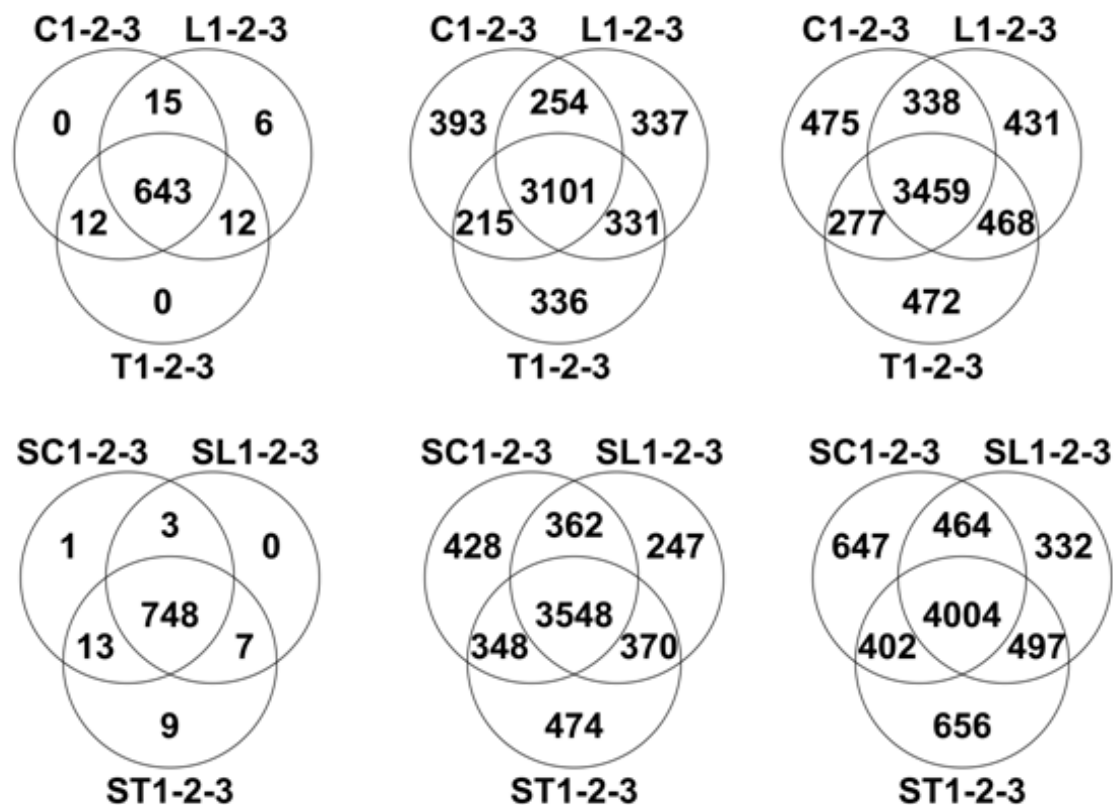


Fig. 4.4: Venn diagram for the output of differentially expressed proteins, unique peptides and unique spectra based on Scaffold in the top row – un-stressed group (C = Control-water, LA = LCO 10^{-6} M, TA = Th17 10^{-9} M) and the bottom row – salt stressed group (CS = 250 mM NaCl Control, LAS = LCO 10^{-6} M + 250 mM NaCl, TAS = Th17 10^{-9} M + 250 mM NaCl. 1-2-3= biological replicates data grouped).

Table 4.2a: Grouping of proteins in *Arabidopsis thaliana* rosettes, that was significant in contrasts based on Fold change.

Treatment contrasts <i>A. thaliana</i>	Control vs. LCO	Control vs. Th17	LCO vs. Th17	Control 250 mM NaCl vs. LCO + 250 mM NaCl	Control 250 mM NaCl vs. Th17 + 250 mM NaCl	LCO 250 mM NaCl vs. Th17 + 250 mM NaCl
Total significant proteins	114	93	80	93	92	80
Known proteins	97	80	68	72	80	64
Putative proteins	10	8	8	13	15	11
Hypothetical proteins	3	1	2	1	-	1
Unknown proteins	4	4	2	7	7	4

Table 4.2b: Grouping of proteins in *Arabidopsis thaliana* rosettes, that were significant in contrasts based on Fisher's Exact test.

Treatment contrasts <i>A. thaliana</i>	Control vs. LCO	Control vs. Th17	LCO vs. Th17	Control 250 mM NaCl vs. LCO + 250 mM NaCl	Control 250 mM NaCl vs. Th17 + 250 mM NaCl	LCO 250 mM NaCl vs. Th17 + 250 mM NaCl
Total significant proteins	63	42	26	25	40	25
Known proteins	55	33	22	21	34	20
Putative Proteins	7	8	2	4	5	5
Hypothetical proteins	1	1	1	-	-	-
Unknown proteins	-	-	1	-	1	-

Based on the known and predicted proteins, some of the up-regulated proteins in unstressed control rosettes included O-methyltransferase, pyrophosphatase, COR15A and B, legume lectin family, actin 7, membrane associated progesterone binding protein, legume lectin family, a chloroplast drought induced stress protein, phosphoglycerate kinase, mitochondrial HSP70, thiamin C, profiling, TIC 40 (TRANSLOCON AT THE INNER ENVELOPE MEMBRANE OF CHLOROPLASTS) universal stress protein and a putative jasmonate inducible protein. Some of the notable proteins up-regulated in LCO treated plants were members of 40 and 60 S ribosomal protein family, phosphoenolpyruvate carboxylase (PEPC) 1 and 2, proteins of the photosystem I subunit and photosystem II 47kD, D1 and D2 proteins, acetyl CoA carboxylase, calcium sensing receptor (CaS), lipoxygenase, RUBISCO large subunit, members of oxidoreductases, fibrillin family, TIC 40 and 110, LEA protein family, peroxisomal glycolate oxidase, cadmium sensitive, cell division cycle related protein and vestitone reductase. Th17 treated rosettes had all of the above proteins up-regulated in LCO treated rosettes in addition to COR13, hydroxyl-proline rich, a major latex protein, catalase, light harvesting complex proteins LHB1B1, LHCA2, LHCB5, LHCB6, nodulin related, Zn binding oxidoreductases and progesterone binding protein [(Refer Appendix II for fold change (Table 4.3a,b,c) and Fisher's exact test results (Table 4.4a,b,c) for *A. thaliana* signals group contrasts].

The number of significant proteins identified in the salt stressed signals group did not alter much in number, but did so in the types of proteins that seemed to be regulated in response to salt stress. The control 250 mM salt stress showed an up-regulation of 40, 50 and 60 S ribosomal proteins, a methyl jasmonate esterase, CaS, cadmium sensitive protein 1, pyruvate decarboxylase, phosphoglycerate kinase, seed maturation protein, stromal ascorbate peroxidase, TIC 40, cinnamyl-alcohol dehydrogenase, pyruvate kinase, peroxidase, Fe-superoxide dismutase, chitinase, plastocyanin, and profiling 1. The LCO treated and salt stressed group however up-regulated a very different set of proteins comprised of COR15A, cytochrome B5 isoform E, glucose-phosphate-6-isomerase, LHCB 4.2 and protein D1 of photosystem II, nodulin related protein, photosystem 1 P700 chlorophyll apoprotein A1, plastid-lipid associated protein, NADH-cytochrome B5 reductase, NADPH oxidoreductases, allene oxide synthase and cyclase. Th17 treated and

250 mM NaCl stressed rosettes up-regulated proteins, some of which were common to both the salt control and LCO with salt groups; apart from those observed in these treatments (listed above for the LCO group), also affected were: ATP citrate synthase, alcohol and aldehyde dehydrogenases, seed maturation protein, cinnamyl-alcohol dehydrogenase 4, cadmium sensitive, glutathione synthase transferase, PIP1B (a plasma membrane water channel protein), importin subunit, APE2 (Acclimation of leaf photosynthesis), myo-inositol, isocitrate dehydrogenase and vestitone reductase. [Please refer Appendix II for Fold change (Table 4.3d,e,f) and Fisher's exact test results (Table 4.4d,e,f) for *A. thaliana* signals group contrasts].

Based on Blast2GO Pro results, the enzyme code distribution for both the unstressed and salt stressed rosettes were studied. A sharp increase in some of the main enzyme classes was observed in the salt stress group, as compared to the unstressed group (Fig. 4.5). While the oxidoreductases, hydrolases, lyases, isomerases and ligases increased by 16.05, 17.14, 2.5, 6.1 and 1.3 %, respectively, transferases decreased by a marginal 1.01 % (Table 4.5). The sharp increase in oxidoreductases and hydrolases could be explained through possible roles in salt stress alleviation.

The GO function distribution characteristics of the unstressed and salt stressed groups also indicated that the proteins identified were mostly associated with ATP, GTP, protein and nucleotide binding, metal ion binding and specific to zinc, copper, cadmium, cobalt, magnesium and calcium, response to salt and cold, glycolysis, pentose-phosphate shunt, gluconeogenesis, thylakoid associated, photorespiration, oxidation-reduction processes and photosystem II assembly (Table 4.7; Fig 4.6a,b,c; Fig 4.7).

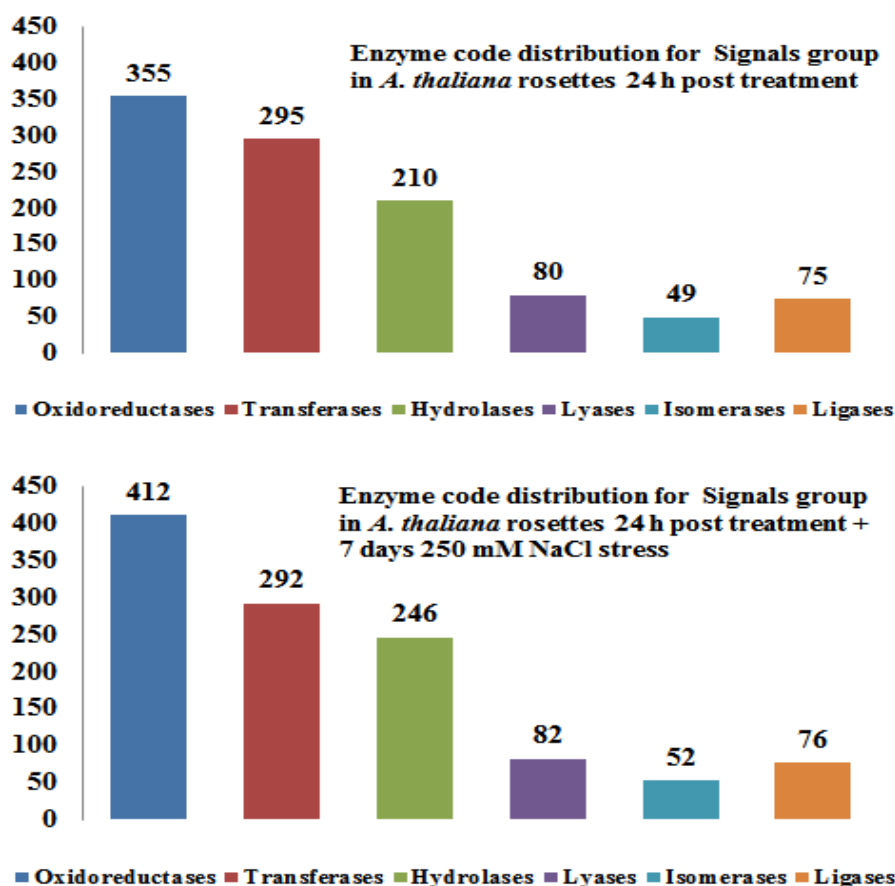
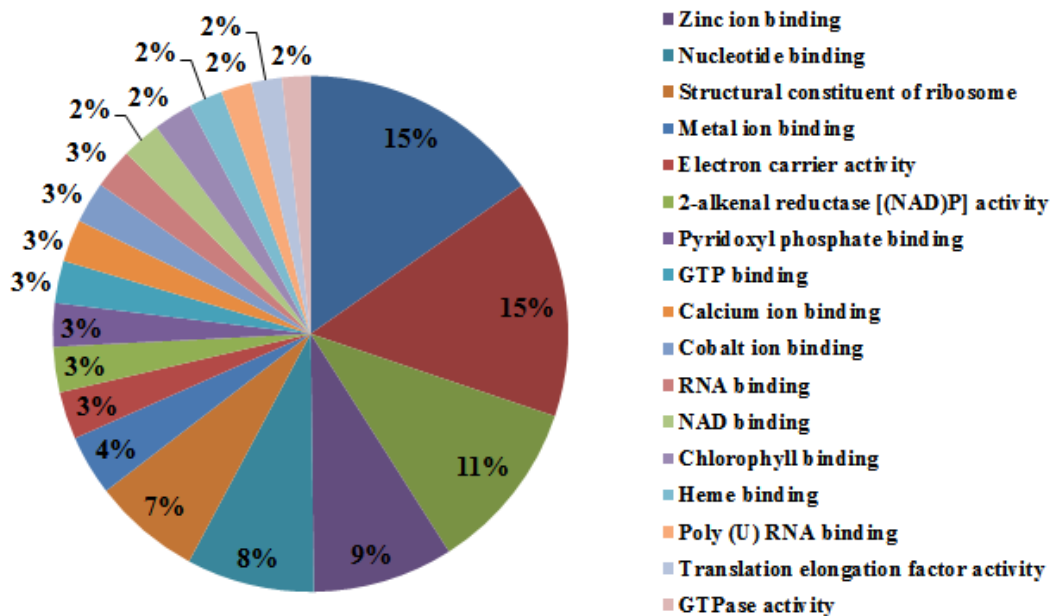


Fig. 4.5: Enzyme code distribution categorized based on main enzyme classes – *Arabidopsis thaliana*

Table 4.5: Enzyme code distribution in un-stressed and salt stressed groups. The % increase or decrease in the main enzyme classes in the salt stress group is mentioned in the brackets.

Main enzyme classes	Sequence distribution in signals group	Sequence distribution in signals + salt group
Oxidoreductases	355	412 (↑ 16.05 %)
Transferases	295	292 (↓ 1.01 %)
Hydrolases	210	246 (↑ 17.14 %)
Lyases	80	82 (↑ 2.5 %)
Isomerases	49	52 (↑ 6.1 %)
Ligases	75	76 (↑ 1.3 %)

Molecular function - Signals group
Arabidopsis thaliana 24 h post treatment



Molecular function - Signals + Salt group
Arabidopsis thaliana 24 h treatment +
 7 days exposure to 250 mM NaCl

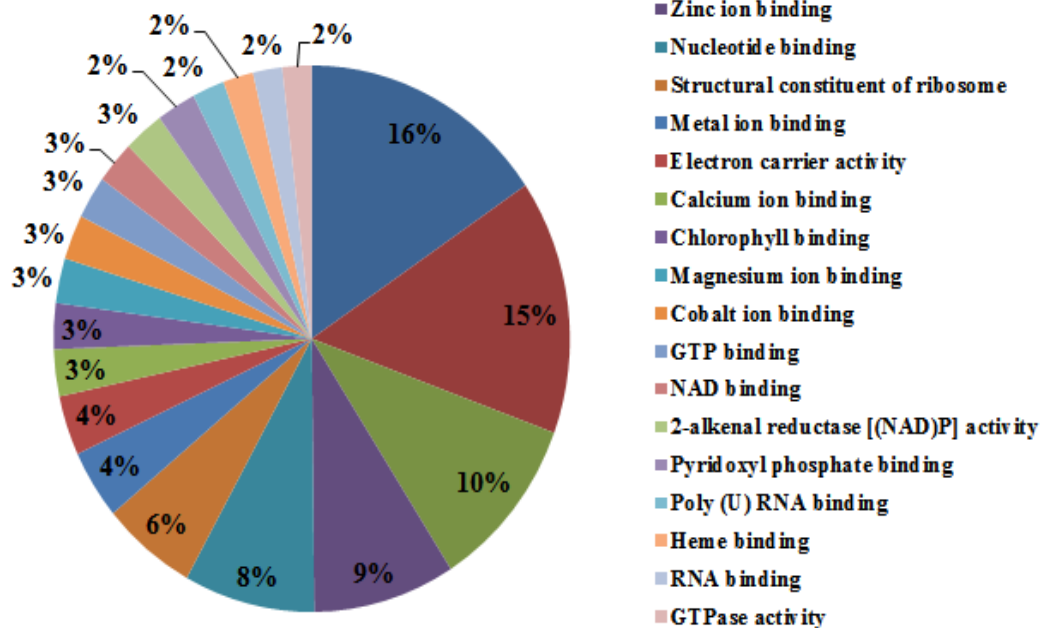


Fig. 4.6a: Pie chart representation of functional classification of GO distribution for molecular function in unstressed group and Signals + 250 mM Salt stressed groups in *Arabidopsis thaliana* rosettes.

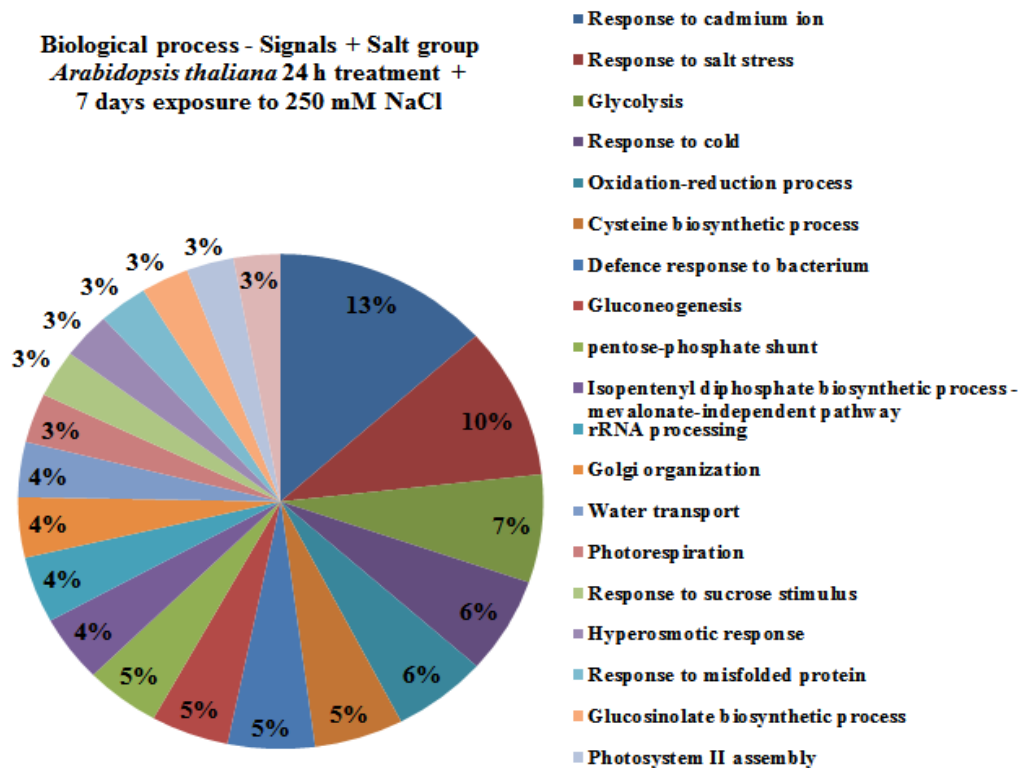
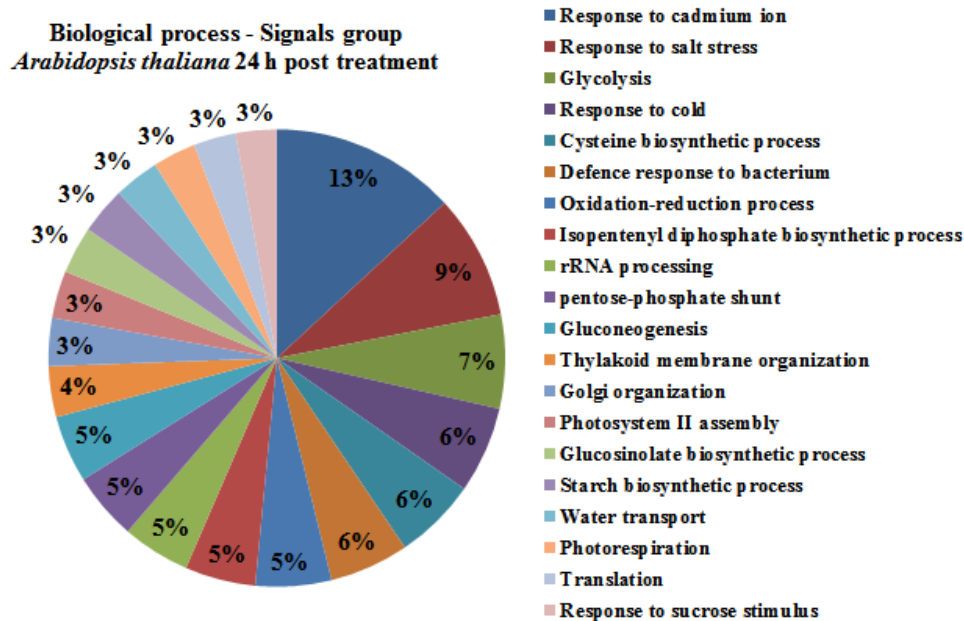
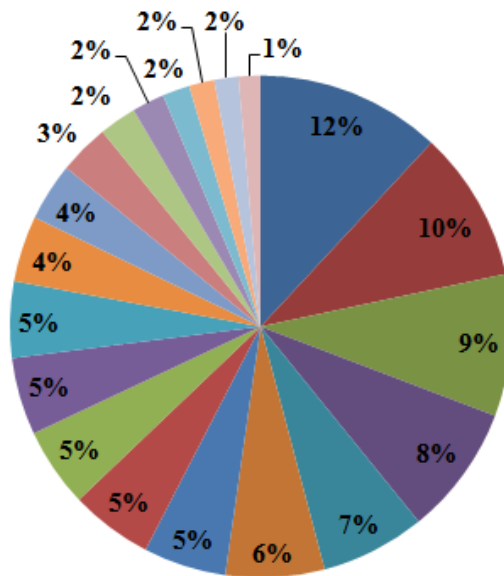


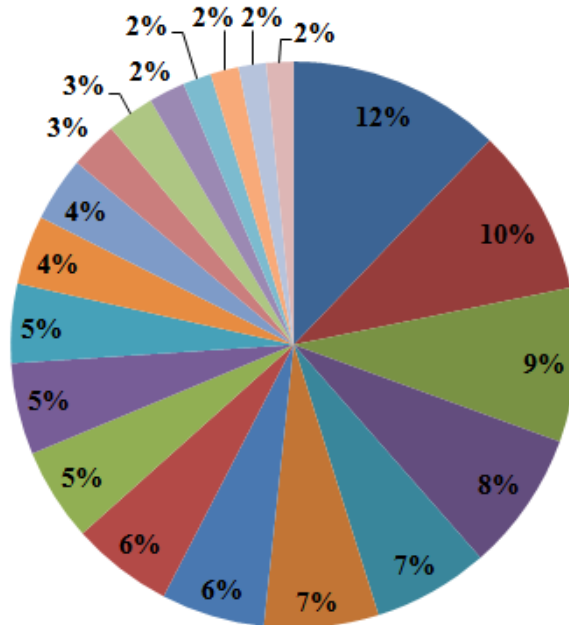
Fig. 4.6b: Pie chart representation of functional classification of GO distribution for biological process in unstressed and signals + 250 mM NaCl stress in *Arabidopsis thaliana* rosettes.

Cellular components - Signals group
Arabidopsis thaliana 24 h post treatment



- Cytosol
- Chloroplast stroma
- Plasma membrane
- Chloroplast envelope
- Apoplast
- Plasmodesmata
- Mitochondrion
- Chloroplast
- Golgi apparatus
- Chloroplast thylakoid
- Nucleus
- Vacuolar membrane
- Cell wall
- Nucleolus
- Vacuole
- Membrane
- Plastoglobule
- Thylakoid
- Stroma
- Extra cellular region

Cellular component - Signals + Salt group
Arabidopsis thaliana 24 h treatment +
7 days exposure to 250 mM NaCl



- Cytosol
- Plasma membrane
- Chloroplast stroma
- Chloroplast envelope
- Plasmodesmata
- Apoplast
- Nucleus
- Chloroplast
- Golgi apparatus
- Mitochondrion
- Chloroplast thylakoid
- Vacuolar membrane
- Cell wall
- Vacuole
- Nucleolus
- Membrane
- Cytosolic ribosome
- Plastoglobule
- Thylakoid
- Plant-type cell wall

Fig. 4.6c: Pie chart representation of functional classification of GO distribution for cellular components in unstressed and signals + 250 mM NaCl stress in *Arabidopsis thaliana* rosettes.

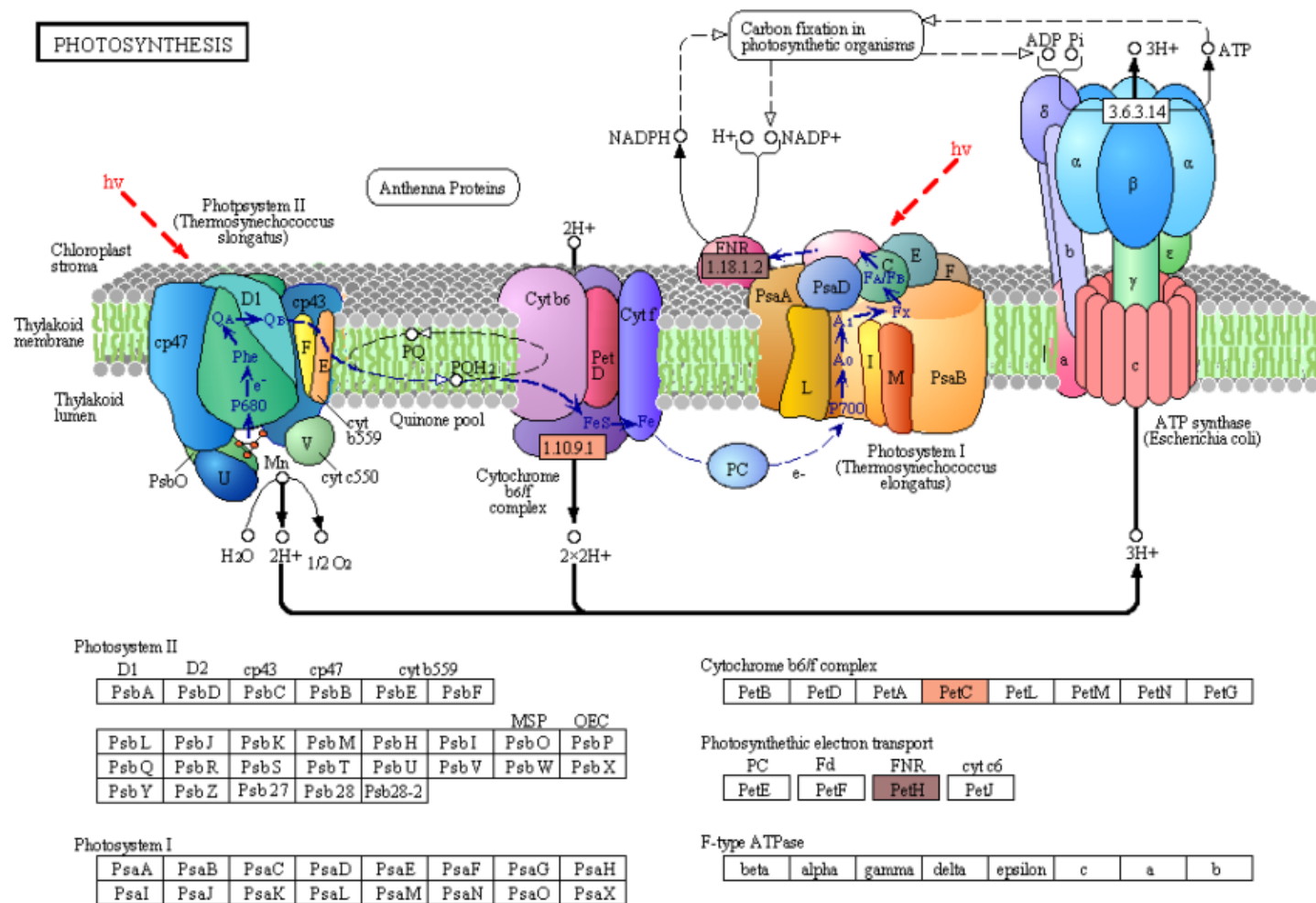


Fig. 4.7: KEGG pathway depicting the role of photosystem I and II (KEGG Pathway).

Table 4.7: GO function categories amongst un-stressed and salt stressed groups in *Arabidopsis thaliana* rosettes

Molecular function	No of seq Signals	No of seq Salt	Biological process	No of seq Signals	No of seq Salt	Cellular Component	No of seq Signals	No of seq Salt
ATP binding	230	246	Response to cadmium ion	421	471	Cytosol	541	610
Protein binding	225	239	Response to salt stress	281	350	Chloroplast stroma	441	441
Copper ion binding	163	164	Glycolysis	213	249	Plasma membrane	415	481
Zinc ion binding	133	141	Response to cold	196	222	Chloroplast envelope	380	400
Nucleotide binding	121	130	Cysteine biosynthetic process	187	194	Apoplast	306	328
Structural constituent of ribosome	102	94	Defence response to bacterium	180	189	Plasmodesmata	289	332
Metal ion binding	57	65	Oxidation-reduction	172	206	Mitochondrion	242	262

			process					
Electron carrier activity	45	56	Isopentenyl diphosphate biosynthetic process - mevalonate-independent pathway	160	154	Chloroplast	241	291
2-alkenal reductase [(NAD)P] activity	43	40	rRNA processing	154	153	Golgi apparatus	232	267
Pyridoxyl phosphate binding	41	39	pentose-phosphate shunt	153	163	Chloroplast thylakoid	226	227
GTP binding	40	40	Gluconeogenesis	152	169	Nucleus	223	296
Calcium ion binding	40	44	Thylakoid membrane organization	115	0	Vacuolar membrane	193	198
Cobalt ion binding	39	42	Golgi organization	109	139	Cell wall	170	185
RNA binding	38	29	Photosystem II assembly	107	103	Nucleolus	147	136
NAD binding	37	40	Glucosinolate	107	104	Vacuole	109	137

			biosynthetic process					
Chlorophyll binding	37	43	Starch biosynthetic process	106	0	Membrane	95	104
Heme binding	32	30	Water transport	103	127	Plastoglobule	80	81
Poly (U) RNA binding	29	32	Photorespiration	98	114	Thylakoid	74	81
Translation elongation factor activity	29	0	Translation	96	0	Stromule	71	0
GTPase activity	27	29	Response to sucrose stimulus	93	109	Extracellular region	64	0
Magnesium ion binding	0	42	Response to misfolded protein	0	107	Cytosolic ribosome	0	81
			Proteasome core complex assembly	0	102	Plant-type cell wall	0	78
			Hyperosmotic response	0	107			

Molecular function, biological processes and cellular components were all affected in both unstressed and salt-stressed conditions. Translation, translation elongation factor activity, thylakoid membrane organization proteins, starch biosynthetic process, proteins of the stroma and the extracellular region were all arrested in the salt stressed group. However, magnesium ion binding proteins, proteins related to misfolded protein responses, proteasome core complex assembly and hyperosmotic stress response, cytosolic ribosome and plant-type cell wall were all prominent in the salt stressed group. Apart from these, proteins in the cytosol, plasma membrane, chloroplast and its envelope, apoplast, plasmodesmata, nucleus and the vacuole were all up-regulated. Very little change was observed in GTP binding and GTPase activity, copper ion binding, rRNA processing, photosystem II assembly, plastoglobule, vacuole membrane, chloroplast thylakoid and stroma.

4.5 Discussion:

Nod Bj V (C18:1; MeFuc), a major LCO molecule produced by *B. japonicum* 532C, isolated and identified in our laboratory, has been reported to have a positive and direct effect on both legume and non-legume seed germination, plant growth and development (Prithiviraj et al., 2003). Other than soybean and common bean, LCO can also enhance seed germination and seedling establishment in maize, rice, canola, apple and grapes, and is accompanied by increased photosynthetic rates (Zhang and Smith, 2001). Investigations into these effects, at the molecular level, led us to transcriptomic studies, and microarray studies on soybean leaves sprayed with LCOs under optimal and sub-optimal growth conditions. The optimal condition microarray revealed 639 differentially expressed genes out of which 13 were related to abiotic stress, 14 related to biotic stress, 3 to salicylic acid and 7 to cytochrome P450s at 48 h post treatment (Lindsay, 2007). The sub-optimal stress microarray revealed the differential expression of over 600 genes. Many of these were defense and stress response related, or transcription factors suggesting the effects of LCO on the transcriptome of the leaves at 48 h post treatment (Wang et al., 2012). These results suggest a need to further explore the mechanisms by which microbe-to-plant signals might help plants accommodate abiotic and biotic stress conditions. Th17 however, has not been studied as well as LCO,

as it is more recently isolated. We have some information regarding its effects on soybean and corn plant growth. The leaves of two-week-old soybean leaves sprayed with Th17 showed increased activities of lignification-related and antioxidative enzymes and their isoforms. Both leaf spray and root drench of soybean and corn with Th17 stimulated plant growth (Jung et al., 2008a, Lee et al., 2009).

Hence, in this study we subjected *A. thaliana* plants to salt stress to evaluate the efficacy of both LCO and Th17 under unstressed and salt stressed conditions for proteome profiling. *A. thaliana* is a glycophyte and sensitive to salt. The roots of *A. thaliana* seedlings were severely affected at 200 mM NaCl, in a Petri plate assay used to study salt stress (0, 50, 100, 150, 200, 250 mM NaCl) (Jiang et al., 2007). Our study shows that, in the presence of the bacterial signal compounds *A. thaliana* showed retarded root growth only at 250 mM NaCl. These compounds alleviated salt stress up to 250 mM NaCl when *A. thaliana* grown in trays were exposed to NaCl stress. At 300 mM NaCl stress, obvious stress related symptoms such as retarded plant growth and loss of turgor in the leaves were observed.

Proteins play central roles in essentially all metabolic processes. The advances in instrumentation and bioinformatic analysis have increased our understanding of proteins and their effects, which can provide key evidence regarding shifts in plant physiology. Despite these advances, proteome profiling in systems biology are still a major challenge; but the amount of information they can add to the understanding of a biological system is impressive. In this study we used the label free proteomics approach to understand *A. thaliana* proteomic responses in the presence of microbial signal compounds and under unstressed and 250 mM NaCl stressed conditions.

Translation, translation elongation factor activity, thylakoid membrane organization proteins, starch biosynthetic process, proteins of the stroma and the extracellular region were all arrested in the salt stressed group, suggesting that the plants were arresting these processes in order to compensate for energy dependent activities associated with Na⁺ ion flushing from the cytosol. However, magnesium ion binding proteins, proteins related to cadmium response, misfolded protein responses, proteasome core complex assembly and hyperosmotic stress response, cytosolic ribosome and plant-

type cell wall were all prominent in the salt stressed group. Ligands for metals such as cadmium (Cd), copper (Cu), nickel (Ni) and zinc (Zn) are seen in all plant tissues and in abundance in the xylem sap where they form complexes with histidine and citrates in the xylem sap moving from roots to leaves. The Cd binding complexes are found in both the cytosol and, predominantly, in the vacuole of the cell (Rauser, 1999).

Apart from these, proteins in the cytosol, plasma membrane, chloroplast and its envelope, apoplast, plasmodesmata, nucleus and the vacuole were all up-regulated, while very little change was observed in GTP binding and GTPase activity, copper ion binding, rRNA processing, photosystem II assembly, plastoglobule, vacuole membrane, chloroplast thylakoid and stroma.

The significant findings in our study were the up-regulation of the chloroplast proteins and the proteins from photosystems I and II, since these are generally strongly and negatively affected by salt stress. During abiotic stresses, photosynthetic capacity is reduced due to damage to photosynthetic pigments of the photosystems I and II, resulting in reduced light absorption capacity (Zhang et al., 2011; Ashraf and Harris, 2013). The stromal proteome of Arabidopsis chloroplasts represented 10 % of the 241 proteins identified to be involved in chloroplast protein synthesis and biogenesis, with 75 % being associated with the oxidative pentose phosphate pathway, glycolysis and Calvin cycle, 5 – 7 % with nitrogen metabolism and the rest with other biosynthetic pathways such as fatty acid metabolism, amino acid metabolism, nucleotides, vitamins B1 and 2, tetrapyrroles, lipooxygenase 2 and a carbonic anhydrase (Peltier et al., 2006).

Plants are exposed to various levels of light in nature and one of the ways they compensate for this is by regulating their thylakoid membrane proteins. Light harvesting protein complex protein phosphorylation is catalyzed by light-dependent protein kinase mediated by plastoquinone and is driven by the electron transport system based on light dosage (Ranjeva and Boudet, 1987). Photosystem II light interception is mediated by pigment proteins that belong to a large class of antenna pigments. Light harvesting complex II (LHC II) is the most abundant of the photosystem II proteins; the apoprotein and pigment-protein holocomplex is structurally very heterogeneous. The LHC II apoproteins Lhcb1, Lhcb2 and Lhcb3 are coded by *Lhcb1*, *Lhcb2* and *Lhcb3* genes. Once

synthesized in the cytoplasm as precursors, these are transported into the chloroplast by post-translational modifications (Jackowski et al., 2001). A short term post-translational redistribution of LHC and a long term chloroplast DNA transcription, balance the regulation of photosystems I and II, and is dictated by the redox state of plastoquinone which is in turn controlled by chloroplast sensor kinase (CSK) (Allen et al., 2011).

Exposure to light stress causes oxidative and nitrosative stress and the proteins of photosystem I and II are affected differentially. Amino acid oxidation products are determined mostly in the photosystem II reaction center, and this often leads to tyrosine and tryptophan oxidation or nitration (Galetskiy et al., 2011). About 80-200 proteins present in the thylakoid lumen are closely associated with the light harvesting complexes and the other proteins regulating photosynthesis. Following an 8 h light exposure, PsbP and PsbQ subunits of photosystem II were seen to increase along with a major plastocyanin and various proteins of unknown function. These proteins also seem to be similarly expressed at the transcription level (Granlund et al., 2009). The excess light energy perceived by plants is channeled into the chloroplasts and dispersed by the mitochondrial respiratory chain. The type II NAD(P)H dehydrogenases in the inner membrane of the mitochondria, cyanide-resistant alternative oxidase and phosphorylating pathway complexes I, III and IV regulate this energy processing. Along with the glycine decarboxylase complex (GDC), these pathways regulate the energy balance between chloroplast and mitochondria under stressful conditions, wherein these pathways are up-regulated to maximise photosynthetic efficiency (Noguchi and Yoshida, 2008).

The plastoglobule proteome of the chloroplast includes a M48 metallopeptidase, Absence of bc1 complex (ABC1) kinases and fibrillins, together constituting about 70 % of the plastoglobule protein biomass. The fibrillins present in other parts of the chloroplast are partitioned, probably based on their isoelectric point and hydrophobicity, to specific functions such as chlorophyll degradation and senescence, plastid proteolysis, isoprenoid biosynthesis, redox and phosphoregulation of the electron flow, although most of the functions of the associated proteins are still not clear (Lundquist et al., 2012).

Despite the high salt stress levels imposed on the plants in this experiment, the photosystem proteins were still up-regulated in the LCO and Th17 treatments, suggesting

that these two signals are preventing the damage of these photosystem proteins in a way we still do not understand.

The other up-regulated proteins in this experiment include those of phosphoenolpyruvate carboxylase (PEPC) and phosphoenolpyruvate carboxylase kinase (PPCK), that are two major cytosolic enzymes central to plant metabolism. During phosphate deprivation, *A. thaliana* responds by phosphorylating PEPC subunits to modulate the metabolic adaptations of lower phosphate availability (Gregory et al., 2009). The plant type - PEPC genes encode for 110-kDa polypeptides. These peptides are homotetrameric and contained several conserved sites for serine-phosphorylation and lysine-mono-ubiquitination (O'Leary et al., 2011; and references therein).

Carbonylation of proteins in organisms is an irreversible and oxidative process that increases with age and leads to disfunction of modified proteins in the system. In Arabidopsis, protein carbonylation is found to increase as the plant grows, but is seen to decrease drastically during the onset of bolting and flowering. Hsp70, ATP synthases, RUBISCO large subunit and proteins of the light harvesting complex and of energy transfer are all targets of this mechanism (Johansson et al., 2004).

The up-regulation of the proteasome pathway indicates that the stress generated toxic proteins might be degraded by this system. In previous studies, the 20S proteasome pathway was seen to be up-regulated in both RNA and protein levels of cadmium stressed Arabidopsis leaves, suggesting that this proteasome pathway might help with degrading stress generated oxidized proteins (Polge et al., 2009). Also, the 26 S proteasome of *Arabidopsis thaliana* contains 26 unique proteins with at least 13 of them containing tryptophan residues as identified using nano-flow liquid chromatography (Russel et al., 2013). Post-transcriptional gene regulation is, in part, controlled by RNA-binding proteins (RBP). The *A. thaliana* genome encodes for more than 200 RBPs and they contribute to diverse developmental processes, chromatin modification and environmental adaptation (Lorkovic, 2009).

LEA proteins, initially discovered and researched in seeds, are now reported to be present in other vegetative tissues and have a wide range of sequence diversity and

intercellular localization, with expression patterns depending on environmental conditions. The majority of the predicted LEA proteins are highly hydrophilic and found mostly in unfolded conditions, being involved largely with cellular dehydration tolerance. In *Arabidopsis*, 9 distinct groups of LEA proteins, encoded by 51 different LEA protein genes, have been reported; most harbor abscisic acid response (ABRE) and/or low temperature response (LTRE) elements in their promoters (Hundertmark and Hinch, 2008).

Progesterone 1 was detected in apple seeds as early as 1968, but due to technical challenges in instrumentation and reliability of assays, the role of progesterone in plants was conclusively established only in 1991 by Saden-Krehula et al., (Janeczko and Skoczowski, 2005). It has now been detected in a variety of dicots and monocots such as adzuki bean, mung bean, pea, tomato, potato, apple, onion, rice and *Arabidopsis*, with the shoots having relatively more abundant progesterone 1 than inflorescences, seeds, roots and tubers. Progesterone 1 was also seen to promote plant growth at very low concentrations (range of 0.01–1 μ M) suggesting that this could be playing the role of a hormone in plants, regulating growth and development (Iino et al., 2007; Nakano and Yokota, 2007).

Nodulin genes once thought to be specialized genes present only in legumes have been observed in some non-legumes. The role of nodulin genes might be diverse and related to general organogenesis, rather than restricted to nodulation. Nodulin genes are found in high transcript levels in floral tissues (Szczyglowski and Amyot, 2003). Other *enod40* genes have been cloned from non-legumes include tomato (Velghels et al., 2003), maize (Compaan et al., 2003), rye grass (*Lolium*) and barley (*Hordeum*) (Knud, 2003). *Enod40* levels are elevated during arbuscular mycorrhizal root colonization of tobacco (*Nicotiana bentana*) and alfalfa (*Medicago truncatula*) (Sinvany et al., 2002). *Azorhizobium caulinodans* ORS571 colonized the roots of *Arabidopsis thaliana* through lateral root cracks and the colonization was improved upon addition of flavanoids naringenin and daidzein. Both colonization and flavanoid stimulation were *Nod gene* independent (Gough et al., 1997). Early nodulin like protein has been observed to accumulate during the early stages of sieve cell differentiation (Khan et al., 2007).

Investigation of transgenic lines of *Arabidopsis* for early nodulin gene *enod40* function showed reduction in cell size of selected tissues in the plant, such as the leaf mesophyll and the epidermal internode cells (Guzzo et al., 2005). Nodulin protein analogues in watermelon control fruit development and ripening (Wechter et al., 2008). Roles of nodulin genes have been reported in tomato fruit development and ripening (Lemaire-Chamley et al., 2005).

4.6 Conclusion:

In this study, we compared the effects of LCO and Th17 under unstressed and salt-stressed conditions; this is the first study conducted to determine the effects of these signals, in combination with stressful levels of salt, on *A. thaliana* proteome. *A. thaliana* is a glycophyte and is sensitive to salt stress. LCO is commercially available (products such as Optimize with LCO promoter technology) and is known to accelerate plant growth in the field. The comparison between LCO and Th17 and the effects on the proteome of the rosettes under stressed and unstressed conditions is another step to understanding the effects of these compounds, at the proteome level, during plant growth. This study also increases our understanding of plant-microbe interactions, mainly in the use of such growth promoting technologies, boosting the potential for decreased use of synthetic chemical inputs on cultivated land, and perhaps enhanced crop productivity on salinized soils around the world.

CHAPTER 5

A proteomic approach to Lipo-chitooligosaccharide and Thuricin 17 effects on soybean salt stress responses

Sowmyalakshmi Subramanian¹, Emily Ricci², Alfred Souleimanov¹, Donald L. Smith¹

¹Department of Plant Sciences,

² Department of Natural Resource Sciences

Macdonald Campus, McGill University, 21111 Lakeshore Road, Sainte Anne de Bellevue, Quebec H9X3V9, Canada

Corresponding author e-mail: donald.smith@mcgill.ca

CONNECTING STATEMENT TO CHAPTER 5

The content of Chapter 5 is derived from an article recently submitted (reformatted here to fit the thesis), co-authored by Subramanian S, Ricci E, Souleimanov A and Smith DL, entitled “A proteomic approach to Lipo-chitooligosaccharide and Thricin 17 effects on soybean salt stress responses”. The results of this study, authored by myself, Ricci E, Souleimanov A and Smith DL were also presented as a poster at the North American Nitrogen Fixation Conference – July 14-17, 2013 Minnesota, USA.

From the previous chapters 3 and 4, it is very clear that the bacterial signals LCO and Th17 provoked differential expression of phytohormones under unstressed conditions. The differences between the unstressed and the salt stressed proteome groups, and especially the shut-down of most parts of the photosynthetic pathways in the control salt stressed condition, while activity is clearly retained in the signal treated plants, suggests that the signal compounds activate mechanisms that allow the plants to deal with the challenge of high salt stress, effectively imparting tolerance to the plants by regulating their carbon, nitrogen, energy and antioxidant metabolisms. Since *Arabidopsis thaliana* is a model plant and the information generated from studying this system needs to be translated to a crop of commercial importance, we studied soybean from whose rhizosphere the signal compounds were first isolated and characterized. This is the first attempt to study the proteome responses of bacterial signals in soybean. In this chapter 5, we hypothesized that the LCO and Th17 promoted soybean seed germination under unstressed conditions and alleviated the negative effects of high salt stress on seed germination. Consequently the objectives of this work were to screen the compounds for seed germination under unstressed and a series of salt stress conditions, followed by label free proteomics on the unstressed and the most effective signal treatments under salt stressed conditions, using LC-MS/MS.

5.1 Abstract

Salt stress is an important abiotic stressor affecting crop growth and productivity. Of the 20 % of the terrestrial earth's surface available as agricultural land, 50 % is estimated by the United Nations Environment Program (The UNEP) to be salinized to the level that crops growing on it will be salt-stressed. Increased soil salinity has profound effects on seed germination and germinating seedlings as they are frequently confronted with much higher salinities than vigorously growing plants, because germination usually occurs in surface soils, the site of greatest soluble salt accumulation. The growth of soybean exposed to 40 mM NaCl is negatively affected, while an exposure to 80 mM NaCl is often lethal. When treated with the bacterial signal compounds lipochitooligosaccharide (LCO) and thuricin 17 (Th17), soybean seeds (variety Absolute RR) responded positively at salt stress of up to 150 mM NaCl. Shotgun proteomics of unstressed and 100 mM NaCl stressed seeds (48 h) in combination with the LCO and Th17 revealed many known, predicted, hypothetical and unknown proteins. In all, carbon, nitrogen and energy metabolic pathways were affected under both unstressed and salt stressed conditions when treated with signals. PEP carboxylase, Rubisco oxygenase large subunit, pyruvate kinase, and isocitrate lyase were some of the noteworthy proteins enhanced by the signals, along with antioxidant glutathione-S-transferase and other stress related proteins. These findings suggest that the germinating seeds alter their proteome based on bacterial signals and on stress, the specificity of this response plays a crucial role in organ maturation and transition from one stage to another in the plants life cycle; understanding this response is of fundamental importance in agriculture and, as a result, global food security.

5.2 Introduction

Soil salinization, one of the most serious agricultural limitations worldwide, is exacerbated by a number of factors including climate (degree of water deficit), the inherent salt content of the soil, topography, underlying geology and hydrology (Wiebe et al., 2007). It is estimated that approximately 20 % of irrigated land, which yields one third of the world's food, is affected by salinity (Yan, 2008; Xu et al., 2011). A significant proportion of recently cultivated agricultural land has become saline because

of land clearing or irrigation (Munns, 2005) and the impact of irrigation-related salinity on agricultural productivity has been recognized in many parts of the world (Rengasamy, 2008). In Canada, dry-land salinity is a significant agronomic problem across the prairies (Acton and Gregorich 1995) where approximately 1 million ha is affected by moderate to severe topsoil salinity (Wiebe et al., 2007). A government of Alberta report suggests the dominant salts in prairie saline seeps are calcium (Ca), magnesium (Mg), sodium (Na) cations and sulfate (SO_4) anions, and that the impact of moderate to severe soil salinity [electrical conductivity of a saturated paste extract (ECe) of 8 to 16 dS m^{-1} and $\text{ECe} > 16 \text{ dS m}^{-1}$, respectively] is apparent for almost all crops produced under dry-land agriculture conditions in this region, with yield reductions up to 50% in cereals and oilseeds crops (Wiebe et al., 2007).

Sodium chloride (NaCl), is a dominant salt in nature; it reduces the ability of plants to take up water (water deficit effect) and other essential nutrients (ion-excess effect) (Munns et al., 2005, 2006). Salt stress causes changes in plant growth due to (1) osmotically-induced water stress, (2) specific ion toxicity due to high concentration of sodium and chloride, (3) nutrient ion imbalance, due to high level of Na^+ and Cl^- which reduce the uptake of K^+ , NO_3^- , PO_4^{3-} and (4) increased production of reactive oxygen species which damage macromolecules inside plant tissue, all of which result in plant growth reduction (Greenway and Munns, 1980). For instance, salt stress enhances the accumulation of NaCl in chloroplasts of higher plants which affects their growth rate, and is often associated with a decrease in photosynthetic electron transport activities (Kirst, 1990). Additionally, in higher plants, it inhibits photosystem (PS)-II activity (Kao et al., 2003; Parida et al., 2003). Therefore, the presence of saline soils substantially alters plant metabolic processes (Levitt, 1980).

Soybean, an important crop legume grown commercially around the world; it is known for the high oil and protein contents of its seeds (Qui and Chang, 2010). Globally, it is one of the main sources for edible vegetable oil and protein and an important livestock feed. For example, the United States of America produced 83,171,600 t while Canada produced 4,246,300 t of soybean in 2011 (FAO Stat, 2013). In addition, soybean cultivation improves soil health through its ability to fix atmospheric nitrogen (thereby

reducing the need for synthetic nitrogen fertilizers) and its deep root system (allowing for soil carbon sequestration) (Qui and Chang, 2010). However, soybean is a salt-sensitive crop (Lauchli, 1984), and its production is severely affected by saline soils (Xu et al., 2011). Soybean exposed to 40 mM NaCl was strongly and negatively affected, while an exposure to 80 mM NaCl was lethal for cv. Enrei (Sobhanian et al., 2010). High salinity results in inhibited seed germination and seedling growth, decreased chlorophyll content, reduced nodulation, decreased biomass accumulation, lowered pod numbers and decreased seed weight, and finally, reduced yields (Essa, 2002; Hamayun et al., 2010). In addition, it was shown that salinity inhibits the expansion and curling of root-hairs and reduced the number of nodules in faba bean (Tu, 1981).

Apart from its nutritive value, the soybean-*Bradyrhizobium* symbiosis is one of the most studied in biological nitrogen fixation. A successful interaction between a legume plant and the appropriate rhizobial bacterium leads to the formation of a new plant organ, the nodule, which is generally formed on plant roots; bacteria reside inside the nodule, in the form of bacteroids, and fix atmospheric dinitrogen into ammonia (Perret et al., 2000). Nodule formation is a highly specialized two step process that requires cross-talk between the bacteria and the host plant, wherein the host plants release signal molecules such as flavonoids and iso-flavonoids, which induce the transcription of bacterial nodulation genes leading to the biosynthesis and secretion of lipochitooligosaccharides (LCOs), called Nod factors, which act as bacteria-to-plant signal molecules (Currier and Strobel, 1976; Firmin et al., 1986; D'Haeze and Holsters, 2002). Nod factors consist of a chitooligosaccharide backbone of three to five β -1,4-linked N-acetyl-D-glucosamine residues, substituted by a fatty acyl chain of varying lengths and with varying degrees of unsaturation, attached at the non-reducing end (Maj et al., 2009). Signal molecules, such as LCOs, have been shown to affect aspects of plant metabolism and enhance growth for a variety of agriculturally important plants. For example, LCO has been shown to induce rapid and transient alkalization of tobacco (Baier et al., 1999) and tomato cells (Staehelin et al., 1994) in suspension cultures. Restoration of cell division and embryo development in temperature-sensitive mutants of carrot (De Jong et al., 1993) was observed. LCO treatment of clover seeds enhanced clover nodulation and growth (Maj et al., 2009). Inoculation with rhizobia or application of Nod factors (lipo-

chitooligosaccharides, LCOs) causes transient increases in cytosolic calcium concentration in root hairs of legume plants (Supanjani et al., 2006), leading to enhanced plant growth. Positive LCO effects have also been reported from our laboratory related to enhanced germination and early plant growth in corn, rice, beet, cotton and mung bean (Prithiviraj et al., 2003). The first microarray study in our laboratory used spray of LCO on (nodulating OAC Bayfield and non-nodulating Evans x L66-2470); this showed an increase in guaiacol peroxidase activity, while chitinase and β -1,3-glucanase were unaffected (Lindsay 2007). More recent research in our laboratory, on soybean leaves treated with LCOs and under sub-optimal growth conditions, revealed the up-regulation of over 600 genes, of which the largest group of known genes are related to defense and stress, and transcription factors of genes in this category. The microarray results show that the transcriptome of the leaves is highly responsive to LCO treatment at 48 h post treatment under low temperature stress (Wang et al., 2012). The results of microarray analysis suggested the need to investigate more carefully the mechanisms by which microbe-to-plant signals aid plants in accommodating abiotic stress conditions.

Some rhizobacteria produce bacteriocins, which increase their adaptability and competitiveness in their specific ecological niche (Kirkup and Riley, 2004). Bacteriocins are bacterially produced proteins/peptides that are either bacteriostatic or bacteriocidal against strains related to the producer strain (Jack et al., 1995), thus, they provide competitive advantage for the producer strain (Wilson et al., 1998) and may enhance nodule occupancy when the producer strain is an appropriate member of the rhizobia (Oresnik et al., 1999). In addition, PGPRs can promote plant growth and development via direct and indirect mechanisms (Jung et al., 2008a). Antibiotic production is one of the mechanisms that PGPR employ to promote plant growth, thereby playing an important role in the bio-control of plant pathogens (Bloemberg and Lugtenberg, 2001; Fravel, 1988 and Riley and Wertz, 2002). For example, *Bacillus thuringiensis* NEB17 is a non-bradyrhizobium endophytic bacterium, a PGPR isolated from soybean root tissue (Bai et al., 2002) that releases the class II δ bacteriocin thuricin 17 (Th17), (3,162 Da) (Gray et al., 2006a,b). Bacteriocins such as thuricin 17 have been shown to enhance plant growth in a variety of crops. Application of Th17 to leaves (spray) or roots (drench) directly stimulates the growth of both soybean and corn (Lee et al., 2009). Furthermore,

when applied as a co-inoculant with *Bradyrhizobium japonicum* 532C, *B. thuringiensis* NEB17 has been shown to enhance soybean root nodulation and plant growth (Bai et al., 2003).

Seeds and young seedlings are frequently confronted with much higher salinities than vigorously growing plants, because germination usually occurs in the uppermost soil layers, which is generally the site of highest soluble salt accumulation (Almansouri et al., 2001). Since plant species vary in how well they tolerate salt-affected soils, it would be beneficial to enhance crop salt tolerance, using cost effective strategies, in order to meet rising global food demand. Although studies on the role of PGPRs under unstressed conditions are plentiful, the characterization of the beneficial responses to salt stressed plants are few. We attempted to study the modes of action of LCO and Th17 in germinating soybean seeds under unstressed and salt-stressed conditions using a shotgun proteomics approach. In addition, there is limited information available regarding salt-response genes, and the proteins they code for, in the soybean-bradyrhizobium symbiosis. The objective of this work was to understand plant proteomic responses to LCO and Th17 treatment under unstressed and salt-stressed conditions.

5.3 Materials and methods

5.3.1 Plant material

Soybean seeds (*Glycine max* (L.) Merrill, cv. Absolute RR) were procured from BelCan, QC, Canada, and used for all the studies on germination and proteomics reported herein.

5.3.2 Extraction and purification of Lipo-chitooligosaccharides (LCO)

The extraction and purification of LCOs followed the method of Souleimanov et al. (2002b). In brief, *B. japonicum* cultures were extracted with 40% HPLC-grade 1-butanol. The culture supernatant was carefully removed and condensed in a low-pressure rotary evaporator system (Yamato RE500, Yamato, USA) at 50 °C at a speed of 125 rpm, until dryness, and the dried extract was resuspended in 4 mL of 18 % acetonitrile. The resuspended extract was loaded onto a C-18 column (PRESEP™ Fisher Scientific,

Montreal, Canada) and eluted three times using 10 mL of 30% acetonitrile and finally using, 60% acetonitrile. The Nod factors were further isolated and purified by HPLC (Waters 501 pumps, a Waters 401 detector set at 214 nm and a WISP712 autosampler using a C18 reverse phase column (0.46 X 25 cm, 5 μ m) - Vydac, CA, USA; catalogue # 218TP54). Chromatography was conducted for 45 min using a linear gradient of acetonitrile from 18 to 60 % as described by Souleimanov et al. (2002b). Identification of Nod factors was conducted by comparing the retention time of standard Nod factors from strain 532C (identified by mass spectrometry).

5.3.3 Extraction of Thuricin 17 (Th17)

Bacillus thuringiensis NEB17 was cultured in King's B medium (King et al., 1954) as previously described (Gray et al., 2006a). In brief, the culture in King's B medium was incubated on an orbital shaker for 32 h after which this inoculum was subcultured into 4.0 L flasks containing 2.0 L of medium and allowed to grow for 48 h. Th17 isolation and purification was carried out using High Performance Liquid Chromatography (HPLC) using the procedures of Gray et al. (2006b). The collected material was denoted as partially purified Th17 and stored at 4° C.

For all experiments, LCO and Th17 were dissolved in water (Cat no. 95304, HPLC grade, Sigma-Aldrich Co., St. Louis, MO, USA) to produce uniform stock solutions and were diluted to the desired concentrations. In all germination experiments LCO concentrations of 10^{-6} and 10^{-8} M, and Th17 concentrations of 10^{-9} and 10^{-11} M were used. These are the concentrations which were found to be the best in previous plant growth response studies (Prithiviraj et al., 2000; Souleimanov et al., 2002a; Lee et al., 2009).

5.3.4 Seed germination

Uniform medium sized seeds were selected and were placed in Petri dishes (Cat. no. 431760, sterile 100 mm x 15 mm polystyrene Petri dish, Fisher Scientific Co., Whitby, ON, Canada) lined with filter paper (09-795D, Qualitative P8, porosity coarse, Fisher Scientific Co., Pittsburg, PA, USA) and containing salt 0, 100, 125, 150, 175 and 200 mM NaCl. Each of the salt concentrations were combined with 10^{-6} M and 10^{-8} M

LCO and 10^{-9} M and 10^{-11} M Th17 in order to determine levels of salt tolerance imparted by these bacterial compounds. The plates were incubated in a germination chamber set at 25 °C and 70 % RH in darkness. Percentage germination was scored at 24, 30, 36 and 48 h after the experiment was initiated.

5.3.5 Label free proteomics

For the proteome analysis, germinated seeds from the unstressed condition, including the water-only control, 10^{-6} M LCO, 10^{-9} M Th17, and the salt stressed condition, including 100 mM NaCl as the salt-stressed control, and combinations of 100 mM NaCl with 10^{-6} M LCO and 10^{-9} M Th17, were sampled and total proteins extracted using a protein extraction kit (Cat. no. PE-0230, Plant total protein extraction kit, Sigma-Aldrich, Co., St. Louis, MO, USA).

5.3.5.1 Protein extraction

In brief, the sampled (pool of 10 seeds per replicate) seeds were ground to a fine powder in liquid nitrogen. Approximately 100 mg of the fine powder was placed in sterile eppendorf tubes and 1 mL of ice cold methanol (Cat no. 15468-7, Sigma-Aldrich Co., St. Louis, MO, USA) was added, vortexed, incubated in -20 °C for 20 min. and centrifuged (Micro12, Fisher Scientific, Denver Instrument Co., USA) at 13,000 rpm for 7 min. at 4 °C. The supernatant was discarded and the procedure was repeated twice more, followed by similar incubation in acetone (Cat. no. 179124, Sigma-Aldrich, Co., St. Louis, MO, USA), both steps in order to remove phenolics and secondary metabolites that might otherwise interfere with LC-MS/MS analysis. The RW2 solution was added to the samples after removing acetone, vortexed for 30s and incubated at room temperature (22 °C) for 15 min. The samples were then centrifuged at 13,000 rpm for 10 min and the supernatant carefully collected in a fresh sterile tubes. The supernatant constituted total proteins from that sample. The proteins were then diluted and quantified using the Lowry method, and samples of 10 µg in 20 µL of 1M urea were taken to the Institut de recherches cliniques de Montréal (IRCM) for label free proteomic analysis using LC-MS/MS.

5.3.5.2 Proteome profiling

The total proteins extracted were then digested with trypsin and subjected to LC-MS/MS using a Velos Orbitrap instrument (Thermo Fisher, MA, USA). Tandem mass spectra were extracted, charge state deconvoluted and deisotoped and all MS/MS samples were analyzed using Mascot (Matrix Science, London, UK; version 2.3.02). Mascot was set up to search the Soybean_20120801 database (unknown version, 80416 entries) assuming the digestion enzyme trypsin. Mascot searched with a fragment ion mass tolerance of 0.60 Da and a parent ion tolerance of 15 PPM. Carbamidomethyl of cysteine was specified in Mascot as a fixed modification. Oxidation of methionine was specified in Mascot as a variable modification.

Criteria for protein identification - Scaffold (version Scaffold_3.4.7, Proteome Software Inc., Portland, OR), was used to validate MS/MS based peptide and protein identifications. Peptide identifications were accepted if they could be established at greater than 95.0 % probability, as specified by the Peptide Prophet algorithm (Keller et al., 2002). Protein identifications were accepted if they could be established at greater than 99.0 % probability and contained at least 2 identified peptides. Protein probabilities were assigned by the Protein Prophet algorithm (Nesvizhskii, 2003). Proteins that contained similar peptides, and could not be differentiated based on MS/MS analysis alone, were grouped to satisfy the principle of parsimony.

5.3.6 Data analysis

Experiments were structured following a completely randomized design. The SAS statistical package 9.3 (SAS Institute Inc., Cary, NC, USA.) was utilized. The Proc Mixed procedure and Tukey's multiple means comparison were used to determine differences among means at the 95 % confidence level.

Scaffold 3.4.7 was used to analyze the proteomics data for fold change and Fisher's exact test of the identified proteins, after subjecting the quantitative value of the spectra to the embedded normalization. Scatter plots of the contrasts were also generated using this software, while the FASTA file generated was analyzed using Blast2GO-Pro V.2.6.6 (Conesa et al., 2005; Conesa and Götz, 2008; Götz et al., 2008, 2011), for the

functional annotation and analysis of the protein sequences. Apart from these, Enzyme code (EC), KEGG maps and InterPro motifs were queried directly using the InterProScan web service.

5.4 Results

5.4.1 Seed germination

In order to evaluate the role of the bacterial signal compounds LCO and Th17 on soybean seed germination and under salt stress, germination pattern was studied on seeds treated with two concentrations of LCO (10^{-6} and 10^{-8} M) and Th17 (10^{-9} and 10^{-11} M) in combination with 100, 125, 150, 175 and 200 mM NaCl. Salinity stress severely affected seed germination by delaying the onset of germination in this cultivar (Fig. 5.1a,b,c; Please refer to Table 5.1 in Appendix III), and the evaluated signals compounds substantially helped overcome the negative effects of salt stress, however, in the absence of stress the compounds did not result in statistically significant differences in the germination pattern.



Fig. 5.1a: Soybean seed germination 48h post treatment (un-stressed) at 25 °C in dark, at 70 % relative humidity.



Fig. 5.1b: Soybean seed germination 48 h post treatment under 100 mM NaCl stress at 25 °C in dark, at 70 % relative humidity.

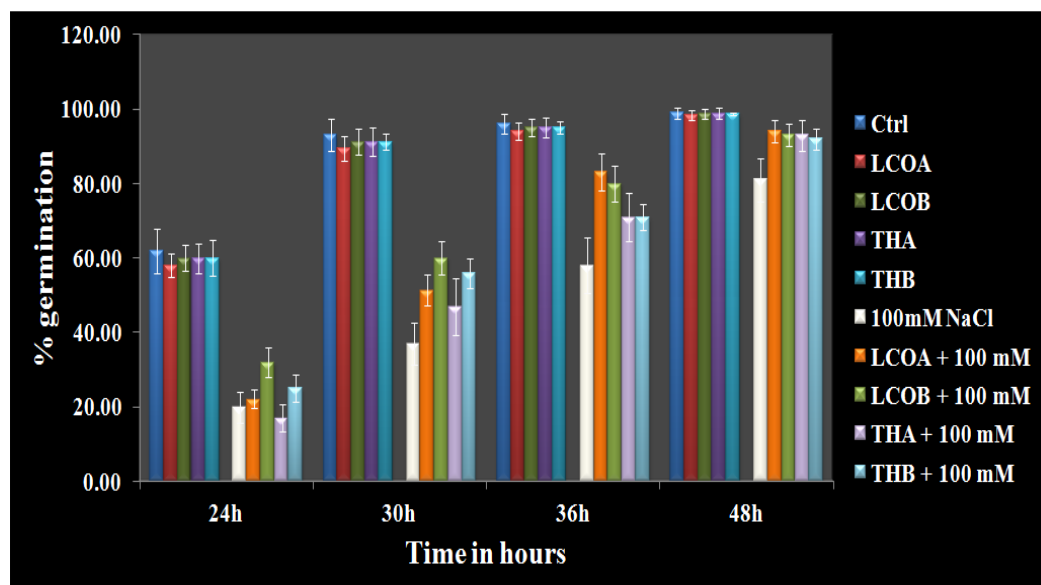


Fig. 5.1c: Bar chart representing soybean seed germination under optimal and 100 mM NaCl stress at 25 °C in dark, at 70 % relative humidity (Ctrl - Water control, LCOA - 10^{-6} M; LCOB - 10^{-8} M; THA - 10^{-9} M; THB - 10^{-11} M).

LCO and Th17 helped germinating soybean seeds overcome salinity stress and did this most effectively at 100 mM NaCl, when measured at 48 h after the onset of germination, although seeds continued to germinate at higher levels of stress. In order to study the effects of the signal compounds and salt stress on germination, 48 h germinated seeds from the unstressed and salt stressed at 100 mM NaCl treatments, in the presence of signals, were sampled for label free proteomics.

5.4.2 Proteome profiling

To understand the effect of LCO and Th17 on unstressed and salt stressed germinated seeds, total proteins were extracted from the samples and subjected to LC-MS based proteome profiling. Based on the quantitative value of the identified spectra, and at 99 % protein probability, with 2 minimum peptides and 95 % peptide probability, 424 proteins were identified at a 0.0 % protein FDR (False discovery rate) with 55358 spectra at 0.0 % peptide FDR for the signals without stress group (Fig. 5.2). Similarly, for the signals with 100 mM NaCl group, 372 proteins were identified at 0.0 % protein FDR, with 52261 spectra at 0.0 % peptide FDR (Fig. 5.2). The treatment contrasts were then analyzed for fold-change after normalization, and Fisher's Exact test was used to narrow down the set of up- and down-regulated proteins, to predict their probable functions at the 48 h time point. It is likely that we missed some of the proteins due to very strict criteria for difference detection during data analysis; however, this level of stringency was utilized for ease of subsequent functional interpretation.

According to the fold-change patterns and Fisher's Exact test of the contrasts, the proteins were categorized as known proteins, predicted proteins, unknown proteins and unnamed protein products (Table 5.2a, 5.2b).

Table 5.2a: Grouping of proteins that were significant in the contrasts based on Fold change.

Treatment contrasts (Fold change)	Control vs. LCO	Control vs. Th17	LCO vs. Th17	Control 100 mM NaCl vs. LCO + 100 mM NaCl	Control 100 mM NaCl vs. Th17 + 100 mM NaCl	LCO 100 mM NaCl vs. Th17 + 100 mM NaCl
Total significant proteins	78	82	25	34	26	28
Known proteins	10	14	3	3	2	6
Predicted proteins	30	32	10	10	9	12
Unknown proteins	25	24	7	18	9	6
Unnamed protein products	13	12	5	3	6	4

Table 5.2b: Grouping of proteins that were significant based on Fisher's Exact test.

Treatment contrasts (Fisher's Exact test)	Control vs. LCO	Control vs. Th17	LCO vs. Th17	Control 100 mM NaCl vs. LCO + 100 mM NaCl	Control 100 mM NaCl vs. Th17 + 100 mM NaCl	LCO 100 mM NaCl vs. Th17 + 100 mM NaCl
Total significant proteins	82	111	13	14	23	24
Known proteins	28	37	10	10	10	14
Predicted proteins	20	33	1	2	6	4
Unknown proteins	20	25	1	2	3	4
Unnamed protein products	14	16	1	0	4	2

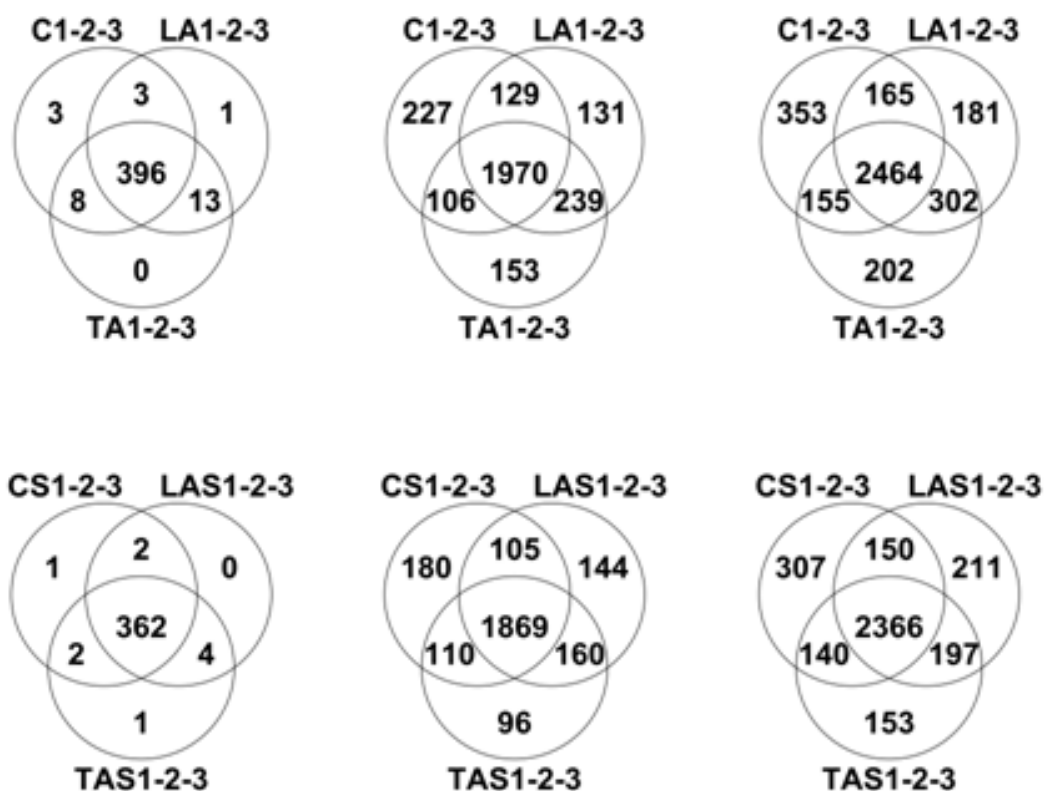


Fig. 5.2: Venn diagram for the output of differentially expressed proteins, unique peptides and unique spectra based on Scaffold in the top row – un-stressed group (C = Control-water, LA = LCO 10^{-6} M, TA = Th17 10^{-9} M) and the bottom row – salt stressed group (CS = 100 mM NaCl Control, LAS = LCO 10^{-6} M + 100 mM NaCl, TAS = Th17 10^{-9} M + 100 mM NaCl. 1-2-3 = biological replicates data grouped)

Based on the known and predicted proteins, some of the prominent proteins in unstressed control seeds included metallothionein, stearyl-acyl carrier, thioredoxin, phosphogluconate dehydrogenase, a 97 kDa heat shock protein (HSP), α and β -subunits of conglycinin, glycinin, lipoxygenase 1, 2 and 3, embryonic protein DC8 like and sucrose binding protein. Glutathione S transferase, peroxisomal voltage dependent anionic channel (VDAC) protein, PEP carboxylase, uricase, alcohol dehydrogenase, arginosuccinate synthase, phosphoglycerate kinase, importin subunit, IN2 homologue, oleosin isoform, and universal stress protein were some of the notable proteins up-regulated by LCO treatment. The Th17 treated seeds were up-regulated for the proteins just mentioned for LCO treatment, and also showed a marked increases (2-fold and above) in auxin-like protein, Rubisco oxygenase large subunit, Kunitz type trypsin inhibitor, stearyl acyl carrier, isocitrate lyase and pyruvate kinase. Both LCO and Th17 caused up-regulation of PEP carboxylase but the α - and β -subunits of conglycinin, glycinin showed a marked down-regulation as compared to control. [Please refer Appendix II for Fold change (Table 5.3a,b,c) and Fisher's Exact test results (Table 5.4a,b,c) for soybean signals group contrasts and scatter plots of contrasts (Fig 5.4a,b,c)].

The number of significant proteins identified in the salt stressed signals group was remarkably lower than the signals-only group, especially in the Control vs LCO and Control vs Th17 contrasts. The salt stress control (salt stress in the absence of signals) resulted in up-regulation of aspartic proteinase, PEP carboxylase, lipoxygenase 1, predicted dehydrin-like protein and mannose phosphate isomerase, while the salt stress with LCO caused up-regulation of glutathione-S- transferase, a predicted auxin-induced protein, pyruvate kinase, importin subunit, and predicted PR5 protein. The salt stress with Th17 treatment caused up-regulation of aspartic proteinase, predicted auxin-induced protein, mannose phosphate isomerase, glyceraldehydes phosphate dehydrogenase, Lea protein, Bowman-Birk proteinase inhibitor, oleosin isoform A and B and a dehydrin-like protein, as compared to salt stress alone (control for this group) and LCO. [Please refer Appendix II for Fold change (Table 5.3d,e,f) and Fisher's exact test results (Table 5.4d,e,f) for soybean signals and salt group contrasts and scatter plot for contrasts (Fig 5.4d,e,f)].

Based on Blast2GO Pro results, the enzyme code distribution for both the unstressed and salt stressed seeds were studied. A sharp decrease in some of the main enzyme classes was observed in the salt stress group as compared to the unstressed group (Fig. 5.3). While the oxidoreductases, hydrolases, lyases and isomerases decreased by 21.02, 37.9, 27.45 and 16 %, respectively, transferases and ligases decreased by 2 and 7 %, respectively (Table 5.5).

The GO function distribution characteristics of the unstressed and salt stressed groups also indicated that the proteins identified were mostly associated with the carbon metabolism, respiratory electron transport, tricarboxylic acid cycle metabolism, amino acid metabolism, protein import, protein processing, protein assembly, transcription, membrane transport, antioxidant defense, nutrient reservoir proteins, and proteins associated with abiotic stresses such as salt, cold and heat (Fig. 5.5a, 5.5b, 5.5c). Molecular function, biological processes and cellular components were all affected in both unstressed and salt-stressed conditions. There was a down-regulation of most of the important components in all the above mentioned functions under salt stress, and especially so with ATPase activity, heme binding, oxidation-reduction processes, proteosome core and regulatory complex subunits, photorespiration, meristem structural organization, response to oxidative stress and leaf morphogenesis related proteins. However, other functional classes such as cation binding, nucleotidyltransferase activities, nucleosome and nucleosome assembly, GTP catabolic processes, cytoskeleton organization and mature ribosome assembly proteins were up-regulated in the salt stress group. There was no change in the patterns of GTP binding, protein heterodimerization activity, translation elongation factor activity, protein folding, cytoplasmic and mitochondria proteins (Table 5.6).

Based on the known and predicted proteins, as identified using fold-change and Fisher's exact test, we generated a metabolic pathway map (Fig. 5.6) that could explain, at least in part, the reason how and why the signal compounds LCO and Th17 promoted seed germination under unstressed conditions and compensate for negative effects on germination under salt stress.

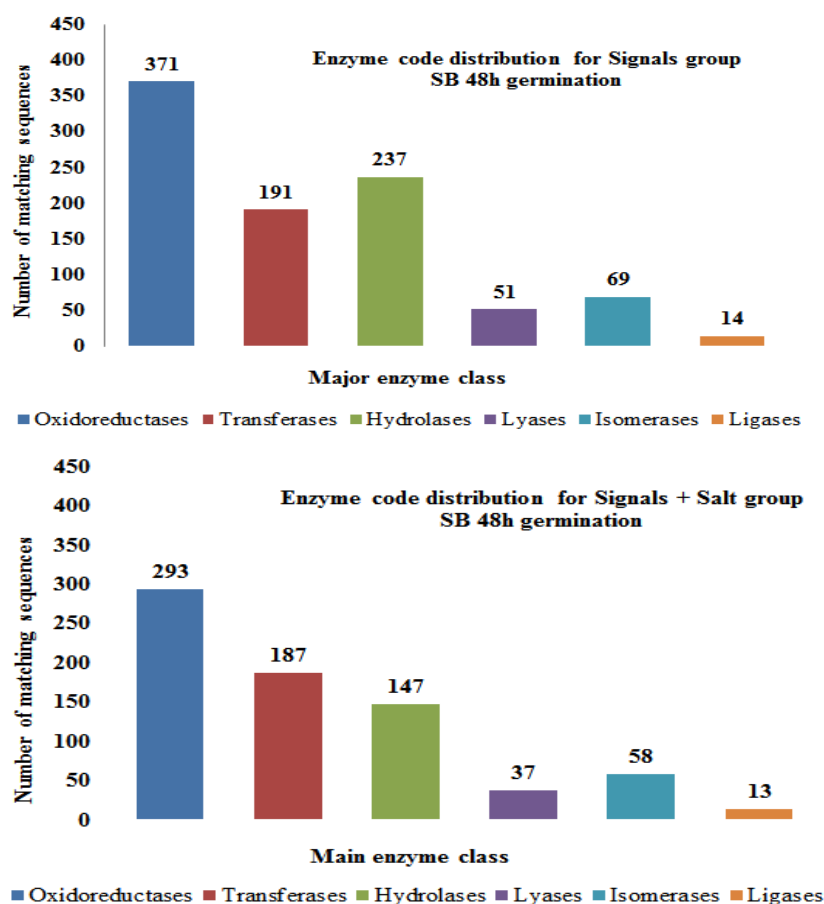
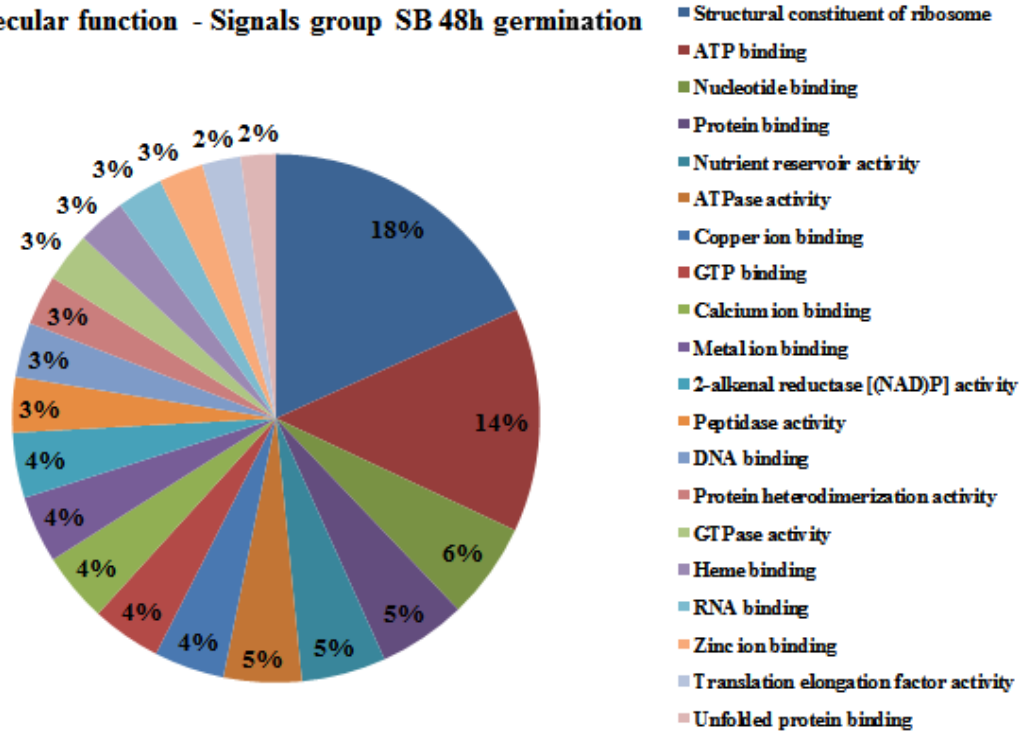


Fig. 5.3: Enzyme code distribution categorized based on main enzyme classes in signals group and signals + salt group

Table 5.5: Enzyme code distribution in un-stressed and salt stress groups. The % decrease in the main enzyme classes in the salt stress group is mentioned in the brackets.

Main enzyme classes	Sequence distribution in signals group	Sequence distribution in signals + salt group
Oxidoreductases	371	293 (↓ 21%)
Transferases	191	187 (↓ 2%)
Hydrolases	237	147 (↓ 37.9%)
Lyases	51	37 (↓ 27.45%)
Isomerases	69	58 (↓ 16%)
Ligases	14	13 (↓ 7%)

Molecular function - Signals group SB 48h germination



Molecular function - Signals and Salt stressed group SB 48h germination

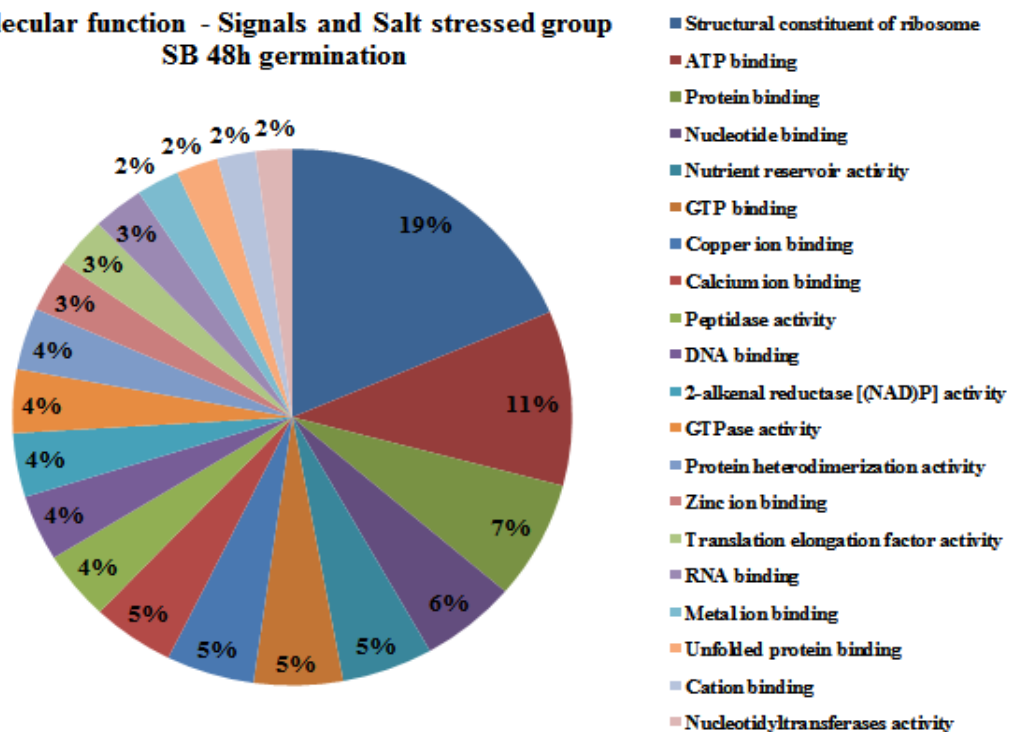
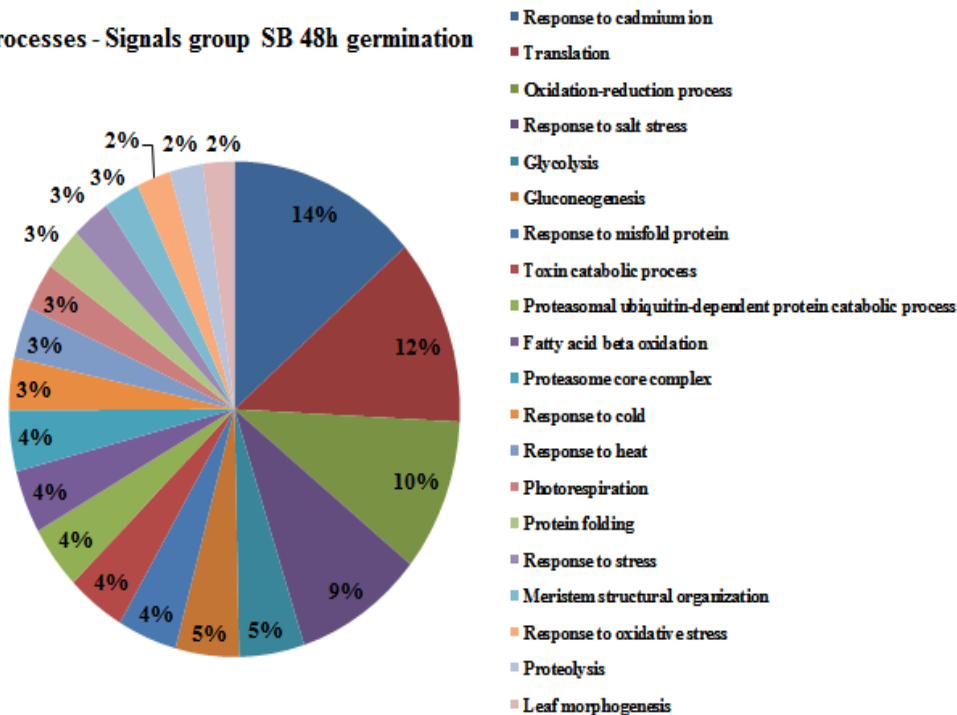


Fig. 5.5a: Pie chart representation of functional classification of the GO distribution for molecular function in the unstressed and salt stressed groups.

Biological processes - Signals group SB 48h germination



Biological processes - Signals and Salt stressed group SB 48h germination

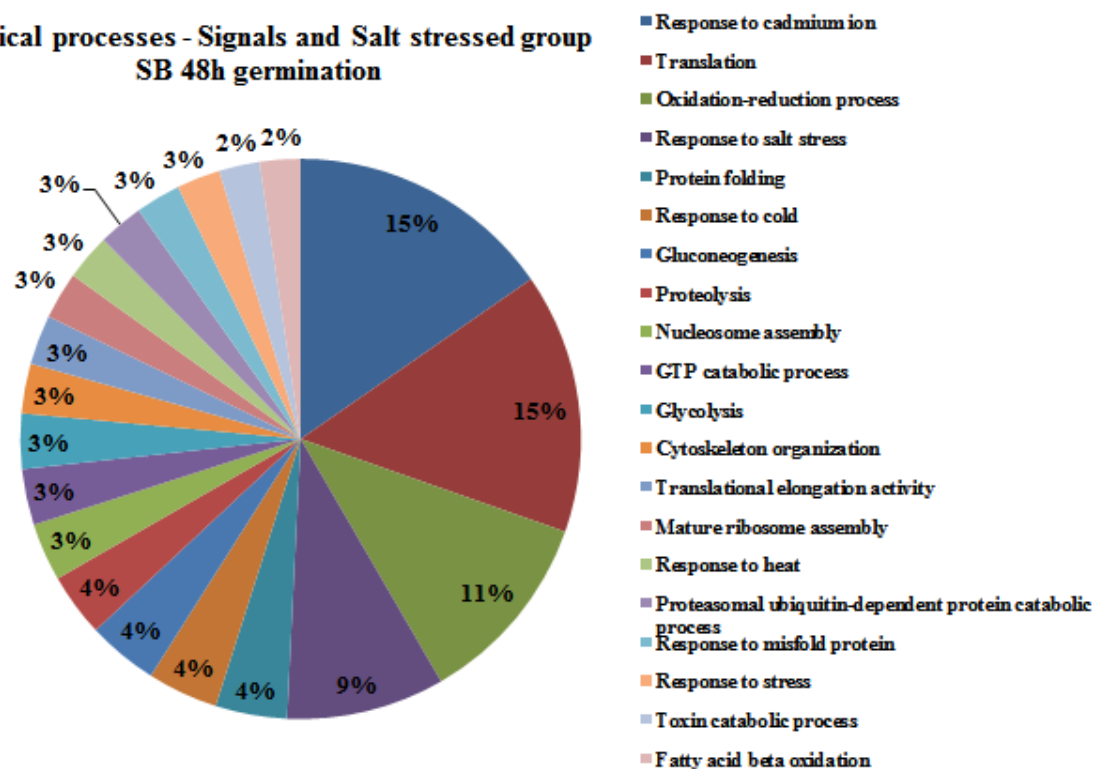
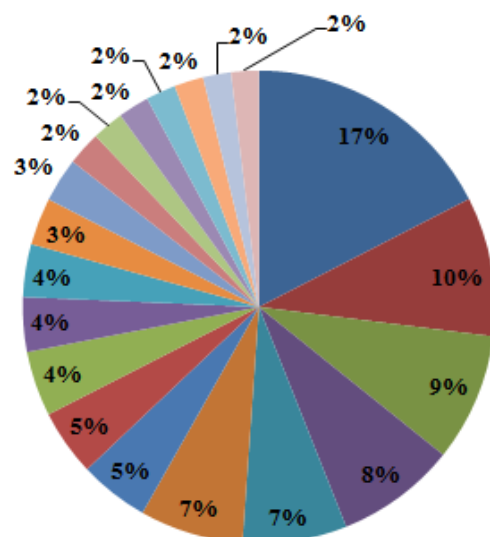


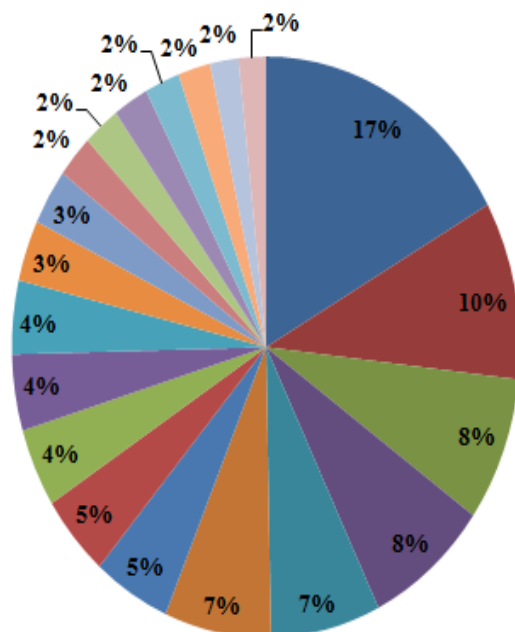
Fig. 5.5b: Pie chart representation of functional classification of the GO distribution for biological process in unstressed and salt stressed groups.

Cellular components - Signals group
SB 48h germination



- Plasmamembrane
- Cholorplast
- Cytosol
- Nucleus
- Vacuole
- Nucleolus
- Cytosolic ribosome
- Apoplast
- Cell wall
- Cytoplasm
- Mitochondrion
- Chloroplast stroma
- Cholorplast envelope
- Proteasome regulatory particle, base subcomplex
- Ribosome
- Membrane
- Plant-type cell wall
- Cytosolic large ribosome
- Integral to membrane
- Small ribosomal subunit

Cellular components - Signals and Salt stressed group
SB 48h germination



- Plasmamembrane
- Cholorplast
- Vacuole
- Nucleus
- Cytosol
- Nucleolus
- Cytosolic ribosome
- Apoplast
- Cytoplasm
- Mitochondrion
- Cell wall
- Chloroplast stroma
- Cholorplast envelope
- Plant-type cell wall
- Ribosome
- Membrane
- Cytosolic large ribosome
- Small ribosomal subunit
- Integral to membrane
- Nucleosome

Fig. 5.5c: Pie chart representation of functional classification of the GO distribution for cellular components in unstressed and salt stressed groups.

Table 5.6: GO function categories amongst un-stressed and salt stressed groups

Molecular function	No. of seq Signals	No. of seq Salt	Biological process	No. of seq Signals	No. of seq Salt	Cellular component	No. of seq Signals	No of seq Salt
Structural constituent of ribosome	356	300	Response to cadmium ion	384	294	Plasma membrane	721	584
ATP binding	267	170	Translation	343	288	Cholorplast	394	344
Nucleotide binding	115	390	Oxidation-reduction process	280	0	Cytosol	362	242
Protein binding	105	115	Response to salt stress	260	175	Nucleus	340	273
Nutrient reservoir activity	101	85	Glycolysis	132	61	Vacuole	295	279
ATPase activity	93	0	Gluconeogenesis	128	78	Nucleolus	293	235
Copper ion binding	84	82	Response to misfold protein	120	50	Cytosolic ribosome	197	170
<i>GTP binding</i>	83	83	Toxin catabolic process	118	45	Apoplast	187	159
Calcium ion binding	83	77	Proteasomal ubiquitin-dependent protein catabolic process	117	50	Cell wall	184	142
Metal ion binding	80	40	Fatty acid beta	116	45	<i>Cytoplasm</i>	<i>154</i>	<i>152</i>

			oxidation					
2-alkenal reductase [(NAD)P] activity	78	62	Proteasome core complex	112	0	Mitochondrion	149	147
Peptidase activity	66	67	Response to cold	96	78	Chloroplast stroma	134	118
DNA binding	65	64	Response to heat	95	51	Chloroplast envelope	125	108
Protein heterodimerization activity	60	60	Photorespiration	87	0	Proteasome regulatory particle, base subcomplex	95	0
GTPase activity	59	62	Protein folding	79	79	Ribosome	90	81
Heme binding	58	0	Response to stress	78	48	Membrane	88	78
RNA binding	55	48	Meristem structural organization	72	0	Plant-type cell wall	84	82
Zinc ion binding	53	51	Response to oxidative stress	68	0	Cytosolic large ribosome	83	77
Translation elongation factor activity	46	49	Proteolysis	67	70	Integral membrane to	79	63
Unfolded protein binding	42	39	Leaf morphogenesis	64	0	Small ribosomal subunit	78	71

Nucleotidyltransferases activity	0	34	Nucleosome assembly	0	64	Nucleosome	0	60
Cation binding	0	36	GTP catabolic process	0	61			
			Cytoskeleton organization	0	55			
			Mature ribosome assembly	0	52			

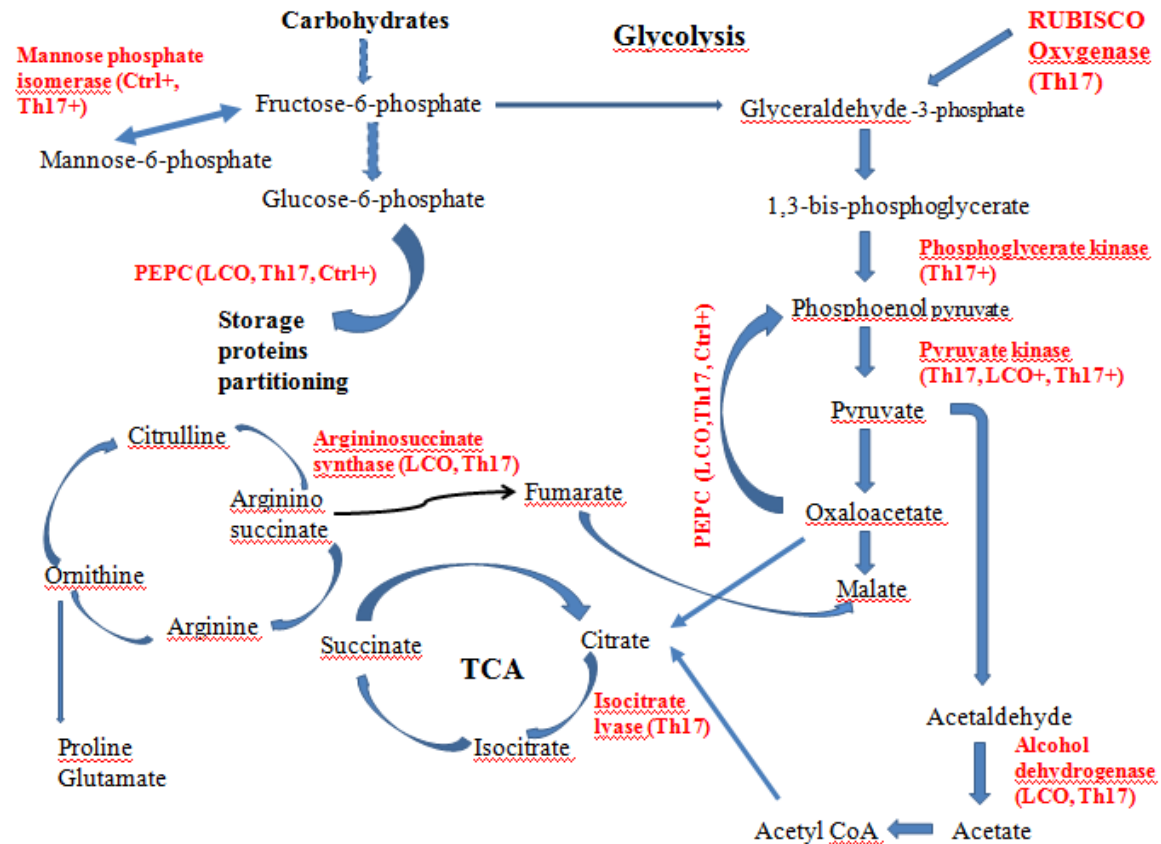


Fig. 5.6: Co-regulation of metabolic pathway components in soybean seeds after 48 h from the onset of germination, as reflected by label free proteomics data. Unstressed group includes Control (Ctrl), 10^{-6} M LCO (LCO), 10^{-9} M Th17 (Th17); and the salt stressed group includes Control 100 mM NaCl (Ctrl+), 10^{-6} M LCO + 100 mM NaCl (LCO+), 10^{-9} M Th17 + 100 mM NaCl (Th17+). Those in red are the up-regulated proteins in the different treatments mentioned in brackets.

5.5 Discussion:

Seed germination is an important event in the initiation of a plant's life and hence is a complicated physiological process, and is also important in agriculture. Under favourable circumstances, many biochemical processes are revoked and new processes are initiated for the development and establishment of a new seedling. The major LCO molecule produced by *B. japonicum* 532C, Nod Bj V (C18:1; MeFuc), isolated and identify confirmed in our laboratory, has been reported to have a positive and direct effects on both legume and non-legume seed germination, and plant growth and development (Prithiviraj et al., 2003). LCO can enhance seed germination and seedling establishment for soybean, common bean, maize, rice, canola, apple and grapes, and can be accompanied by increased photosynthetic rates (Zhang and Smith, 2001). Our investigations into these effects, at molecular level, led us to transcriptomic studies, and microarray studies from our laboratory, on soybean leaves treated with LCOs under sub-optimal growth conditions, revealed the up-regulation of over 600 genes. Many of these were defense and stress response related, or transcription factors related to these responses, suggesting that the effect of LCO at the transcriptome of the leaves at 48 h post treatment is at least partly centred around stress responses (Wang et al., 2012). These results suggest the need to further investigate the mechanisms by which microbe-to-plant signals might help plants accommodate abiotic and biotic stress conditions. However, Th17 has not been as well studied as LCO, as it is was more recently isolated, although we have some information regarding its effects on soybean and corn plant growth (Jung et al., 2008a; Lee et al., 2009).

Hence, in this study we performed germination tests to evaluate the efficacy of both LCOs and Th17 on germination under unstressed and salt stressed conditions for the soybean cultivar absolute RR. These compounds alleviated salt stress inhibition of germination up to 150 mM NaCl, with the best response (greatest reversal of salt stress inhibition) was seen at 100 mM NaCl. As the concentration of salt increased in the treatments, higher salt concentrations resulted in reduced seed germination and was similar in pattern to previous studies on soybean germination under salt stress, despite differences in the cultivar studied (Komatsu et al., 2009a).

With the advances in instrumentation and bioinformatic analysis, it is now becoming evident that proteins and effects on proteins can provide key evidence regarding shifts in plant physiology, since they play central roles in essentially all metabolic processes. Despite these advances, proteome profiling in systems biology is still a major challenge. However, the amount of information they can add to the understanding of a biological system is impressive. In this study we used the label free proteomics approach to understand soybean seed germination in the presence of microbial signal compounds and under unstressed and 100 mM NaCl stressed conditions.

From the known and predicted proteins identified, some of the up-regulated proteins in unstressed control seeds included a metallothionein. Metallothioneins are a group of proteins with highly conserved cysteines and have metal binding attributes that are important for plant nutrient acquisition, survival and development (Leszczyszyn et al., 2013). Plant metallothioneins are of at least of four types, 1-4 (pMT); some information is available regarding soybean pMT type 4, the transcripts of which are approximately 375 fold more abundant in seeds than to other soybean seed pMTs (Pagani et al., 2012). The presence of metallothionein in our study might indicate the up-regulation of molecular functions related to copper, zinc, heme, metal ion binding, and the nutrient reservoir activities.

Thioredoxins comprise a group of proteins that modulate redox potential and regulate various enzymatic processes in metabolic pathways, and act as functional components of antioxidant pathways (Arnér and Holmgren, 2000; Meyer et al., 2005). Thioredoxin from soybean nodules has been reported to play an important role in the nodulation process and in nitrogen metabolism (Lee et al., 2005; Du et al., 2010). During nodulation, nodulin-35, a subunit of uricase is proposed to be a possible target for thioredoxin (Du et al., 2010). The presence of phosphoenol pyruvate carboxylase in our contrasts is not surprising since, the interactions of thioredoxins with the enzymes of carbon metabolism have been demonstrated earlier (Montrichard et al., 2009).

The major storage proteins of soybean seeds are α and β -subunits of conglycinin and glycinin; β -conglycinin and glycinin degrade rapidly and their degradation products accumulate or degrade further as the seeds germinate. This degradation, by proteolysis,

provides amino acids and energy for the growing seedlings (Kim et al., 2011). Both LCO and Th17 caused up-regulation of PEP carboxylase, and degraded the α - and β -subunits of conglycinin, and glycinin as compared to the levels in control treatment seeds. In addition, degradation of seed storage proteins is carried out by thioredoxins in cereals (Wong et al., 1995), and it is probable that similar mechanisms occur in soybean seeds as well, given the faster rate of storage protein depletion in LCO and Th17 treated seeds. In non-photosynthetic tissues such as oil-containing seeds, phosphoenol pyruvate plays an important role in channelizing carbohydrates to plastidic fatty acid oxidation, production of ATP in the mitochondria, replenishing tricarboxylic acid pathway intermediates and synthesis of organic acids for the biosynthesis of essential amino acids and in nitrogen assimilation. All these coordinate the efficacious use of seed storage proteins during seedling establishment (Plaxton and Podesta', 1996; Ruuska et al., 2002; Schwender et al., 2004; Turner et al., 2005).

This is indicative of efficient storage protein utilization in conjunction with thioredoxin and PEP carboxylase, a probable reason why we have often observed better germination patterns at early stages of germination (up to 48 h) for signal compound treated seeds. Lipoxygenase 1, 2 and 3 are essential for storage protein break down and also for the biosynthesis of chloroplasts in soybean seeds (Vernooy-Gerritsen et al., 1983; Siedow, 1991). Embryonic protein DC8 like, and sucrose binding protein, were the other proteins up-regulated in control seeds as compared to LCO and Th17 treated seeds, suggesting a functional role in lipid metabolism and the glycolytic pathway in the germinating seeds.

Glutathione-S-transferase and an associated IN2 homologue, peroxisomal voltage dependent anionic channel (VDAC) protein, alcohol dehydrogenase, arginosuccinate synthase, phosphoglycerate kinase, importin subunit, oleosin isoform (an oil body membrane protein that acts as an emulsifier for lipid storage in seeds), LEA and universal stress protein were some of the notable proteins up-regulated in germinating LCO treated seeds. Glutathione-S-transferase and an associated IN2-1 homologue B-like protein are the major antioxidant proteins observed in soybean seeds (Xu et al., 2011). Although the function of GST in seeds is not fully understood, its presence during stress responses is

indicative of probable oxidative damage protection. Reports that GST has some control over the regulation of the phytohormones GA and ABA (Kim et al., 2008) is encouraging in that the regulation of these hormones during seed germination by LCO and Th17 could be of significance in agriculture. The fold change increase in alcohol dehydrogenase in LCO and Th17 treated seeds was not a surprise, as the decreased levels of oxygen in germinating seeds favours fermentation, and this in turn could also increase the success of germination (Rolletschek et al., 2003). LEA proteins are seen to accumulate during the final stages of seed development (Baker et al., 1988) and seen to be expressed in soybean seeds during salt stress (Soulages et al., 2002). Along with the universal stress proteins, LEA proteins probably help seeds adapt for eventual salt stress responses. Voltage dependent anionic channel proteins are recognized as those that are primary transporters of ions and metabolites across organelle membranes, especially so with outer mitochondrial membrane and peroxisomes (Shoshan-Barmatz and Gincel, 2003). Peroxisomes control fatty acid metabolism, energy metabolism (the pentose-phosphate pathway) and glyoxylate metabolism of germinating seeds, allowing conversion of storage lipids into sugars (Gabaldon, 2010). The up-regulation of peroxisomal voltage dependent anionic channels (pVDAC) in both LCO and Th17 treated seeds suggests increased energy metabolism associated with mitochondrial function, as seen from the GO function outputs.

The Th17 treated seeds manifested the above mentioned proteins, seeds also manifested them as a result of LCO treatment, but LCO treatment also caused a marked increase (2-fold and above) in auxin-like protein, down regulation of rubisco oxygenase large subunit, Kunitz type trypsin inhibitor, stearyl acyl carrier, isocitrate lyase and pyruvate kinase. Stearyl acyl carrier up-regulation indicates the regulation of stearic acid contents in the seeds, which is of importance in soybean seed oil composition (Ruddle et al., 2013). Soybean cv. Jefferson has been reported to up-regulate β -conglycinin, glycinin, Kunitz trypsin inhibitor, alcohol dehydrogenase, Gm Bd 28K allergen, seed maturation proteins and sucrose binding proteins in seeds during germination (Mooney and Thelen, 2004; Natrajan et al., 2005). Transgenic soybean seeds have higher amounts of malondialdehyde, ascorbate peroxidase, glutathione reductase, and catalase (29.8, 30.6, 71.4, and 35.3 %, respectively) than non-transgenic seeds.

Precursors of glycinin, allergen Gly m Bd 28k, actin and sucrose binding proteins were the other proteins identified (Brandao et al., 2010; Barbosa et al., 2012).

The number of proteins identified in the salt stressed signals group was remarkably lower than the unstressed signals group, especially in the control vs LCO and control vs Th17 contrasts; this is very typical of soybean seed salt tolerance responses, as found in previous studies of soybean salt stress (Aghaie et al., 2009). The salt stress control showed up-regulation of aspartic proteinase, which has been observed regularly under salt stress, although its function in salt stress is unknown. In the salt-stress control seeds PEP carboxylase, lipxygenase 1, and mannose phosphate isomerase manifested increased glycolytic processes, while the predicted dehydrin-like protein could be used for compensation related to the water deficit effects of salt stress (Nylander et al., 2001). Salt stress in the presence of LCO resulted in up-regulation of glutathione-S-transferase, a predicted auxin-induced protein, pyruvate kinase, importin subunit, and predicted PR5 protein. GST and PR5 protein are stress regulators (Marrs, 1996; Kosova et al., 2013). Salt stress in combination with Th17 caused up-regulation of aspartic proteinase, predicted auxin-induced protein, mannose phosphate isomerase, glyceraldehydes phosphate dehydrogenase, Lea proteins, Bowman-Birk proteinase inhibitor, oleosin isoform A and B and a dehydrin-like protein, as compared to salt stress control treatment and salt stress with LCO treatment. Kunitz trypsin inhibitor and Bowman-Birk proteinase inhibitor are the two major trypsin inhibitors of soybean that control the degradation of storage proteins. Along with GST, they help protect seeds from predators (Kim et al., 2011).

In previous studies of salt stressed soybean seeds, the levels of proteins such as kinesin motor protein, trypsin inhibitor, alcohol dehydrogenase and annexin, were found to change, suggesting that these proteins might play roles in soybean salt tolerance and adaptation (Sobhanian et al., 2010; 2011). The percentage germination was not affected in soybean cultivars Lee68 and N2899 (salt-tolerant and salt-sensitive respectively) when exposed to 100 mM NaCl. The mean germination time for Lee68 (0.3 days) and N2899 (1.0 day) was delayed, compared with control plants. Hormonal responses to salt stress differed between these cultivars. Increased abscisic acid levels and decreased gibberellic

acid (GA 1, 3) and isopentyladenosine concentrations was seen in both these cultivars; auxin (IAA) increased in Lee68, but remained unchanged in N2899. Two dimensional gel electrophoresis, followed by MALDI-TOF-MS analysis, also suggested increases in ferritin and the 20S proteasome subunit β -6 in both the cultivars while, glyceraldehyde 3-phosphate dehydrogenase, glutathione *S*-transferase (GST) 9, GST 10, and seed maturation protein PM36 were down-regulated in Lee68. These proteins were present at low concentrations in N2899 in the absence of stress, and were seen to up-regulate following exposure to salt stress (Xu et al., 2011).

In our study, although strict statistical criteria were used to identify and understand the role of these proteins in unstressed and salt stressed seeds, this combination of up- and down-regulated proteins suggested a metabolic shift and represents a strategy used by soybean seeds to enhance tolerance of, or adaptation to, salt stress in the presence of LCO and Th17. However, relaxation of statistical criteria could reveal the presence of more proteins, and provide broader insights; however, these would be associated with a lesser degree of certainty. Although functional roles for all the known proteins identified by label free proteomics needs future meticulous work, it would be inappropriate to reject the role of the many hypothetical, unknown proteins and the unnamed protein products that were up-regulated in the seeds, as they could also add to our understanding of currently known adaptation strategies.

5.6 Conclusions:

In this study, we compared the effects of LCO and Th17 under unstressed and salt-stressed conditions; this is the first study conducted to determine chronic exposure effects of these signals, in combination with stressful levels of salt, on germinating soybean seeds. This subtropical crop requires temperatures of 25 – 30 °C for optimum growth and is severely affected by salinity stress. Although LCO is commercially available (Optimize with LCO promoter technology, and a wide range of similar products) and is known to speedup plant growth in the field, the comparison between LCO and Th17 for seed germination and the effects on the proteome of these seeds under stressed and unstressed conditions enhances its potential for better commercialization. This work is being continued as another project wherein soybean plants at different stages

of growth is being evaluated, both in response to LCO and Th17 and various abiotic stresses. In addition, the use of such growth promoting technologies might help invigorate elements of the native soil microflora and create synergies among them, promoting the potential for decreased use of chemical inputs in the cultivable land, and perhaps enhanced crop productivity on salinized soils around the world.

CHAPTER 6

SUMMARY, CONCLUSIONS AND FUTURE DIRECTIONS

6.1 General summary and conclusions

LCO and Th17 are bacterial compounds isolated from rhizobacteria of the soybean rhizosphere. The strain producing Th17 was isolated from plants growing at the Emile A. Lods Agronomy Research Centre/Horticultural Centre of the Macdonald Campus of McGill University. Since 2000 (Prithiviraj et al., 2000; Souleimanov et al., 2002a; Prithiviraj et al., 2003; Khan et al., 2008), our laboratory has tested LCO for plant growth and development effects, both under field conditions and in the laboratory, to determine effects on plant growth, while Th17 has been studied since 2006 when it was first identified as a bacteriocin (Gray et al., 2006a, b; Jung et al., 2008a; Lee et al., 2009). All the work done so far has shown promising results with LCO and Th17 as plant growth promoters of both legumes and non-legumes. Under controlled conditions, however, the responses were more pronounced under stress conditions, such as low temperature and drought (unpublished results), which resulted in probing the possible role of these compounds in alleviating salt stress. Two microarray studies conducted on LCO effects in our laboratory suggested that a transient increase in expression of salicylic acid occurred at 24 h after spray treatment of soybean leaves and was accompanied by enhanced expression of stress responsive genes under optimal conditions; while application of LCO after an initial period of low temperature stress resulted in a shift from one set of stress related genes, presumably active due to low temperature conditions, to another set that might help prevent the effects of low temperature because of LCO stimulation (Lindsay, 2007; Wang et al., 2012).

Hence in Chapter 3, we attempted to quantify plant hormone levels to determine possible roles of these in plant growth responses to LCO and Th17 treatments. Phytohormones form an important component of a plant's intracellular regulatory mechanisms. Responses of *Arabidopsis thaliana* rosettes to LCO and Th17, at 24 h after exposure, were not identical. LCO treated rosettes showed decreased levels of total IAA, cytokinins, gibberellins and jasmonic acid, and increases in ABA and SA, while Th17

treated rosettes had decreased levels of cytokinins, gibberellins, jasmonic acid and ABA; and increases in IAA and SA. However, both signal compounds caused decreased JA levels, suggesting that these two compounds may not be inducing the classic induced systemic resistance like responses in *A. thaliana*, and suggesting a new phytohormone response network regulating plant growth promotion in non-legumes.

In all our studies, treatment with LCO and Th17 under optimal plant growth conditions resulted in small positive responses, while imposition of stress conditions such as low temperature, drought (unpublished data) and salt stress caused clearer positive plant responses. Hence salt stress was studied to further our knowledge of plant-microbe relations under stress conditions. *Arabidopsis thaliana* plants responded positively to salt stress of up to 250 mM NaCl in a 15 day salt tolerance evaluation. Shotgun proteomics of unstressed and 250 mM NaCl stressed *A. thaliana* rosettes (7 days post stress), in combination with the LCO and Th17, revealed higher levels of many known, putative, hypothetical and unknown proteins. Carbon and energy metabolic pathways were the most affected, under both unstressed and salt stressed conditions, when treated with these microbe-to-plant signals. PEP carboxylase, Rubisco-oxygenase large subunit, pyruvate kinase, chloroplast proteins and proteins of photosystem I and II were some of the noteworthy proteins whose levels were enhanced by the signals, along with a range of stress related proteins. Higher levels of the chloroplast proteins and those of photosystem I and II proteins in the signal-treated, salt-stressed plants is a significant finding, resulting in improved plant growth under high levels of salt stress. If this finding can be translated to field grown crops, an important management input would be added to crop production systems, allowing enhanced global food production and improved global food security. Hence we also studied this phenomenon in soybean, a commercially important crop in Eastern Canada.

In Chapter 5, we studied soybean, from whose rhizosphere these compounds can be isolated, in order to determine their effects on soybean germination. Soybean is a subtropical crop requiring temperatures of 25 – 30 °C for optimum growth and is severely affected by salinity stress. Soybean growth is negatively affected when the plant is exposed to 40 mM NaCl and 80 mM NaCl can be lethal (Sobhanian et al., 2010). Hence

our first goal was to evaluate the variety absolute RR, to determine the best salt stress level for testing the effects of LCO and Th17 on salt-stress tolerance of germinating seeds. Germinating soybean seeds responded positively to the bacterial signal compounds LCO and Th17 at salt stress levels of up to 150 mM NaCl. Shotgun proteomics of unstressed and 100 mM NaCl stressed seeds (48 h) in combination with the LCO and Th17 revealed many known, predicted, hypothetical and unknown proteins. Carbon, nitrogen and energy metabolic pathways were affected under both unstressed and salt stressed conditions when treated with LCO and Th17 signals. PEP carboxylase, Rubisco oxygenase large subunit, pyruvate kinase, and isocitrate lyase were some of the noteworthy proteins enhanced by the signals, along with antioxidant glutathione-S-transferase and other stress related proteins. These findings suggested that the germinating seeds altered their proteome following exposure to bacterial signals and salt stress. These specific responses might play an important role in organ maturation and transition from one stage to another in a plant's life cycle. Understanding these responses is of fundamental importance in agriculture and, as a result, to global food security.

6.2 Suggestions for future research

To expand the work reported here and to further clarify the role of LCO and Th17 on plant growth, particularly under abiotic stress, the following research remains to be done.

1. Expand the range of time points for hormone analysis study and include ethylene in future work.

In our study, due to funding restrictions, we were able to study only one time point and also only two pooled biological replicates. Expanding the hormone response study to include ethylene and also to include a series of time points, such as 12, 36 and 48 h, based on circadian rhythm points, will be helpful in establishing a pattern of responses over time. Similarly application of the treatments at different times of the day will be of help in suggesting an effective application time for field conditions, since time of treatments may change the results, based on the plant's internal oscillations.

2. Expand the time points for proteome analysis, based on developmental stage.

In our study we conducted research on the proteome of *A. thaliana* only at 24 h post treatment. A broader analysis of proteome responses at say 6, 12, 36, and 48 h after application could give us more detail regarding regulation of the proteome and this could be related to the levels of phytohormones following a study of the type suggested immediately above. In addition, these time points are appropriate for studies such as how responses elicited at these times redirect plant growth and development, as indicated by earlier plant-microbe interaction studies.

3. Studying protein-protein interaction of various organelles.

Th17 being a protein, is a good candidate for studying protein-protein interactions. Since we have found specific sets of proteins to be up-regulated in *A. thaliana* rosettes, it would be useful to expand this knowledge to organelle based studies, in order to target specific proteins that regulate plant growth, with a view to fine tuning current understanding of the mechanism of action of Th17.

4. Studying *A. thaliana* root responses to bacterial signals using systems biology.

Despite our best efforts, we were unable to study the responses of the root system to LCO and Th17 treatments. A proteomic study similar to the one conducted on the rosettes, and perhaps at the time points indicated above, will highlight the partitioning of photosynthates and other root growth parameters. This will also be helpful in suggesting anchorage, nutrient availability and carbon sequestration capabilities in the root zone.

5. Expand our knowledge of *A. thaliana* proteomics responses to LCO and Th17 to the economically important crops such as soybean and corn.

In the work reported in chapter 5, we evaluated germinated soybean seeds at the proteome level. However, a good deal of work remains to be conducted in this area:

1. Studying soybean and corn, and subsequently other crop, root responses to bacterial signals using systems biology.

2. Extended study of both soybean and corn to differentiate between responses of a legume and a non-legume crop.

6. Sequencing of *B. thuringiensis* NEB17

Since our knowledge of *B. thuringiensis* NEB17 is not complete, it would be appropriate to obtain a full and annotated genome sequence for future use.

LIST OF REFERENCES

- Abaidoo RC, Keyser HH, Singleton PW, Dashiell KE, Sanginga N (2007) Population size, distribution, and symbiotic characteristics of indigenous *Bradyrhizobium* spp. that nodulate TGx soybean genotypes in Africa. *Applied Soil Ecology*, 35: 57-67.
- Acton DF and Gregorich LJ (1995) Center for Land and Biological Resources Research (Canada): The health of our soils: toward sustainable agriculture in Canada. Ottawa, ON: Centre for Land and Biological Resources Research.
- Aebersold R, Mann M (2003) Mass spectrometry-based proteomics. *Nature*, 422: 198-207.
- Aghaei K, Ehsanpour AA, Shah AH, Komatsu S (2009) Proteome analysis of soybean hypocotyl and root under salt stress. *Amino Acids*, 36: 91-98.
- Agri-Facts: Salt tolerance of Plants: <http://www1.agric.gov.ab.ca> Nov 2001 (last accessed 12th July 2012).
- Ahsan N, Donnart T, Nouri M-Z, Komatsu S (2010) Tissue-specific defense and thermoadaptive mechanisms of soybean seedlings under heat stress revealed by proteomic approach. *Journal of Proteome Research*, 9: 4189-4204.
- Ahsan N and Komatsu S (2009) Comparative analyses of the proteomes of leaves and flowers at various stages of development reveal organ specific functional differentiation of proteins in soybean. *Proteomics*, 9: 4889-4907.
- Alabadi D, Bla'zquez MA (2009) Molecular interactions between light and hormone signaling to control plant growth. *Plant Molecular Biology*, 69: 409-417.
- Alam I, Lee D-G, Kim K-H, Park C-H, Sharmin S A, Lee H, Oh K-W, Yun B-W, Lee B-H (2010) Proteome analysis of soybean roots under water logging stress at an early vegetative stage. *Journal of Biosciences*, 35: 49-62.
- Albenne C, Canut H, Jamet E (2013) Plant cell wall proteomics: the leadership of *Arabidopsis thaliana*. *Frontiers in Biology*, 4: 1-17.
- Allen JF, Santabarbara S, Allen CA, Puthiyaveetil S (2011) Discrete redox signaling pathways regulate photosynthetic light-harvesting and chloroplast gene transcription. *PLoS ONE* 6(10): e26372. doi:10.1371/journal.pone.0026372.
- Almansouri M, Kinet JM, Lutts S (2001) Effect of salt and osmotic stresses on germination in durum wheat (*Triticum durum* Desf.). *Plant Soil*, 231: 243-254.
- Alves BJR, Boddey RM, Urquiaga S (2003) The success of BNF in soybean in Brazil. *Plant and Soil*, 252: 1-9.
- Amalraj RS, Selvaraj N, Veluswamy GK, Ramanujan RP, Muthurajan R, Agrawal GK, Rakwal R, Viswanathan R (2010) Sugarcane proteomics: establishment of a protein extraction method for 2-DE in stalk tissues and initiation of sugarcane proteome reference map. *Electrophoresis*, 31: 1959-1974.
- Anderson PP (2001) The future world food situation and the role of plant diseases. [www.aspnet.org/Education/feature/Food security](http://www.aspnet.org/Education/feature/Food%20security).

Arabidopsis Biological Resource Center – <http://abrc.osu.edu> (last visited 23rd March 2010).

Arabidopsis hormone database - <http://ahd.cbi.pku.edu.cn> (last visited May 2013).

Arai Y, Hayashi M, Nishimura M (2008) Proteomic identification and characterization of a novel peroxisomal adenine nucleotide transporter supplying ATP for fatty acid β -oxidation in soybean and Arabidopsis. *The Plant Cell*, 20: 3227-3240.

Argueso CT, Ferreira FJ, Epple P, To JPC, Hutchison CE, Schaller GE, Dangl JL, Kieber JJ (2012) Two-component elements mediate interactions between cytokinin and salicylic acid in plant immunity. *PLoS Genetics*, 8: 1-13.

Arner ES and Holmgren A (2000) Physiological functions of thioredoxin and thioredoxin reductase. *European Journal of Biochemistry*, 267: 6102-6109.

Ashraf M and Harris PJC (2013) Photosynthesis under stressful environments: An overview. *Photosynthetica*, 51: 163-190.

Bai Y, D'Aoust F, Smith DL, Driscoll BT (2002a) Isolation of plant-growth-promoting *Bacillus strains* from soybean root nodules. *Canadian Journal of Microbiology*, 48: 230-238.

Bai Y, Souleimanov A, Smith DL (2002b) An inducible activator produced by a *Serratia proteamaculans* strain and its soybean growth-promoting activity under greenhouse conditions. *Journal of Experimental Botany*, 373: 1495-1502.

Bai Y, Zhou X, Smith DL (2003) Enhanced soybean plant growth resulting from co-inoculation of *Bacillus* strains with *Bradyrhizobium japonicum*. *Crop Science*, 43: 1774-1781

Baier R, Schiene K, Kohring B, Flaschel E, Niehaus K (1999) Alfalfa and tobacco cells react differently to chitin oligosaccharides and sinorhizobium meliloti nodulation factors. *Planta*, 210: 157-164.

Baker J, Steele C, Dure L (1988) Sequence and characterization of 6 lea proteins and their genes from cotton. *Plant Molecular Biology*, 11: 277-291.

Baldani JJ, Reis VM, Baldani VLD, Doberner J (2002) A brief story of nitrogen fixation in sugarcane – reasons for success in Brazil. *Functional Plant Biology*, 29: 417-423.

Barbosa HS, Arruda SCC, Azevedo RA, Arruda MAZ (2012) New insights on proteomics of transgenic soybean seeds: evaluation of differential expressions of enzymes and proteins. *Analytical and Bioanalytical Chemistry*, 402: 299-314.

Barcellos FG, Batista JS, Menna P, Hungria M (2009) Genetic differences between *Bradyrhizobium japonicum* variant strains contrasting in N₂-fixation efficiency revealed by representational difference analysis. *Archives in Microbiology*, 191: 113-22.

Batista JS, Torres AR, Hungria M (2010) Towards a two-dimensional proteomic reference map of *Bradyrhizobium japonicum* CPAC 15: spotlighting "hypothetical proteins". *Proteomics*, 10: 3176-89.

Bielach A, Podlešáková K, Marhavý P, Duclercq J, Cuesta C, Müller B, Grunewald W, Petr Tarkowski P, Benková E (2012) Spatiotemporal regulation of lateral root organogenesis in Arabidopsis by cytokinin. *The Plant Cell*, 24: 3967-3981.

- Bla'zquez M, Tre'nor M, Weigel D (2002) Independent control of gibberellin biosynthesis and flowering time by the circadian clock in *Arabidopsis*. *Plant Physiology*, 130: 1770–1775.
- Bleeker AB, Estelle MA, Summerville C, Kende H (1988) Insensitivity to ethylene conferred by a dominant mutation in *Arabidopsis thaliana*. *Science*, 241: 1086-1089.
- Bloemberg GV and Lugtenberg BJ (2001) Molecular basis of plant growth promotion and biocontrol by rhizobacteria. *Current opinion in plant biology*, 4: 343-350.
- Boddey RM, Urquiaga S, Alves BJR, Reis V (2003) Endophytic nitrogen fixation in sugarcane: present knowledge and future applications. *Plant and Soil*, 252: 139–149.
- Boudart G, Jamet E, Rossignol M, Lafitte C, Borderies G, Jauneau A, Esquerré-Tugayé M-T, Pont-Lezica R (2005) Cell wall proteins in apoplastic fluids of *Arabidopsis thaliana* rosettes: Identification by mass spectrometry and bioinformatics. *Proteomics*, 5: 212–221.
- Bradyrhizobium japonicum* database - <http://www.kazusa.or.jp/index.html> (last accessed 12th July 2012).
- Brandao AR, Barbosa HS, Arruda MAZ (2010) Image analysis of two-dimensional gel electrophoresis for comparative proteomics of transgenic and non-transgenic soybean seeds. *Journal of proteomics*, 73: 1433-1440.
- Brechenmacher L, Lee J, Sachdev S, Song Z, Nguyen THN, Joshi T, Oehrle N, Libault M, Mooney B, Xu D, Cooper B, Stacey G (2009) Establishment of a protein reference map for soybean root hair cells. *Plant Physiology*, 149: 670-682.
- C'erny' M, Dyc'ka F, Boba'l'ova' J, Brzobohaty B (2011) Early cytokinin response proteins and phosphoproteins of *Arabidopsis thaliana* identified by proteome and phosphoproteome profiling. *Journal of Experimental Botany*, 62: 921–937.
- Caesar K, Thamm AMK, Witthoft J, Elgass K, Huppenberger P, Grefen C, Horak J, Harter K (2011) Evidence for the localization of the *Arabidopsis* cytokinin receptors AHK3 and AHK4 in the endoplasmic reticulum. *Journal of Experimental Botany*, 62: 5571–5580.
- Campo RJ and Hungria M (2004) Sources of nitrogen to reach high soybean yields: In: *Proceedings of VII World Soybean Research Conference, IV International Soybean Processing and Utilization Conference, III Congresso Brasileiro de Soja Brazilian Soybean Congress*, Foz do Iguassu, PR, Brazil, 29 February–5 March 2004, pp. 1275-1280.
- Cao H, Glazebrook J, Clarke J D, Volko S, Dong X (1997) The *Arabidopsis NPR1* gene that controls systemic acquired resistance encodes a novel protein containing ankyrin repeats. *Cell*, 88: 57-63.
- Carlson R, Price N, Stacey G (1994) The biosynthesis of rhizobial lipo-oligosaccharide nodulation signal molecules. *Molecular Plant Microbe Interactions*, 7: 684-95.
- Carroll AJ (2013) The *Arabidopsis* cytosolic ribosomal proteome: from form to function. *Frontiers in Plant Science*, 4: 1-14.
- Carter C, Pan S, Zouhar J, Avila EL, Girke T, Raikhel NV (2004) The vegetative vacuole proteome of *Arabidopsis thaliana* reveals predicted and unexpected proteins. *The Plant Cell*, 16: 3285–3303.

- Charmont S, Jamet E, Pont-Lezica R, Canut H (2005) Proteomic analysis of secreted proteins from *Arabidopsis thaliana* seedlings: improved recovery following removal of phenolic compounds. *Phytochemistry*, 66: 453-461.
- Chen C, McIver J, Yang Y, Bai Y, Schultz B, McIver A (2007) Foliar application of lipo-chitooligosaccharides (Nod factors) to tomato (*Lycopersicon esculentum*) enhances flowering and fruit production. *Canadian Journal of Plant Science*, 87: 365-372.
- Chen Z, Cui Q, Liang C, Sun L, Tian J, Liao H (2011) Identification of differentially expressed proteins in soybean nodules under phosphorus deficiency through proteomic analysis. *Proteomics*, 11: 4648-4659.
- Chinnusamy V, Schumaker K, Zhu JK (2004) Molecular genetic perspectives on cross-talk and specificity in abiotic stress signalling in plants. *Journal of Experimental Botany*, 55: 225–236.
- Choudhary DK and Johri BN (2009) Interactions of *Bacillus* spp. and plants – with special reference to induced systemic resistance (ISR). *Microbiology Research*, 164: 493-513.
- Chowdhary G, Kataya ARA, Lingner T, Reumann S (2012) Non-canonical peroxisome targeting signals: identification of novel PTS1 tripeptides and characterization of enhancer elements by computational permutation analysis. *BMC Plant Biology*, 12: 142-156.
- Ciesielska A, Ruszkowski M, Kasperska A, Femiak I, Michalski Z, Sikorski MM (2012) New insights into the signaling and function of cytokinins in higher plants. *Journal of Biotechnology, Computational Biology and Bionanotechnology*, 93: 400-413.
- Cilia M, Fish T, Yang X, McLaughlin M, Thannhauser TW, Gray S (2009) A comparison of protein extraction methods suitable for gel-based proteomic studies of aphid proteins. *Journal of Biomolecular Techniques*, 20: 201-215.
- Compaan B, Ruttink T, Albrecht C, Meeley R, Bisseling T, Franssen H (2003) Identification and characterization of a *Zea mays* line carrying a transposon-tagged ENOD40. *Biochemica et Biophysica Acta*, 1629: 84–91.
- Compant S, Clément C, Sessitsch A (2010) Plant growth promoting bacteria in the rhizo- and endosphere of plants. Their role, colonization, mechanisms involved and prospects for utilization. *Soil Biol Biochem*, 42: 669–678.
- Compant S, Mitter B, Colli-Mull JG, Gangl H, Sessitsch A (2011) Endophytes of Grapevine Flowers, Berries, and Seeds: Identification of Cultivable Bacteria, Comparison with Other Plant Parts, and Visualization of Niches of Colonization. *Microb Ecol*, 62: 188–197
- Conesa A and S. Götz (2008) Blast2GO: A comprehensive suite for functional analysis in plant genomics. *International Journal of Plant Genomics*, 1-13.
- Conesa A, Götz S, Garcia-Gomez M, Terol J, Talon M, Robles M (2005) Blast2GO: a universal tool for annotation, visualization and analysis in functional genomics research. *Bioinformatics*, 21: 3674-3676.
- Cook D, Dreyer D, Bonnet D, Howell M, Nony E, VandenBosch K (1995) Transient induction of a peroxidase gene in *Medicago truncatula* precedes infection by *Rhizobium meliloti*. *The Plant Cell*, 7: 43-55.

- Covington MF and Harmer SL (2007) The circadian clock regulates auxin signaling and responses in Arabidopsis. *PLoS Biol* 5(8): e222. doi:10.1371/journal.pbio.0050222.
- Covington MF, Maloof JN, Straume M, Kay SA, Harmer SL (2008) Global transcriptome analysis reveals circadian regulation of key pathways in plant growth and development. *Genome Biology*, 9: R130.
- Cui Z, Carter TE, Gai J, Qui J, Nelson RL (1999) Origin, description, and pedigree of Chinese soybean cultivars released from 1923 to 1995. U.S. Department of Agriculture, Agricultural Research Service, Tech. Bull; No. 1871.
- Culligan EP, Marchesi JR, Hill C, Sleator RD (2012) Mining the human gut microbiome for novel stress resistance genes. *Gut Microbes*, 3: 394-397.
- Currier W and Strobel G (1976) Chemotaxis of *Rhizobium* spp. to plant root exudates. *Plant Physiology*, 57: 820-823.
- Czaja LF, Hogenkamp C, Lamm P, Maillet F, Martinez EA, Samain E, Dénarié J, Küster H, Hohnjec N (2012) Transcriptional responses toward diffusible signals from symbiotic microbes reveal *MtNFP*- and *MtDMI3*-dependent reprogramming of host gene expression by arbuscular mycorrhizal fungal lipochitooligosaccharides. *Plant Physiology*, 159: 1671-1685.
- D'Haeze W and Holsters M (2002) Nod factor structures, responses, and perception during initiation of nodule development. *Glycobiology*, 12: 79-105.
- da Silva Batista JS, Hungria M (2012) Proteomics reveals differential expression of proteins related to a variety of metabolic pathways by genistein-induced *Bradyrhizobium japonicum* strains. *Journal of Proteomics*, 75:1211-9.
- Dabuxilatu MI and Ikeda M (2005) Distribution of K, Na and Cl in root and leaf cells of soybean and cucumber plants grown under salinity conditions. *Soil Science and Plant Nutrition*, 51: 1053-7.
- Dawe AL, Mu R, Rivera G, Salamon JA (2011) Molecular methods for studying the *Cryphonectria parasitica* - hypovirus experimental system. *Methods in Molecular Biology*, 722: 225-236.
- De Jong AJ, Heidstra R, Spaik HP, Hartog MV, Meijer EA, Hendriks T, Schiavo FL, Terzi M, Bisseling T, Van Kammen A (1993) *Rhizobium* lipooligosaccharides rescue a carrot somatic embryo mutant. *The Plant cell*, 5: 615-620.
- Delahunty C and Yates JR (2005) Protein identification using 2D-LC-MS/MS. *Methods*, 35: 248-255.
- Delaney TP, Friedrich L, Ryals JA (1995) Arabidopsis signal transduction mutant defective in chemically and biologically induced disease resistance. *Proceedings of National Academy of Sciences, USA*, 92: 6602-6606.
- Delmotte N, Ahrens CH, Knief C, Qeli E, Koch M, Fischer HM, Vorholt JA, Hennecke H, Pessi G (2010) An integrated proteomics and transcriptomics reference data set provides new insights into the *Bradyrhizobium japonicum* bacteroid metabolism in soybean root nodules. *Proteomics*, 10: 1391-400.

- Denarie J and Cullimore J (1993) Lipo-oligosaccharide nodulation factors: a minireview new class of signaling molecules mediating recognition and morphogenesis. *Cell*, 74: 951-954.
- Dimkpa C, Weinand T, Asch F (2009) Plant–rhizobacteria interactions alleviate abiotic stress conditions. *Plant, Cell and Environment*, 32: 1682–1694.
- Djordjevic MA, Oakes M, Li DX, Hwang CH, Hocart CH, and Gresshoff PM (2007) The glycine max xylem sap and apoplast proteome. *Journal of Proteome Research*, 6: 3771-3779.
- Dona` M, Macovei A, Fae` M, Carbonera D, Balestrazzi A (2013) Plant hormone signaling and modulation of DNA repair under stressful conditions. *Plant Cell Rep*, DOI 10.1007/s00299-013-1410-9.
- Dong Z, Canny MJ, McCully ME, Roboredo MR, Cabadilla CF, Ortega E, Rodés R (1994) A nitrogen-fixing endophyte of sugarcane stems' A new role for the apoplast. *Plant Physiology*, 105: 1139-1147.
- Doornbos RF, Geraats BPJ, Kuramae EE, Van Loon LC, Bakker PAHM (2011) Effects of Jasmonic Acid, Ethylene, and Salicylic Acid Signaling on the Rhizosphere Bacterial Community of *Arabidopsis thaliana*. *MPMI*, 24: 395–407.
- Dora R, Carsten M, Ole MJB, John M (2000) Fusion genetic analysis of gibberellin signaling mutants. *Plant Journal*, 22: 427-438.
- Dreher K and Callis J (2007) Ubiquitin, hormones and biotic stress in plants. *Annals of Botany*, 99: 787-822.
- Du H, Kim S, Nam KH, Lee M-S, Son O, Lee S-H, Cheon C-I (2010) Identification of uricase as a potential target of plant thioredoxin: implication in the regulation of nodule development. *Biochemical and Biophysical Research Communications*, 397: 22-26.
- Du W, Xu Y, Liu D (2003) Lipase-catalysed transesterification of soya bean oil for biodiesel production during continuous batch operation. *Biotechnology and Applied Biochemistry*, 38: 103-6.
- Duan L, Dietrich D, Ng CH, Chan PMY, Bhalarao R, Bennett MJ, Dinneny JR (2013) Endodermal ABA signaling promotes lateral root quiescence during salt stress in *Arabidopsis* seedlings. *The Plant Cell*, 25: 324–341.
- Dyachok J, Tobin A, Price N, von Arnold S (2000) Rhizobial Nod factors stimulate somatic embryo development in *Picea abies*. *Plant Cell Reports*, 19: 290-297.
- Dyachok J, Wiweger M, Kenne L, von Arnold S (2002) Endogenous nod-factor-like signal molecules promote early somatic embryo development in Norway spruce. *Plant Physiology*, 128: 523-533.
- Elmore JM, Liu J, Smith B, Phinney B, Coaker G (2012) Quantitative proteomics reveals dynamic changes in the plasma membrane during *Arabidopsis* immune signaling. *Molecular & Cellular Proteomics*, 11: 1–13.
- Essa TA (2002) Effect of salinity stress on growth and nutrient composition of three soybean (*Glycine max* L. Merrill) cultivars. *Journal of Agronomy and Crop Science*, 188: 86-93.
- ExPASy Proteomics server, available at <http://www.expasy.org>

Falkowski PG, Fenchel T, Delong EF (2008) The microbial engines that drive earth's biogeochemical cycles. *Science*, 320: 1034-9.

Fan W and Dong X (2002) *In vivo* interaction between NPR1 and transcription factor TGA2 leads to salicylic acid-mediated gene activation in *Arabidopsis*. *Plant Cell*, 14: 1377-1389.

FAO (2011; 2013) *FAOSTAT*. Food and Agriculture Organization of the United Nations, Rome, Italy. Available at: <http://faostat.fao.org> (last accessed 8 July 2013).

Fasim F, Ahmed N, Parsons R, Gadd GM (2002) Solubilization of zinc salts by a bacterium isolated from the air environment of a tannery. *FEMS Microbiology Letters*, 213: 1-6.

Ferro M, Seigneurin-Berny D, Rolland N, Chapel A, Salvi D, Garin J, Joyard J (2000) Organic solvent extraction as a versatile procedure to identify hydrophobic chloroplast membrane proteins. *Electrophoresis*, 21: 3517-3526.

Firmin J, Wilson K, Rossen L, Johnston AWB (1986) Flavonoid activation of nodulation genes in *Rhizobium* reversed by other compounds present in plants. *Nature*, 324: 90-92.

Fravel DR (1988) Role of Antibiosis in the Biocontrol of Plant-Diseases. *Annual Review of Phytopathology*, 26: 75-91.

Fré̄bort I, Kowalska M, Hluska T, Fré̄bortová J, Galuszka P (2011) Evolution of cytokinin biosynthesis and degradation. *Journal of Experimental Botany*, 62: 2431-2452.

Frigerio M, Alabad D, Pērez-Gōmez J, Garcí̄a-Cārcel L, Phillips AL, Hedden P, Blāzquez MA (2006) Transcriptional regulation of gibberellin metabolism genes by auxin signaling in *Arabidopsis*. *Plant Physiology*, 142: 553-563.

Fujita Y, Fujita M, Shinozaki K, Yamaguchi-Shinozaki K (2011) ABA-mediated transcriptional regulation in response to osmotic stress in plants. *Journal of Plant Research*, 124: 509-525.

Gabaldón T (2010). Peroxisome diversity and evolution. *Philos Trans R Soc Lond B Biological Science*, 365: 765-73.

Galant A, Koester RP, Ainsworth EA, Hicks LM, Jez JM (2012) From climate change to molecular response: redox proteomics of ozone-induced responses in soybean. *New Phytologist*, 194: 220-229.

Galetskiy D, Lohscheider JN, Kononikhin AS, Popov IA, Nikolaev EN, Adamska I (2011) Mass spectrometric characterization of photooxidative protein modifications in *Arabidopsis thaliana* thylakoid membranes. *Rapid Communications in Mass Spectrometry*, 25: 184-190.

Godoy LP, Vasconcelos ATR, Chueire LMO, Souza RC (2008) Genomic panorama of *Bradyrhizobium japonicum* CPAC 15, a commercial inoculant strain largely established in Brazilian soils and belonging to the same serogroup as USDA 123. *Soil Biology and Biochemistry*, 40: 2743-2753.

Gong Z, Koiwa H, Cushman MA, Ray A, Bufford D, Kore-eda S, Matsumoto T, Zhu J, Cushman J, Bressan RA, Hasegawa PM (2001) Genes that are uniquely stress-regulated in salt overly sensitive (sos) mutants. *Plant Physiology*, 126: 363-375.

Götz S (2008) et al. High-throughput functional annotation and data mining with the Blast2GO suite. *Nucleic Acids Research*, 36: 3420-3435.

- Götz S (2011) et al. B2G-FAR, a species centered GO annotation repository. *Bioinformatics*, 27: 919-924.
- Gough C, Vassel J, Galera C, Webster G, Cocking E, D'enari'e J (1997) Interactions between bacterial diazotrophs and non-legume dicots: *Arabidopsis thaliana* as a model plant. *Plant and Soil*, 194: 123–130.
- Graham PH and Vance CP (2000) Nitrogen fixation in perspective: an overview of research and extension needs. *Field Crops Research*, 65: 93-106.
- Graham PH and Vance CP (2003) Legumes: Importance and constraints to greater use. *Plant Physiology*, 131: 872-877.
- Granlund I, Hall M, Kieselbach T, Schroder WP (2009) Light induced changes in protein expression and uniform regulation of transcription in the thylakoid lumen of *Arabidopsis thaliana*. *PLoS ONE* 4(5): e5649. doi:10.1371/journal.pone.0005649.
- Gray EJ, Di Falco M, Souleimanov A, Smith DL (2006a) Proteomic analysis of the bacteriocin, Thuricin-17 produced by *Bacillus thuringiensis* NEB17. *FEMS Microbiology Letters*, 255: 27-32.
- Gray EJ, Lee K, Di Falco M, Souleimanov A, Zhou X, Smith DL (2006b) A novel bacteriocin, thuricin 17, produced by PGPR strain *Bacillus thuringiensis* NEB17: isolation and classification. *Journal of Applied Microbiology*, 100: 545-554.
- Gray EJ and Smith DL (2005) Intracellular and extracellular PGPR: commonalities and distinctions in the plant-bacterium signaling processes. *Soil Biology and Biochemistry*, 37: 395-412.
- Greenway H and Munns R (1980) Mechanisms of salt tolerance in non-halophytes. *Annual Reviews in Plant Physiology*, 31:149-190.
- Gregory AL, Hurley BA, Tran HT, Valentine AJ, She Y-M, Knowles VL, Plaxton WC (2009) *In vivo* regulatory phosphorylation of the phosphoenolpyruvate carboxylase AtPPC1 in phosphate-starved *Arabidopsis thaliana*. *Journal of Biochemistry*, 420: 57–65.
- Grobei MA, Qeli E, Brunner E, Rehrauer H, Zhang R, Roschitzki B, Basler K, Ahrens CH, Grossniklaus U (2009) Deterministic protein inference for shotgun proteomics data provides new insights into *Arabidopsis* pollen development and function. *Genome Research*, 19: 1786–1800.
- Guzzo F, Portaluppi P, Grisi R, Barone S, Zampieri S, Franssen H, Levi M (2005) Reduction of cell size induced by enod40 in *Arabidopsis thaliana*. *Journal of Experimental Botany*, 56: 507–513.
- Hajdich M, Ganapathy A, Stein JW, Thelen JJ (2005) A systematic proteomic study of seed filling in soybean. Establishment of high-resolution two-dimensional reference maps, expression profiles, and an interactive proteome database. *Plant Physiology*, 137: 1397-1419.
- Hamayun M, Khan SA, Khan AL, Shinwari ZK, Hussain J, Sohn EY, Kang SM, Kim YH, Khan MA, Lee IJ (2010) Effect of salt stress on growth attributes and endogenous growth hormones of soybean cultivar Hwangkeumkong. *Pakistan Journal of Botany*, 42: 3103-3112.
- Hammond-Kosack KE and Jones JDG (1996) Resistance gene-dependent plant defense responses. *Plant Cell*, 8: 1773-1791.

Hanano H, Domagalska MA, Nagy F, Davis SJ (2006) Multiple phytohormones influence distinct parameters of the plant circadian clock. *Genes to Cells*, 11: 1381–1392.

Hasegawa PM, Bressan RA, Zhu JK, Bohnert HJ (2000) Plant cellular and molecular responses to high salinity. *Annual Review of Plant Molecular and Plant Physiology*, 51: 463–499.

Hashiguchi A, Sakata K, Komatsu S (2009) Proteome analysis of early-stage soybean seedlings under flooding stress. *Journal of Proteome Research*, 8: 2058–2069.

He Y, Dai S, Dufresne CP, Zhu N, Pang Q (2013) Integrated proteomics and metabolomics of *Arabidopsis* acclimation to gene-dosage dependent perturbation of isopropylmalate dehydrogenases. *PLoS ONE*, 8: e57118. doi:10.1371/journal.pone.0057118.

Hempel J, Zehner S, Göttfert M, Patschkowski T (2009) Analysis of the secretome of the soybean symbiont *Bradyrhizobium japonicum*. *Journal of Biotechnology*, 10: 51–8.

Herbert BR, Molloy MP, Gooley AA, Walsh BJ, Bryson WG, Williams KL (1998) Improved protein solubility in two-dimensional electrophoresis using tributyl phosphine as reducing agent. *Electrophoresis*, 19: 845–51.

Hirsch S and Oldroyd G (2009) Integrated Nod factor signaling in plants. In: *Signaling in Plants* Springer Berlin Heidelberg. pp 71–90.

Horiguchi G, Molla´-Morales A, Pe´ rez-Pe´ rez JM, Kojima K, Robles P, Ponce MR, Micol JL, Tsukaya H (2011) Differential contributions of ribosomal protein genes to *Arabidopsis thaliana* leaf development. *The Plant Journal*, 65: 724–736.

Hotta CT, Gardner MJ, Hubbard KE, Baek SJ, Dalchau N, Suhita D, Dodd AN, Webb AAR (2007) Modulation of environmental responses of plants by circadian clocks. *Plant, Cell and Environment*, 30: 333–349.

Houston NL, Lee D-G, Stevenson SE, Ladics GS, Bannon GA, McClain S, Privalle L, Stagg N, Herouet-Guicheney C, MacIntosh SC, Thelen JJ (2011) Quantitation of soybean allergens using tandem mass spectrometry. *Journal of Proteome Research*, 10: 763–773.

<http://www.oilseedproteomics.missouri.edu/soybean.php> (last accesses 15th Oct 2012).

Hughes RM and Herridge DF (1989) Effect of tillage on yield, nodulation and nitrogen fixation of soybean in far north-coastal New South Wales. *Australian Journal of Experimental Agriculture*, 29: 671–677.

Hummel M, Cordewener JHG, Groot JCM, Smeekens S, America AHP, Hanson J (2012) Dynamic protein composition of *Arabidopsis thaliana* cytosolic ribosomes in response to sucrose feeding as revealed by label free MSE proteomics. *Proteomics*, 12, 1024–1038.

Hundertmark M, Hinch DK (2008) LEA (Late Embryogenesis Abundant) proteins and their encoding genes in *Arabidopsis thaliana*. *BMC Genomics*, 9: 118–130.

Huo H, Wang M, Bloyd C, Putsche V (2009) Life-cycle assessment of energy use and greenhouse gas emissions of soybean-derived biodiesel and renewable fuels. *Environmental Science and Technology*, 43: 750–6.

Hymowitz T and Harlan JR (1983) Introduction of soybean to North America by Samuel Bowen in 1765. *Economic Botany*, 37: 371–379.

- Iino M, Nomura T, Tamaki Y, Yamada Y, Yoneyama K, Takeuchi Y, Mori M, Asami T, Nakano T, Yokota T (2007) Progesterone: Its occurrence in plants and involvement in plant growth. *Phytochemistry* 68: 1664–1673.
- Inui H, Yamaguchi Y, Hirano S (1997) Elicitor actions of N-acetylchitoooligosaccharides and laminarioligosaccharides for chitinase and L-phenylalanine ammonia-lyase induction in rice suspension culture. *Bioscience, Biotechnology and Biochemistry*, 61: 975-978.
- Irshad M, Canut H, Borderies G, Pont-Lezica R, Jamet E (2008) A new picture of cell wall protein dynamics in elongating cells of *Arabidopsis thaliana*: Confirmed actors and newcomers. *BMC Plant Biology*, 8: 94 - 101.
- Jack RW, Tagg JR, Ray B (1995) Bacteriocins of gram-positive bacteria. *Microbiological reviews*, 59:171-200.
- Jackowski G, Kacprzak K, Jansson S (2001) Identification of Lhcb1/Lhcb2/Lhcb3 heterotrimers of the main light harvesting chlorophyll a/b protein complex of Photosystem II (LHC II). *Biochimica et Biophysica Acta*, 1504: 340-345.
- James EK (2000) Nitrogen fixation in endophytic and associative symbiosis. *Field Crops Research* 65, 197–209.
- Jamet J, Albenne C, Boudart G, Irshad M, Canut H, Pont-Lezica R (2008) Recent advances in plant cell wall proteomics. *Proteomics*, 8: 893–908.
- Janeczko A and Skoczowski A (2005) Mammalian sex hormones in plants. *Folia Histochemistry and Cytobiology*, 43: 71–79.
- Jefferson RA, Kavanagh TA, Bevan MW (1987) GUS fusions: β -glucuronidase as a sensitive and versatile gene fusion marker in higher plants. *The EMBO Journal*, 6: 3901-3907.
- Jiang J, Yang B, Harris NS, Deyholos MK (2007) Comparative proteomic analysis of NaCl stress-responsive proteins in *Arabidopsis* roots. *Journal of Experimental Botany*, 58: 3591–3607.
- Johansson E, Olsson O, Nyström T (2004) Progression and Specificity of Protein Oxidation in the Life Cycle of *Arabidopsis thaliana*. *The Journal of Biological Chemistry*, 279: 22204–22208.
- Joshi T, Patil K, Fitzpatrick MR, Franklin LD, Yao Q, Jeffrey R, Cook JR, Wang Z, Libault M, Brechenmacher L, Valliyodan B, Wu X, Cheng J, Stacey G, Nguyen HT, Xu D (2012) Soybean Knowledge Base (SoyKB): a web resource for soybean translational genomics. *BMC Genomics*, 13 (Suppl 1): S15.
- Jun L, Wen-Li X, Ming-chao MA, Da-wei G, Xin J, Feng-ming C, DeLong S, Hui-jun C, Li L (2011) Proteomic study on two *Bradyrhizobium japonicum* strains with different competitiveness for nodulation. *Journal of Integrative Agriculture*, 10: 1072-1079.
- Jung G, Matsunami T, Oki Y, Kokubun M (2008b) Effects of water logging on nitrogen fixation and photosynthesis in supernodulating soybean cultivar Kanto 100. *Plant Production Science*, 11: 291-297.
- Jung W, Mabood F, Souleimanov A, Zhou X, Jaoua S, Kamoun F, Smith DL (2008a) Stability and antibacterial activity of bacteriocins produced by *Bacillus thuringiensis* and *Bacillus thuringiensis* ssp. *Kurstaki*. *Journal of Microbiology and Biotechnology*, 18: 1836–1840.

- Kamst E, Spaink HP, Kafetzopoulos D (1998) Biosynthesis and secretion of rhizobial lipochitin-oligosaccharide signal molecules. Pages 29-71 in: Subcellular Biochemistry 29: Plant-Microbe Interactions. B. B. Biswas and H. K. Das, eds. Plenum Press, New York
- Kaneko T, Nakamura Y, Sato S, Minamisawa K, Uchiumi T, Sasamoto S, Watanabe A, Idesawa K, Iriguchi M, Kawashima K, Kohara M, Matsumoto M, Shimpo S, Tsuruoka H, Wada T, Yamada M, Tabata S (2002a) Complete genomic sequence of nitrogen-fixing symbiotic bacterium *Bradyrhizobium japonicum* USDA110. DNA Research, 9: 189-197.
- Kaneko T, Nakamura Y, Sato S, Minamisawa K, Uchiumi T, Sasamoto S, Watanabe A, Idesawa K, Iriguchi M, Kawashima K, Kohara M, Matsumoto M, Shimpo S, Tsuruoka H, Wada T, Yamada M, Tabata S (2002b) Complete genomic sequence of nitrogen-fixing symbiotic bacterium *Bradyrhizobium japonicum* USDA110 (supplement). DNA Research, 9: 225-256.
- Kao WY, Tsai TT, Shih CN (2003) Photosynthetic gas exchange and chlorophyll a fluorescence of three wild soybean species in response to NaCl treatments. Photosynthetica, 41: 415-419.
- Katsir L, Chung HS, Koo AJK, Howe GA (2008) Jasmonate signaling: a conserved mechanism of hormone sensing. Current Opinion in Plant Biology, 11: 1-8.
- KEGG pathway - <http://www.genome.jp/kegg/>
- Keller A, Nesvizhskii AI, Kolker E, Aebersold R (2002) Empirical statistical model to estimate the accuracy of peptide identifications made by MS/MS and database search. Analytical Chemistry, 74: 5383-92.
- Kessmann H and Ryals J (1993) Requirement of salicylic acid for the induction of systemic acquired resistance. Science, 261: 754-756.
- Khan JA, Wang Q, Sjöstrand RJ, Schulz A, Thompson GA (2007) An early nodulin-like protein accumulates in the sieve element plasma membrane of *Arabidopsis*. Plant Physiology, 143: 1576-1589.
- Khan NA, Takahashi R, Abe J, Komatsu S (2009) Identification of cleistogamy-associated proteins in flower buds of near-isogenic lines of soybean by differential proteomic analysis. Peptides, 30: 2095-2102.
- Khan W (2003) Signal compounds involved with plant perception and response to microbes alter plant physiological activities and growth of crop plants. PhD Thesis, McGill University.
- Khan WM, Prithiviraj B, Smith DL (2008) Nod factor [Nod Bj V (C18:1, MeFuc)] and lumichrome enhance photosynthesis and growth of corn and soybean. Journal of Plant Physiology, 165: 1342-1351.
- Kim HS and Delaney TP (2002a) Over-expression of TGA5, which encodes a bZIP transcription factor that interacts with NIM1/NPR1, confers SAR-independent resistance in *Arabidopsis thaliana* to *Peronospora parasitica*. The Plant Journal, 32: 151-163.
- Kim HS and Delaney TP (2002b) Arabidopsis SON1 is an F-Box protein that regulates a novel induced defense response independent of both salicylic acid and systemic acquired resistance. The Plant Cell, 14: 1469-1482.

- Kim KY, Jordan D, McDonald GA (1998) Effect of phosphate solubilizing bacteria and vesicular–arbuscular mycorrhizae on tomato growth and soil microbial activity. *Biol. Fertil. Soil*, 26: 79–87.
- Kim ST, Kang SY, Wang Y, Kim SG, Hwang DH, Kang KY (2008) Analysis of embryonic protein modulation by GA and ABA from germinating rice seeds. *Proteomics*, 8: 3577–3587.
- Kim YC, Leveau J, Gardener BBM, Pierson EA, Pierson LS, Ryu C-M (2011) The multifactorial basis for plant health promotion by plant-associated bacteria. *Applied and Environmental Microbiology*, 77: 1548–1555.
- King EO, Ward MK, Raney DE (1954) Two simple media for the demonstration of phycocyanin and fluorescein. *Journal of Laboratory and Clinical Medicine*, 44: 301–307.
- Kinkema M, Fan W, Dong X (2000) Nuclear localization of NPR1 is required for activation of PR gene expression. *Plant Cell*, 12: 2339–2350.
- Kinross JM, von Roon AC, Holmes E, Darzi A, Nicholson JK (2008) The human gut microbiome: Implications for future health care. *Current Gastroenterology Reports*, 10: 396–403.
- Kirkup BC and Riley MA (2004) Antibiotic-mediated antagonism leads to a bacterial game of rock-paper-scissors *in vivo*. *Nature*, 428: 412–414.
- Kirst G (1990) Salinity tolerance of eukaryotic marine algae. *Annual Reviews in Plant Physiology*, 41: 21.
- Klaenhammer T (1993) Genetics of bacteriocins produced by lactic acid bacteria. *FEMS Microbiology Letters*, 12: 39–86.
- Kloepper JW and Schroth MN (1978) Plant growth-promoting rhizobacteria on radishes. *Proceedings of the 4th International Conference on Plant Pathogenic Bacteria*, 2: 879–882.
- Knud L (2003) Molecular cloning and characterization of a cDNA encoding a ryegrass (*Lolium perenne*) ENOD40 homologue. *Journal of Plant Physiology*, 160: 675–687.
- Koay SY and Gam LH (2011) Method development for analysis of proteins extracted from the leaves of *Orthosiphon aristatus*. *Journal of Chromatography B. Analytical Technologies in The Biomedical and Life Sciences*, 879: 2179–2183.
- Komatsu S, Wada T, Abale'a Y, Nouri M-Z, Nanjo Y, Nakayama N, Shimamura S, Yamamoto R, Nakamura T, Furukawa K (2009a) Analysis of plasma membrane proteome in soybean and application to flooding stress response. *Journal of Proteome Research*, 8: 4487–4499.
- Komatsu S, Yamamoto A, Nakamura T, Nouri M-Z, Nanjo Y, Nishizawa K, Furukawa K (2011) Comprehensive analysis of mitochondria in roots and hypocotyls of soybean under flooding stress using proteomics and metabolomics techniques. *Journal of Proteome Research*, 10: 3993–4004.
- Komatsu S, Yamamoto R, Nanjo Y, Mikami Y, Yunokawa H, Sakata K (2009b) A comprehensive analysis of the soybean genes and proteins expressed under flooding stress using transcriptome and proteome techniques. *Journal of Proteome Research*, 8: 4766–4778.

- Kosová K, Prášil IT, Vítámvás P (2013) Protein contribution to plant salinity response and tolerance acquisition. *International Journal of Molecular Science*, 14: 6757-6789.
- Krishnan HB (2002) Evidence for accumulation of the β -subunit of β -conglycinin in soybean [*Glycine max* (L) Merr.] embryonic axes. *Plant Cell report*, 20: 869-875.
- Krishnan HB, Nelson RL (2011) Proteomic analysis of high protein soybean (*Glycine max*) accessions demonstrates the contribution of novel glycinin subunits. *Journal of Agriculture and Food Chemistry*, 59: 2432-2439.
- Kunihiro A, Yamashino T, Nakamichi N, Niwa Y, Nakanishi H, Mizuno T (2011) PHYTOCHROME-INTERACTING FACTOR 4 and 5 (PIF4 and PIF5) activate the homeobox ATHB2 and auxin-Inducible IAA29 genes in the coincidence mechanism underlying photoperiodic control of plant growth of *Arabidopsis thaliana*. *Plant Cell Physiol*, 52: 1315–1329.
- Lahner B, Gong J, Mahmoudian M, Smith EL, Abid KB, Rogers EE, Guerinot ML, Harper JF, Ward JM, McIntyre L (2003) Genomic scale profiling of nutrient and trace elements in *Arabidopsis thaliana*. *Nature Biotechnology*, 21: 1215–1221.
- Lau OS and Deng XW (2010) Plant hormone signaling lightens up: integrators of light and hormones. *Current Opinion in Plant Biology*, 13: 571–577.
- Lauchli A and Staples RC (1984) Salinity tolerance in plants: strategies for crop improvement. New York: John Wiley and Sons: Salt exclusion: an adaptation of legume crops and pastures under saline conditions. Staples RC, Toeniessen GH, editors Salinity tolerance in plants: strategies for crop improvement. p: 171-187.
- Lauressergues D, Delaux P-M, Formey D, Lelandais-Brière C, Fort S, Cottaz S, Bécard G, Niebel A, Roux C, Combier J-P (2012) The microRNA miR171h modulates arbuscular mycorrhizal colonization of *Medicago truncatula* by targeting *NSP2*. *The Plant Journal*, 72: 512–522.
- Layzell DB and Atkins CA (1997) The physiology and biochemistry of legume N₂ fixation. In *Plant Metabolism* ed. Dennis DT, Turpin DH, Lefebvre DD and Layzell DB pp. 495–505. Harlow: Addison Wesley Longman.
- Lee CP, Taylor NL, Millar AH (2013) Recent advances in the composition and heterogeneity of the *Arabidopsis* mitochondrial proteome. *Frontiers in Plant Science*, 4: 1-8.
- Lee J, Garrett WM, Cooper B (2007) Shotgun proteomic analysis of *Arabidopsis thaliana* leaves. *Journal of Separation Science*, 30: 2225 – 2230.
- Lee K, Gray EJ, Mabood F, Jung W, Charles T, Clark SRD, Ly A, Souleimanov A, Zhou X, Smith DL (2009) The class IId bacteriocin thuricin-17 increases plant growth. *Planta*, 229: 747-755.
- Lee M-Y, Shin K-H, Kim Y-K, Suh J-Y, Gu Y-Y, Kim M-R, Hur Y-S, Son O, Kim J-S, ong E, Lee M-S, Nam KH, Hwang KH, Sung M-K, Kim H-J, Chun J-Y, Park M, Ahn T-I, Hong CB, Lee S-H, Park HJ, Park J-S, Verma DPS, Cheon C-I (2005) Induction of thioredoxin is required for nodule development to reduce reactive oxygen species levels in soybean roots. *Plant Physiology*, 139: 1881–1889.

- Lemaire-Chamley M, Petit J, Garcia V, Just D, Baldet P, Germain V, Fagard M, Mouassite M, Cheniclet C, Rothan C (2005) Changes in transcriptional profiles are associated with early fruit tissue specialization in tomato. *Plant Physiology*, 139: 750–769.
- Leon-Reyes A, Does DV, De Lange ES, Delker C, Wasternack C, Van Wees SCM, Ritsema T, Li L, Hou X, Tsuge T, Ding M, Aoyama T, Oka A, Gu H, Zhao Y, Qu L-J (2010) The possible action mechanisms of indole-3-acetic acid methyl ester in *Arabidopsis*. *Plant Cell Rep*, 27: 575–584.
- Leszczyszyn OI, Imam HT, Blindauer CA (2013) Diversity and distribution of plant metallothioneins: a review of structure, properties and functions. *Metallomics*, DOI: 10.1039/c3mt00072a.
- Levitt J (1980) Responses of plants to environmental stresses, 2nd edn. New York: Academic Press.
- Li L, Hou X, Tsuge T, Ding M, Aoyama T, Oka A, Gu H, Zhao Y, Qu L-J (2008) The possible action mechanisms of indole-3-acetic acid methyl ester in *Arabidopsis*. *Plant Cell Reports*, 27: 575–584.
- Lill J (2003) Proteomic tools for quantitation by mass spectrometry. *Mass Spectrometry Reviews*, 22: 182–194.
- Lindsay JK (2007) The effect of lipo-chitooligosaccharide from *Bradyrhizobium japonicum*, on soybean salicylic acid, pathogen-related protein activity and gene expression (Master's Thesis, McGill University).
- Liu H, Sadygov RG, Yates JR (2004) A model for random sampling and estimation of relative protein abundance in shotgun proteomics. *Analytical Chemistry*, 76: 4193–4201.
- Loiret FG, Ortega E, Kleiner D, Ortega-Rode's P, Rode's R, Dong Z (2004) A putative new endophytic nitrogen-fixing bacterium *Pantoea* sp. from sugarcane. *Journal of Applied Microbiology*, 97: 504–511.
- López-Lara I, Drift K, Brussel A, Haverkamp J, Lugtenberg B, Thomas-Oates J, Spaink H (1995) Induction of nodule primordia on *Phaseolus* and *Acacia* by lipo-chitin oligosaccharide nodulation signals from broad-host-range rhizobium strain GRH2. *Plant Molecular Biology*, 29: 465–477.
- Lorkovic ZJ (2009) Role of plant RNA-binding proteins in development, stress response and genome organization. *Trends in plant science*, 14: 229–236.
- Lowry OH, Rosebrough NJ, Farr AL, Randall RJ (1951) Protein measurement with Folin phenol reagent. *Journal of Biological Chemistry*, 193: 265–275.
- Lugtenberg B and Kamilova F (2009) Plant-growth-promoting rhizobacteria. *Annual Reviews in Microbiology*, 63: 541–556.
- Lui K (2004) Soybeans as a powerhouse of nutrients and phytochemicals. In *Soybeans as functional foods and ingredients*; Lui K., Ed.; AOCS Press: Champaign, IL, p: 1–53.
- Lumba S, Cutler S, McCourt P (2010) Plant nuclear hormone receptors: a role for small molecules in protein–protein interactions. *Annual Review of Cell Developmental Biology*, 26: 445–469.

- Lundquist PK, Poliakov A, Bhuiyan NH, Zybaïlov B, Sun Q, van Wijk KJ (2012) The functional network of the *Arabidopsis* plastoglobule proteome based on quantitative proteomics and genome-wide coexpression analysis. *Plant Physiology*, 158: 1172–1192.
- Mabood F and Smith DL (2005) Pre-incubation of *Bradyrhizobium japonicum* with jasmonates accelerates nodulation and nitrogen fixation in soybean (*Glycine max*) at optimal and suboptimal root zone temperatures. *Physiologia Plantarum*, 125: 311–325.
- Mabood F, Gray EJ, Lee KD, Supanjani, Smith DL (2006) Exploiting inter-organismal chemical communication for improved inoculants. *Canadian Journal of Plant Science*, 86: 951–966.
- Mabood F, Souleimanov A, Khan W, Smith DL (2006a) Jasmonates induce Nod factor production by *Bradyrhizobium japonicum*. *Plant Physiology and Biochemistry*, 44: 759–765.
- Mabood F, Zhou X, Smith DL (2006b) Pre-incubation of *Bradyrhizobium japonicum* cells with methyl jasmonate (MeJA) increases soybean nodulation and nitrogen fixation under short season field conditions. *Agronomy Journal*, 98: 289–294.
- Mabood F, Zhou X, Lee KD, Smith DL (2006c) Methyl jasmonate, alone or in combination with genistein, and *Bradyrhizobium japonicum* increases soybean (*Glycine max* L.) plant dry matter production and grain yield under short season conditions. *Field Crops Research*, 95: 412–419.
- Maillet F, Poinot V, André O, Puech-Pagès V, Haouy A, Gueunier M, Cromer L, Giraudet D, Formey D, Niebel A, Martinez EA, Driguez H, Bécard G, Dénarié J (2011) Fungal lipochitooligosaccharide symbiotic signals in arbuscular mycorrhizal. *Nature*, 469: 58–63.
- Maj D, Wielbo J, Marek-Kozaczuk M, Martyniuk S, Skorupska A (2009) Pretreatment of clover seeds with nod factors improves growth and nodulation of *Trifolium pratense*. *Journal of chemical ecology*, 35: 479–487.
- Malamy J, Carr J P, Klessig D F, Raskin I (1990) Salicylic Acid - A likely endogenous signal in the resistance response of tobacco to viral infection. *Science*, 250: 1002–1004.
- Mandadi KK, Misra A, Ren S, McKnight TD (2009) BT2, a BTB protein, mediates multiple responses to nutrients, stresses, and hormones in *Arabidopsis*. *Plant Physiology*, 150: 1930–1939.
- Mandal KG, Sahab KP, Ghosha PH, Hatia KM, Bandyopadhyaya KK (2002) Bioenergy and economic analysis of soybean-based crop production systems in central India. *Biomass and Bioenergy*, 23: 337–345.
- Mandel MJ, Schaefer AL, Brennan CA, Heath-Heckman EAC, DeLoney-Marino CR, McFall-Ngai MJ, Ruby EG (2012) Squid-derived chitin oligosaccharides are a chemotactic signal during colonization by *Vibrio fischeri*. *Applied and Environmental Microbiology*, 78: 4620–4626.
- Marhavy P, Bielach A, Abas L, Abuzeineh A, Duclercq J, Tanaka H, Parezova M, Petrašek J, Friml J, Kleine-Vehn J, Benkova E (2011) Cytokinin modulates endocytic trafficking of PIN1 auxin efflux carrier to control plant organogenesis development. *Cell*, 127: 796–804.
- Marrs KA (1996) The functions and regulation of glutathione S-transferases in plants. *Annual Review of Plant Physiology*, 47: 127–158.
- Mateos PF, Baker DL, Petersen M, Velázquez E, Jiménez-Zurdo JJ, Martínez-Molina E, Squartini A, Orgambide G, Hubbell DH, Dazzo FB (2001) Erosion of root epidermal cell walls by

rhizobium polysaccharide-degrading enzymes as related to primary host infection in the rhizobium–legume symbiosis. *Canadian Journal of Microbiology*, 47: 475-487.

Mathesius U, Djordjevic MA, Oakes M, Goffard N, Haerizadeh F, Weiller GF, Singh MB, Bhalla PL (2011) Comparative proteomic profiles of the soybean (*Glycine max*) root apex and differentiated root zone. *Proteomics*, 11: 1707-1719.

Meinke DW, Cherry JM, Dean C, Rounsley SD, Koornneef M (1998) *Arabidopsis thaliana*: A Model Plant for Genome Analysis. *Science*, 282: 662-682.

Meyer Y, Reichheld JP, Vignols F (2005) Thioredoxins in *Arabidopsis* and other plants. *Photosynthetic Research*, 86: 419–433.

Michael TP, Breton G, Hazen SP, Priest H, Mockler TC, Kay SA, Chory J (2008) A morning-specific phytohormone gene expression program underlying rhythmic plant growth. *PLoS Biol* 6: 1887-1898.

Mohammadi PP, Moieni A, Hiraga S, Komatsu S (2012) Organ specific proteomic analysis of drought-stressed soybean seedlings. *Journal of proteomics*, 75: 1906-1923.

Molloy MP, Herbert BR, Walsh BJ, Tyler MI, Traini M, Sanchez JC, Hochstrasser DF, Williams KL, Gooley AA (1998) Extraction of membrane proteins by differential solubilization for separation using two-dimensional gel electrophoresis. *Electrophoresis*, 19: 837-44.

Montrichard F, Alkhalfioui F, Yano H, Vensel WH, Hurkman WJ, Buchanan BB (2009) Thioredoxin targets in plants: the first 30 years. *Journal of Proteomics*, 72: 452–474.

Mooney BP and Thelen JJ (2004) High-throughput peptide mass fingerprinting of soybean seed proteins: automated workflow and utility of UniGene expressed sequence tag databases for protein identification. *Phytochemistry*, 65: 1733-1744.

Müller J, Boller T, Wiemken A (2001) Trehalose becomes the most abundant non-structural carbohydrate during senescence of soybean nodules. *Journal of Experimental Botany*, 52: 943-7.

Munns R (2005) Genes and salt tolerance: bringing them together. *New phytologist*, 167: 645.

Munns R, James RA, Lauchli A (2006) Approaches to increasing the salt tolerance of wheat and other cereals. *Journal of experimental botany*, 57: 1025-1043.

Munns, R (2002) Comparative physiology of salt and water stress. *Plant Cell Environ*, 25: 239–250.

Murashige T and Skoog F (1962) A revised medium for rapid growth and bioassays with tobacco tissue cultures. *Physiologia Plantarum* 15: 473-479.

Mushrush GW, Wynne JH, Willauer HD, Lloyd CL (2006) Soybean-derived biofuels and home heating fuels. *Journal of Environmental Science and Health. Part A-Toxic/Hazardous Substances and Environmental Engineering*, 41: 2495-2502.

Nakano T and Yokota T (2007) Progesterone: Its occurrence in plants and involvement in plant growth. *Phytochemistry*, 68: 1664–1673.

Nanjo Y, Nouri M-Z, Komatsu S (2011) Quantitative proteomic analyses of crop seedlings subjected to stress conditions; a commentary. *Phytochemistry*, 72: 1263-1272.

- Nanjo Y, Skultety L, Ashraf Y, Komatsu S (2010) Comparative proteomic analysis of early-stage soybean seedlings responses to flooding by using gel and gel-free techniques. *Journal of Proteome Research*, 9: 3989-4002.
- Nanjo Y, Skultety L, Uváčková L, Klubicová K, Hajduch M, Komatsu S (2012) Mass spectrometry-based analysis of proteomic changes in the root tips of flooded soybean seedlings. *Journal of Proteome Research*, 11: 372-385.
- Natarajan SS, Xu C, Bae H, Caperna TJ, Garrett WM (2006) Characterization of storage proteins in wild (*Glycine soja*) and cultivated (*Glycine max*) soybean seeds using proteomic analysis. *Journal of Agriculture and Food Chemistry*, 54: 3114-3120.
- Natarajan SS, Xu C, Caperna TJ, Garrett WM (2005) Comparison of protein solubilization methods suitable for proteomic analysis of soybean seed proteins. *Analytical Biochemistry*, 342: 214-220.
- Ndakidemi PA, Dakora FD, Nkonya EM, Ringo D, Mansoor H (2006) Yield and economic benefits of common bean (*Phaseolus vulgaris*) and soybean (*Glycine max*) inoculation in northern Tanzania. *Australian Journal of Experimental Agriculture*, 46: 571-577.
- Nemhauser JL, Hong F, Chory J (2006) Different plant hormones regulate similar processes through largely non overlapping transcriptional responses. *Cell*, 126: 467-475.
- Nesvizhskii AI, Keller A, Kolker E, Aebersold R (2003) A statistical model for identifying proteins by tandem mass spectrometry. *Analytical Chemistry*, 75: 4646-58.
- Newbould P (1989) The use of nitrogen fertilizers in agriculture. Where do we go practically and ecologically? *Plant Soil*, 115: 297-311.
- Ng W-L and Bassler L (2009) Bacterial quorum-sensing network architectures. *Annual Review of Genetics*, 43: 197-222.
- Niell S, Desikan R, Hancock J (2002) Hydrogen peroxide signaling. *Current Opinion in Plant Biology*, 5: 388-395.
- Nishiyama R, Watanabe Y, Fujita Y, Le DT, Kojima M, Werner T, Vankova R, Yamaguchi-Shinozaki K, Shinozaki K, Kakimoto T, Sakakibara H, Schmu'ling T, Tran LP (2011) Analysis of cytokinin mutants and regulation of cytokinin metabolic genes reveals important regulatory roles of cytokinins in drought, salt and abscisic acid responses, and abscisic acid biosynthesis. *The Plant Cell*, 23: 2169-2183.
- Noguchi K and Yoshida K (2008) Interaction between photosynthesis and respiration in illuminated leaves. *Mitochondrion*, 8: 87-99.
- Nouri M-Z and Komatsu S (2010) Comparative analysis of soybean plasma membrane proteins under osmotic stress using gel-based and LC MS/MS-based proteomics approaches. *Proteomics*, 10: 1930-1945.
- Novozymes-<http://bioag.novozymes.com/en/products/unitedstates/biofertility/Pages/default.aspx>
- Nylander M, Sevensson J, Palva ET, Welin BV (2001) Stress-induced accumulation and tissue-specific localization of dehydrins in *Arabidopsis thaliana*. *Plant Molecular Biology*, 45: 263-275.

- O'Leary B, Park J, Plaxton WC (2011) The remarkable diversity of plant PEPC (phosphoenolpyruvate carboxylase): recent insights into the physiological functions and post-translational controls of non-photosynthetic PEPCs. *The Biochemical Journal*, 436: 15–34.
- Oerhle NW, Sarma AD, Waters JK, Emerich DW (2008) Proteomic analysis of soybean nodule cytosol. *Phytochemistry*, 69: 2426-2438.
- Oláh B, Brière C, Bécard G, Dénarié J, Gough C (2005) Nod factors and a diffusible factor from arbuscular mycorrhizal fungi stimulate lateral root formation in *Medicago truncatula* via the DMI1/DMI2 signalling pathway. *Plant Journal*, 44: 195-207.
- Oresnik IJ, Twelker S, Hynes MF (1999) Cloning and characterization of a *Rhizobium leguminosarum* gene encoding a bacteriocin with similarities to RTX toxins. *Applied and environmental microbiology*, 65: 2833-2840.
- Pagani MA, Tomas M, Carrillo J, Bofill R, Capdevila M, Atrian S, Andreo CS (2012) The response of the different soybean metallothionein isoforms to cadmium intoxication. *Journal of inorganic Chemistry*, 117: 306-315.
- Panter S, Thomson R, de Bruxelles G, Laver D, Trevaskis B, Udvardi M (2000) Identification with proteomics of novel proteins associated with the peribacteroid membrane of soybean root nodules. *Molecular Plant Microbe Interactions*, 13: 325-333.
- Paoletti AC, Zybaylov B, Washburn MP (2004) Principles and applications of multidimensional protein identification technology. *Expert Review of Proteomics*, 1: 275-282.
- Parida AK and Das AB (2005) Salt tolerance and salinity effects on plants: a review. *Exotoxicology and Environmental Safety*, 60: 324-49.
- Parida AK, Das AB, Mitra B (2003) Effects of NaCl stress on the structure, pigment complex composition, and photosynthetic activity of mangrove *Bruguiera parviflora* chloroplasts. *Photosynthetica*, 41: 191-200.
- Peltier J-B, Cai Y, Sun Q, Zabrouskov V, Giacomelli L, Rudella A, Ytterberg AJ, Rutschow H, van Wijk KJ (2006) The oligomeric stromal proteome of *Arabidopsis thaliana* chloroplasts. *Molecular and Cellular Proteomics*, 5: 114–133.
- Peng Z-Y, Zhou X, Li L, Yu X, Li H, Jiang Z, Cao G, Bai M, Wang X, Jiang C, Lu H, Hou X, Qu L, Wang Z, Zuo J, Fu X, Su Z, Li S, Guo H (2009) Arabidopsis Hormone Database: a comprehensive genetic and phenotypic information database for plant hormone research in Arabidopsis. *Nucleic Acids Research*, 37: D975-D982.
- Penninckx IAMA, Thomma BPHJ, Buchala A, Metraux JP, Broekaert WF (1998) Concomitant activation of jasmonate and ethylene response pathways is required for induction of a plant defensin gene in Arabidopsis. *Plant Cell*, 10: 2103-2113.
- Perret X, Staehelin C, Broughton WJ (2000) Molecular basis of symbiotic promiscuity. *Microbiology and Molecular Biology Reviews*, 64: 180-201.
- Pestana-Calsa MC, Pacheco CM, de Castro RC, de Almeida RR, de Lira NP, Junior TC (2012) Cell wall, lignin and fatty acid-related transcriptome in soybean: Achieving gene expression patterns for bioenergy legume. *Genetics and Molecular Biology*, 35(1 (suppl)): 322-330.

- Pham J and Desikan R (2012) Modulation of ROS production and hormone levels by AHK5 during abiotic and biotic stress signaling. *Plant Signaling and Behavior*, 7: 893-897.
- Pieterse CMJ, Van Pelt JA, Saskia CM, van Wees, Ton J, Léon-Kloosterzeil KM, Keurentjes JJB, Verhagen BWM, Knoester M, Van der Sluis I, Bakker PAHM, van Loon LC (2001) Rhizobacteria-mediated induced systemic resistance: triggering, signaling and expression. *European Journal of Plant Pathology*, 107: 51-61.
- Pisa G, Magnani GS, Weber H, Souza EM, Faoro H, Monteiro RA, Daros E, Baura V, Bessalho JP, Pedrosa FO, Cruz LM (2011) Diversity of *16S rRNA* genes from bacteria of sugarcane rhizosphere soil. *Brazilian Journal of Medical and Biological Research*, 44: 1215-1221.
- Plaxton WC and Podesta' FE (2006) The functional organization and control of plant respiration. *Critical Reviews in Plant Science*, 25: 159-198.
- Polge C, Jaquinod M, Holzer F, Bourguignon J, Walling L, Brouquisse R (2009) Evidence for the existence in *Arabidopsis thaliana* of the proteasome proteolytic pathway, activation in response to cadmium. *The Journal of Biological Chemistry*, 284: 35412-35424.
- Prithiviraj B, Souleimanov A, Zhou X, Smith DL (2000) Differential response of soybean (*Glycine max* (L.) Merr.) genotypes to lipo-chito-ligosaccharide Nod Bj-V (C_{18:1} MeFuc). *Journal of Experimental Botany*, 51: 2045-2051.
- Prithiviraj B, Zhou X, Souleimanov A, Khan WM, Smith DL (2003) A host-specific bacteria-to-plant signal molecule (Nod factor) enhances germination and early growth of diverse crop plants. *Planta*, 216: 437-445.
- Proietti S, Bertini L, Timperio AM, Zolla L, Caporale C, Caruso C (2013) Crosstalk between salicylic acid and jasmonate in *Arabidopsis* investigated by an integrated proteomic and transcriptomic approach. *Molecular Biosystems*, DOI: 10.1039/c3mb25569g.
- Provorov NA, Tsyganova AV, Brewin NJ, Tsyganov VE, Vorobyov NI (2012) Evolution of symbiotic bacteria within the extra- and intra-cellular plant compartments: experimental evidence and mathematical simulation (Mini-review). *Symbiosis*, 58: 39-50.
- Pugsley AP (1984) The ins and outs of colicins. II. Lethal action, immunity and ecological implications. *Microbiological Sciences*, 1: 203-205.
- Qiu Q, Guo Y, Dietrich M, Schumaker KS, Zhu JK (2002) Regulation of SOS1, a plasma membrane Na⁺/H⁺ exchanger in *Arabidopsis thaliana*, by SOS2 and SOS3. *Proceedings of National Academy of Sciences, USA*, 99: 8436-8441.
- Quecine MC, Araújo WL, Rossetto PB, Ferreira A, Tsui S, Lacava PT, Mondin M, Azevedo JL, Pizzirani-Kleiner AA (2012) Sugarcane growth promotion by the endophytic bacterium *Pantoea agglomerans* 33.1. *Applied and Environmental Microbiology*, 78: 7511-7518.
- Qui L-J and Chang R-Z (2010) The origin and history of soybean. In *The soybean: botany, production and uses* / edited by Guriqbal Singh. Pp- 1-23, CAB International.
- Rader BA, Kremer N, Apicella MA, Goldman WE, McFall-Ngai MJ (2012) Modulation of symbiont lipid A signaling by host alkaline phosphatases in the squid-Vibrio symbiosis. *MBio* 3: doi: 10.1128.

- Ramu S, Peng H, Cook DR (2002) Nod factor induction of reactive oxygen species production is correlated with expression of the early nodulin gene *rip1* in *Medicago truncatula*. *Molecular Plant Microbe Interaction*, 15: 522–528.
- Ranjeva R and Boudet AM (1987) Phosphorylation of proteins in plants: Regulatory effects and potential involvement in stimulus/response coupling. *Annual Review of Plant Physiology*, 38: 73–93.
- Rao JR and Cooper JE (1994) Rhizobia catabolize gene-inducing flavanoid via C-ring fission mechanisms. *Journal of Bacteriology*, 176: 5409–5413.
- Rapala-Kozik M, Wolak N, Kujda M, Banas AK (2012) The upregulation of thiamine (vitamin B1) biosynthesis in *Arabidopsis thaliana* seedlings under salt and osmotic stress conditions is mediated by abscisic acid at the early stages of this stress response. *BMC Plant Biology*, 12: 2–15.
- Rausser WE (1999) Structure and function of metal chelators produced by plants -the case for organic acids, amino acids, phytin, and metallothioneins. *Cell Biochemistry and Biophysics*, 19–48.
- Rengasamy P (2008) Salinity in the landscape: A growing problem in Australia. *Geotimes*, 53: 34–39.
- Riley MA and Wertz JE (2002): Bacteriocins: evolution, ecology, and application. *Annual review of microbiology*, 56: 117–137.
- Robertson FC, Skeffington AW, Gardner MJ, Webb AAR (2009) Interactions between circadian and hormonal signalling in plants. *Plant Molecular Biology*, 69: 419–427.
- Rodriguez H and Fraga R (1999) Phosphate solubilizing bacteria and their role in plant growth promotion. *Biotechnology Advances*, 17: 319–339.
- Rolletschek H, Weber H, Borisjuk L (2003) Energy status and its control on embryogenesis of legumes. Embryo photosynthesis contributes to oxygen supply and is coupled to biosynthetic fluxes. *Plant Physiology*, 132: 1196–1206.
- Ruddle P, Whetten R, Cardinal A, Upchurch RG, Miranda L (2013) Effect of a novel mutation in a $\Delta 9$ -stearoyl-ACP-desaturase on soybean seed oil composition. *Theoretical and Applied Genetics*, 126: 241–249.
- Russell JD, Scalf M, Book AJ, Lador DT, Vierstra RD, Smith LM, Coon JJ (2013) Characterization and quantification of intact 26S proteasome proteins by real-time measurement of intrinsic fluorescence prior to top-down mass spectrometry. *PLoS ONE* 8(3): e58157. doi:10.1371/journal.pone.0058157.
- Ruuska SA, Girke T, Benning C, Ohlrogge JB (2002) Contrapuntal networks of gene expression during *Arabidopsis* seed filling. *Plant Cell*, 14: 1191–1206.
- Ryu C-M, Farag MA, Hu C-H, Reddy MS, Wei H-X, Pare PW, Kloepper JW (2003) Bacterial volatiles promote growth in *Arabidopsis*. *Proceedings of National Academy of Sciences*, 100: 4927–4932.
- Sa´nchez-Rodríguez C, Rubio-Somoza I, Sibout R, Persson S (2010) Phytohormones and the cell wall in *Arabidopsis* during seedling growth. *Trends in Plant Science*, 15: 291–301.

- Sadowsky MJ and Graham PH (1998) Soil biology of the Rhizobiaceae. In: (Spaink HP, Kondorosi A, Hooykaas PJJ. ed. The Rhizobiaceae, 155-172. (Kluwer: Dordrecht, The Netherlands).
- Salminen SO and Streeter JG (1986) Uptake and metabolism of carbohydrates by *Bradyrhizobium japonicum* bacteroids. Plant Physiology, 83: 535-540.
- Salvagiotti F, Cassman KG, Specht JE, Walters DT, Weiss A, Dobermann A (2008) Nitrogen uptake, fixation and response to fertilizer N in soybeans: A review. Field Crops Research, 108: 1-13.
- Santi C, Bogusz D, Franche C (2013) Biological nitrogen fixation in non-legume plants. Annals of Botany, Page 1 of 25.
- Sarma AD and Emerich DW (2005) Global protein expression pattern of *Bradyrhizobium japonicum* bacteroids: a prelude to functional proteomics. Proteomics, 5: 4170-84.
- Schmidt J, Rohrig H, John M, Wieneke U, Stacey G, Koncz C, Schell J (1993) Alteration of plant growth and development by *Rhizobium* nodA and nodB genes involved in the synthesis of oligosaccharide signal molecules. Plant Journal, 4: 651-658.
- Schmidt MA, Barbazuk WB, Sandford M, May G, Song Z, Zhou W, Nikolau BJ, Herman EM (2011) Silencing of soybean seed storage proteins results in a rebalanced protein composition preserving seed protein content without major collateral changes in the metabolome and transcriptome. Plant Physiology, 156: 330-345.
- Schultze M and Kondorosi Á (1996) The role of lipochitooligosaccharides in root nodule organogenesis and plant cell growth. Current Opinion in Genetics and Development, 6: 631-638.
- Schultze M and Kondorosi Á (1998) Regulation of symbiotic root nodule development. Annual Reviews in Genetics, 32: 33-57.
- Schwender J, Ohlrogge JB, Shachar-Hill Y (2004) Understanding flux in plant metabolic networks. Current Opinion in Plant Biology, 7: 309-317.
- Scott F, Gilbert SF, Sapp J, Tauber AI (2012) A symbiotic view of life: We have never been individuals. The Quarterly Review of Biology, 87: 325-341.
- Seung D, Risopatron JPM, Jones BJ, Marc J (2012) Circadian clock-dependent gating in ABA signalling networks. Protoplasma, 249: 445-457.
- Sha Valli Khan PS, Hoffmann L, Renaut J, Hausman JF (2007) Current initiatives in proteomics for the analysis of plant salt tolerance, Current Science, 93: 6-11.
- Shapiro AD and Zhang C (2001) The role of NDR1 in avirulence gene-directed signaling and control of programmed cell death in Arabidopsis. Plant Physiology, 127: 1089-1101.
- Shinozaki K and Yamaguchi-Shinozaki K (1997) Gene expression and signal transduction in water stress response. Plant Physiology, 115: 327-334.
- Shiraiwa T, Sakashita M, Yagi Y, Horie T (2006) Nitrogen fixation and seed yield in soybean under moderate high-temperature stress. Plant Production Science, 9: 165-167.

- Shoshan-Barmatz V and Gincel D (2003) The voltage dependent anion channel; characterization, modulation and role in mitochondrial function in cell's life and death. *Cell Biochemistry and Biophysics*, 39: 279-292.
- Siedow JN (1991) Plant lipoxygenase: structure and function. *Annual Reviews in Plant Physiology and Plant Molecular Biology*, 42: 145–188.
- Sinvany G, Kapulnik Y, Wininger S, Badani H, Jurkevitch E (2002) The early nodulin *enod40* is induced by, and also promotes arbuscular mycorrhizal root colonization. *Physiology and Molecular Plant Pathology*, 60: 103-109.
- Sobhanian H, Aghaei K, Komatsu S (2011) Changes in the plant proteome resulting from salt stress: Towards the creation of salt tolerant crops? *Journal of proteomics*, 74: 1323-1337.
- Sobhanian H, Razavizadeh R, Nanjo Y, Ehsanpour AA, Rastgar Jazii F, Motamed N, Komatsu S (2010) Proteome analysis of soybean leaves, hypocotyls and roots under salt stress. *Proteome Science*, 8: 1-15.
- Soulages JL, Kim K, Walters C, Cushman JC (2002) Temperature induced extended helix/random coil transitions in a group 1 late embryogenesis-abundant protein from soybean. *Plant physiology*, 128: 822-832.
- Souleimanov A, Prithiviraj B, Carlson RW, Jeyaretnam B, Smith DL (2002b) Isolation and characterization of the major nod factor of *Bradyrhizobium japonicum* strain 532C. *Microbiological Research*, 157: 25-28.
- Souleimanov A, Prithiviraj B, Smith DL (2002a) The major Nod factor of *Bradyrhizobium japonicum* promotes early growth of soybean and corn. *Journal of Experimental Botany*, 53: 1929-1934.
- Spaink H (2000) Root nodulation and infection factors produced by rhizobial bacteria. *Annual Review of Microbiology*, 54: 257-288.
- Spaink H, Wijfjes A, Lugtenberg B (1995) Rhizobium NodI and NodJ proteins play a role in the efficiency of secretion of lipochitin oligosaccharides. *Journal of Bacteriology*, 177: 6276-6281.
- Spoel SH and Dong X (2008) Making sense of hormone crosstalk during plant immune responses. *Cell Host and Microbe*, 3: 348-351.
- Sridhara S, Thimmegowda S, Prasad TG (1995) Effect of water regimes and moisture stress at different growth stages on nodule dynamics, nitrogenase activity and nitrogen fixation in soybean [*Glycine max* (L.) Merrill]. *Journal of Agronomy and Crop Science*, 174: 111-115.
- Staehelin C, Granado J, Muller J, Wiemken A, Mellor RB, Felix G, Regenass M, Broughton WJ, Boller T (1994) Perception of rhizobium nodulation factors by tomato cells and inactivation by root chitinases. *Proceedings of National Academy of Sciences, USA*, 91: 2196-2200.
- Staswick P E, Su W, Howell S H (1992) Methyl jasmonate inhibition of root growth and induction of a leaf protein are decreased in an *Arabidopsis thaliana* mutant. *Proceedings of National Academy of Sciences, USA*, 89: 6837-6840.
- Staswick PE, Serban B, Rowe M, Tiriyaki I, Maldonado MT, Maldonado MC, Suza W (2005) Characterization of an Arabidopsis enzyme family that conjugates amino acids to indole-3-Acetic acid. *The Plant Cell*, 17: 616–627.

- Steenhoudt O and Vanderleyden J (2000) *Azospirillum*, a free-living nitrogen-fixing bacterium closely associated with grasses: genetic, biochemical and ecological aspects. *FEMS Microbiology Reviews*, 24: 487-506.
- Streeter JG and Gomez ML (2006) Three enzymes for trehalose synthesis in *Bradyrhizobium* cultured bacteria and in bacteroids from soybean nodules. *Applied and Environmental Microbiology*, 72: 4250-4255.
- Su Y-H, Liu Y-B, Zhang X-S (2011) Auxin–Cytokinin interaction regulates meristem development. *Molecular Plant*, 4: 616–625.
- Sudre D, Gutierrez-Carbonell E, Lattanzio G, Rellán-Álvarez R, Gaymard F, Wohlgemuth G, Oliver Fiehn, Álvarez-Fernández A, Zamarreño AM, Bacaicoa E, Duy D, García-Mina J-M, Abadía J, Philippar K, López-Millán A-F, Briat J-F (2013) Iron-dependent modifications of the flower transcriptome, proteome, metabolome, and hormonal content in an *Arabidopsis* ferritin mutant. *Journal of Experimental Botany* doi:10.1093/jxb/ert112.
- Süss C, Hempel J, Zehner S, Krause A, Patschkowski T, Göttfert M (2006) Identification of genistein-inducible and type III-secreted proteins of *Bradyrhizobium japonicum*. *Journal of Biotechnology*, 126: 69-77.
- Sugawara M, Cytryn EJ, Sadowsky MJ (2010) Functional role of *Bradyrhizobium japonicum* trehalose biosynthesis and metabolism genes during physiological stress and nodulation. *Applied and Environmental Microbiology*, 76: 1071-81.
- Supanjani S, Habib A, Mabood F, Lee KD, Donnelly D, Smith DL (2006) Nod factor enhances calcium uptake by soybean. *Plant physiology and biochemistry : PPB / Societe francaise de physiologie vegetale*, 44: 866-872.
- Surpin M, Zheng H, Morita MT, Saito C, Avila E, Blakeslee JJ, Bandyopadhyay A, Kovaleva V, Carter D, Murphy A, Tasaka M, Raikhel N (2003) The VTI family of SNARE proteins is necessary for plant viability and mediates different protein transport pathways. *Plant Cell*, 15: 2885–2899.
- Szczyglowski K and Amyot L (2003) Symbiosis, inventiveness by recruitment? *Plant Physiology*, 131: 935–940.
- Tagg J, Daiani A, Wannamaker L (1976) Bacteriocins of gram-positive bacteria. *Bacteriological Reviews*, 40: 722-756.
- Thines B, Katsir L, Melotto M, Niu Y, Mandaokar A, Liu G, Nomura K, He S Y, Howe G A, Browse J (2007) JAZ repressor proteins are targets of the SCFCOI1 complex during jasmonate signaling. *Nature*, 448: 661-665.
- To JPC, Haberer G, Ferreira FJ, Deruere J, Mason MG, Schaller GE, Alonso JM, Ecker JR, Keiber JJ (2004) Type-A *Arabidopsis* Response Regulators Are Partially Redundant Negative Regulators of Cytokinin Signaling. *Plant Cell* 16: 658-671
- Toorchi M, Yukawa K, Nouri M-Z, Komatsu S (2009) Proteomics approach for identifying osmotic-stress-related proteins in soybean roots. *Peptides*, 30: 2108-2117.
- Triplett EW (1996) Diazotrophic endophytes: progress and prospects for nitrogen fixation in monocots. *Plant and Soil*, 186: 29–38.

- Tu JC (1981) Effect of salinity on rhizobium-root-hair interaction, nodulation and growth of soybean. *Canadian Journal of Plant Science*, 61: 231-239.
- Turner WL, Knowles VL, Plaxton WC (2005) Cytosolic pyruvate kinase: subunit composition, activity, and amount in developing castor and soybean seeds, and biochemical characterization of the purified castor seed enzyme. *Planta*, 222: 1051–1062.
- Uknes S, Mauch-Mani B, Moyer M, Potter S, Williams S, Dincher S, Chandler D, Slusarenko A, Ward E, Ryals J (1992) Acquired resistance in *Arabidopsis*. *Plant Cell*, 4: 645-56.
- Ulmasov T, Murfett J, Hagen G, Guilfoyle (1997) Aux/IAA Proteins Repress Expression of Reporter Genes Containing Natural and Highly Active Synthetic Auxin Response Elements. *Plant Cell*, 9: 1963-1971.
- van Wees SCM, Pieterse CMJ, Trijssenaar A, Van't Westende YAM, Hartog F, van Loon LC (1997) Differential induction of systemic resistance in *Arabidopsis* by biocontrol bacteria. *Molecular Plant-Microbe Interaction*, 6: 716-724.
- Vance CP (1998) Legume symbiotic nitrogen fixation: agronomic aspects. In *The Rhizobiaceae: Molecular biology of model Plant-Associated bacteria*, eds., Spaink HP, Kondorosi A, Hooykaas PJJ, Dordrecht, The Netherlands: Kluwer Academic Publishers, pp. 509-530.
- Vance CP (2001) Symbiotic nitrogen fixation and phosphorus acquisition: plant nutrition in a world of declining renewable resources. *Plant Physiology*, 127: 390-397.
- Vazquez M, Santana O, Quinto C (1993) The NodI and NodJ proteins from *Rhizobium* and *Bradyrhizobium* strains are similar to capsular polysaccharide secretion proteins from gram-negative bacteria. *Molecular Microbiology*, 8: 369-377.
- Velázquez E, Rojas M, Lorite MJ, Rivas R, Zurdo-Piñeiro JL, Heydrich M, Bedmar EJ (2008) Genetic diversity of endophytic bacteria which could be find in the apoplastic sap of the medullary parenchyma of the stem of healthy sugarcane plants. *Journal of Basic Microbiology*, 48: 118–124.
- Vernooy-Gerritse M, Bos ALM, Veldink GA, Vliegthart JFG (1983) Localization of lipoxygenases 1 and 2 in germinating soybean seeds by an indirect immunofluorescence technique. *Plant Physiology*, 73: 262-267.
- Vessey JK (2003) Plant growth promoting rhizobacteria as biofertilizers. *Plant Soil*, 255: 571-586.
- Vick BA and Zimmerman DC (1984) Biosynthesis of jasmonic acid by several plant species. *Plant Physiology*, 75: 458-461.
- Von Bulow JFW and Dobereiner J (1975) Potential for nitrogen fixation in maize genotypes in Brazil. *Proceedings of the National Academy of Sciences, USA*, 72: 2389-2393.
- Wan J, Torres M, Ganapathy A, Thelen J, DaGue BB, Mooney B, Xu D, Gary Stacey (2005) Proteomic analysis of soybean root hairs after infection by *Bradyrhizobium japonicum*. *Molecular Plant Microbe Interactions*, 18: 458–467.
- Wang N, Khan W, Smith DL (2012) Changes in soybean global gene expression after application of Lipo-chitooligosaccharide from *Bradyrhizobium japonicum* under sub-optimal temperature. *PLoS ONE*, 7(2): e31571.

- Washburn MP, Ulaszek R, Deciu C, Schieltz DM, Yates JR. III (2002) Analysis of quantitative proteomic data generated via multidimensional protein identification technology. *Analytical Chemistry*, 74: 1650-1657.
- Wasternack C (2007) Jasmonates: An Update on Biosynthesis, Signal Transduction and Action in Plant Stress Response, Growth and Development. *Annals of Botany*, 7: 1–17.
- Wechter WP, Levi A, Harris KR, Davis AR, Fei Z, Katzir N, Giovannoni JJ, Ayelet Salman-Minkov A, Hernandez A, Thimmapuram J, Tadmor Y, Portnoy V, Trebitsh T (2008) Gene expression in developing watermelon fruit. *BMC Genomics*. 9: 275.
- Whipps JM (2001) Microbial interactions and biocontrol in the rhizosphere. *Journal of Experimental Botany*, 52: 487-511.
- Whiteman S-A, Serazetdinova L, Jones AME, Sanders D, Rathjen J, Peck SC, Maathuis FJM (2008) Identification of novel proteins and phosphorylation sites in a tonoplast enriched membrane fraction of *Arabidopsis thaliana*. *Proteomics*, 8: 3536–3547.
- Wiebe BH (2007) Application of a risk indicator for assessing trends in dryland salinization risk on the Canadian Prairies. *Canadian journal of soil science*, 87: 213.
- Wilson RA, Handley BA, Beringer JE (1998) Bacteriocin production and resistance in a field population of *Rhizobium leguminosarum* biovar *Viciae*. *Soil Biology and Biochemistry*, 30: 413-417.
- Wittstock U and Burow M (2010) Glucosinolate Breakdown in *Arabidopsis*: Mechanism, Regulation and Biological Significance. *The Arabidopsis Book*. First published on July 12, 2010 10.1199/tab.0134.
- Wong JH, Kobrehel K, Buchanan BB (1995) Thioredoxin and seed proteins. *Methods in Enzymology*, 252: 228–240.
- Xing M and Xue H (2012) A proteomics study of auxin effects in *Arabidopsis thaliana*. *Acta Biochim Biophys Sin*, 44: 783–796.
- Xiong L, Schumaker KS, Zhu J-K (2002) Cell Signaling during Cold, Drought, and Salt Stress. *The Plant Cell*, S165–S183.
- Xu XM and Moller SG (2011) The value of *Arabidopsis* research in understanding human disease states. *Current Opinion in Biotechnology*, 22: 300-307.
- Xu X-Y, Fan R, Zheng R, Li C-M, Yu D-Y (2011) Proteomic analysis of seed germination under salt stress in soybeans. *Journal Zhejiang Univ-Sci B (Biomedicine and Biotechnology)*, 12: 507-517.
- Yamaguchi M, Valliyodan B, Zhang J, Lenoble ME, Yu O, Rogers EE, Nguyen HT, Sharp RE (2010) Regulation of growth response to water stress in the soybean primary root. I. Proteomic analysis reveals region-specific regulation of phenylpropanoid metabolism and control of free iron in the elongation zone. *Plant, Cell and Environment*, 33: 223-243.
- Yan L (2008) Effect of salt stress on seed germination and seedling growth of three salinity plants. *Pakistan Journal of Biological Sciences*, 11: 1268-1272.

- Yang H, Huang Y, Zhi H, Yu D (2011) Proteomics-based analysis of novel genes involved in response toward soybean mosaic virus infection. *Molecular Biology Reports*, 38: 511-521.
- Zhang F and Smith DL (2001) Interorganismal signaling in suboptimum environments: the legume–rhizobia symbiosis. *Advances in Agronomy*, 76: 125–161.
- Zhang L-T, Zhang Z-S, Gao H-Y, Meng X-L, Yang C, Lui J-G, Meng Q-W (2011) Mitochondrial alternative oxidase pathway protects plants against photoinhibition by alleviating inhibition of the repair of photodamaged PSII through preventing formation of reactive oxygen species in *Rumex* K-1 leaves. *Plant Physiology*, 143: 396-407.
- Zhao Z, Zhang W, Stanley BA, Assmann SM (2008) Functional proteomics of *Arabidopsis thaliana* guard cells uncovers new stomatal signaling pathways. *The Plant Cell*, 20: 3210–3226.
- Zhen Y, Qia J-L, Wanga S-S, Sua J, Xua G-H, Zhanga M-S, Miaoa L, Pengb X-X, Tiana D and Yanga Y-H (2007) Comparative proteome analysis of differentially expressed proteins induced by Al toxicity in soybean. *Physiologia Plantarum*, 131: 542-554.
- Zhou R, Cutler AJ, Ambrose SJ, Galka MM, Nelson KM, Squires TM, Loewen MK, Jadhav AS, Ross ARS, Taylor DC, Abrams SR (2004) A new abscisic acid catabolic pathway. *Plant Physiology*, 134: 361–369.
- Zhu JK (2000) Genetic analysis of plant salt tolerance using *Arabidopsis thaliana*. *Plant Physiology*, 124: 941-948.
- Zhu J-K (2001a) Plant salt tolerance. *Trends in Plant Science*, 6: 66-71.
- Zhu J-K (2001b) Cell signaling under salt, water and cold stresses. *Current Opinion in Plant Biology*, 4: 401–406.

APPENDIX I

CHAPTER 3

Table 3.1: Phytohormones and their catabolites/conjugates analyzed in three-week-old *Arabidopsis thaliana* rosette, 24 h after LCO and Th17 treatments (LCO - 10^{-6} M, Th17 - 10^{-9} M) [24 h post signal compound treatment – UPLC-ESI-MS/MS; Analysis conducted at the National Research Council (NRC)-Plant Biology Institute (PBI), Saskatoon]

Auxins	
IAA	Indole-3-acetic acid
IAA-Asp	N-(Indole-3-yl-acetyl)-aspartic acid
IAA-Glu	N-(Indole-3-yl-acetyl)-glutamic acid
IAA-Ala	N-(Indole-3-yl-acetyl)-alanine
IAA-Leu	N-(Indole-3-yl-acetyl)-leucine
IBA	Indole-3-butyric acid
Cytokinins	
t-ZOG	(trans) Zeatin-O-glucoside
c-ZOG	(cis) Zeatin-O-glucoside
t-Z	(trans) Zeatin
c-Z	(cis) Zeatin
dhZ	Dihydrozeatin
t-ZR	(trans) Zeatin riboside
c-ZR	(cis) Zeatin riboside
dhZR	Dihydrozeatin riboside
2iP	Isopentenyladenine
Gibberellins	
GA1	Gibberellin 1
GA3	Gibberellin 3
GA4	Gibberellin 4
GA7	Gibberellin 7
GA8	Gibberellin 8
GA9	Gibberellin 9
GA19	Gibberellin 19
GA20	Gibberellin 20
GA24	Gibberellin 24
GA29	Gibberellin 29
GA34	Gibberellin 34
GA44	Gibberellin 44
GA51	Gibberellin 51
GA53	Gibberellin 53
ABA & metabolites	

ABA	cis-Absciscic acid
ABAGE	Absciscic acid glucose ester
DPA	Dihydrophaseic acid
PA	Phaseic acid
7'OH-ABA	7'-Hydroxy-absciscic acid
neo-PA	neo-Phaseic acid
t-ABA	trans-Absciscic acid
Free Salicylic acid	
Free Jasmonic acid	

APPENDIX II

CHAPTER 4

Table 4.3a: Fold change of spectral count in *Arabidopsis thaliana* rosette Contrast 1 - Control Vs LCO

	Fold change for Contrast 1 - Control Vs LCO				
	Identified Proteins <i>Arabidopsis thaliana</i> rosettes	NCBI Accession	MW	Control	LCO
1	[acyl-carrier-protein] S-malonyltransferase/ binding / catalytic/ transferase	gi 18402286	42 kDa	2.1	0.5
2	40S ribosomal protein S3 (RPS3B)	gi 15232352	27 kDa	0.3	3.4
3	40S ribosomal protein S3A (RPS3aB)	gi 15236171 (+1)	30 kDa	0.1	7.0
4	4-alpha-hydroxytetrahydrobiopterin dehydratase	gi 15241386	24 kDa	3.6	0.3
5	50S ribosomal protein L21, chloroplast / CL21 (RPL21)	gi 15219695	24 kDa	2.5	0.4
6	60S ribosomal protein L10 (RPL10B)	gi 15223382 (+3)	25 kDa	0.3	3.9
7	60S ribosomal protein L17 (RPL17B)	gi 15220431 (+2)	20 kDa	0.3	3.8
8	60S ribosomal protein L18 (RPL18C)	gi 15241061	21 kDa	0.4	2.3
9	60S ribosomal protein L30 (RPL30C)	gi 15230183	12 kDa	0.3	3.9
10	60S ribosomal protein L6 (RPL6C)	gi 15221126 (+1)	26 kDa	0.1	7.3
11	AAC1 (ADP/ATP CARRIER 1); ATP:ADP antiporter/ binding	gi 15231937	41 kDa	0.4	2.3
12	AILP1	gi 15239658 (+1)	25 kDa	2.7	0.4
13	AKR2 (ANKYRIN REPEAT-CONTAINING PROTEIN 2); protein binding	gi 15237008 (+1)	37 kDa	0.4	2.3
14	AOS (ALLENE OXIDE SYNTHASE); allene oxide synthase/ hydro-lyase/ oxygen binding	gi 15239032 (+2)	58 kDa	0.5	2.1
15	ASP1 (ASPARTATE AMINOTRANSFERASE 1); L-aspartate:2-oxoglutarate aminotransferase	gi 15224592	48 kDa	2.2	0.5
16	ASP2 (ASPARTATE AMINOTRANSFERASE 2); L-aspartate:2-oxoglutarate aminotransferase	gi 15239772 (+1)	44 kDa	2.1	0.5
17	AT103	gi 1033195	44 kDa	0.3	3.4

18	At2g34460/T31E10.20	gi 15912295 (+2)	27 kDa	0.4	2.9
19	AT3g52500/F22O6_120	gi 16209647 (+1)	51 kDa	4.1	0.2
20	AT4G38220	gi 227202560 (+3)	44 kDa	0.5	2.0
21	AtMAPR2 (Arabidopsis thaliana membrane-associated progesterone binding protein 2); heme binding	gi 15224648 (+2)	11 kDa	2.2	0.5
22	ATOMT1 (O-METHYLTRANSFERASE 1); caffeate O-methyltransferase/ myricetin 3'-O-methyltransferase/ quercetin 3-O-methyltransferase	gi 15239571 (+1)	40 kDa	2.8	0.4
23	ATPPC1 (PHOSPHOENOLPYRUVATE CARBOXYLASE 1); catalytic/ phosphoenolpyruvate carboxylase	gi 15219272 (+1)	110 kDa	0.4	2.7
24	ATPPC2 (PHOSPHOENOLPYRUVATE CARBOXYLASE 2); catalytic/ phosphoenolpyruvate carboxylase	gi 240254631	110 kDa	0.3	3.1
25	ATRP1 (PPDK REGULATORY PROTEIN); phosphoprotein phosphatase/ protein kinase	gi 15233554 (+2)	44 kDa	3.1	0.3
26	CaS (Calcium sensing receptor)	gi 15237201	41 kDa	0.4	2.5
27	CDSP32 (CHLOROPLASTIC DROUGHT-INDUCED STRESS PROTEIN OF 32 KD)	gi 15222954 (+1)	34 kDa	3.3	0.3
28	COR15A (COLD-REGULATED 15A)	gi 15227963 (+1)	15 kDa	7.0	0.1
29	COR15B (COLD REGULATED 15B)	gi 15227952 (+1)	15 kDa	2.9	0.3
30	COS1 (COI1 SUPPRESSOR1); 6,7-dimethyl-8-ribityllumazine synthase	gi 15224809	24 kDa	0.3	3.8
31	DEGP1 (DegP protease 1); serine-type endopeptidase/ serine-type peptidase	gi 22331378	47 kDa	2.4	0.4
32	diaminopimelate epimerase family protein	gi 15231841 (+1)	39 kDa	0.3	2.9
33	dicarboxylate/tricarboxylate carrier (DTC)	gi 15241167	32 kDa	0.4	2.4
34	dihydrolipoamide acetyltransferase	gi 11994364 (+2)	60 kDa	2.1	0.5
35	DNA-binding family protein / remorin family protein	gi 15233068	23 kDa	0.3	3.0
36	ELI3-1 (ELICITOR-ACTIVATED GENE 3-1); binding / catalytic/ oxidoreductase/ zinc ion binding	gi 15233642 (+1)	38 kDa	3.3	0.3

37	elongation factor 1-beta / EF-1-beta	gi 145324076 (+3)	29 kDa	0.4	2.5
38	emb1138 (embryo defective 1138); ATP binding / ATP-dependent helicase/ RNA binding / helicase/ nucleic acid binding / zinc ion binding	gi 30690260 (+2)	81 kDa	0.4	2.2
39	emb2386 (embryo defective 2386); structural constituent of ribosome	gi 15218602	25 kDa	0.3	3.9
40	emb2726 (embryo defective 2726); RNA binding / translation elongation factor	gi 18417320	104 kDa	0.4	2.3
41	FQR1 (FLAVODOXIN-LIKE QUINONE REDUCTASE 1); FMN binding / oxidoreductase, acting on NADH or NADPH, quinone or similar compound as acceptor	gi 15239652	22 kDa	2.4	0.4
42	FSD1 (FE SUPEROXIDE DISMUTASE 1); copper ion binding / superoxide dismutase	gi 15234913 (+3)	24 kDa	2.6	0.4
43	FTSZ2-1; protein binding / structural molecule	gi 18404086	51 kDa	2.1	0.5
44	GDCH; glycine dehydrogenase (decarboxylating)	gi 15226973	18 kDa	2.7	0.4
45	Glu-tRNA(Gln) amidotransferase subunit A	gi 11078533 (+1)	57 kDa	2.1	0.5
46	glycine-rich RNA-binding protein	gi 829254 (+4)	14 kDa	4.3	0.2
47	GRF10 (GENERAL REGULATORY FACTOR 10); ATP binding / protein binding / protein phosphorylated amino acid binding	gi 18395103 (+2)	29 kDa	0.4	2.3
48	GUN5 (GENOMES UNCOUPLED 5); magnesium chelatase	gi 15240675 (+2)	154 kDa	0.2	4.7
49	late embryogenesis abundant family protein / LEA family protein	gi 15224810 (+1)	36 kDa	0.5	2.0
50	legume lectin family protein	gi 15228229	31 kDa	10.5	0.1
51	LTPG1 (GLYCOSYLPHOSPHATIDYLINOSITOL-ANCHORED LIPID PROTEIN TRANSFER 1)	gi 15217777 (+1)	20 kDa	0.4	2.5
52	mitochondrial elongation factor Tu	gi 1149571 (+1)	51 kDa	2.5	0.4
53	MLP43 (MLP-LIKE PROTEIN 43)	gi 15223275	18 kDa	3.7	0.3
54	MST1 (MERCAPTOPYRUVATE SULFURTRANSFERASE 1); 3-mercaptopyruvate sulfurtransferase/ sulfurtransferase/ thiosulfate sulfurtransferase	gi 18412307 (+1)	42 kDa	4.3	0.2
55	MTHSC70-2 (MITOCHONDRIAL HSP70 2); ATP binding	gi 15242459	73 kDa	3.6	0.3
56	NADH-ubiquinone oxidoreductase-related	gi 18423437	19 kDa	0.4	2.8

57	NPQ4 (NONPHOTOCHEMICAL QUENCHING); chlorophyll binding / xanthophyll binding	gi 15219418 (+1)	28 kDa	0.3	3.7
58	NTF2A (NUCLEAR TRANSPORT FACTOR 2A); Ran GTPase binding / protein transporter	gi 15223491	14 kDa	3.0	0.3
59	NTF2B (NUCLEAR TRANSPORT FACTOR 2B); Ran GTPase binding / protein transporter	gi 145324046 (+2)	15 kDa	2.0	0.5
60	oxygen-evolving complex-related	gi 18411110 (+1)	27 kDa	5.1	0.2
61	PAB1 (PROTEASOME SUBUNIT PAB1); endopeptidase/ peptidase/ threonine-type endopeptidase	gi 15219257 (+1)	26 kDa	2.0	0.5
62	PAC1; endopeptidase/ peptidase/ threonine-type endopeptidase	gi 15233268 (+1)	27 kDa	2.0	0.5
63	PAE1; endopeptidase/ peptidase/ threonine-type endopeptidase	gi 15220961	26 kDa	3.1	0.3
64	PBF1; peptidase/ threonine-type endopeptidase	gi 15232965 (+2)	25 kDa	2.5	0.4
65	PBP1 (PYK10-BINDING PROTEIN 1); copper ion binding	gi 15228198 (+1)	32 kDa	2.0	0.5
66	pfkB-type carbohydrate kinase family protein	gi 15224669	35 kDa	2.8	0.4
67	PGY1 (PIGGYBACK1); RNA binding / structural constituent of ribosome	gi 18401451	24 kDa	0.4	2.6
68	phosphoprotein phosphatase (EC 3.1.3.16) 2A-4 (version 2) [similarity]	gi 11262975 (+4)	34 kDa	2.0	0.5
69	photosystem II 47 kDa protein	gi 7525059 (+1)	56 kDa	0.3	3.8
70	photosystem II D2 protein	gi 27435857 (+1)	35 kDa	0.4	2.6
71	photosystem II family protein	gi 18379115	19 kDa	2.1	0.5
72	photosystem II protein D1	gi 7525013	39 kDa	0.4	2.7
73	PKT3 (PEROXISOMAL 3-KETOACYL-COA THIOLASE 3); acetyl-CoA C-acyltransferase	gi 15225798 (+1)	49 kDa	2.1	0.5
74	PLDALPHA1 (PHOSPHOLIPASE D ALPHA 1); phospholipase D	gi 15232671	92 kDa	0.4	2.6
75	PP2AA3 (PROTEIN PHOSPHATASE 2A SUBUNIT A3); binding / protein phosphatase type 2A regulator	gi 22329534 (+5)	66 kDa	0.5	2.1
76	PSAL (photosystem I subunit L)	gi 15235490 (+1)	23 kDa	0.3	4.0

77	PYK10; beta-glucosidase/ copper ion binding / fucosidase/ hydrolase, hydrolyzing O-glycosyl compounds	gi 15232626 (+3)	60 kDa	6.1	0.2
78	RecName: Full=Aconitate hydratase 3, mitochondrial; Short=Aconitase 3; AltName: Full=Citrate hydro-lyase 3; Flags: Precursor	gi 118572817 (+2)	108 kDa	4.6	0.2
79	RecName: Full=ATP-dependent Clp protease proteolytic subunit 1; AltName: Full=Endopeptidase ClpP1; Short=pClpP	gi 160332321 (+1)	22 kDa	0.3	2.9
80	RecName: Full=DEAD-box ATP-dependent RNA helicase 15	gi 110283023 (+6)	48 kDa	0.1	8.3
81	RecName: Full=Photosystem II CP43 chlorophyll apoprotein; AltName: Full=PSII 43 kDa protein; AltName: Full=Photosystem II 44 kDa reaction center protein; AltName: Full=Protein CP-43; AltName: Full=Protein P6; Flags: Precursor	gi 172045852 (+1)	50 kDa	0.4	2.4
82	RHM1 (RHAMNOSE BIOSYNTHESIS 1); UDP-L-rhamnose synthase/ UDP-glucose 4,6-dehydratase/ catalytic	gi 15218420	75 kDa	2.5	0.4
83	ribosomal protein S11 (probable start codon at bp 67)	gi 166867 (+1)	20 kDa	0.2	4.5
84	RPL23AB (RIBOSOMAL PROTEIN L23AB); RNA binding / nucleotide binding / structural constituent of ribosome	gi 145332857 (+4)	17 kDa	0.3	3.6
85	RPL27AB; structural constituent of ribosome	gi 15220698 (+1)	16 kDa	0.3	3.6
86	RPS6 (RIBOSOMAL PROTEIN S6); structural constituent of ribosome	gi 15236042	28 kDa	0.4	2.5
87	RPT1A (REGULATORY PARTICLE TRIPLE-A 1A); ATPase	gi 15220930 (+1)	48 kDa	4.5	0.2
88	SOUL heme-binding family protein	gi 15220033	25 kDa	2.5	0.4
89	SQD1; UDPsulfoquinovose synthase/ sulfotransferase	gi 15234041 (+4)	53 kDa	0.4	2.8
90	THIC (ThiaminC); ADP-ribose pyrophosphohydrolase/ catalytic/ iron-sulfur cluster binding	gi 15227584	72 kDa	2.2	0.5
91	thylakoid lumenal 15 kDa protein, chloroplast	gi 18406661 (+1)	24 kDa	3.1	0.3
92	TIC110 (TRANSLOCON AT THE INNER ENVELOPE MEMBRANE OF CHLOROPLASTS 110)	gi 15221009 (+2)	112 kDa	0.2	6.2
93	TIC40	gi 15237382	49 kDa	7.5	0.1

94	TSB1 (TRYPTOPHAN SYNTHASE BETA-SUBUNIT 1); tryptophan synthase	gi 15239755	51 kDa	2.8	0.4
95	universal stress protein (USP) family protein	gi 18401345	18 kDa	2.3	0.4
96	UXS3 (UDP-GLUCURONIC ACID DECARBOXYLASE 3); UDP-glucuronate decarboxylase/ catalytic	gi 145334845 (+2)	40 kDa	4.8	0.2
97	vestitone reductase-related	gi 15236930	44 kDa	0.3	3.4
	Putative protein				
1	26S proteasome regulatory subunit, putative	gi 145334543 (+2)	29 kDa	3.0	0.3
2	adenylosuccinate lyase, putative / adenylosuccinase, putative	gi 22328773	60 kDa	0.4	2.6
3	ATP-dependent Clp protease proteolytic subunit, putative	gi 18414804 (+1)	33 kDa	2.5	0.4
4	beta-hydroxyacyl-ACP dehydratase, putative	gi 18399910	24 kDa	0.3	3.0
5	caffeoyl-CoA 3-O-methyltransferase, putative	gi 15235213	29 kDa	2.1	0.5
6	calmodulin, putative	gi 15221284 (+1)	17 kDa	2.2	0.4
7	fructose-bisphosphate aldolase, putative	gi 15226185	42 kDa	2.3	0.4
8	nuclear RNA-binding protein, putative	gi 145334757 (+2)	32 kDa	0.2	5.1
9	phosphoethanolamine N-methyltransferase 2, putative (NMT2)	gi 15221909 (+1)	54 kDa	3.8	0.3
10	thiol methyltransferase, putative	gi 145331123 (+2)	27 kDa	2.7	0.4
	Hypothetical protein				
1	hypothetical protein	gi 10998936 (+1)	56 kDa	0.4	2.6
2	hypothetical protein	gi 110736982 (+1)	25 kDa	2.2	0.5
3	hypothetical protein	gi 110740330 (+1)	63 kDa	0.1	8.5
	Unknown protein				
1	unknown protein	gi 18398135 (+1)	39 kDa	2.1	0.5
2	unknown protein	gi 18411555 (+1)	18 kDa	0.2	6.0
3	unknown protein	gi 15239049 (+7)	40 kDa	0.3	3.9
4	unknown protein	gi 18410256 (+2)	40 kDa	2.0	0.5

Table 4.3b: Fold change of spectral count in *Arabidopsis thaliana* rosette Contrast 2 - Control Vs Th17

	Fold change for Contrast 2 - Control Vs Th17				
	Identified Proteins <i>Arabidopsis thaliana</i> rosette	NCBI Accession	MW	Control	Th17
1	2-oxoacid dehydrogenase family protein	gi 15240454	50 kDa	5.9	0.2
2	4-alpha-hydroxytetrahydrobiopterin dehydratase	gi 15241386	24 kDa	2.7	0.4
3	60S ribosomal protein L30 (RPL30C)	gi 15230183	12 kDa	0.3	2.9
4	AILP1	gi 15239658 (+1)	25 kDa	3.3	0.3
5	AKR2 (ANKYRIN REPEAT-CONTAINING PROTEIN 2); protein binding	gi 15237008 (+1)	37 kDa	0.3	3.1
6	ALDH2C4; 3-chloroallyl aldehyde dehydrogenase/ aldehyde dehydrogenase (NAD)/ coniferyl-aldehyde dehydrogenase	gi 18404212	54 kDa	5.8	0.2
7	aldose 1-epimerase family protein	gi 15228261	40 kDa	3.0	0.3
8	At2g34460/T31E10.20	gi 15912295 (+2)	27 kDa	0.2	4.8
9	AT3g06720/F3E22_14	gi 13605661 (+2)	59 kDa	2.3	0.4
10	AT3g07390/F21O3_10	gi 18426884 (+2)	16 kDa	0.5	2.0
11	AT3g52500/F22O6_120	gi 16209647 (+1)	51 kDa	2.6	0.4
12	ATCAP1 (ARABIDOPSIS THALIANA CYCLASE ASSOCIATED PROTEIN 1); actin binding	gi 15236128	51 kDa	0.3	3.0
13	ATNAP6 (NON-INTRINSIC ABC PROTEIN 6); protein binding / transporter	gi 18398463 (+1)	53 kDa	3.2	0.3
14	ATPPC1 (PHOSPHOENOLPYRUVATE CARBOXYLASE 1); catalytic/ phosphoenolpyruvate carboxylase	gi 15219272 (+1)	110 kDa	0.4	2.7
15	ATPPC2 (PHOSPHOENOLPYRUVATE CARBOXYLASE 2); catalytic/ phosphoenolpyruvate carboxylase	gi 240254631	110 kDa	0.3	3.0
16	ATSAR1B (SECRETION-ASSOCIATED RAS 1 B); GTP binding	gi 15223516	22 kDa	2.7	0.4
17	CaS (Calcium sensing receptor)	gi 15237201	41 kDa	0.4	2.3
18	CB5-E (CYTOCHROME B5 ISOFORM E); heme binding	gi 15238776	15 kDa	2.0	0.5
19	CDSP32 (CHLOROPLASTIC DROUGHT-INDUCED STRESS PROTEIN OF 32 KD)	gi 15222954 (+1)	34 kDa	2.4	0.4

20	Clp amino terminal domain-containing protein	gi 18416540 (+1)	26 kDa	0.3	2.9
21	COR15A (COLD-REGULATED 15A)	gi 15227963 (+1)	15 kDa	4.9	0.2
22	CORI3 (CORONATINE INDUCED 1); cystathionine beta-lyase/ transaminase	gi 15236533	47 kDa	0.4	2.4
23	CP12-1	gi 30690673	13 kDa	0.5	2.1
24	CP29; RNA binding / poly(U) binding	gi 15231817 (+2)	36 kDa	7.5	0.1
25	curculin-like (mannose-binding) lectin family protein	gi 15219200 (+1)	49 kDa	0.4	2.6
26	cytochrome b6	gi 7525063	24 kDa	0.5	2.0
27	diaminopimelate epimerase family protein	gi 15231841 (+1)	39 kDa	0.4	2.6
28	dihydrolipoamide acetyltransferase	gi 11994364 (+2)	60 kDa	2.2	0.4
29	DNA-binding family protein / remorin family protein	gi 15233068	23 kDa	0.2	6.4
30	ECT2; protein binding	gi 30682679 (+3)	72 kDa	4.2	0.2
31	FTSZ2-1; protein binding / structural molecule	gi 18404086	51 kDa	2.1	0.5
32	Glu-tRNA(Gln) amidotransferase subunit A	gi 11078533 (+1)	57 kDa	2.1	0.5
33	GUN5 (GENOMES UNCOUPLED 5); magnesium chelatase	gi 15240675 (+2)	154 kDa	0.4	2.9
34	hydroxyproline-rich glycoprotein family protein	gi 18411523 (+2)	49 kDa	0.4	2.8
35	KAS I (3-KETOACYL-ACYL CARRIER PROTEIN SYNTHASE I); catalytic/ fatty-acid synthase/ transferase, transferring acyl groups other than amino-acyl groups	gi 15237422 (+2)	50 kDa	0.4	2.6
36	legume lectin family protein	gi 15228229	31 kDa	10.9	0.1
37	leucine-rich repeat family protein	gi 15222811	54 kDa	2.1	0.5
38	LTPG1 (GLYCOSYLPHOSPHATIDYLINOSITOL-ANCHORED LIPID PROTEIN TRANSFER 1)	gi 15217777 (+1)	20 kDa	0.4	2.5
39	major latex protein-related / MLP-related	gi 15231561 (+1)	18 kDa	0.5	2.0
40	MAM1 (METHYLTHIOALKYLMALATE SYNTHASE 1); 2-isopropylmalate synthase/ methylthioalkylmalate synthase	gi 15237194 (+2)	55 kDa	2.5	0.4
41	mitochondrial elongation factor Tu	gi 1149571 (+1)	51 kDa	3.3	0.3
42	MLP43 (MLP-LIKE PROTEIN 43)	gi 15223275	18 kDa	2.7	0.4
43	MTHSC70-2 (MITOCHONDRIAL HSP70 2); ATP binding	gi 15242459	73 kDa	7.4	0.1
44	myo-inositol-1-phosphate synthase	gi 1161312 (+5)	56 kDa	3.9	0.3

45	nodulin-related	gi 15227642	20 kDa	0.5	2.1
46	NPQ4 (NONPHOTOCHEMICAL QUENCHING); chlorophyll binding / xanthophyll binding	gi 15219418 (+1)	28 kDa	0.3	3.6
47	NTF2A (NUCLEAR TRANSPORT FACTOR 2A); Ran GTPase binding / protein transporter	gi 15223491	14 kDa	2.8	0.4
48	NTF2B (NUCLEAR TRANSPORT FACTOR 2B); Ran GTPase binding / protein transporter	gi 145324046 (+2)	15 kDa	4.3	0.2
49	oxidoreductase, zinc-binding dehydrogenase family protein	gi 15235549	34 kDa	4.5	0.2
50	oxygen-evolving complex-related	gi 18411110 (+1)	27 kDa	2.6	0.4
51	PAB1 (PROTEASOME SUBUNIT PAB1); endopeptidase/ peptidase/ threonine-type endopeptidase	gi 15219257 (+1)	26 kDa	4.2	0.2
52	PAE1; endopeptidase/ peptidase/ threonine-type endopeptidase	gi 15220961	26 kDa	3.0	0.3
53	PBF1; peptidase/ threonine-type endopeptidase	gi 15232965 (+2)	25 kDa	2.6	0.4
54	PBP1 (PYK10-BINDING PROTEIN 1); copper ion binding	gi 15228198 (+1)	32 kDa	2.1	0.5
55	pfkB-type carbohydrate kinase family protein	gi 15224669	35 kDa	2.8	0.4
56	phosphoprotein phosphatase (EC 3.1.3.16) 2A-4 (version 2) [similarity]	gi 11262975 (+4)	34 kDa	2.1	0.5
57	photosystem II 47 kDa protein	gi 7525059 (+1)	56 kDa	0.3	3.2
58	photosystem II D2 protein	gi 27435857 (+1)	35 kDa	0.4	2.5
59	photosystem II protein D1	gi 7525013	39 kDa	0.4	2.7
60	plastid-lipid associated protein PAP / fibrillin family protein	gi 30688146	27 kDa	2.0	0.5
61	PRF1 (PROFILIN 1); actin binding	gi 15224838	14 kDa	3.2	0.3
62	PSAL (photosystem I subunit L)	gi 15235490 (+1)	23 kDa	0.4	2.6
63	PYK10; beta-glucosidase/ copper ion binding / fucosidase/ hydrolase, hydrolyzing O-glycosyl compounds	gi 15232626 (+3)	60 kDa	2.9	0.3
64	RecName: Full=ATP-dependent Clp protease proteolytic subunit 1; AltName: Full=Endopeptidase ClpP1; Short=pClpP	gi 160332321 (+1)	22 kDa	0.4	2.2
65	RecName: Full=DEAD-box ATP-dependent RNA helicase 15	gi 110283023 (+6)	48 kDa	0.3	3.3

66	RecName: Full=Spermidine synthase 1; Short=SPDSY 1; AltName: Full=Putrescine aminopropyltransferase 1	gi 12230014 (+1)	37 kDa	2.0	0.5
67	RHM1 (RHAMNOSE BIOSYNTHESIS 1); UDP-L-rhamnose synthase/ UDP-glucose 4,6-dehydratase/ catalytic	gi 15218420	75 kDa	2.4	0.4
68	ribosomal protein L1 family protein	gi 15229443 (+1)	38 kDa	0.4	2.3
69	RPT1A (REGULATORY PARTICLE TRIPLE-A 1A); ATPase	gi 15220930 (+1)	48 kDa	4.5	0.2
70	SAL1; 3'(2'),5'-bisphosphate nucleotidase/ inositol or phosphatidylinositol phosphatase	gi 145359623 (+1)	44 kDa	5.1	0.2
71	SBP1 (selenium-binding protein 1); selenium binding	gi 15236385	54 kDa	2.1	0.5
72	SPR1 (SPIRAL1)	gi 15227691	12 kDa	3.1	0.3
73	Strong similarity to S. pombe leucyl-tRNA synthetase (gb Z73100)	gi 2160156 (+1)	123 kDa	0.2	4.1
74	SWIB complex BAF60b domain-containing protein	gi 18397658 (+2)	16 kDa	0.4	2.5
75	THIC (ThiaminC); ADP-ribose pyrophosphohydrolase/ catalytic/ iron-sulfur cluster binding	gi 15227584	72 kDa	2.3	0.4
76	thylakoid lumenal 15 kDa protein, chloroplast	gi 18406661 (+1)	24 kDa	2.3	0.4
77	TIC40	gi 15237382	49 kDa	2.4	0.4
78	universal stress protein (USP) family protein	gi 18401345	18 kDa	2.4	0.4
79	UXS3 (UDP-GLUCURONIC ACID DECARBOXYLASE 3); UDP-glucuronate decarboxylase/ catalytic	gi 145334845 (+2)	40 kDa	2.1	0.5
80	vestitone reductase-related	gi 15236930	44 kDa	0.3	3.1
	Putative proteins				
1	30S ribosomal protein S10, chloroplast, putative	gi 15231154	21 kDa	2.6	0.4
2	adenylosuccinate lyase, putative / adenylosuccinase, putative	gi 22328773	60 kDa	0.4	2.8
3	beta-hydroxyacyl-ACP dehydratase, putative	gi 18399910	24 kDa	0.3	2.9
4	chaperonin, putative	gi 15240317 (+1)	60 kDa	2.3	0.4
5	cysteine protease inhibitor, putative / cystatin, putative	gi 18399630 (+2)	22 kDa	10.0	0.1
6	fructose-bisphosphate aldolase, putative	gi 15226185	42 kDa	4.7	0.2
7	NADH-cytochrome b5 reductase, putative	gi 18420117	36 kDa	3.0	0.3

8	tetrahydrofolate dehydrogenase/cyclohydrolase, putative	gi 15230449 (+1)	32 kDa	2.2	0.5
	Hypothetical protein				
1	hypothetical protein	gi 10998936 (+1)	56 kDa	0.4	2.7
	Unknown proteins				
1	unknown protein	gi 18398135 (+1)	39 kDa	2.3	0.4
2	unknown protein	gi 18411555 (+1)	18 kDa	0.2	5.0
3	unknown protein	gi 15230039	10 kDa	0.3	3.1
4	unknown protein	gi 15239049 (+7)	40 kDa	0.2	4.9

Table 4.3c: Fold change of spectral count in *Arabidopsis thaliana* rosette Contrast 3 - LCO Vs Th17

	Fold change for Contrast 3 - LCO Vs Th17				
	Identified Proteins <i>Arabidopsis thaliana</i> rosette	NCBI Accession	MW	LCO	Th17
1	2-oxoacid dehydrogenase family protein	gi 15240454	50 kDa	3.4	0.3
2	40S ribosomal protein S3A (RPS3aB)	gi 15236171 (+1)	30 kDa	7.3	0.1
3	50S ribosomal protein L21, chloroplast / CL21 (RPL21)	gi 15219695	24 kDa	0.4	2.5
4	60S ribosomal protein L10 (RPL10B)	gi 15223382 (+3)	25 kDa	3.8	0.3
5	60S ribosomal protein L17 (RPL17B)	gi 15220431 (+2)	20 kDa	3.7	0.3
6	60S ribosomal protein L4/L1 (RPL4A)	gi 15232723 (+1)	45 kDa	4.9	0.2
7	60S ribosomal protein L6 (RPL6C)	gi 15221126 (+1)	26 kDa	7.6	0.1
8	adenylate kinase family protein	gi 22327339 (+1)	66 kDa	3.1	0.3
9	ALDH2C4; 3-chloroallyl aldehyde dehydrogenase/ aldehyde dehydrogenase (NAD)/ coniferyl-aldehyde dehydrogenase	gi 18404212	54 kDa	3.0	0.3
10	APM1 (AMINOPEPTIDASE M1); aminopeptidase	gi 22329112	98 kDa	3.1	0.3
11	AT103	gi 1033195	44 kDa	3.0	0.3
12	AT3g06720/F3E22_14	gi 13605661 (+2)	59 kDa	2.4	0.4
13	AT3g14930/K15M2_7	gi 16323119 (+2)	46 kDa	0.5	2.0

14	ATKRS-1 (ARABIDOPSIS THALIANA LYSYL-TRNA SYNTHETASE 1); ATP binding / aminoacyl-tRNA ligase/ lysine-tRNA ligase/ nucleic acid binding / nucleotide binding	gi 15229833	71 kDa	3.9	0.3
15	AtMAPR2 (Arabidopsis thaliana membrane-associated progesterone binding protein 2); heme binding	gi 15224648 (+2)	11 kDa	0.5	2.2
16	ATRAB1C; GTP binding	gi 15236555 (+2)	22 kDa	2.9	0.3
17	ATRP1 (PPDK REGULATORY PROTEIN); phosphoprotein phosphatase/ protein kinase	gi 15233554 (+2)	44 kDa	0.3	2.9
18	BIP1; ATP binding	gi 15241844	74 kDa	4.0	0.2
20	CB5-E (CYTOCHROME B5 ISOFORM E); heme binding	gi 15238776	15 kDa	4.0	0.3
22	CP29; RNA binding / poly(U) binding	gi 15231817 (+2)	36 kDa	5.4	0.2
23	CR88; ATP binding	gi 15228059 (+2)	89 kDa	6.3	0.2
24	DEGP1 (DegP protease 1); serine-type endopeptidase/ serine-type peptidase	gi 22331378	47 kDa	0.4	2.5
25	DEGP2; serine-type endopeptidase/ serine-type peptidase	gi 18407488 (+1)	67 kDa	0.4	2.3
26	dicarboxylate/tricarboxylate carrier (DTC)	gi 15241167	32 kDa	2.2	0.4
27	DNA-binding family protein / remorin family protein	gi 15233068	23 kDa	0.5	2.2
28	ECT2; protein binding	gi 30682679 (+3)	72 kDa	3.6	0.3
29	ELI3-1 (ELICITOR-ACTIVATED GENE 3-1); binding / catalytic/ oxidoreductase/ zinc ion binding	gi 15233642 (+1)	38 kDa	0.4	2.7
30	EMB2296 (embryo defective 2296); structural constituent of ribosome	gi 15227954	28 kDa	3.2	0.3
31	emb2386 (embryo defective 2386); structural constituent of ribosome	gi 15218602	25 kDa	3.9	0.3
32	FDH (FORMATE DEHYDROGENASE); NAD or NADH binding / binding / catalytic/ cofactor binding / oxidoreductase, acting on the CH-OH group of donors, NAD or NADP as acceptor	gi 15241492 (+2)	42 kDa	0.5	2.1
33	FSD1 (FE SUPEROXIDE DISMUTASE 1); copper ion binding / superoxide dismutase	gi 15234913 (+3)	24 kDa	0.2	4.0
34	GDCH; glycine dehydrogenase (decarboxylating)	gi 15226973	18 kDa	0.5	2.2
35	glycine-rich RNA-binding protein	gi 829254 (+4)	14 kDa	0.5	2.2

36	HSP81-2 (HEAT SHOCK PROTEIN 81-2); ATP binding	gi 15241115 (+4)	80 kDa	2.3	0.4
38	leucine-rich repeat family protein	gi 15222811	54 kDa	2.1	0.5
39	MAM1 (METHYLTHIOALKYLMALATE SYNTHASE 1); 2-isopropylmalate synthase/ methylthioalkylmalate synthase	gi 15237194 (+2)	55 kDa	2.1	0.5
40	MST1 (MERCAPTOPYRUVATE SULFURTRANSFERASE 1); 3-mercaptopyruvate sulfurtransferase/ sulfurtransferase/ thiosulfate sulfurtransferase	gi 18412307 (+1)	42 kDa	0.3	2.9
41	MTHSC70-2 (MITOCHONDRIAL HSP70 2); ATP binding	gi 15242459	73 kDa	2.0	0.5
42	NTF2B (NUCLEAR TRANSPORT FACTOR 2B); Ran GTPase binding / protein transporter	gi 145324046 (+2)	15 kDa	2.1	0.5
43	oxidoreductase, zinc-binding dehydrogenase family protein	gi 15235549	34 kDa	4.4	0.2
44	PAB1 (PROTEASOME SUBUNIT PAB1); endopeptidase/ peptidase/ threonine-type endopeptidase	gi 15219257 (+1)	26 kDa	2.1	0.5
45	PAB8 (POLY(A) BINDING PROTEIN 8); RNA binding / translation initiation factor	gi 18402769	73 kDa	2.1	0.5
46	plastid-lipid associated protein PAP / fibrillin family protein	gi 30688146	27 kDa	2.0	0.5
47	PP2AA3 (PROTEIN PHOSPHATASE 2A SUBUNIT A3); binding / protein phosphatase type 2A regulator	gi 22329534 (+5)	66 kDa	2.9	0.3
48	PRF1 (PROFILIN 1); actin binding	gi 15224838	14 kDa	4.1	0.2
49	PTAC4 (PLASTID TRANSCRIPTIONALLY ACTIVE4)	gi 18408237	36 kDa	0.4	2.2
50	PYK10; beta-glucosidase/ copper ion binding / fucosidase/ hydrolase, hydrolyzing O-glycosyl compounds	gi 15232626 (+3)	60 kDa	0.5	2.1
51	RecName: Full=Aconitate hydratase 3, mitochondrial; Short=Aconitase 3; AltName: Full=Citrate hydro-lyase 3; Flags: Precursor	gi 118572817 (+2)	108 kDa	0.3	3.1
52	RecName: Full=DEAD-box ATP-dependent RNA helicase 15	gi 110283023 (+6)	48 kDa	2.5	0.4
53	ribosomal protein S11 (probable start codon at bp 67)	gi 166867 (+1)	20 kDa	2.6	0.4
55	RPS6 (RIBOSOMAL PROTEIN S6); structural constituent of ribosome	gi 15236042	28 kDa	2.1	0.5
57	TIC110 (TRANSLOCON AT THE INNER ENVELOPE MEMBRANE OF CHLOROPLASTS 110)	gi 15221009 (+2)	112 kDa	6.4	0.2

58	TIC40	gi 15237382	49 kDa	0.3	3.1
59	TOC75-III (TRANSLOCON AT THE OUTER ENVELOPE MEMBRANE OF CHLOROPLASTS 75-III); P-P-bond-hydrolysis-driven protein transmembrane transporter	gi 15232625	89 kDa	2.6	0.4
60	TSB1 (TRYPTOPHAN SYNTHASE BETA-SUBUNIT 1); tryptophan synthase	gi 15239755	51 kDa	0.5	2.2
62	UXS3 (UDP-GLUCURONIC ACID DECARBOXYLASE 3); UDP-glucuronate decarboxylase/ catalytic	gi 145334845 (+2)	40 kDa	0.4	2.3
	Putative protein				
1	2,3-biphosphoglycerate-independent phosphoglycerate mutase, putative / phosphoglyceromutase, putative	gi 15231939	61 kDa	0.5	2.0
2	ATP-dependent Clp protease proteolytic subunit, putative	gi 18414804 (+1)	33 kDa	0.4	2.6
3	caffeoyl-CoA 3-O-methyltransferase, putative	gi 15235213	29 kDa	0.4	2.6
4	chaperonin, putative	gi 15240317 (+1)	60 kDa	4.0	0.3
5	cysteine protease inhibitor, putative / cystatin, putative	gi 18399630 (+2)	22 kDa	7.5	0.1
6	diaminopimelate decarboxylase, putative / DAP carboxylase, putative	gi 18416698	54 kDa	0.4	2.4
7	fructose-bisphosphate aldolase, putative	gi 15226185	42 kDa	2.0	0.5
8	phosphoethanolamine N-methyltransferase 2, putative (NMT2)	gi 15221909 (+1)	54 kDa	0.5	2.2
	Hypothetical protein				
1	hypothetical protein	gi 110736982 (+1)	25 kDa	0.4	2.8
2	hypothetical protein	gi 110740330 (+1)	63 kDa	5.5	0.2
	Unknown protein				
1	Unknown protein	gi 13899087 (+1)	25 kDa	0.3	3.2
2	unknown protein	gi 15230039	10 kDa	0.3	3.4

Table 4.3d: Fold change of spectral count in *Arabidopsis thaliana* rosette Contrast 4 - Control 250 mM NaCl Vs LCO + 250 mM NaCl

	Fold change for Contrast 4 - Control 250 mM NaCl Vs LCO + 250 mM NaCl				
	Identified Proteins in <i>Arabidopsis thaliana</i> rosette	NCBI Accession	MW	250 mM NaCl Control	LCO + 250 mM NaCl
1	[acyl-carrier-protein] S-malonyltransferase/ binding / catalytic/ transferase	gi 18402286 (+1)	42 kDa	0.5	2.1
2	40S ribosomal protein S7 (RPS7C)	gi 15237278 (+1)	22 kDa	2.8	0.4
3	50S ribosomal protein L21, chloroplast / CL21 (RPL21)	gi 15219695	24 kDa	6.6	0.2
4	60S acidic ribosomal protein P0 (RPP0B)	gi 15232603 (+1)	34 kDa	0.4	2.3
5	60S acidic ribosomal protein P1-like protein	gi 21553441	11 kDa	0.4	2.3
6	60S ribosomal protein L4/L1 (RPL4D)	gi 15242558 (+2)	45 kDa	2.9	0.3
7	6-phosphogluconate dehydrogenase family protein	gi 15232888	54 kDa	2.2	0.4
8	ACL (ACETONE-CYANOHYDRIN LYASE); hydrolase/ hydrolase, acting on ester bonds / methyl indole-3-acetate esterase/ methyl jasmonate esterase/ methyl salicylate esterase	gi 15227863 (+1)	30 kDa	2.8	0.4
9	aconitate hydratase, cytoplasmic / citrate hydro-lyase / aconitase (ACO)	gi 15233349	98 kDa	0.3	3.9
10	ADK2 (ADENOSINE KINASE 2); adenosine kinase/ copper ion binding / kinase	gi 15242717	38 kDa	2.4	0.4
11	AILP1	gi 15239658 (+1)	25 kDa	2.3	0.4
12	aldo/keto reductase family protein	gi 18404526 (+1)	35 kDa	11.8	0.1
13	aldose 1-epimerase family protein	gi 15228261	40 kDa	2.0	0.5
14	ASN2 (ASPARAGINE SYNTHETASE 2); asparagine synthase (glutamine-hydrolyzing)	gi 30698086 (+2)	65 kDa	3.1	0.3
15	ASP2 (ASPARTATE AMINOTRANSFERASE 2); L-aspartate:2-oxoglutarate aminotransferase	gi 15239772	44 kDa	2.0	0.5
16	AT3g52500/F22O6_120	gi 16209647 (+1)	51 kDa	2.1	0.5
17	At3g63410	gi 108385436 (+4)	38 kDa	2.1	0.5
18	ATGCN1; transporter	gi 15239436	67 kDa	0.3	3.8

19	ATRB45C; RNA binding	gi 18416906 (+1)	45 kDa	0.3	3.0
20	avirulence-responsive protein-related / avirulence induced gene (AIG) protein-related	gi 15242451	20 kDa	4.1	0.2
21	BCAT3 (BRANCHED-CHAIN AMINOTRANSFERASE 3); branched-chain-amino-acid transaminase/ catalytic	gi 18408919 (+3)	45 kDa	0.4	2.6
22	binding / catalytic/ coenzyme binding	gi 30685117	68 kDa	4.5	0.2
23	binding / catalytic/ coenzyme binding	gi 18398333	32 kDa	0.3	3.8
24	CAD1 (CADMIUM SENSITIVE 1); cadmium ion binding / copper ion binding / glutathione gamma-glutamylcysteinyltransferase	gi 15240084 (+4)	54 kDa	2.1	0.5
25	calcium-binding EF hand family protein	gi 18406507	16 kDa	2.0	0.5
26	CaS (Calcium sensing receptor)	gi 15237201	41 kDa	2.0	0.5
27	CB5-E (CYTOCHROME B5 ISOFORM E); heme binding	gi 15238776	15 kDa	0.3	3.7
28	COR15A (COLD-REGULATED 15A)	gi 15227963 (+1)	15 kDa	0.4	2.7
29	CP29; RNA binding / poly(U) binding	gi 15231817 (+2)	36 kDa	12.2	0.1
30	DPE2 (DISPROPORTIONATING ENZYME 2); 4-alpha-glucanotransferase/ heteroglycan binding	gi 42569818	110 kDa	0.5	2.2
31	DXR (1-DEOXY-D-XYLULOSE 5-PHOSPHATE REDUCTOISOMERASE); 1-deoxy-D-xylulose-5-phosphate reductoisomerase	gi 15241970	52 kDa	2.2	0.5
32	emb2394 (embryo defective 2394); structural constituent of ribosome	gi 15220443 (+1)	25 kDa	2.9	0.4
33	FED A; 2 iron, 2 sulfur cluster binding / electron carrier/ iron-sulfur cluster binding	gi 15219837	16 kDa	4.2	0.2
34	GAMMA CAL2 (GAMMA CARBONIC ANHYDRASE-LIKE 2); transferase	gi 15228424 (+2)	28 kDa	0.4	2.7
35	HSP60-2 (HEAT SHOCK PROTEIN 60-2); ATP binding	gi 30685604	62 kDa	0.5	2.0
36	immunophilin / FKBP-type peptidyl-prolyl cis-trans isomerase family protein	gi 15224305	24 kDa	6.0	0.2
37	LHCB4.2 (light harvesting complex PSII); chlorophyll binding	gi 15231990	31 kDa	0.2	5.5
38	LTI78 (LOW-TEMPERATURE-INDUCED 78)	gi 15242967 (+1)	78 kDa	0.4	2.7
39	LTPG1 (GLYCOSYLPHOSPHATIDYLINOSITOL-ANCHORED LIPID PROTEIN TRANSFER 1)	gi 15217777 (+1)	20 kDa	2.1	0.5

40	mitochondrial phosphate transporter	gi 15241291 (+1)	40 kDa	2.0	0.5
42	nodulin-related	gi 15227642	20 kDa	0.2	4.2
43	oxidoreductase, zinc-binding dehydrogenase family protein	gi 15235549	34 kDa	2.2	0.5
44	PATL2 (PATELLIN 2); transporter	gi 15219901	76 kDa	0.3	3.0
45	peptidyl-prolyl cis-trans isomerase cyclophilin-type family protein	gi 15240008 (+2)	28 kDa	2.3	0.4
47	peptidyl-prolyl cis-trans isomerase TLP38, chloroplast / thylakoid lumen PPIase of 38 kDa / cyclophilin / rotamase	gi 42564190	50 kDa	2.6	0.4
48	pfkB-type carbohydrate kinase family protein	gi 22330456 (+1)	41 kDa	0.3	3.8
49	PGR5-LIKE A	gi 145333783 (+2)	35 kDa	0.3	3.3
51	photosystem I P700 chlorophyll a apoprotein A1	gi 7525033	83 kDa	0.4	2.4
52	photosystem II protein D1	gi 7525013	39 kDa	0.5	2.0
53	PIP1B (NAMED PLASMA MEMBRANE INTRINSIC PROTEIN 1B); water channel	gi 145331415 (+3)	29 kDa	0.5	2.0
54	plastid-lipid associated protein PAP-related / fibrillin-related	gi 15241221 (+1)	26 kDa	0.3	3.0
55	pyruvate decarboxylase family protein	gi 15237954	61 kDa	3.0	0.3
56	RecName: Full=ATP-dependent Clp protease proteolytic subunit 1; AltName: Full=Endopeptidase ClpP1; Short=pClpP	gi 160332321 (+1)	22 kDa	2.1	0.5
57	RecName: Full=DEAD-box ATP-dependent RNA helicase 15	gi 110283023 (+6)	48 kDa	3.6	0.3
58	RGP1 (REVERSIBLY GLYCOSYLATED POLYPEPTIDE 1); cellulose synthase (UDP-forming)	gi 15232865	41 kDa	0.3	2.9
59	RPS6 (RIBOSOMAL PROTEIN S6); structural constituent of ribosome	gi 15236042 (+3)	28 kDa	2.4	0.4
61	RPT5B (26S proteasome AAA-ATPase subunit RPT5B); ATPase/ calmodulin binding	gi 15217431 (+4)	47 kDa	3.2	0.3
62	SAM-2 (S-ADENOSYLMETHIONINE SYNTHETASE 2); copper ion binding / methionine adenosyltransferase	gi 15234354	43 kDa	2.2	0.5
63	seed maturation protein	gi 110739182 (+2)	67 kDa	4.5	0.2
64	serine/threonine protein phosphatase type 2A regulatory subunit A	gi 1254996 (+2)	66 kDa	0.5	2.2
65	SIR; sulfite reductase (ferredoxin)/ sulfite reductase	gi 15238217 (+2)	72 kDa	2.2	0.4

66	stromal ascorbate peroxidase	gi 1419388	40 kDa	2.4	0.4
67	Strong similarity to <i>S. pombe</i> leucyl-tRNA synthetase (gb Z73100)	gi 2160156 (+1)	123 kDa	2.1	0.5
68	TIC40	gi 15237382	49 kDa	4.5	0.2
69	TUA3; structural constituent of cytoskeleton	gi 15241168	50 kDa	0.2	5.6
70	TUB4; structural constituent of cytoskeleton	gi 15241472	50 kDa	0.1	8.4
71	universal stress protein (USP) family protein	gi 18407428	17 kDa	0.4	2.5
72	universal stress protein (USP) family protein	gi 18399413 (+4)	21 kDa	0.4	2.6
	Putative protein				
1	26S proteasome regulatory subunit, putative	gi 145334543 (+1)	29 kDa	6.9	0.1
2	ATP-dependent Clp protease proteolytic subunit, putative	gi 18414804 (+1)	33 kDa	2.6	0.4
3	chaperonin, putative	gi 18396719 (+1)	59 kDa	2.2	0.4
4	cinnamyl-alcohol dehydrogenase, putative (CAD)	gi 15239741 (+1)	36 kDa	3.6	0.3
5	lactoylglutathione lyase, putative / glyoxalase I, putative	gi 15220397	39 kDa	3.0	0.3
6	mannose 6-phosphate reductase (NADPH-dependent), putative	gi 15226489	35 kDa	0.3	2.9
7	NADH-cytochrome b5 reductase, putative	gi 18420117	36 kDa	0.2	5.9
8	NADH-ubiquinone oxidoreductase B8 subunit, putative	gi 15238831	11 kDa	2.2	0.4
9	NADPH oxidoreductase, putative; 14094-12769	gi 10092264 (+1)	34 kDa	0.2	4.5
10	nascent polypeptide-associated complex (NAC) domain-containing protein / BTF3b-like transcription factor, putative	gi 15220876 (+1)	18 kDa	2.7	0.4
11	putative glycyl tRNA synthetase	gi 15292923 (+2)	82 kDa	2.1	0.5
12	pyruvate kinase, putative	gi 145332819 (+4)	52 kDa	2.2	0.5
13	UTP--glucose-1-phosphate uridylyltransferase, putative / UDP-glucose pyrophosphorylase, putative / UGPase, putative	gi 15237947	52 kDa	3.1	0.3
	Hypothetical protein				
1	hypothetical protein	gi 110740330 (+2)	63 kDa	2.7	0.4
	Unknown protein				
1	unknown	gi 24417262 (+1)	44 kDa	0.3	3.7

2	Unknown protein	gi 17065226 (+1)	25 kDa	2.1	0.5
3	unknown protein	gi 30689549	32 kDa	0.3	3.8
4	unknown protein	gi 15239993	28 kDa	2.9	0.3
5	unknown protein	gi 18411555 (+1)	18 kDa	0.5	2.1
6	unknown protein	gi 15241839	48 kDa	0.4	2.8
7	unknown protein	gi 15235021 (+1)	15 kDa	0.3	3.3

Table 4.3e: Fold change of spectral count in *Arabidopsis thaliana* rosette Contrast 5 - Control 250 mM NaCl Vs Th17 + 250 mM NaCl

Fold change for Contrast 5 - Control 250 mM NaCl Vs Th17 + 250 mM NaCl					
	Identified Proteins <i>Arabidopsis thaliana</i> rosette	NCBI Accession	MW	Control 250 mM NaCl	TH + 250 mM NaCl
1	[acyl-carrier-protein] S-malonyltransferase/ binding / catalytic/ transferase	gi 18402286 (+1)	42 kDa	0.3	2.9
2	40S ribosomal protein S2 (RPS2C)	gi 15227443 (+1)	31 kDa	2.6	0.4
3	50S ribosomal protein L21, chloroplast / CL21 (RPL21)	gi 15219695	24 kDa	2.3	0.4
4	60S acidic ribosomal protein P2 (RPP2B)	gi 15226230	11 kDa	2.0	0.5
5	ACLB-1; ATP citrate synthase	gi 15230764 (+1)	66 kDa	0.2	5.5
6	aconitate hydratase, cytoplasmic / citrate hydro-lyase / aconitase (ACO)	gi 15233349	98 kDa	0.4	2.7
7	ALDH10A8; 3-chloroallyl aldehyde dehydrogenase/ oxidoreductase	gi 18410730	54 kDa	0.3	3.0
8	aldo/keto reductase family protein	gi 18404526 (+1)	35 kDa	2.2	0.5
9	aldose 1-epimerase family protein	gi 15228261	40 kDa	2.1	0.5
10	AOC4 (ALLENE OXIDE CYCLASE 4); allene-oxide cyclase	gi 15222241	28 kDa	4.7	0.2
11	ASP2 (ASPARTATE AMINOTRANSFERASE 2); L-aspartate:2-oxoglutarate aminotransferase	gi 15239772	44 kDa	2.1	0.5
12	At1g35160/T32G9_30	gi 14532442 (+1)	30 kDa	0.5	2.1
13	At1g69410/F10D13.8	gi 13937159 (+1)	17 kDa	0.4	2.6
14	At3g55410	gi 28416717 (+2)	115 kDa	0.4	2.6

15	AT4G38220	gi 227202560 (+3)	44 kDa	0.3	3.6
16	AT5g26830/F2P16_90	gi 15081626 (+3)	77 kDa	0.3	3.2
17	ATCAD4; cinnamyl-alcohol dehydrogenase	gi 15230382 (+2)	39 kDa	0.3	3.5
18	ATCAD5 (CINNAMYL ALCOHOL DEHYDROGENASE 5); cinnamyl-alcohol dehydrogenase	gi 15235295 (+1)	39 kDa	0.2	4.1
19	ATCAP1 (ARABIDOPSIS THALIANA CYCLASE ASSOCIATED PROTEIN 1); actin binding	gi 15236128	51 kDa	2.8	0.4
20	ATGCN1; transporter	gi 15239436	67 kDa	0.3	3.8
21	avirulence-responsive protein-related / avirulence induced gene (AIG) protein-related	gi 15242451	20 kDa	2.0	0.5
22	BCAT3 (BRANCHED-CHAIN AMINOTRANSFERASE 3); branched-chain-amino-acid transaminase/ catalytic	gi 18408919 (+3)	45 kDa	0.4	2.6
23	binding / catalytic/ coenzyme binding	gi 18398333	32 kDa	0.4	2.7
24	CAC1 (CHLOROPLASTIC ACETYLCOENZYME A CARBOXYLASE 1); acetyl-CoA carboxylase/ biotin binding	gi 42573385 (+3)	27 kDa	3.0	0.3
25	CaS (Calcium sensing receptor)	gi 15237201	41 kDa	2.8	0.4
26	CB5-E (CYTOCHROME B5 ISOFORM E); heme binding	gi 15238776	15 kDa	0.3	3.6
27	CHLM (magnesium-protoporphyrin IX methyltransferase); magnesium protoporphyrin IX methyltransferase	gi 15234905 (+2)	34 kDa	0.5	2.0
28	Clp amino terminal domain-containing protein	gi 18416540 (+1)	26 kDa	4.8	0.2
29	CLPB3 (CASEIN LYTIC PROTEINASE B3); ATP binding / ATPase/ nucleoside-triphosphatase/ nucleotide binding / protein binding	gi 18417676	109 kDa	3.6	0.3
30	COR15A (COLD-REGULATED 15A)	gi 15227963 (+1)	15 kDa	0.4	2.3
31	CP29; RNA binding / poly(U) binding	gi 15231817 (+2)	36 kDa	7.4	0.1
32	CXIP2 (CAX-INTERACTING PROTEIN 2); electron carrier/ protein disulfide oxidoreductase	gi 18404699	32 kDa	6.2	0.2
33	CYN (CYANASE); DNA binding / cyanate hydratase/ hydro-lyase	gi 15229458 (+1)	19 kDa	2.4	0.4

34	DXR (1-DEOXY-D-XYLULOSE 5-PHOSPHATE REDUCTOISOMERASE); 1-deoxy-D-xylulose-5-phosphate reductoisomerase	gi 15241970	52 kDa	2.2	0.5
35	emb2386 (embryo defective 2386); structural constituent of ribosome	gi 15218602	25 kDa	0.4	2.2
36	FSD1 (FE SUPEROXIDE DISMUTASE 1); copper ion binding / superoxide dismutase	gi 15234913 (+3)	24 kDa	2.3	0.4
37	GAMMA CA2 (GAMMA CARBONIC ANHYDRASE 2); carbonate dehydratase	gi 15220153	30 kDa	0.4	2.5
38	GER1 (GERMIN-LIKE PROTEIN 1); oxalate oxidase	gi 15218535 (+3)	22 kDa	2.1	0.5
39	glutathione S-transferase	gi 15375408 (+2)	25 kDa	0.5	2.2
40	GRP-3 (GLYCINE-RICH PROTEIN 3)	gi 15224548 (+1)	14 kDa	2.3	0.4
41	GTP binding	gi 15221444 (+1)	44 kDa	2.2	0.5
42	HSP70 (heat shock protein 70); ATP binding	gi 15230534	71 kDa	0.5	2.1
43	immunophilin / FKBP-type peptidyl-prolyl cis-trans isomerase family protein	gi 15224305	24 kDa	2.1	0.5
44	IMPL1 (MYO-INOSITOL MONOPHOSPHATASE LIKE 1); 3'(2'),5'-bisphosphate nucleotidase/ inositol or phosphatidylinositol phosphatase/ inositol-1(or 4)-monophosphatase	gi 18397837 (+2)	40 kDa	0.4	2.5
46	late embryogenesis abundant domain-containing protein / LEA domain-containing protein	gi 15229066 (+2)	33 kDa	0.3	3.2
47	LHCB4.2 (light harvesting complex PSII); chlorophyll binding	gi 15231990	31 kDa	0.2	4.3
48	LTI78 (LOW-TEMPERATURE-INDUCED 78)	gi 15242967 (+1)	78 kDa	0.4	2.7
49	mitochondrial phosphate transporter	gi 15241291 (+1)	40 kDa	0.2	4.5
50	nodulin-related	gi 15227642	20 kDa	0.2	4.8
51	PAD1 (20s proteasome alpha subunit pad1); endopeptidase/ peptidase/ threonine-type endopeptidase	gi 15230435	27 kDa	2.4	0.4
52	PATL1 (PATELLIN 1); transporter	gi 15218382	64 kDa	0.5	2.1
53	PATL2 (PATELLIN 2); transporter	gi 15219901	76 kDa	0.1	9.9

54	PBC1 (PROTEASOME BETA SUBUNIT C1); peptidase/ threonine-type endopeptidase	gi 18395025 (+2)	23 kDa	0.5	2.2
55	peroxidase	gi 1402914 (+1)	40 kDa	7.8	0.1
56	PETE1 (PLASTOCYANIN 1); copper ion binding / electron carrier	gi 15222956 (+2)	18 kDa	2.0	0.5
58	PGR5-LIKE A	gi 145333783 (+2)	35 kDa	0.3	3.9
59	phospholipid hydroperoxide glutathione peroxidase-like protein	gi 2760606 (+1)	19 kDa	2.4	0.4
60	photosystem I P700 chlorophyll a apoprotein A1	gi 7525033	83 kDa	0.5	2.1
61	photosystem II protein D1	gi 7525013	39 kDa	0.4	2.3
62	PIP1B (NAMED PLASMA MEMBRANE INTRINSIC PROTEIN 1B); water channel	gi 145331415 (+3)	29 kDa	0.4	2.7
63	plastid-lipid associated protein PAP-related / fibrillin-related	gi 15241221 (+1)	26 kDa	0.2	6.1
64	PRF1 (PROFILIN 1); actin binding	gi 15224838	14 kDa	2.3	0.4
65	PSAG (PHOTOSYSTEM I SUBUNIT G)	gi 15222757	17 kDa	3.4	0.3
66	RecName: Full=ATP-dependent Clp protease proteolytic subunit 1; AltName: Full=Endopeptidase ClpP1; Short=pClpP	gi 160332321 (+1)	22 kDa	0.3	3.1
67	RGP1 (REVERSIBLY GLYCOSYLATED POLYPEPTIDE 1); cellulose synthase (UDP-forming)	gi 15232865	41 kDa	4.0	0.2
68	ROC2 (ROTAMASE CYCLOPHILIN 2); cyclosporin A binding / peptidyl-prolyl cis-trans isomerase	gi 15228814	19 kDa	2.4	0.4
69	RPL18 (RIBOSOMAL PROTEIN L18); structural constituent of ribosome	gi 15230011 (+2)	21 kDa	0.5	2.2
70	RPL23AB (RIBOSOMAL PROTEIN L23AB); RNA binding / nucleotide binding / structural constituent of ribosome	gi 145332857 (+4)	17 kDa	2.8	0.4
73	SAM1 (S-ADENOSYLMETHIONINE SYNTHETASE 1); methionine adenosyltransferase	gi 15217781 (+1)	43 kDa	0.4	2.4
74	serine/threonine protein phosphatase type 2A regulatory subunit A	gi 1254996 (+2)	66 kDa	0.2	4.1

76	SUS1 (SUCROSE SYNTHASE 1); UDP-glycosyltransferase/ sucrose synthase	gi 15242073	93 kDa	0.3	2.9
77	threonine synthase	gi 1448917 (+1)	58 kDa	0.4	2.7
78	TIC40	gi 15237382	49 kDa	4.6	0.2
79	TUB4; structural constituent of cytoskeleton	gi 15241472	50 kDa	0.2	4.2
80	xylose isomerase	gi 21537178	54 kDa	0.2	5.2
	Putative protein				
1	3-isopropylmalate dehydrogenase, chloroplast, putative	gi 15221631 (+1)	44 kDa	2.3	0.4
2	chaperonin, putative	gi 18396719 (+1)	59 kDa	0.4	2.7
3	chitinase, putative	gi 15224308	30 kDa	2.4	0.4
4	fructose-bisphosphate aldolase, putative	gi 15236768	38 kDa	0.5	2.2
5	importin beta-2, putative	gi 15238758 (+1)	96 kDa	0.4	2.6
6	mannose 6-phosphate reductase (NADPH-dependent), putative	gi 15226489	35 kDa	0.4	2.6
7	NADPH oxidoreductase, putative; 14094-12769	gi 10092264 (+1)	34 kDa	0.2	4.4
8	phosphoglycerate kinase, putative	gi 15223484 (+1)	50 kDa	2.1	0.5
9	putative dihydroxyacid dehydratase	gi 14532594 (+1)	65 kDa	0.3	3.6
10	putative elongation factor P (EF-P); 66839-65711	gi 12322730 (+1)	21 kDa	2.3	0.4
11	putative glycyl tRNA synthetase	gi 15292923 (+2)	82 kDa	3.0	0.3
12	putative methylenetetrahydrofolate reductase	gi 13877629 (+2)	67 kDa	0.5	2.1
13	succinyl-CoA ligase (GDP-forming) alpha-chain, mitochondrial, putative / succinyl-CoA synthetase, alpha chain, putative / SCS-alpha, putative	gi 15241592	36 kDa	0.5	2.1
14	thiol methyltransferase, putative	gi 145331123 (+2)	27 kDa	2.5	0.4
15	ubiquitin-conjugating enzyme, putative	gi 18394416	17 kDa	2.7	0.4
	Unknown protein				
1	unknown protein	gi 24417262 (+1)	44 kDa	0.2	4.6
2	unknown protein	gi 116831573 (+3)	23 kDa	4.7	0.2
3	unknown protein	gi 20465634 (+2)	149 kDa	0.3	3.8

4	unknown protein	gi 30689549	32 kDa	0.2	6.6
5	unknown protein	gi 18411555 (+1)	18 kDa	0.2	5.2
6	unknown protein	gi 15241839	48 kDa	0.4	2.7
7	unknown protein	gi 15236659 (+1)	28 kDa	0.3	2.9

Table 4.3f: Fold change of spectral count in *Arabidopsis thaliana* rosette Contrast 6 – LCO + 250 mM NaCl Vs Th17 + 250 mM NaCl

	Fold change for Contrast 6 - LCO + 250 mM NaCl Vs Th17 + 250 mM NaCl				
	Identified Proteins <i>Arabidopsis thaliana</i> rosette	NCBI Accession	MW	LCO + 250 mM NaCl	TH + 250 mM NaCl
1	50S ribosomal protein L21, chloroplast / CL21 (RPL21)	gi 15219695	24 kDa	0.4	2.8
2	60S ribosomal protein L4/L1 (RPL4D)	gi 15242558 (+2)	45 kDa	0.3	3.1
3	ACL (ACETONE-CYANOHYDRIN LYASE); hydrolase/ hydrolase, acting on ester bonds / methyl indole-3-acetate esterase/ methyl jasmonate esterase/ methyl salicylate esterase	gi 15227863 (+1)	30 kDa	0.3	2.9
4	ACLB-1; ATP citrate synthase	gi 15230764 (+1)	66 kDa	0.3	3.7
5	ADH1 (ALCOHOL DEHYDROGENASE 1); alcohol dehydrogenase	gi 15223838 (+1)	41 kDa	0.4	2.3
6	aldo/keto reductase family protein	gi 18404526 (+1)	35 kDa	0.2	5.3
7	allene oxide synthase	gi 1890152	59 kDa	2.3	0.4
8	AOC4 (ALLENE OXIDE CYCLASE 4); allene-oxide cyclase	gi 15222241	28 kDa	4.0	0.3
9	APE2 (ACCLIMATION OF PHOTOSYNTHESIS TO ENVIRONMENT 2); antiporter/ triose-phosphate transmembrane transporter	gi 145334749 (+5)	45 kDa	0.3	3.0
10	ASN2 (ASPARAGINE SYNTHETASE 2); asparagine synthase (glutamine-hydrolyzing)	gi 30698086 (+2)	65 kDa	0.4	2.8
11	At3g63410	gi 108385436 (+4)	38 kDa	0.3	4.0
12	AT5g26830/F2P16_90	gi 15081626 (+3)	77 kDa	0.3	2.9

13	ATCAD5 (CINNAMYL ALCOHOL DEHYDROGENASE 5); cinnamyl-alcohol dehydrogenase	gi 15235295 (+1)	39 kDa	0.4	2.7
14	ATCAP1 (ARABIDOPSIS THALIANA CYCLASE ASSOCIATED PROTEIN 1); actin binding	gi 15236128	51 kDa	2.0	0.5
15	ATJ3; protein binding	gi 15229874 (+1)	46 kDa	0.5	2.1
16	ATRB45C; RNA binding	gi 18416906 (+1)	45 kDa	3.1	0.3
17	avirulence-responsive protein-related / avirulence induced gene (AIG) protein-related	gi 15242451	20 kDa	0.5	2.0
18	binding / catalytic/ coenzyme binding	gi 30685117	68 kDa	0.2	5.1
19	CAD1 (CADMIUM SENSITIVE 1); cadmium ion binding / copper ion binding / glutathione gamma-glutamylcysteinyltransferase	gi 15240084 (+4)	54 kDa	0.3	3.8
20	CARB (CARBAMOYL PHOSPHATE SYNTHETASE B); ATP binding / carbamoyl-phosphate synthase/ catalytic	gi 18397283	130 kDa	0.4	2.3
21	Clp amino terminal domain-containing protein	gi 18416540 (+1)	26 kDa	3.6	0.3
22	CLPB3 (CASEIN LYTIC PROTEINASE B3); ATP binding / ATPase/ nucleoside-triphosphatase/ nucleotide binding / protein binding	gi 18417676	109 kDa	2.6	0.4
23	CXIP2 (CAX-INTERACTING PROTEIN 2); electron carrier/ protein disulfide oxidoreductase	gi 18404699	32 kDa	3.4	0.3
24	CYN (CYANASE); DNA binding / cyanate hydratase/ hydro-lyase	gi 15229458 (+1)	19 kDa	3.3	0.3
25	emb2386 (embryo defective 2386); structural constituent of ribosome	gi 15218602	25 kDa	0.3	3.3
26	emb2394 (embryo defective 2394); structural constituent of ribosome	gi 15220443 (+1)	25 kDa	0.4	2.8
27	FED A; 2 iron, 2 sulfur cluster binding / electron carrier/ iron-sulfur cluster binding	gi 15219837	16 kDa	0.2	4.6
28	glutathione S-transferase	gi 15375408 (+2)	25 kDa	0.4	2.4
29	GRP-3 (GLYCINE-RICH PROTEIN 3)	gi 15224548 (+1)	14 kDa	2.5	0.4
30	GTP binding	gi 15221444 (+1)	44 kDa	2.1	0.5
31	HSP70 (heat shock protein 70); ATP binding	gi 15230534	71 kDa	0.4	2.2

32	immunophilin / FKBP-type peptidyl-prolyl cis-trans isomerase family protein	gi 15224305	24 kDa	0.4	2.8
33	mitochondrial phosphate transporter	gi 15241291 (+1)	40 kDa	0.1	9.1
34	MLP43 (MLP-LIKE PROTEIN 43)	gi 15223275	18 kDa	0.4	2.4
35	MSRB2 (methionine sulfoxide reductase B 2); peptide-methionine-(S)-S-oxide reductase	gi 18415779	22 kDa	2.7	0.4
36	PAA2 (20S PROTEASOME SUBUNIT PAA2); endopeptidase/ peptidase/ threonine-type endopeptidase	gi 15224993 (+1)	27 kDa	2.0	0.5
37	PATL2 (PATELLIN 2); transporter	gi 15219901	76 kDa	0.3	3.3
38	PBC1 (PROTEASOME BETA SUBUNIT C1); peptidase/ threonine-type endopeptidase	gi 18395025 (+2)	23 kDa	0.4	2.8
39	peptidyl-prolyl cis-trans isomerase TLP38, chloroplast / thylakoid lumen PPIase of 38 kDa / cyclophilin / rotamase	gi 42564190	50 kDa	0.4	2.6
40	peroxidase	gi 1402914 (+1)	40 kDa	4.9	0.2
41	pfkB-type carbohydrate kinase family protein	gi 22330456 (+1)	41 kDa	3.7	0.3
42	PGI1 (PHOSPHOGLUCOSE ISOMERASE 1); glucose-6-phosphate isomerase	gi 30686602 (+2)	67 kDa	2.0	0.5
43	phospholipid hydroperoxide glutathione peroxidase-like protein	gi 2760606 (+1)	19 kDa	2.5	0.4
44	plastid-lipid associated protein PAP-related / fibrillin-related	gi 15241221 (+1)	26 kDa	0.5	2.0
45	POR C (PROTOCHLOROPHYLLIDE OXIDOREDUCTASE); NADPH dehydrogenase/ oxidoreductase/ protochlorophyllide reductase	gi 15218860 (+2)	44 kDa	0.5	2.0
46	PRF1 (PROFILIN 1); actin binding	gi 15224838	14 kDa	3.2	0.3
47	PSAG (PHOTOSYSTEM I SUBUNIT G)	gi 15222757	17 kDa	2.5	0.4
48	pyruvate decarboxylase family protein	gi 15237954	61 kDa	0.5	2.1
49	RecName: Full=Aconitate hydratase 3, mitochondrial; Short=Aconitase 3; AltName: Full=Citrate hydro-lyase 3; Flags: Precursor	gi 118572817 (+2)	108 kDa	0.4	2.5
50	RecName: Full=ATP-dependent Clp protease proteolytic subunit 1; AltName: Full=Endopeptidase ClpP1; Short=pClpP	gi 160332321 (+1)	22 kDa	0.2	6.5

51	RGP1 (REVERSIBLY GLYCOSYLATED POLYPEPTIDE 1); cellulose synthase (UDP-forming)	gi 15232865	41 kDa	11.7	0.1
52	ROC2 (ROTAMASE CYCLOPHILIN 2); cyclosporin A binding / peptidyl-prolyl cis-trans isomerase	gi 15228814	19 kDa	2.1	0.5
53	RPT5B (26S proteasome AAA-ATPase subunit RPT5B); ATPase/ calmodulin binding	gi 15217431 (+4)	47 kDa	0.2	4.2
54	SAM1 (S-ADENOSYLMETHIONINE SYNTHETASE 1); methionine adenosyltransferase	gi 15217781 (+1)	43 kDa	0.3	3.7
55	seed maturation protein	gi 110739182 (+2)	67 kDa	0.1	6.8
56	SEX1 (STARCH EXCESS 1); alpha-glucan, water dikinase	gi 18391200 (+1)	157 kDa	0.2	5.1
57	SIR; sulfite reductase (ferredoxin)/ sulfite reductase	gi 15238217 (+2)	72 kDa	0.3	3.5
58	Strong similarity to S. pombe leucyl-tRNA synthetase (gb Z73100)	gi 2160156 (+1)	123 kDa	0.3	3.7
59	SUS1 (SUCROSE SYNTHASE 1); UDP-glycosyltransferase/ sucrose synthase	gi 15242073	93 kDa	0.4	2.3
60	thioredoxin reductase like protein	gi 110739775 (+2)	30 kDa	0.4	2.8
61	TUA3; structural constituent of cytoskeleton	gi 15241168	50 kDa	3.2	0.3
62	vestitone reductase-related	gi 15236930	44 kDa	0.4	2.5
63	XYL1 (ALPHA-XYLOSIDASE 1); alpha-N-arabinofuranosidase/ hydrolase, hydrolyzing O-glycosyl compounds / xylan 1,4-beta-xylosidase	gi 15221437 (+1)	102 kDa	0.5	2.1
64	xylose isomerase	gi 21537178	54 kDa	0.3	3.1
	Putative protein				
1	3-isopropylmalate dehydrogenase, chloroplast, putative	gi 15221631 (+1)	44 kDa	3.3	0.3
2	ATP-dependent Clp protease proteolytic subunit, putative	gi 18414804 (+1)	33 kDa	0.4	2.5
3	caffeoyl-CoA 3-O-methyltransferase, putative	gi 15235213	29 kDa	0.5	2.1
4	chaperonin, putative	gi 18396719 (+1)	59 kDa	0.2	6.0
5	cinnamyl-alcohol dehydrogenase, putative (CAD)	gi 15239741 (+1)	36 kDa	0.2	4.2
6	fructose-bisphosphate aldolase, putative	gi 15236768	38 kDa	0.5	2.1

7	isocitrate dehydrogenase, putative / NADP+ isocitrate dehydrogenase, putative	gi 22326811 (+1)	54 kDa	0.0	22.6
8	lactoylglutathione lyase, putative / glyoxalase I, putative	gi 15220397	39 kDa	0.3	3.4
9	NADH-cytochrome b5 reductase, putative	gi 18420117	36 kDa	6.9	0.1
10	ubiquitin-conjugating enzyme, putative	gi 18394416	17 kDa	2.4	0.4
11	UTP--glucose-1-phosphate uridylyltransferase, putative / UDP-glucose pyrophosphorylase, putative / UGPase, putative	gi 15237947	52 kDa	0.3	3.6
	Hypothetical protein				
1	hypothetical protein	gi 110740330 (+2)	63 kDa	0.4	2.7
	Unknown protein				
1	unknown protein	gi 20465634 (+2)	149 kDa	0.4	2.7
2	unknown protein	gi 15239993	28 kDa	0.5	2.1
3	unknown protein	gi 18411555 (+1)	18 kDa	0.4	2.5
4	unknown protein	gi 15235021 (+1)	15 kDa	3.0	0.3

Table 4.4a: Fisher's Exact test (P-value) (Spectral counts) for *Arabidopsis thaliana* rosette Contrast 1. Control Vs LCO

	Fisher's exact test for Contrast 1. Control Vs. LCO					
	Identified Proteins <i>Arabidopsis thaliana</i> rosette	NCBI Accession Number	MW	Control	LCO	Fisher's Exact Test (P-Value)
1	40S ribosomal protein S3 (RPS3B)	gi 15232352	27 kDa	5	17	95% (0.0097)
2	40S ribosomal protein S3A (RPS3aA)	gi 15229364	30 kDa	0	6	95% (0.017)
3	40S ribosomal protein S3A (RPS3aB)	gi 15236171 (+1)	30 kDa	1	8	95% (0.021)
4	4-alpha-hydroxytetrahydrobiopterin dehydratase	gi 15241386	24 kDa	10	3	95% (0.042)
5	60S ribosomal protein L15 (RPL15A)	gi 15235851 (+2)	24 kDa	0	5	95% (0.033)
6	60S ribosomal protein L4/L1 (RPL4A)	gi 15232723 (+1)	45 kDa	0	14	95% (0.000071)
7	60S ribosomal protein L6 (RPL6C)	gi 15221126 (+1)	26 kDa	1	8	95% (0.021)

8	60S ribosomal protein L9 (RPL90B)	gi 18398753 (+1)	22 kDa	13	25	95% (0.042)
9	AAC1 (ADP/ATP CARRIER 1); ATP:ADP antiporter/ binding	gi 15231937	41 kDa	9	21	95% (0.025)
10	ACT7 (ACTIN 7); structural constituent of cytoskeleton	gi 15242516	42 kDa	127	97	95% (0.018)
11	AGT (ALANINE:GLYOXYLATE AMINOTRANSFERASE); alanine-glyoxylate transaminase/ serine-glyoxylate transaminase/ serine-pyruvate transaminase	gi 15225026	44 kDa	42	74	95% (0.0027)
12	At1g07930/T6D22_3	gi 13605682 (+4)	50 kDa	72	98	95% (0.037)
13	At3g63410	gi 108385436 (+4)	38 kDa	0	5	95% (0.033)
14	ATKRS-1 (ARABIDOPSIS THALIANA LYSYL-TRNA SYNTHETASE 1); ATP binding / aminoacyl-tRNA ligase/ lysine-tRNA ligase/ nucleic acid binding / nucleotide binding	gi 15229833	71 kDa	0	5	95% (0.033)
15	ATOMT1 (O-METHYLTRANSFERASE 1); caffeate O-methyltransferase/ myricetin 3'-O-methyltransferase/ quercetin 3-O-methyltransferase	gi 15239571 (+1)	40 kDa	12	4	95% (0.035)
16	AtPPa6 (Arabidopsis thaliana pyrophosphorylase 6); inorganic diphosphatase/ pyrophosphatase	gi 15242465	33 kDa	27	15	95% (0.038)
17	ATPPC1 (PHOSPHOENOLPYRUVATE CARBOXYLASE 1); catalytic/ phosphoenolpyruvate carboxylase	gi 15219272 (+1)	110 kDa	7	20	95% (0.011)
18	ATPPC2 (PHOSPHOENOLPYRUVATE CARBOXYLASE 2); catalytic/ phosphoenolpyruvate carboxylase	gi 240254631	110 kDa	19	60	95% (0.0000032)
19	ATRAB1C; GTP binding	gi 15236555 (+2)	22 kDa	0	6	95% (0.017)
20	BIP1; ATP binding	gi 15241844	74 kDa	0	16	95% (0.000018)
21	CAC3; acetyl-CoA carboxylase	gi 18404621 (+1)	85 kDa	0	5	95% (0.033)
22	COR15A (COLD-REGULATED 15A)	gi 15227963 (+1)	15 kDa	29	4	95% (0.0000041)
23	COR15B (COLD REGULATED 15B)	gi 15227952 (+1)	15 kDa	37	13	95% (0.00035)
24	CP29; RNA binding / poly(U) binding	gi 15231817 (+2)	36 kDa	76	56	95% (0.037)
25	CR88; ATP binding	gi 15228059 (+2)	89 kDa	0	12	95% (0.00028)

26	ELI3-1 (ELICITOR-ACTIVATED GENE 3-1); binding / catalytic/ oxidoreductase/ zinc ion binding	gi 15233642 (+1)	38 kDa	12	4	95% (0.035)
27	emb2726 (embryo defective 2726); RNA binding / translation elongation factor	gi 18417320	104 kDa	9	21	95% (0.025)
28	GDCH; glycine dehydrogenase (decarboxylating)	gi 15226973	18 kDa	29	12	95% (0.0047)
29	GLU1 (GLUTAMATE SYNTHASE 1); glutamate synthase (ferredoxin)	gi 18414469 (+1)	177 kDa	92	121	95% (0.038)
30	glyceraldehyde 3-phosphate dehydrogenase A subunit	gi 166702 (+3)	38 kDa	199	267	95% (0.0019)
31	GRF2 (GENERAL REGULATORY FACTOR 2); protein binding / protein phosphorylated amino acid binding	gi 18411901 (+1)	29 kDa	14	27	95% (0.035)
32	GS2 (GLUTAMINE SYNTHETASE 2); glutamate-ammonia ligase	gi 15238559	47 kDa	207	173	95% (0.028)
33	heat shock cognate 70 kDa protein 3 (HSC70-3) (HSP70-3)	gi 15232682	71 kDa	55	92	95% (0.0021)
34	HSC70-1 (HEAT SHOCK COGNATE PROTEIN 70-1); ATP binding	gi 15241849 (+1)	71 kDa	108	141	95% (0.031)
35	legume lectin family protein	gi 15228229	31 kDa	9	1	95% (0.0098)
36	LOX2 (LIPOXYGENASE 2); lipoxygenase	gi 18407921	102 kDa	116	175	95% (0.00060)
37	mitochondrial elongation factor Tu	gi 1149571 (+1)	51 kDa	20	8	95% (0.015)
38	MLP43 (MLP-LIKE PROTEIN 43)	gi 15223275	18 kDa	15	4	95% (0.0085)
39	NPQ4 (NONPHOTOCHEMICAL QUENCHING); chlorophyll binding / xanthophyll binding	gi 15219418 (+1)	28 kDa	4	14	95% (0.017)
40	PAE1; endopeptidase/ peptidase/ threonine-type endopeptidase	gi 15220961	26 kDa	12	4	95% (0.035)
41	photosystem II 47 kDa protein	gi 7525059 (+1)	56 kDa	3	11	95% (0.031)
42	PLDALPHA1 (PHOSPHOLIPASE D ALPHA 1); phospholipase D	gi 15232671	92 kDa	7	19	95% (0.017)
43	PSAL (photosystem I subunit L)	gi 15235490 (+1)	23 kDa	5	19	95% (0.0039)
44	RBP31 (31-KDA RNA BINDING PROTEIN); RNA binding / poly(U) binding	gi 15233980 (+5)	36 kDa	0	11	95% (0.00055)
45	RecName: Full=ATP synthase subunit alpha, mitochondrial	gi 14916970	55 kDa	42	62	95% (0.039)
46	RecName: Full=DEAD-box ATP-dependent RNA helicase 15	gi 110283023 (+6)	48 kDa	1	8	95% (0.021)

47	RecName: Full=Phosphoglycerate kinase, chloroplastic; Flags: Precursor	gi 12644295	50 kDa	172	129	95% (0.0044)
48	RHM1 (RHAMNOSE BIOSYNTHESIS 1); UDP-L-rhamnose synthase/ UDP-glucose 4,6-dehydratase/ catalytic	gi 15218420	75 kDa	22	9	95% (0.013)
49	ribulose-1,5-bisphosphate carboxylase/oxygenase large subunit	gi 7525041	53 kDa	1374	1560	95% (0.0016)
50	SAL1; 3'(2'),5'-bisphosphate nucleotidase/ inositol or phosphatidylinositol phosphatase	gi 145359623 (+1)	44 kDa	5	0	95% (0.030)
51	SHM4 (serine hydroxymethyltransferase 4); catalytic/ glycine hydroxymethyltransferase/ pyridoxal phosphate binding	gi 15236375	52 kDa	35	22	95% (0.047)
52	SUR1 (SUPERROOT 1); S-alkylthiohydroximate lyase/ carbon-sulfur lyase/ transaminase	gi 15225387 (+1)	51 kDa	6	0	95% (0.015)
53	TIC40	gi 15237382	49 kDa	7	1	95% (0.033)
54	TUB7; structural constituent of cytoskeleton	gi 15227559	51 kDa	0	7	95% (0.0084)
55	vestitone reductase-related	gi 15236930	44 kDa	3	10	95% (0.050)
	Putative protein					
1	(S)-2-hydroxy-acid oxidase, peroxisomal, putative / glycolate oxidase, putative / short chain alpha-hydroxy acid oxidase, putative	gi 15231850	40 kDa	74	102	95% (0.029)
2	adenylosuccinate lyase, putative / adenylosuccinase, putative	gi 22328773	60 kDa	7	19	95% (0.017)
3	elongation factor 1B-gamma, putative / eEF-1B gamma, putative	gi 18391048	47 kDa	20	35	95% (0.035)
4	lactoylglutathione lyase, putative / glyoxalase I, putative	gi 15220397 (+1)	39 kDa	20	10	95% (0.044)
5	phosphoglycerate kinase, putative	gi 15223484 (+1)	50 kDa	43	27	95% (0.029)
6	monodehydroascorbate reductase, putative	gi 18407925 (+3)	53 kDa	37	23	95% (0.039)
7	putative jasmonate inducible protein	gi 110738521 (+3)	52 kDa	5	0	95% (0.030)
	Hypothetical protein					
1	hypothetical protein	gi 110740330 (+1)	63 kDa	1	10	95% (0.0065)

Table 4.4b: Fisher Exact test (P-value) (Spectral counts) for *Arabidopsis thaliana* rosette Contrast 2 - Control Vs Th17

Fisher's Exact test Contrast 2 - Control Vs. Th17						
	Identified Proteins <i>Arabidopsis thaliana</i> rosette	NCBI Accession Number	M W	Control	Th17	Fisher's Exact Test (P-Value)
1	2-oxoacid dehydrogenase family protein	gi 15240454	50 kDa	10	2	95% (0.018)
2	ACT7 (ACTIN 7); structural constituent of cytoskeleton	gi 15242516	42 kDa	127	95	95% (0.013)
3	AGT (ALANINE:GLYOXYLATE AMINOTRANSFERASE); alanine-glyoxylate transaminase/ serine-glyoxylate transaminase/ serine-pyruvate transaminase	gi 15225026	44 kDa	42	72	95% (0.0043)
4	At3g63410	gi 108385436 (+4)	38 kDa	0	5	95% (0.033)
5	ATPPC1 (PHOSPHOENOLPYRUVATE CARBOXYLASE 1); catalytic/ phosphoenolpyruvate carboxylase	gi 15219272 (+1)	110 kDa	7	19	95% (0.016)
6	ATPPC2 (PHOSPHOENOLPYRUVATE CARBOXYLASE 2); catalytic/ phosphoenolpyruvate carboxylase	gi 240254631	110 kDa	19	57	95% (0.000011)
7	binding / catalytic/ coenzyme binding	gi 18404496	35 kDa	54	34	95% (0.017)
8	catalase	gi 1246399 (+1)	57 kDa	75	101	95% (0.039)
9	chlorophyll A-B-binding protein 2 precursor, 5' partial; 1-750	gi 12324161 (+3)	27 kDa	59	89	95% (0.012)
10	COR15A (COLD-REGULATED 15A)	gi 15227963 (+1)	15 kDa	29	6	95% (0.000046)
11	COR15B (COLD REGULATED 15B)	gi 15227952 (+1)	15 kDa	37	19	95% (0.0091)
12	CORI3 (CORONATINE INDUCED 1); cystathionine beta-lyase/ transaminase	gi 15236533	47 kDa	12	29	95% (0.0069)
13	CP29; RNA binding / poly(U) binding	gi 15231817 (+2)	36 kDa	76	12	95% (0.000000000000039)
14	ESM1 (epithiospecifier modifier 1); carboxylesterase/ hydrolase, acting on ester bonds	gi 15231805 (+2)	44 kDa	77	47	95% (0.0032)

15	F5M15.5	gi 8778617	117 kDa	103	138	95% (0.020)
16	GLU1 (GLUTAMATE SYNTHASE 1); glutamate synthase (ferredoxin)	gi 18414469 (+1)	177 kDa	92	131	95% (0.0080)
17	heat shock cognate 70 kDa protein 3 (HSC70-3) (HSP70-3)	gi 15232682	71 kDa	55	82	95% (0.017)
18	HPR; glycerate dehydrogenase/ poly(U) binding	gi 15220620	42 kDa	59	81	95% (0.048)
19	KAS I (3-KETOACYL-ACYL CARRIER PROTEIN SYNTHASE I); catalytic/ fatty-acid synthase/ transferase, transferring acyl groups other than amino-acyl groups	gi 15237422 (+2)	50 kDa	8	21	95% (0.014)
20	legume lectin family protein	gi 15228229	31 kDa	9	1	95% (0.0099)
21	LHB1B1; chlorophyll binding	gi 18403549	28 kDa	51	83	95% (0.0050)
22	LHCA2; chlorophyll binding	gi 186511289 (+1)	28 kDa	27	44	95% (0.034)
23	LHCB5 (LIGHT HARVESTING COMPLEX OF PHOTOSYSTEM II 5); chlorophyll binding	gi 15235029 (+1)	30 kDa	49	69	95% (0.050)
24	LHCB6 (LIGHT HARVESTING COMPLEX PSII SUBUNIT 6); chlorophyll binding	gi 15218330 (+1)	28 kDa	14	27	95% (0.034)
25	LOX2 (LIPOXYGENASE 2); lipoxygenase	gi 18407921	102 kDa	116	180	95% (0.00022)
26	mitochondrial elongation factor Tu	gi 1149571 (+1)	51 kDa	20	6	95% (0.0040)
27	MLP43 (MLP-LIKE PROTEIN 43)	gi 15223275	18 kDa	15	6	95% (0.035)
28	MTHSC70-2 (MITOCHONDRIAL HSP70 2); ATP binding	gi 15242459	73 kDa	7	1	95% (0.033)
29	NPQ4 (NONPHOTOCHEMICAL QUENCHING); chlorophyll binding / xanthophyll binding	gi 15219418 (+1)	28 kDa	4	13	95% (0.027)
30	PAE1; endopeptidase/ peptidase/ threonine-type endopeptidase	gi 15220961	26 kDa	12	4	95% (0.035)
31	RHM1 (RHAMNOSE BIOSYNTHESIS 1); UDP-L-rhamnose synthase/ UDP-glucose 4,6-dehydratase/ catalytic	gi 15218420	75 kDa	22	9	95% (0.013)
32	ribosomal protein L1 family protein	gi 15229443 (+1)	38 kDa	8	19	95% (0.029)

33	ribulose-1,5-bisphosphate carboxylase/oxygenase large subunit	gi 7525041	53 kDa	1,374	1,630	95% (0.0000090)
	Putative protein					
1	3-isopropylmalate dehydrogenase, chloroplast, putative	gi 15241338	44 kDa	37	20	95% (0.014)
2	adenylosuccinate lyase, putative / adenylosuccinase, putative	gi 22328773	60 kDa	7	20	95% (0.011)
3	chaperonin, putative	gi 15231255	63 kDa	114	86	95% (0.020)
4	cysteine protease inhibitor, putative / cystatin, putative	gi 18399630 (+2)	22 kDa	9	1	95% (0.0099)
5	fructose-bisphosphate aldolase, putative	gi 18420348	43 kDa	196	167	95% (0.048)
6	fructose-bisphosphate aldolase, putative	gi 15226185	42 kDa	9	2	95% (0.030)
7	putative jasmonate inducible protein	gi 110738521 (+3)	52 kDa	5	0	95% (0.030)
8	ubiquitin-conjugating enzyme, putative	gi 18394416	17 kDa	6	0	95% (0.015)
	Unknown protein					
1	Unknown protein	gi 14423536 (+1)	34 kDa	8	0	95% (0.0036)

Table 4.4c: Fisher's Exact test (P-value) (Spectral counts) for Arabidopsis thaliana rosette Contrast 3 - LCO Vs Th17

	Fishers's Exact test for Contrast 3 - LCO Vs Th17					
	Identified Proteins <i>Arabidopsis thaliana</i> rosette	NCBI Accession	MW	LCO	Th17	Fisher's Exact Test (P-Value)
1	40S ribosomal protein S3A (RPS3aA)	gi 15229364	30 kDa	6	0	95% (0.016)
2	40S ribosomal protein S3A (RPS3aB)	gi 15236171 (+1)	30 kDa	8	1	95% (0.020)
3	60S ribosomal protein L15 (RPL15A)	gi 15235851 (+2)	24 kDa	5	0	95% (0.031)
4	60S ribosomal protein L4/L1 (RPL4A)	gi 15232723 (+1)	45 kDa	14	3	95% (0.0064)
5	60S ribosomal protein L6 (RPL6C)	gi 15221126 (+1)	26 kDa	8	1	95% (0.020)
6	60S ribosomal protein L9 (RPL90B)	gi 18398753 (+1)	22 kDa	25	12	95% (0.024)
7	AT5g52920/MXC20_15	gi 15081612 (+2)	64 kDa	5	0	95% (0.031)

8	BIP1; ATP binding	gi 15241844	74 kDa	16	4	95% (0.0060)
9	CAC3; acetyl-CoA carboxylase	gi 18404621 (+1)	85 kDa	5	0	95% (0.031)
10	CAD1 (CADMIUM SENSITIVE 1); cadmium ion binding / copper ion binding / glutathione gamma-glutamylcysteinyltransferase	gi 15240084 (+4)	54 kDa	5	0	95% (0.031)
11	CDC48 (CELL DIVISION CYCLE 48); ATPase/ identical protein binding	gi 15232776	89 kDa	22	11	95% (0.040)
12	CP29; RNA binding / poly(U) binding	gi 15231817 (+2)	36 kDa	56	12	95% (0.000000031)
13	CR88; ATP binding	gi 15228059 (+2)	89 kDa	12	2	95% (0.0065)
14	elongation factor 1-beta / EF-1-beta	gi 145324076 (+3)	29 kDa	5	0	95% (0.031)
15	ESM1 (epithiospecifier modifier 1); carboxylesterase/ hydrolase, acting on ester bonds	gi 15231805 (+2)	44 kDa	75	47	95% (0.0072)
16	FIB (FIBRILLIN); structural molecule	gi 15233357	35 kDa	0	5	95% (0.031)
17	GAPB (GLYCERALDEHYDE-3-PHOSPHATE DEHYDROGENASE B SUBUNIT); glyceraldehyde-3-phosphate dehydrogenase (NADP+)/ glyceraldehyde-3-phosphate dehydrogenase	gi 15217555 (+1)	48 kDa	184	149	95% (0.032)
18	GDCH; glycine dehydrogenase (decarboxylating)	gi 15226973	18 kDa	12	24	95% (0.032)
19	oxidoreductase, zinc-binding dehydrogenase family protein	gi 15220854 (+1)	41 kDa	18	33	95% (0.024)
20	RBP31 (31-KDA RNA BINDING PROTEIN); RNA binding / poly(U) binding	gi 15233980 (+5)	36 kDa	11	0	95% (0.00049)
21	SHM1 (SERINE TRANSHYDROXYMETHYLTRANSFERASE 1); glycine hydroxymethyltransferase/ poly(U) binding	gi 15235745 (+1)	57 kDa	86	119	95% (0.012)
22	TUB7; structural constituent of cytoskeleton	gi 15227559	51 kDa	7	0	95% (0.0078)
	Putative protein					
1	cysteine protease inhibitor, putative / cystatin, putative	gi 18399630 (+2)	22 kDa	7	1	95% (0.035)
2	nuclear RNA-binding protein, putative	gi 145334757 (+2)	32 kDa	5	0	95% (0.031)
	Hypothetical protein					

	(phosphorylating)/ glyceraldehyde-3-phosphate dehydrogenase					
10	GAPB (GLYCERALDEHYDE-3-PHOSPHATE DEHYDROGENASE B SUBUNIT); glyceraldehyde-3-phosphate dehydrogenase (NADP+)/ glyceraldehyde-3-phosphate dehydrogenase	gi 15217555 (+1)	48 kDa	112	146	95% (0.033)
11	GER3 (GERMIN 3); oxalate oxidase	gi 15242028 (+2)	22 kDa	55	34	95% (0.012)
12	HSP60-2 (HEAT SHOCK PROTEIN 60-2); ATP binding	gi 30685604	62 kDa	12	25	95% (0.029)
13	KIN1	gi 15237228 (+1)	6 kDa	40	62	95% (0.026)
14	KIN2	gi 15237236	7 kDa	52	86	95% (0.0039)
15	LTI78 (LOW-TEMPERATURE-INDUCED 78)	gi 15242967 (+1)	78 kDa	11	32	95% (0.0013)
16	photosystem I P700 chlorophyll a apoprotein A1	gi 7525033	83 kDa	8	18	95% (0.044)
17	RecName: Full=DEAD-box ATP-dependent RNA helicase 15	gi 110283023 (+6)	48 kDa	10	3	95% (0.041)
18	RGP1 (REVERSIBLY GLYCOSYLATED POLYPEPTIDE 1); cellulose synthase (UDP-forming)	gi 15232865	41 kDa	7	20	95% (0.012)
19	SAM-2 (S-ADENOSYLMETHIONINE SYNTHETASE 2); copper ion binding / methionine adenosyltransferase	gi 15234354	43 kDa	49	25	95% (0.0024)
20	TUA3; structural constituent of cytoskeleton	gi 15241168	50 kDa	3	17	95% (0.0016)
21	TUB4; structural constituent of cytoskeleton	gi 15241472	50 kDa	4	32	95% (0.0000014)
	Putative proteins					
1	fructose-bisphosphate aldolase, putative	gi 18399660	43 kDa	101	136	95% (0.023)
2	lactoylglutathione lyase, putative / glyoxalase I, putative	gi 15220397	39 kDa	16	6	95% (0.022)

3	phosphoglycerate kinase, putative	gi 15223484 (+1)	50 kDa	53	34	95% (0.019)
4	UTP--glucose-1-phosphate uridylyltransferase, putative / UDP-glucose pyrophosphorylase, putative / UGPase, putative	gi 15237947	52 kDa	13	5	95% (0.042)

Table 4.4e: Fisher Exact test (P-value) (Spectral counts) for *Arabidopsis thaliana* rosette contrasts 5. Control 250 mM NaCl Vs Th17 + 250 mM NaCl

Fisher's Exact test for Contrast 5 - Control 250 mM NaCl Vs Th17 + 250 mM NaCl						
	Identified Proteins <i>Arabidopsis thaliana</i> rosette	Accession Number	MW	Control 250 mM NaCl	Th17 + 250 mM NaCl	Fisher's Exact Test (P-Value)
1	ribulose-1,5-bisphosphate carboxylase/oxygenase large subunit	gi 7525041	53 kDa	858	1,213	95% (0.0000000000041)
2	aconitate hydratase, cytoplasmic / citrate hydro-lyase / aconitase (ACO)	gi 15233349	98 kDa	5	16	95% (0.019)
3	ADK2 (ADENOSINE KINASE 2); adenosine kinase/ copper ion binding / kinase	gi 15242717	38 kDa	33	21	95% (0.041)
4	AT5g26000/T1N24_7	gi 15809938 (+3)	61 kDa	120	98	95% (0.028)
5	ATS9 (ARABIDOPSIS NON-ATPASE SUBUNIT 9)	gi 15218845 (+3)	47 kDa	0	6	95% (0.019)
6	CLPP4 (CLP PROTEASE P4); serine-type endopeptidase	gi 18422548 (+3)	32 kDa	18	33	95% (0.041)
7	COR15A (COLD-REGULATED 15A)	gi 15227963 (+1)	15 kDa	142	324	95% (0.0000000000000021)
8	COR47 (COLD-REGULATED 47)	gi 15217937 (+1)	30 kDa	22	46	95% (0.0054)
9	CP29; RNA binding / poly(U) binding	gi 15231817 (+2)	36 kDa	32	5	95% (0.0000015)
10	F1O19.10/F1O19.10	gi 13926229	15 kDa	145	205	95% (0.0051)
11	F3F9.11	gi 8052534	77 kDa	66	43	95% (0.0071)

12	FDH (FORMATE DEHYDROGENASE); NAD or NADH binding / binding / catalytic/ cofactor binding / oxidoreductase, acting on the CH-OH group of donors, NAD or NADP as acceptor	gi 15241492 (+2)	42 kDa	59	42	95% (0.027)
13	GAPA-2 (GLYCERALDEHYDE 3-PHOSPHATE DEHYDROGENASE A SUBUNIT 2); NAD or NADH binding / binding / catalytic/ glyceraldehyde-3-phosphate dehydrogenase (phosphorylating)/ glyceraldehyde-3-phosphate dehydrogenase	gi 15222111 (+1)	43 kDa	92	56	95% (0.00050)
14	GAPC1 (GLYCERALDEHYDE-3-PHOSPHATE DEHYDROGENASE C SUBUNIT 1); glyceraldehyde-3-phosphate dehydrogenase (phosphorylating)/ glyceraldehyde-3-phosphate dehydrogenase	gi 15229231	37 kDa	105	63	95% (0.00016)
15	HEMC (HYDROXYMETHYLBILANE SYNTHASE); hydroxymethylbilane synthase	gi 15241573 (+1)	41 kDa	31	18	95% (0.026)
16	HSP70 (heat shock protein 70); ATP binding	gi 15230534	71 kDa	14	31	95% (0.014)
17	KIN2	gi 15237236	7 kDa	52	82	95% (0.016)
18	LHB1B1; chlorophyll binding	gi 18403549	28 kDa	55	80	95% (0.045)
19	LHCB3 (LIGHT-HARVESTING CHLOROPHYLL B-BINDING PROTEIN 3); structural molecule	gi 15239602	29 kDa	16	31	95% (0.033)
20	LTI30 (LOW TEMPERATURE-INDUCED 30)	gi 15230361	21 kDa	12	25	95% (0.037)
21	LTI78 (LOW-TEMPERATURE-	gi 15242967 (+1)	78 kDa	11	33	95% (0.0013)

	INDUCED 78)					
22	mitochondrial phosphate transporter	gi 15241291 (+1)	40 kDa	2	10	95% (0.025)
23	PATL2 (PATELLIN 2); transporter	gi 15219901	76 kDa	1	10	95% (0.0078)
24	peroxidase	gi 1402914 (+1)	40 kDa	8	1	95% (0.015)
25	photosystem II 47 kDa protein	gi 7525059	56 kDa	24	42	95% (0.033)
26	photosystem II protein D1	gi 7525013	39 kDa	9	22	95% (0.023)
27	ROC3; peptidyl-prolyl cis-trans isomerase	gi 15227259	18 kDa	47	33	95% (0.040)
28	SAM1 (S-ADENOSYLMETHIONINE SYNTHETASE 1); methionine adenosyltransferase	gi 15217781 (+1)	43 kDa	9	24	95% (0.011)
29	SAM-2 (S-ADENOSYLMETHIONINE SYNTHETASE 2); copper ion binding / methionine adenosyltransferase	gi 15234354	43 kDa	49	29	95% (0.0072)
30	SEX1 (STARCH EXCESS 1); alpha-glucan, water dikinase	gi 18391200 (+1)	157 kDa	0	5	95% (0.037)
31	threonine synthase	gi 1448917 (+1)	58 kDa	5	14	95% (0.043)
32	translational inhibitor protein like	gi 110739384 (+2)	28 kDa	29	18	95% (0.046)
33	TUB4; structural constituent of cytoskeleton	gi 15241472	50 kDa	4	17	95% (0.0055)
34	VDAC2 (VOLTAGE DEPENDENT ANION CHANNEL 2); voltage-gated anion channel	gi 15240765	30 kDa	29	17	95% (0.032)
	Putative proteins					
1	26S proteasome regulatory subunit, putative	gi 145334543 (+1)	29 kDa	6	0	95% (0.013)
2	ACLB-1; ATP citrate synthase	gi 15230764 (+1)	66 kDa	2	12	95% (0.0090)
3	isocitrate dehydrogenase, putative / NADP+ isocitrate dehydrogenase, putative	gi 22326811 (+1)	54 kDa	0	19	95% (0.0000035)
4	phosphoglycerate kinase, putative	gi 15223484 (+1)	50 kDa	53	29	95% (0.0022)

5	putative elongation factor P (EF-P); 66839-65711	gi 12322730 (+1)	21 kDa	14	6	95% (0.043)
	Unknown proteins					
1	unknown protein	gi 30689549	32 kDa	1	7	95% (0.043)

Table 4.4f: Fisher Exact test (P-value) (Spectral counts) for *Arabidopsis thaliana* rosette contrasts 6. LCO + 250 mM NaCl Vs Th17 + 250 mM NaCl

	Fisher's Exact test for Contrast 6 - LCO + 250 mM NaCl Vs Th17 + 250 mM NaCl					
	Identified Proteins <i>Arabidopsis thaliana</i> rosette	Accession number	MW	LCO + 250 mM NaCl	Th17 + 250 mM NaCl	Fisher's Exact Test (P-Value)
1	ACLB-1; ATP citrate synthase	gi 15230764 (+1)	66 kDa	3	12	95% (0.021)
2	ADH1 (ALCOHOL DEHYDROGENASE 1); alcohol dehydrogenase	gi 15223838 (+1)	41 kDa	8	20	95% (0.022)
3	aspartic proteinase	gi 1354272 (+1)	52 kDa	26	46	95% (0.018)
4	ATS9 (ARABIDOPSIS NON-ATPASE SUBUNIT 9)	gi 15218845 (+3)	47 kDa	0	6	95% (0.017)
5	beta-glucosidase homolog	gi 6651430	60 kDa	92	70	95% (0.030)
6	COR15A (COLD-REGULATED 15A)	gi 15227963 (+1)	15 kDa	376	324	95% (0.0076)
7	COR13 (CORONATINE INDUCED 1); cystathionine beta-lyase/transaminase	gi 15236533	47 kDa	99	78	95% (0.040)
8	DHAR1 (dehydroascorbate reductase); copper ion binding / glutathione dehydrogenase (ascorbate)	gi 15223576	24 kDa	87	68	95% (0.047)
9	F1O19.10/F1O19.10	gi 13926229	15 kDa	163	205	95% (0.036)
10	GAPC1 (GLYCERALDEHYDE-3-PHOSPHATE DEHYDROGENASE C SUBUNIT 1); glyceraldehyde-3-phosphate dehydrogenase (phosphorylating)/ glyceraldehyde-3-phosphate dehydrogenase	gi 15229231	37 kDa	93	63	95% (0.0053)

11	HEMC (HYDROXYMETHYLBILANE SYNTHASE); hydroxymethylbilane synthase	gi 15241573 (+1)	41 kDa	31	18	95% (0.032)
12	HSP70 (heat shock protein 70); ATP binding	gi 15230534	71 kDa	14	31	95% (0.011)
13	mitochondrial phosphate transporter	gi 15241291 (+1)	40 kDa	1	10	95% (0.0069)
14	PR5 (PATHOGENESIS-RELATED GENE 5)	gi 15222089	25 kDa	23	38	95% (0.049)
15	RecName: Full=ATP-dependent Clp protease proteolytic subunit 1; AltName: Full=Endopeptidase ClpP1; Short=pClpP	gi 160332321 (+1)	22 kDa	1	7	95% (0.039)
16	RGP1 (REVERSIBLY GLYCOSYLATED POLYPEPTIDE 1); cellulose synthase (UDP-forming)	gi 15232865	41 kDa	20	2	95% (0.000043)
17	SAM1 (S-ADENOSYLMETHIONINE SYNTHETASE 1); methionine adenosyltransferase	gi 15217781 (+1)	43 kDa	6	24	95% (0.00099)
18	seed maturation protein	gi 110739182 (+2)	67 kDa	1	7	95% (0.039)
19	TUA3; structural constituent of cytoskeleton	gi 15241168	50 kDa	17	6	95% (0.014)
20	TUB4; structural constituent of cytoskeleton	gi 15241472	50 kDa	32	17	95% (0.016)
	Putative proteins					
1	3-isopropylmalate dehydrogenase, chloroplast, putative	gi 15221631 (+1)	44 kDa	18	5	95% (0.0041)
2	arginase, putative	gi 15236635	38 kDa	36	22	95% (0.032)
3	isocitrate dehydrogenase, putative / NADP+ isocitrate dehydrogenase, putative	gi 22326811 (+1)	54 kDa	1	19	95% (0.000028)
4	lactoylglutathione lyase, putative / glyoxalase I, putative	gi 15220397	39 kDa	6	20	95% (0.0061)
5	UTP--glucose-1-phosphate uridylyltransferase, putative / UDP-glucose pyrophosphorylase, putative / UGPase, putative	gi 15237947	52 kDa	5	17	95% (0.011)

APPENDIX III

CHAPTER 5

Table 5.1: Least square means of germination by soybean seeds treated with lipo-chitooligosaccharide and thuricin 17 under optimal and salt stress conditions. Means associated with the same letter are not significantly different at $p < 0.05$ ($n = 10$).

Treatments	24h	±SEM	30h	±SEM	36h	±SEM	48h	±SEM
P < 0.05	0.7130		0.9847		0.9342		0.1592	
Control (Water)	62.00 ^a	6.03	93.00 ^a	4.28	96.00 ^a	2.59	99.00 ^a	1.50
LCOA	58.00 ^a	3.22	89.50 ^a	3.22	94.00 ^a	2.37	98.50 ^b	1.26
LCOB	60.00 ^a	3.54	91.25 ^a	3.54	95.00 ^a	2.25	98.75 ^a	1.37
THA	60.00 ^a	3.95	91.25 ^a	3.95	95.00 ^a	2.60	98.75 ^{ab}	1.51
THB	60.00 ^a	4.75	91.25 ^a	2.28	95.00 ^a	1.67	98.75 ^{ab}	0.37
P < 0.05	0.0588		0.0427		0.0270		0.1255	
Control (100 mM NaCl)	20.00 ^b	4.22	37.00 ^b	5.78	58.00 ^b	7.42	81.00 ^b	5.67
LCOA + 100 mM NaCl	22.22 ^{ab}	2.48	51.44 ^{ab}	4.23	83.00 ^a	4.96	94.00 ^a	3.06
LCOB +100 mM NaCl	32.00 ^a	3.89	60.00 ^a	4.47	80.00 ^a	4.94	93.00 ^a	3.00
THA + 100 mM NaCl	17.00 ^b	3.67	47.00 ^{ab}	7.61	71.00 ^{ab}	6.40	93.00 ^a	4.23
THB + 100 mM NaCl	25.00 ^{ab}	3.73	56.00 ^a	4.00	71.00 ^{ab}	3.48	92.00 ^{ab}	2.91
P < 0.05	0.6093		0.0181		0.0222		0.6683	
Control (125 mM NaCl)	1.00 ^a	1.00	17.00 ^b	2.60	30.00 ^b	3.94	76.00 ^a	4.27
LCOA + 125 mM NaCl	3.00 ^a	1.53	36.00 ^a	4.76	58.00 ^a	6.46	82.00 ^a	3.89
LCOB +125 mM NaCl	2.00 ^a	1.33	37.00 ^a	5.17	55.00 ^a	6.54	83.00 ^a	3.96
THA + 125 mM NaCl	4.00 ^a	1.63	32.00 ^a	4.67	53.00 ^a	5.97	84.00 ^a	3.71

THB + 125 mM NaCl	2.00^a	1.33	27.00^{ab}	4.73	49.00^a	7.67	81.00^a	4.33
P < 0.05	0.1961		0.0616		0.0086		0.0089	
Control (150 mM NaCl)	0.00^a	0.00	14.00^b	4.00	27.00^c	5.17	88.00^a	2.49
LCOA + 150 mM NaCl	0.00^a	0.00	17.00^{ab}	2.13	41.00^{ab}	3.79	79.00^{bc}	3.79
LCOB +150 mM NaCl	4.00^a	2.21	25.00^a	2.24	51.00^a	4.07	87.00^{ab}	3.67
THA + 150 mM NaCl	3.00^a	2.13	24.00^a	4.00	43.00^{ab}	6.16	80.00^{abc}	3.33
THB + 150 mM NaCl	1.00^a	1.00	16.00^{ab}	3.06	34.00^{bc}	3.40	73.00^c	2.13
P < 0.05	0.5316		0.4041		0.0396		0.1452	
Control (175 mM NaCl)	0.00^a	0.00	11.00^a	3.14	34.00^{bc}	4.00	83.00^{ab}	3.00
LCOA + 175 mM NaCl	1.00^a	1.00	17.00^a	3.96	44.00^{abc}	3.71	78.00^b	4.67
LCOB +175 mM NaCl	2.00^a	2.00	17.00^a	4.48	45.00^{ab}	5.43	90.00^a	3.65
THA + 175 mM NaCl	0.00^a	0.00	12.00^a	3.59	31.00^c	5.47	77.00^b	4.73
THB + 175 mM NaCl	0.00^a	0.00	20.00^a	3.33	49.00^a	4.33	84.00^{ab}	3.06
P<0.05	0.4175		0.4074		0.2012		0.8802	
Control (200 mM NaCl)	1.00^a	1.00	8.00^a	2.00	23.00^a	3.35	66.00^a	5.81
LCOA + 200 mM NaCl	0.00^a	0.00	6.00^a	4.00	17.00^{ab}	4.48	66.00^a	4.76
LCOB +200 mM NaCl	0.00^a	0.00	2.00^a	1.33	10.00^b	2.98	67.00^a	4.73
THA + 200 mM NaCl	0.00^a	0.00	3.00^a	2.13	15.00^{ab}	3.73	69.00^a	2.77
THB + 200 mM NaCl	0.00^a	0.00	3.00^a	2.13	18.00^{ab}	4.16	72.00^a	4.90

Table 5.3a: Fold change (Spectral counts) for contrasts 1. Control Vs LCO

Fold change contrast 1. Control Vs LCO					
	Known proteins [Glycine max]	NCBI Accession	MW	Control	LCO
1	atpA	gi 22739 (+1)	55 kDa	2.8	0.4
2	cytosolic chaperonin, delta subunit	gi 255957394 (+1)	58 kDa	0.3	3.0
3	glutathione S-transferase GST 14, partial	gi 11385443 (+6)	25 kDa	0.4	2.3
4	metallothionein-II protein	gi 2306979 (+1)	8 kDa	2.5	0.4
5	peroxisomal voltage-dependent anion-selective channel protein	gi 167963388 (+5)	30 kDa	0.4	2.3
6	phosphoenolpyruvate carboxylase	gi 218267 (+8)	111 kDa	0.4	2.5
7	poly [ADP-ribose] polymerase 3	gi 351724917 (+2)	92 kDa	0.4	2.4
8	RecName: Full=ATP synthase subunit beta, chloroplastic; AltName: Full=ATP synthase F1 sector subunit beta; AltName: Full=F-ATPase subunit beta	gi 118573752 (+5)	54 kDa	0.3	4.0
9	stearoyl-acyl carrier protein desaturase B	gi 183392958 (+6)	45 kDa	2.5	0.4
10	uricase	gi 1498170 (+8)	35 kDa	0.3	3.0
	Predicted proteins				
1	PREDICTED: 50S ribosomal protein L12, chloroplastic-like	gi 356538549 (+1)	20 kDa	0.3	3.0
2	PREDICTED: 60S acidic ribosomal protein P1-3-like	gi 356506100	11 kDa	0.4	2.7
3	PREDICTED: 6-phosphogluconate dehydrogenase, decarboxylating-like isoform 1	gi 356526581 (+5)	54 kDa	2.5	0.4
4	PREDICTED: 97 kDa heat shock protein-like	gi 356550547	95 kDa	4.0	0.3
5	PREDICTED: aconitate hydratase 1	gi 356496602	99 kDa	3.0	0.3
6	PREDICTED: adenosylhomocysteinase-like	gi 356512439	53 kDa	2.1	0.5
7	PREDICTED: aldehyde dehydrogenase family 2 member B4, mitochondrial-like	gi 356567618	58 kDa	2.8	0.4
8	PREDICTED: alpha-1,4 glucan phosphorylase L isozyme, chloroplastic/amyloplastic-like	gi 356551144	110 kDa	0.1	11.0
9	PREDICTED: ATP-citrate synthase beta chain protein 1-like	gi 356529147 (+1)	66 kDa	0.4	2.5

10	PREDICTED: auxin-induced protein PCNT115-like isoform 1	gi 356517239 (+1)	38 kDa	0.5	2.0
11	PREDICTED: eukaryotic peptide chain release factor GTP-binding subunit ERF3A-like	gi 356513002 (+1)	56 kDa	0.5	2.0
12	PREDICTED: ketol-acid reductoisomerase, chloroplastic-like	gi 356543900 (+1)	63 kDa	0.1	9.0
13	PREDICTED: ketol-acid reductoisomerase, chloroplastic-like	gi 356543032	63 kDa	0.3	3.0
14	PREDICTED: leucine aminopeptidase 1-like isoform 1	gi 356571429	61 kDa	0.5	2.0
15	PREDICTED: LOW QUALITY PROTEIN: adenosine kinase 2-like	gi 356572450	37 kDa	2.0	0.5
16	PREDICTED: LOW QUALITY PROTEIN: argininosuccinate synthase, chloroplastic-like	gi 356514007 (+7)	46 kDa	0.1	8.0
17	PREDICTED: oligopeptidase A-like	gi 356531379	87 kDa	0.5	2.0
18	PREDICTED: probable allantoinase 1-like	gi 356549347	57 kDa	0.5	2.0
19	PREDICTED: quinone oxidoreductase 1-like	gi 356544208	40 kDa	3.5	0.3
20	PREDICTED: stromal 70 kDa heat shock-related protein, chloroplastic-like	gi 356559803	74 kDa	0.5	2.0
21	PREDICTED: sucrose synthase 2-like	gi 356558189	92 kDa	0.5	2.0
22	PREDICTED: T-complex protein 1 subunit alpha-like	gi 356525315	59 kDa	2.0	0.5
23	PREDICTED: T-complex protein 1 subunit beta-like	gi 356539292 (+1)	57 kDa	0.4	2.5
24	PREDICTED: T-complex protein 1 subunit eta-like	gi 356501324 (+1)	60 kDa	2.0	0.5
25	PREDICTED: T-complex protein 1 subunit zeta-like	gi 356527473 (+1)	59 kDa	0.3	4.0
26	PREDICTED: thioredoxin H-type	gi 356564319	13 kDa	3.3	0.3
27	PREDICTED: transaldolase-like	gi 356527464 (+1)	48 kDa	0.3	3.0
28	PREDICTED: uncharacterized protein At2g37660, chloroplastic-like	gi 356567949	28 kDa	6.0	0.2
29	PREDICTED: uncharacterized protein LOC100783299	gi 356570331	76 kDa	2.0	0.5
30	PREDICTED: uncharacterized protein LOC100808941	gi 356570816	16 kDa	2.7	0.4
	Unknown proteins				
1	unknown	gi 255626483 (+4)	17 kDa	2.0	0.5
2	unknown	gi 255642364 (+1)	46 kDa	2.0	0.5
3	unknown	gi 255628369 (+2)	15 kDa	2.0	0.5

4	unknown	gi 255631748 (+2)	24 kDa	0.4	2.3
5	unknown	gi 255627471 (+3)	10 kDa	2.6	0.4
6	unknown	gi 255625799 (+2)	16 kDa	0.2	4.5
7	unknown	gi 255646011 (+3)	35 kDa	0.4	2.5
8	unknown	gi 255626101 (+2)	20 kDa	0.5	2.0
9	unknown	gi 255642137 (+2)	50 kDa	0.3	3.0
10	unknown	gi 255641228 (+9)	43 kDa	0.5	2.2
11	unknown	gi 255645037 (+1)	42 kDa	0.5	2.0
12	unknown	gi 255628633 (+2)	22 kDa	0.4	2.5
13	unknown	gi 255637227 (+1)	29 kDa	0.3	3.0
14	unknown	gi 255626921 (+3)	15 kDa	0.1	7.0
15	unknown	gi 255627607 (+6)	14 kDa	0.3	3.0
16	unknown	gi 255626825 (+1)	13 kDa	3.5	0.3
17	unknown	gi 255627399 (+2)	24 kDa	0.4	2.6
18	unknown	gi 255633168	27 kDa	2.0	0.5
19	unknown	gi 255635052 (+2)	39 kDa	0.3	4.0
20	unknown	gi 255638912 (+1)	37 kDa	0.4	2.7
21	unknown	gi 255627767 (+3)	21 kDa	0.2	5.0
22	unknown	gi 255627023 (+26)	18 kDa	0.3	4.0
23	unknown	gi 255641753 (+12)	22 kDa	2.0	0.5
24	unknown	gi 255640724 (+3)	14 kDa	2.5	0.4
25	unknown	gi 255646799 (+1)	19 kDa	0.5	2.0
	Unnamed protein product				
1	unnamed protein product	gi 296523720 (+2)	65 kDa	0.5	2.0
2	unnamed protein product	gi 219732878 (+30)	47 kDa	0.4	2.3
3	unnamed protein product	gi 227247708 (+2)	17 kDa	4.3	0.2
4	unnamed protein product	gi 291047826 (+2)	53 kDa	3.0	0.3

5	unnamed protein product	gi 257672765 (+2)	90 kDa	0.4	2.6
6	unnamed protein product	gi 227248104 (+4)	23 kDa	0.5	2.0
7	unnamed protein product	gi 296511543 (+2)	18 kDa	0.5	2.0
8	unnamed protein product	gi 219732886 (+61)	50 kDa	2.0	0.5
9	unnamed protein product	gi 219898651 (+4)	11 kDa	0.5	2.0
10	unnamed protein product	gi 227483067 (+1)	79 kDa	0.3	3.0
11	unnamed protein product	gi 219931139 (+2)	27 kDa	3.0	0.3
12	unnamed protein product	gi 253785312 (+13)	16 kDa	3.0	0.3
13	unnamed protein product	gi 219743082 (+12)	38 kDa	3.0	0.3

Table 5.3b: Fold change (Spectral counts) for contrasts 2. Control Vs Th17

	Fold change Contrast 2. Control Vs Th17				
	Known proteins	Accession	MW	Control	Th17
1	beta-conglycinin alpha prime subunit	gi 290563695 (+4)	72 kDa	2.0	0.5
2	beta-conglycinin beta subunit	gi 63852207 (+1)	48 kDa	2.0	0.5
3	cytosolic chaperonin, delta subunit	gi 255957394 (+1)	58 kDa	0.5	2.0
4	glutathione S-transferase GST 14, partial	gi 11385443 (+6)	25 kDa	0.3	3.0
5	metallothionein-II protein	gi 2306979 (+1)	8 kDa	2.5	0.4
6	peroxisomal fatty acid beta-oxidation multifunctional protein	gi 167962162 (+2)	79 kDa	7.0	0.1
7	peroxisomal voltage-dependent anion-selective channel protein	gi 167963388 (+5)	30 kDa	0.3	3.3
8	phosphoenolpyruvate carboxylase	gi 218267 (+8)	111 kDa	0.2	6.5
9	poly [ADP-ribose] polymerase 3	gi 351724917 (+2)	92 kDa	0.4	2.4
10	pyruvate kinase	gi 22296818 (+13)	55 kDa	0.3	3.3
11	RecName: Full=ATP synthase subunit beta, chloroplastic; AltName: Full=ATP synthase F1 sector subunit beta; AltName: Full=F-ATPase subunit beta	gi 118573752 (+5)	54 kDa	0.2	5.0
12	RecName: Full=Beta-conglycinin, alpha chain; Flags: Precursor	gi 121281 (+5)	70 kDa	2.1	0.5
13	RecName: Full=Isocitrate lyase 1; Short=ICL 1; Short=Isocitrase 1;	gi 1168289 (+8)	63 kDa	0.5	2.0

	Short=Isocitratase 1				
14	uricase	gi 1498170 (+8)	35 kDa	0.4	2.3
	Predicted proteins				
1	PREDICTED: 50S ribosomal protein L12, chloroplastic-like	gi 356538549 (+1)	20 kDa	0.4	2.5
2	PREDICTED: 60S acidic ribosomal protein P1-3-like	gi 356506100	11 kDa	0.5	2.0
3	PREDICTED: 6-phosphogluconate dehydrogenase, decarboxylating-like isoform 1	gi 356526581 (+5)	54 kDa	2.5	0.4
4	PREDICTED: 97 kDa heat shock protein-like	gi 356550547	95 kDa	2.0	0.5
5	PREDICTED: adenosylhomocysteinase-like	gi 356512439	53 kDa	2.1	0.5
6	PREDICTED: alpha-1,4 glucan phosphorylase L isozyme, chloroplastic/amyloplastic-like	gi 356551144	110 kDa	0.1	7.0
7	PREDICTED: ATP-citrate synthase beta chain protein 1-like	gi 356529147 (+1)	66 kDa	0.4	2.5
8	PREDICTED: auxin-induced protein PCNT115-like isoform 1	gi 356517239 (+1)	38 kDa	0.1	7.0
9	PREDICTED: bifunctional polymyxin resistance protein ArnA-like	gi 356539350 (+2)	43 kDa	4.0	0.3
10	PREDICTED: endoplasmin homolog	gi 356553371 (+1)	94 kDa	0.3	3.5
11	PREDICTED: eukaryotic peptide chain release factor GTP-binding subunit ERF3A-like	gi 356513002 (+1)	56 kDa	0.4	2.5
12	PREDICTED: ketol-acid reductoisomerase, chloroplastic-like	gi 356543900 (+1)	63 kDa	0.1	12.0
13	PREDICTED: ketol-acid reductoisomerase, chloroplastic-like	gi 356543032	63 kDa	0.3	3.5
14	PREDICTED: leucine aminopeptidase 1-like isoform 1	gi 356571429	61 kDa	0.4	2.3
15	PREDICTED: LOW QUALITY PROTEIN: argininosuccinate synthase, chloroplastic-like	gi 356514007 (+7)	46 kDa	0.1	10.0
16	PREDICTED: lysosomal alpha-mannosidase-like isoform 1	gi 356561171 (+1)	117 kDa	0.4	2.7
17	PREDICTED: oligopeptidase A-like	gi 356531379	87 kDa	0.5	2.0
18	PREDICTED: phosphoglycerate kinase, chloroplastic-like	gi 356525742	50 kDa	0.5	2.1
19	PREDICTED: stromal 70 kDa heat shock-related protein, chloroplastic-like	gi 356559803	74 kDa	0.5	2.0
20	PREDICTED: sucrose synthase 2-like	gi 356558189	92 kDa	0.5	2.0
22	PREDICTED: T-complex protein 1 subunit beta-like	gi 356539292 (+1)	57 kDa	0.4	2.5

23	PREDICTED: T-complex protein 1 subunit gamma-like	gi 356530989 (+1)	60 kDa	0.5	2.0
24	PREDICTED: T-complex protein 1 subunit zeta-like	gi 356527473 (+1)	59 kDa	0.1	7.0
25	PREDICTED: thioredoxin H-type	gi 356564319	13 kDa	5.0	0.2
26	PREDICTED: transaldolase-like	gi 356527464 (+1)	48 kDa	0.4	2.5
27	PREDICTED: tripeptidyl-peptidase 2-like isoform 1	gi 356530860 (+2)	145 kDa	2.0	0.5
28	PREDICTED: uncharacterized protein At2g37660, chloroplastic-like	gi 356567949	28 kDa	3.0	0.3
29	PREDICTED: uncharacterized protein LOC100783299	gi 356570331	76 kDa	2.0	0.5
30	PREDICTED: uncharacterized protein LOC100785671	gi 356517098	57 kDa	0.5	2.0
31	PREDICTED: uncharacterized protein LOC100808941	gi 356570816	16 kDa	2.0	0.5
32	PREDICTED: uncharacterized protein LOC100819278	gi 356538184	13 kDa	2.2	0.5
	Unknown proteins				
1	unknown	gi 255647576 (+1)	31 kDa	0.3	2.9
2	unknown	gi 255640554 (+2)	23 kDa	0.5	2.0
3	unknown	gi 255626765 (+1)	19 kDa	0.4	2.6
4	unknown	gi 255641166 (+2)	37 kDa	2.0	0.5
5	unknown	gi 255631748 (+2)	24 kDa	0.5	2.0
6	unknown	gi 255627471 (+3)	10 kDa	3.3	0.3
7	unknown	gi 255625799 (+2)	16 kDa	0.2	4.5
8	unknown	gi 255646011 (+3)	35 kDa	0.5	2.0
9	unknown	gi 255627595 (+3)	20 kDa	0.4	2.8
10	unknown	gi 255642137 (+2)	50 kDa	0.3	4.0
11	unknown	gi 255631490 (+1)	15 kDa	2.3	0.4
12	unknown	gi 255628633 (+2)	22 kDa	0.4	2.5
13	unknown	gi 255626921 (+3)	15 kDa	0.2	6.0
14	unknown	gi 255627607 (+6)	14 kDa	0.3	3.5
15	unknown	gi 255626825 (+1)	13 kDa	2.3	0.4
16	unknown	gi 255627399 (+2)	24 kDa	0.3	3.0

17	unknown	gi 255635052 (+2)	39 kDa	0.1	8.0
18	unknown	gi 255640875 (+1)	26 kDa	3.0	0.3
19	unknown	gi 255638912 (+1)	37 kDa	0.3	3.0
20	unknown	gi 255627767 (+3)	21 kDa	0.3	3.0
21	unknown	gi 255633476 (+3)	27 kDa	7.0	0.1
22	unknown	gi 255627023 (+26)	18 kDa	0.5	2.0
23	unknown	gi 255641753 (+12)	22 kDa	0.5	2.0
24	unknown	gi 255646799 (+1)	19 kDa	0.3	3.0
	Unnamed protein product				
1	unnamed protein product	gi 219902785 (+13)	26 kDa	2.0	0.5
2	unnamed protein product	gi 296523720 (+2)	65 kDa	0.4	2.6
3	unnamed protein product	gi 219732878 (+30)	47 kDa	0.4	2.5
4	unnamed protein product	gi 219725202 (+5)	36 kDa	0.4	2.3
5	unnamed protein product	gi 227262746 (+7)	19 kDa	0.4	2.5
6	unnamed protein product	gi 219941197 (+5)	58 kDa	2.0	0.5
7	unnamed protein product	gi 227247708 (+2)	17 kDa	5.2	0.2
8	unnamed protein product	gi 257672765 (+2)	90 kDa	0.4	2.3
9	unnamed protein product	gi 227248104 (+4)	23 kDa	0.5	2.0
10	unnamed protein product	gi 219898651 (+4)	11 kDa	0.5	2.0
11	unnamed protein product	gi 227483067 (+1)	79 kDa	0.3	4.0
12	unnamed protein product	gi 219743082 (+12)	38 kDa	3.0	0.3

Table 5.3c: Fold change (Spectral counts) for contrasts 3. LCO Vs Th17

	Fold change Contrast 3. LCO Vs Th17				
	Known Proteins	Accession	MW	LCO	TH
1	phosphoenolpyruvate carboxylase	gi 218267 (+8)	111 kDa	0.4	2.6
2	RecName: Full=Elongation factor Tu, chloroplastic; Short=EF-Tu; Flags: Precursor	gi 1169494 (+2)	53 kDa	0.4	2.2
3	stearoyl-acyl carrier protein desaturase B	gi 183392958 (+6)	45 kDa	0.3	3.5
	Predicted Proteins				
1	PREDICTED: aconitate hydratase 1	gi 356496602	99 kDa	0.4	2.2
2	PREDICTED: auxin-induced protein PCNT115-like isoform 1	gi 356517239 (+1)	38 kDa	0.3	3.5
3	PREDICTED: endoplasmin homolog	gi 356553371 (+1)	94 kDa	0.4	2.3
4	PREDICTED: galactokinase-like	gi 356521747 (+1)	54 kDa	3.0	0.3
5	PREDICTED: lysosomal alpha-mannosidase-like isoform 1	gi 356561171 (+1)	117 kDa	0.3	4.0
6	PREDICTED: probable allantoinase 1-like	gi 356549347	57 kDa	2.0	0.5
7	PREDICTED: quinone oxidoreductase 1-like	gi 356544208	40 kDa	0.3	3.0
8	PREDICTED: uncharacterized protein At2g37660, chloroplastic-like	gi 356567949	28 kDa	0.5	2.0
9	PREDICTED: uncharacterized protein LOC100785671	gi 356517098	57 kDa	0.3	3.3
	Unknown proteins				
1	unknown	gi 255627595 (+3)	20 kDa	0.5	2.2
2	unknown	gi 255641228 (+9)	43 kDa	2.2	0.4
3	unknown	gi 255633168	27 kDa	0.3	3.5
4	unknown	gi 255640875 (+1)	26 kDa	2.0	0.5
5	unknown	gi 255627023 (+26)	18 kDa	2.0	0.5
6	unknown	gi 255641753 (+12)	22 kDa	0.3	4.0
7	unknown	gi 255638358 (+1)	21 kDa	2.0	0.5
	Unnamed protein product				
1	unnamed protein product	gi 227262746 (+7)	19 kDa	0.5	2.0

2	unnamed protein product	gi 291047826 (+2)	53 kDa	0.3	3.5
3	unnamed protein product	gi 218576558 (+3)	27 kDa	0.4	2.5
4	unnamed protein product	gi 253785312 (+13)	16 kDa	0.3	3.0
5	unnamed protein product	gi 219890664 (+22)	62 kDa	6.0	0.2

Table 5.3d: Fold change (Spectral counts) for contrasts 4. Control 100 mM NaCl Vs LCO + 100 mM NaCl

	Fold change (Spectral counts) Control 100 mM NaCl Vs LCO + 100 mM NaCl				
	Known Proteins	Accession	MW	Control	LCO
1	aspartic proteinase 1	gi 15186732 (+1)	55 kDa	10.4	0.1
2	glutathione S-transferase GST 14, partial	gi 11385443 (+6)	25 kDa	0.4	2.7
3	phosphoenolpyruvate carboxylase	gi 218267 (+8)	111 kDa	3.1	0.3
	Predicted proteins				
1	PREDICTED: 26S proteasome non-ATPase regulatory subunit 2 1A-like	gi 356517488 (+1)	97 kDa	2.4	0.4
2	PREDICTED: auxin-induced protein PCNT115-like isoform 1	gi 356517239 (+5)	38 kDa	0.5	2.2
3	PREDICTED: mannose-6-phosphate isomerase-like	gi 356569059	46 kDa	4.1	0.2
4	PREDICTED: oligopeptidase A-like	gi 356496657	88 kDa	2.2	0.5
5	PREDICTED: phosphoglucomutase, cytoplasmic-like	gi 356513072	64 kDa	2.1	0.5
6	PREDICTED: proteasome subunit alpha type-6-like	gi 356545355	41 kDa	0.4	2.5
7	PREDICTED: protein disulfide isomerase-like 1-4-like isoform 1	gi 356542509 (+1)	64 kDa	0.3	3.3
8	PREDICTED: quinone oxidoreductase 1-like	gi 356544208	40 kDa	2.0	0.5
9	PREDICTED: T-complex protein 1 subunit eta-like	gi 356501324 (+1)	60 kDa	3.2	0.3
10	PREDICTED: tripeptidyl-peptidase 2-like isoform 1	gi 356530860 (+2)	145 kDa	5.3	0.2
	Unknown Proteins				
1	unknown	gi 255642364 (+1)	46 kDa	0.5	2.1
2	unknown	gi 255627471 (+3)	10 kDa	2.2	0.5
3	unknown	gi 255633344 (+4)	28 kDa	0.4	2.3

4	unknown	gi 255626101 (+2)	20 kDa	3.3	0.3
5	unknown	gi 255632936 (+1)	22 kDa	2.2	0.4
6	unknown	gi 255646011 (+3)	35 kDa	0.4	2.3
7	unknown	gi 255638991 (+1)	36 kDa	0.3	3.7
8	unknown	gi 255637227 (+1)	29 kDa	0.4	2.5
9	unknown	gi 255627023 (+24)	18 kDa	2.5	0.4
10	unknown	gi 255637298 (+1)	24 kDa	0.3	3.1
11	unknown	gi 255627767 (+1)	21 kDa	0.5	2.1
12	unknown	gi 255633168	27 kDa	0.5	2.2
13	unknown	gi 255648016 (+1)	41 kDa	4.1	0.2
14	unknown	gi 255627001 (+8)	21 kDa	0.3	3.0
15	unknown	gi 255626769 (+4)	10 kDa	0.4	2.6
16	unknown	gi 255631490 (+1)	15 kDa	3.1	0.3
17	unknown	gi 255626103 (+1)	18 kDa	2.9	0.3
18	unknown	gi 255628253 (+1)	24 kDa	0.3	3.6
	Unnamed proteins				
1	unnamed protein product	gi 219900741 (+16)	62 kDa	0.5	2.1
2	unnamed protein product	gi 218381826 (+17)	15 kDa	0.5	2.2
3	unnamed protein product	gi 219892799 (+6)	42 kDa	0.5	2.2

Table 5.3e: Fold change (Spectral counts) for contrasts 5. Control 100 mM NaCl Vs Th17 + 100 mM NaCl

	Fold change (Spectral counts) Control 100 mM NaCl Vs Th17 + 100 mM NaCl				
	Known proteins	Accession	MW	Control	Th17
1	aspartic proteinase 1	gi 15186732 (+1)	55 kDa	2.6	0.4
2	heat shock protein 90-2	gi 208964722 (+2)	80 kDa	3.3	0.3
	Predicted proteins				

1	PREDICTED: 60S ribosomal protein L5-like	gi 356549759 (+1)	34 kDa	3.0	0.3
2	PREDICTED: auxin-induced protein PCNT115-like isoform 1	gi 356517239 (+5)	38 kDa	0.2	5.3
3	PREDICTED: dehydrin DHN3-like	gi 356548915	15 kDa	2.1	0.5
4	PREDICTED: eukaryotic peptide chain release factor GTP-binding subunit ERF3A-like	gi 356513002 (+1)	56 kDa	2.1	0.5
5	PREDICTED: importin subunit alpha-1-like	gi 356535026 (+1)	59 kDa	2.1	0.5
6	PREDICTED: probable allantoinase 1-like	gi 356549347	57 kDa	2.5	0.4
7	PREDICTED: proteasome subunit alpha type-6-like	gi 356545355	41 kDa	0.5	2.1
8	PREDICTED: staphylococcal nuclease domain-containing protein 1-like	gi 356508886 (+1)	109 kDa	0.5	2.2
9	PREDICTED: T-complex protein 1 subunit eta-like	gi 356501324 (+1)	60 kDa	3.8	0.3
	Unknown proteins				
1	unknown	gi 255641166 (+2)	37 kDa	3.4	0.3
2	unknown	gi 255640554 (+2)	23 kDa	0.5	2.1
3	unknown	gi 255626101 (+2)	20 kDa	3.3	0.3
4	unknown	gi 255628245 (+5)	27 kDa	2.4	0.4
5	unknown	gi 255638991 (+1)	36 kDa	0.3	3.5
6	unknown	gi 255627023 (+24)	18 kDa	7.8	0.1
7	unknown	gi 255626769 (+4)	10 kDa	0.5	2.1
8	unknown	gi 255631490 (+1)	15 kDa	2.8	0.4
9	unknown	gi 255646799 (+1)	19 kDa	0.4	2.8
	Unnamed protein product				
1	unnamed protein product	gi 227307930 (+3)	52 kDa	0.5	2.1
2	unnamed protein product	gi 219900741 (+16)	62 kDa	0.5	2.0
3	unnamed protein product	gi 219902785 (+13)	26 kDa	2.3	0.4
4	unnamed protein product	gi 218381826 (+17)	15 kDa	0.3	3.2
5	unnamed protein product	gi 227470844 (+7)	53 kDa	0.2	4.5
6	unnamed protein product	gi 219892799 (+6)	42 kDa	0.3	3.1

Table 5.3f: Fold change (Spectral counts) for contrasts 6. LCO + 100 mM NaCl Vs Th17 + 100 mM NaCl

Fold change (Spectral counts) LCO + 100 mM NaCl Vs Th17 + 100 mM NaCl					
	Known proteins	Accession	MW	LCO	Th17
1	aspartic proteinase 1	gi 15186732 (+1)	55 kDa	0.2	4.1
2	glutathione S-transferase GST 14, partial	gi 11385443 (+6)	25 kDa	3.1	0.3
3	heat shock protein 90-2	gi 208964722 (+2)	80 kDa	3.5	0.3
4	peroxisomal 3-ketoacyl-CoA thiolase precursor	gi 167963384 (+3)	49 kDa	2.1	0.5
5	phosphoenolpyruvate carboxylase	gi 218267 (+8)	111 kDa	0.2	5.1
6	pyruvate kinase	gi 22296818 (+13)	55 kDa	3.8	0.3
	Predicted protein				
1	PREDICTED: 26S proteasome non-ATPase regulatory subunit 2 1A-like	gi 356517488 (+1)	97 kDa	0.3	3.0
2	PREDICTED: 60S ribosomal protein L5-like	gi 356549759 (+1)	34 kDa	2.7	0.4
3	PREDICTED: auxin-induced protein PCNT115-like isoform 1	gi 356517239 (+5)	38 kDa	0.4	2.5
4	PREDICTED: eukaryotic peptide chain release factor GTP-binding subunit ERF3A-like	gi 356513002 (+1)	56 kDa	2.6	0.4
5	PREDICTED: importin subunit alpha-1-like	gi 356535026 (+1)	59 kDa	2.6	0.4
6	PREDICTED: lysosomal alpha-mannosidase-like isoform 1	gi 356561171 (+1)	117 kDa	0.4	2.5
7	PREDICTED: mannose-6-phosphate isomerase-like	gi 356569059	46 kDa	0.5	2.2
8	PREDICTED: oligopeptidase A-like	gi 356496657	88 kDa	0.4	2.6
9	PREDICTED: PR-5 protein	gi 356513419	24 kDa	3.3	0.3
10	PREDICTED: probable allantoinase 1-like	gi 356549347	57 kDa	3.5	0.3
11	PREDICTED: protein disulfide isomerase-like 1-4-like isoform 1	gi 356542509 (+1)	64 kDa	3.2	0.3
12	PREDICTED: T-complex protein 1 subunit gamma-like	gi 356559977	60 kDa	4.4	0.2
	Unknown protein				
1	unknown	gi 255641166 (+2)	37 kDa	2.6	0.4
2	unknown	gi 255628245 (+5)	27 kDa	3.3	0.3
3	unknown	gi 255627023 (+24)	18 kDa	3.1	0.3

4	unknown	gi 255627767 (+1)	21 kDa	2.9	0.3
5	unknown	gi 255648016 (+1)	41 kDa	0.4	2.3
6	unknown	gi 255628253 (+1)	24 kDa	2.9	0.3
	Unnamed protein product				
1	unnamed protein product	gi 219971748 (+5)	38 kDa	0.4	2.4
2	unnamed protein product	gi 259662381 (+2)	27 kDa	0.3	3.0
3	unnamed protein product	gi 219890664 (+21)	62 kDa	3.6	0.3
4	unnamed protein product	gi 227470844 (+7)	53 kDa	0.4	2.6

Table 5.4a: Fisher Exact test (P-value) (Spectral counts) for contrasts 1. Control Vs LCO

Fisher's Exact Test - Contrast 1. Control Vs LCO						
	Known proteins	Accession	MW	Control	LCO	Fisher's Exact Test (P-Value) Control vs LCO
1	24 kDa protein SC24	gi 18448973 (+2)	25 kDa	12	20	95% (0.033)
2	2S albumin pre-propeptide	gi 2305020 (+5)	18 kDa	230	136	95% (0.0018)
3	34 kDa maturing seed vacuolar thiol protease precursor	gi 1199563 (+14)	43 kDa	137	172	95% (0.000077)
4	alcohol dehydrogenase 1	gi 22597178 (+1)	40 kDa	51	58	95% (0.048)
5	beta-conglycinin alpha prime subunit	gi 290563695 (+4)	72 kDa	1,085	616	95% (0.00000000000017)
6	beta-conglycinin beta subunit	gi 63852207 (+1)	48 kDa	759	435	95% (0.0000000018)
7	Chain A, Crystal Structure Of Basic 7s Globulin From Soybean	gi 330689364 (+3)	44 kDa	260	249	95% (0.033)
8	Chain A, Crystal Structure Of Soybean Lipoygenase-D	gi 118138512 (+5)	97 kDa	47	0	95% (0.00000000000073)
9	Chain A, Crystal Structures Of Recombinant And Native Soybean Beta- Conglycinin Beta Homotrimers Complexes With N-Acetyl-D-Glucosamine	gi 21465628 (+4)	48 kDa	922	588	95% (0.0000017)

	Predicted proteins					
1	PREDICTED: alpha-1,4 glucan phosphorylase L isozyme, chloroplastic/amyloplastic-like	gi 356551144	110 kDa	1	11	95% (0.0010)
2	PREDICTED: ATP synthase subunit beta, mitochondrial-like	gi 356575611	60 kDa	31	40	95% (0.033)
3	PREDICTED: cell division cycle protein 48 homolog	gi 356508699	91 kDa	62	80	95% (0.0037)
4	PREDICTED: embryonic protein DC-8-like	gi 356533407	49 kDa	187	186	95% (0.027)
5	PREDICTED: glyceraldehyde-3-phosphate dehydrogenase-like	gi 356507341	55 kDa	116	146	95% (0.00024)
6	PREDICTED: glyceraldehyde-3-phosphate dehydrogenase-like	gi 356516587	37 kDa	99	126	95% (0.00047)
7	PREDICTED: heat shock 70 kDa protein-like	gi 356562559	71 kDa	64	83	95% (0.0029)
8	PREDICTED: importin subunit alpha-1-like	gi 356535026 (+1)	59 kDa	0	9	95% (0.00073)
9	PREDICTED: ketol-acid reductoisomerase, chloroplastic-like	gi 356543900 (+1)	63 kDa	1	9	95% (0.0043)
10	PREDICTED: leucine aminopeptidase 1-like isoform 1	gi 356571429	61 kDa	9	18	95% (0.018)
11	PREDICTED: LOW QUALITY PROTEIN: argininosuccinate synthase, chloroplastic-like	gi 356514007 (+7)	46 kDa	1	8	95% (0.0088)
12	PREDICTED: luminal-binding protein 5	gi 356523657	73 kDa	71	81	95% (0.022)
13	PREDICTED: P24 oleosin isoform A	gi 356571311	24 kDa	114	125	95% (0.012)
14	PREDICTED: probable pre-mRNA-splicing factor ATP-dependent RNA helicase-like	gi 356499785 (+3)	82 kDa	12	0	95% (0.00080)
15	PREDICTED: protein IN2-1 homolog B-like	gi 356572385	27 kDa	20	28	95% (0.041)
16	PREDICTED: SNF1-related protein kinase regulatory subunit gamma-like PV42a-like	gi 356555078	42 kDa	20	35	95% (0.0038)
17	PREDICTED: T-complex protein 1 subunit beta-like	gi 356539292 (+1)	57 kDa	8	20	95% (0.0040)
18	PREDICTED: uncharacterized protein LOC100780139	gi 356515096	118 kDa	121	135	95% (0.0064)

19	PREDICTED: universal stress protein A-like protein-like	gi 356500401	21 kDa	24	35	95% (0.017)
20	PREDICTED: UTP--glucose-1-phosphate uridylyltransferase-like	gi 356553237	51 kDa	45	56	95% (0.020)
	Unknown proteins					
1	unknown	gi 255647735 (+1)	37 kDa	81	102	95% (0.0019)
2	unknown	gi 255648242 (+1)	48 kDa	25	41	95% (0.0034)
3	unknown	gi 255626917 (+4)	23 kDa	13	20	95% (0.050)
4	unknown	gi 255647576 (+1)	31 kDa	8	15	95% (0.039)
5	unknown	gi 255640108 (+2)	28 kDa	10	17	95% (0.044)
6	unknown	gi 255639366	17 kDa	13	20	95% (0.050)
7	unknown	gi 255640468 (+1)	24 kDa	26	37	95% (0.018)
8	unknown	gi 255625799 (+2)	16 kDa	2	9	95% (0.014)
9	unknown	gi 255646011 (+3)	35 kDa	4	10	95% (0.041)
10	unknown	gi 255641228 (+9)	43 kDa	5	11	95% (0.047)
11	unknown	gi 255626921 (+3)	15 kDa	1	7	95% (0.018)
12	unknown	gi 255641256 (+1)	54 kDa	0	8	95% (0.0016)
13	unknown	gi 255627399 (+2)	24 kDa	5	13	95% (0.017)
14	unknown	gi 255638912 (+1)	37 kDa	27	72	95% (0.000000016)
15	unknown	gi 255626769 (+6)	10 kDa	0	4	95% (0.040)
16	unknown	gi 255648016 (+1)	41 kDa	0	4	95% (0.040)
17	unknown	gi 255633476 (+3)	27 kDa	7	0	95% (0.016)
18	unknown	gi 255626665 (+1)	26 kDa	0	4	95% (0.040)
19	unknown	gi 255633192 (+6)	16 kDa	6	0	95% (0.028)
20	unknown	gi 255638358 (+1)	21 kDa	0	4	95% (0.040)
	Unnamed protein					
1	unnamed protein product	gi 218336143 (+1)	41 kDa	135	142	95% (0.018)
2	unnamed protein product	gi 257676145 (+2)	84 kDa	138	152	95% (0.0054)

3	unnamed protein product	gi 227247986 (+6)	25 kDa	34	43	95% (0.033)
4	unnamed protein product	gi 219764826 (+10)	72 kDa	52	67	95% (0.0076)
5	unnamed protein product	gi 227307930 (+3)	52 kDa	13	20	95% (0.050)
6	unnamed protein product	gi 219909552 (+5)	18 kDa	14	23	95% (0.025)
7	unnamed protein product	gi 296523720 (+2)	65 kDa	8	16	95% (0.026)
8	unnamed protein product	gi 219766739 (+7)	74 kDa	75	82	95% (0.037)
9	unnamed protein product	gi 227247708 (+2)	17 kDa	47	11	95% (0.000034)
10	unnamed protein product	gi 227248782 (+4)	26 kDa	0	5	95% (0.018)
11	unnamed protein product	gi 219764822 (+8)	71 kDa	43	63	95% (0.0017)
12	unnamed protein product	gi 257672765 (+2)	90 kDa	19	49	95% (0.0000048)
13	unnamed protein product	gi 219892799 (+6)	42 kDa	0	5	95% (0.018)
14	unnamed protein product	gi 219890664 (+22)	62 kDa	0	6	95% (0.0081)

Table 5.4b: Fisher Exact test (P-value) (Spectral counts) for contrasts 2. Control Vs Th17

Fisher's Exact test - Contrast Control Vs Th17						
	Known proteins	Accession	MW	Control	Th17	Fisher's Exact Test (P-Value)
1	2S albumin pre-propeptide	gi 2305020 (+5)	18 kDa	230	128	95% (0.00063)
2	51 kDa seed maturation protein precursor	gi 351726078 (+1)	51 kDa	90	101	95% (0.010)
3	alcohol dehydrogenase 1	gi 22597178 (+1)	40 kDa	51	59	95% (0.030)
4	basic 7S globulin isoform	gi 20302594 (+6)	47 kDa	198	188	95% (0.044)
5	beta-conglycinin alpha prime subunit	gi 290563695 (+4)	72 kDa	1,085	542	95% (0.000000000000000000033)
6	beta-conglycinin beta subunit	gi 63852207 (+1)	48 kDa	759	372	95% (0.0000000000000019)
7	Chain A, Beta-AmylaseBETA-Cyclodextrin Complex	gi 157830279 (+11)	56 kDa	202	200	95% (0.015)
8	Chain A, Crystal Structure Of Basic 7s Globulin	gi 330689364 (+3)	44 kDa	260	268	95% (0.0015)

	Full=Glycinin A1a subunit; Contains: RecName: Full=Glycinin Bx subunit; Flags: Precursor					
33	RecName: Full=Glycinin G2; Contains: RecName: Full=Glycinin A2 subunit; Contains: RecName: Full=Glycinin B1a subunit; Flags: Precursor	gi 121277 (+9)	54 kDa	2,214	1,254	95% (0.0000000000000000000000000054)
34	RecName: Full=Glycinin G3; Contains: RecName: Full=Glycinin A subunit; Contains: RecName: Full=Glycinin B subunit; Flags: Precursor	gi 121278 (+3)	54 kDa	905	609	95% (0.00069)
35	RecName: Full=P24 oleosin isoform B; AltName: Full=P91	gi 266689 (+3)	23 kDa	115	144	95% (0.00016)
36	ribulose-1,5-bisphosphate carboxylase/oxygenase large subunit	gi 83595726 (+2)	53 kDa	49	58	95% (0.024)
37	sucrose-binding protein 2	gi 29469054 (+1)	56 kDa	240	233	95% (0.016)
	Predicted proteins					
1	PREDICTED: alpha-1,4 glucan phosphorylase L isozyme, chloroplastic/amyloplastic-like	gi 356551144	110 kDa	1	7	95% (0.016)
2	PREDICTED: ATP synthase subunit beta, mitochondrial-like	gi 356575611	60 kDa	31	55	95% (0.00018)
3	PREDICTED: auxin-induced protein PCNT115-like isoform 1	gi 356517239 (+1)	38 kDa	1	7	95% (0.016)
4	PREDICTED: cell division cycle protein 48 homolog	gi 356508699	91 kDa	62	71	95% (0.021)
5	PREDICTED: embryonic protein DC-8-like	gi 356533407	49 kDa	187	178	95% (0.046)
6	PREDICTED: formate--tetrahydrofolate ligase-like	gi 356576871	67 kDa	17	29	95% (0.0080)
7	PREDICTED: glyceraldehyde-3-phosphate dehydrogenase-like	gi 356507341	55 kDa	116	165	95% (0.00000074)
8	PREDICTED: glyceraldehyde-3-phosphate dehydrogenase-like	gi 356516587	37 kDa	99	144	95% (0.0000018)
9	PREDICTED: heat shock 70 kDa protein-like	gi 356562559	71 kDa	64	83	95% (0.0019)
10	PREDICTED: importin subunit alpha-1-like	gi 356535026 (+1)	59 kDa	0	8	95% (0.0015)
11	PREDICTED: ketol-acid reductoisomerase, chloroplastic-like	gi 356543900 (+1)	63 kDa	1	12	95% (0.00043)

12	PREDICTED: ketol-acid reductoisomerase, chloroplastic-like	gi 356543032	63 kDa	2	7	95% (0.045)
13	PREDICTED: kunitz-type trypsin inhibitor KTI1-like	gi 356527266	23 kDa	78	86	95% (0.021)
14	PREDICTED: leucine aminopeptidase 1-like isoform 1	gi 356571429	61 kDa	9	21	95% (0.0039)
15	PREDICTED: leucine aminopeptidase 3, chloroplastic-like	gi 356498766	60 kDa	19	27	95% (0.035)
16	PREDICTED: LOW QUALITY PROTEIN: argininosuccinate synthase, chloroplastic-like	gi 356514007 (+7)	46 kDa	1	10	95% (0.0019)
17	PREDICTED: luminal-binding protein 5	gi 356523657	73 kDa	71	76	95% (0.042)
18	PREDICTED: P24 oleosin isoform A	gi 356571311	24 kDa	114	135	95% (0.00099)
19	PREDICTED: phosphoglycerate kinase, chloroplastic-like	gi 356525742	50 kDa	14	30	95% (0.0012)
20	PREDICTED: probable pre-mRNA-splicing factor ATP-dependent RNA helicase-like	gi 356499785 (+3)	82 kDa	12	0	95% (0.00090)
21	PREDICTED: protein IN2-1 homolog B-like	gi 356572385	27 kDa	20	27	95% (0.048)
22	PREDICTED: serine/threonine-protein phosphatase 2A 65 kDa regulatory subunit A beta isoform-like	gi 356520585 (+3)	65 kDa	0	4	95% (0.038)
23	PREDICTED: serpin-ZX-like	gi 356510338	43 kDa	0	4	95% (0.038)
24	PREDICTED: serpin-ZX-like	gi 356510338	43 kDa	0	4	95% (0.038)
25	PREDICTED: SNF1-related protein kinase regulatory subunit gamma-like PV42a-like	gi 356555078	42 kDa	20	33	95% (0.0063)
26	PREDICTED: sucrose synthase 2-like	gi 356558189	92 kDa	6	12	95% (0.047)
27	PREDICTED: sucrose-binding protein-like	gi 356536206	58 kDa	330	315	95% (0.010)
28	PREDICTED: T-complex protein 1 subunit beta-like	gi 356539292 (+1)	57 kDa	8	20	95% (0.0034)
29	PREDICTED: T-complex protein 1 subunit zeta-like	gi 356527473 (+1)	59 kDa	1	7	95% (0.016)
30	PREDICTED: thioredoxin H-type	gi 356564319	13 kDa	10	2	95% (0.047)
31	PREDICTED: uncharacterized protein	gi 356515096	118 kDa	121	149	95% (0.00019)

	LOC100780139					
32	PREDICTED: universal stress protein A-like protein-like	gi 356500401	21 kDa	24	36	95% (0.010)
33	PREDICTED: UTP--glucose-1-phosphate uridylyltransferase-like	gi 356553237	51 kDa	45	52	95% (0.040)
	Unknown proteins					
1	unknown	gi 255636164 (+2)	35 kDa	65	71	95% (0.038)
2	unknown	gi 255647735 (+1)	37 kDa	81	116	95% (0.000025)
3	unknown	gi 255645048 (+1)	36 kDa	36	47	95% (0.016)
4	unknown	gi 255648242 (+1)	48 kDa	25	33	95% (0.036)
5	unknown	gi 255626917 (+4)	23 kDa	13	21	95% (0.030)
6	unknown	gi 255647576 (+1)	31 kDa	8	23	95% (0.00071)
7	unknown	gi 255635394 (+3)	50 kDa	11	20	95% (0.019)
8	unknown	gi 255645127 (+3)	22 kDa	11	19	95% (0.028)
9	unknown	gi 255633344 (+4)	28 kDa	9	16	95% (0.037)
10	unknown	gi 255640554 (+2)	23 kDa	7	14	95% (0.033)
11	unknown	gi 255640468 (+1)	24 kDa	26	34	95% (0.036)
12	unknown	gi 255626765 (+1)	19 kDa	5	13	95% (0.016)
13	unknown	gi 255625799 (+2)	16 kDa	2	9	95% (0.013)
14	unknown	gi 255627595 (+3)	20 kDa	4	11	95% (0.022)
15	unknown	gi 255642137 (+2)	50 kDa	2	8	95% (0.025)
16	unknown	gi 255626921 (+3)	15 kDa	1	6	95% (0.033)
17	unknown	gi 255641256 (+1)	54 kDa	0	8	95% (0.0015)
18	unknown	gi 255627607 (+6)	14 kDa	2	7	95% (0.045)
19	unknown	gi 255627399 (+2)	24 kDa	5	15	95% (0.0053)
20	unknown	gi 255635052 (+2)	39 kDa	1	8	95% (0.0080)
21	unknown	gi 255638912 (+1)	37 kDa	27	81	95% (0.000000000081)
22	unknown	gi 255626769 (+6)	10 kDa	0	6	95% (0.0075)

23	unknown	gi 255626665 (+1)	26 kDa	0	5	95% (0.017)
24	unknown	gi 255633192 (+6)	16 kDa	6	0	95% (0.030)
25	unknown	gi 255640867 (+1)	17 kDa	20	0	95% (0.0000083)
	Unnamed protein					
1	unnamed protein product	gi 218336143 (+1)	41 kDa	135	141	95% (0.013)
2	unnamed protein product	gi 257676145 (+2)	84 kDa	138	153	95% (0.0026)
3	unnamed protein product	gi 219734265 (+13)	49 kDa	65	74	95% (0.021)
4	unnamed protein product	gi 219725204 (+6)	36 kDa	60	74	95% (0.0069)
5	unnamed protein product	gi 219764826 (+10)	72 kDa	52	62	95% (0.019)
6	unnamed protein product	gi 227307930 (+3)	52 kDa	13	24	95% (0.0093)
7	unnamed protein product	gi 219909552 (+5)	18 kDa	14	24	95% (0.015)
8	unnamed protein product	gi 296523720 (+2)	65 kDa	8	21	95% (0.0020)
9	unnamed protein product	gi 257676113 (+2)	84 kDa	136	138	95% (0.024)
10	unnamed protein product	gi 219986458 (+2)	31 kDa	10	17	95% (0.039)
11	unnamed protein product	gi 219732878 (+30)	47 kDa	4	10	95% (0.038)
12	unnamed protein product	gi 227262746 (+7)	19 kDa	4	10	95% (0.038)
13	unnamed protein product	gi 227247708 (+2)	17 kDa	47	9	95% (0.0000074)
14	unnamed protein product	gi 227248782 (+4)	26 kDa	0	8	95% (0.0015)
15	unnamed protein product	gi 257672765 (+2)	90 kDa	19	43	95% (0.000057)
16	unnamed protein product	gi 219892799 (+6)	42 kDa	0	4	95% (0.038)

Table 5.4c: Fisher Exact test (P-value) (Spectral counts) for contrasts 3. LCO Vs Th17

	Fisher's Exact test - Contrast LCO Vs Th17					
	Known proteins	Accession	MW	LCO	Th17	Fisher's Exact Test (P-Value)
1	34 kDa maturing seed vacuolar thiol protease precursor	gi 1199563 (+14)	43 kDa	172	120	95% (0.0024)

2	beta-conglycinin alpha prime subunit	gi 290563695 (+4)	72 kDa	616	542	95% (0.036)
3	beta-conglycinin beta subunit	gi 63852207 (+1)	48 kDa	435	372	95% (0.029)
4	Chain A, Crystal Structure Of Soybean Lipoxygenase-D	gi 118138512 (+5)	97 kDa	0	36	95% (0.0000000000097)
5	Chain A, Crystal Structures Of Recombinant And Native Soybean Beta- Conglycinin Beta Homotrimers Complexes With N-Acetyl-D-Glucosamine	gi 21465628 (+4)	48 kDa	588	472	95% (0.00063)
6	glycinin A3B4 subunit	gi 10566449 (+2)	58 kDa	818	623	95% (0.00000083)
7	glycinin A5A4B3 precursor	gi 351734402 (+2)	64 kDa	804	664	95% (0.00053)
8	glycinin G4 subunit [soybeans, Peptide, 560 aa]	gi 255224	64 kDa	786	645	95% (0.00040)
9	phosphoenolpyruvate carboxylase	gi 218267 (+8)	111 kDa	5	13	95% (0.044)
10	RecName: Full=Isocitrate lyase 1; Short=ICL 1; Short=Isocitrase 1; Short=Isocitratase 1	gi 1168289 (+8)	63 kDa	0	8	95% (0.0036)
	Predicted proteins					
1	PREDICTED: uncharacterized protein LOC100785671	gi 356517098	57 kDa	3	10	95% (0.042)
	Unknown proteins					
1	unknown	gi 255640867 (+1)	17 kDa	18	0	95% (0.0000046)
	Unnamed protein					
1	unnamed protein product	gi 219764822 (+8)	71 kDa	63	40	95% (0.019)

Table 5.4d: Fisher Exact test (P-value) (Spectral counts) for contrasts 4. Control 100 mM NaCl Vs LCO + 100 mM NaCl, 5. Control 100 mM NaCl Vs Th17 + 100 mM NaCl, 6. LCO + 100 mM NaCl Vs Th17 + 100 mM NaCl.

	Fisher's Exact Test Contrast Control Vs LCO					
	Known proteins	Accession	MW	Control	LCO	Fisher's Exact Test (P-Value)
1	RecName: Full=Glycinin G1; Contains: RecName: Full=Glycinin A1a subunit; Contains: RecName:	gi 121276 (+10)	56 kDa	1,722	1,853	95% (0.030)

	Full=Glycinin Bx subunit; Flags: Precursor					
2	34 kDa maturing seed vacuolar thiol protease precursor	gi 1199563 (+14)	43 kDa	115	200	95% (0.0000015)
3	aspartic proteinase 1	gi 15186732 (+1)	55 kDa	10	1	95% (0.0055)
4	beta-conglycinin alpha prime subunit	gi 290563695 (+4)	72 kDa	695	801	95% (0.0059)
5	Chain A, Crystal Structures Of Recombinant And Native Soybean Beta- Conglycinin Beta Homotrimers Complexes With N-Acetyl-D-Glucosamine	gi 21465628 (+4)	48 kDa	644	716	95% (0.042)
6	glycinin A3B4 subunit	gi 10566449 (+2)	58 kDa	825	912	95% (0.033)
7	lipoxygenase L-1	gi 161318153 (+2)	94 kDa	435	379	95% (0.017)
8	pyruvate kinase	gi 22296818 (+13)	55 kDa	0	8	95% (0.0041)
9	RecName: Full=Beta-conglycinin, alpha chain; Flags: Precursor	gi 121281 (+5)	70 kDa	977	1,068	95% (0.040)
10	seed biotinylated protein 68 kDa isoform	gi 240254706	68 kDa	160	132	95% (0.045)
	Predicted proteins					
1	PREDICTED: 97 kDa heat shock protein-like	gi 356550547	95 kDa	7	0	95% (0.0075)
2	PREDICTED: T-complex protein 1 subunit gamma-like	gi 356559977	60 kDa	0	5	95% (0.032)
	Unknown proteins					
1	unknown	gi 255630323 (+5)	18 kDa	126	97	95% (0.024)
2	unknown	gi 255625639 (+1)	23 kDa	5	0	95% (0.030)

Table 5.4e: Fisher Exact test (P-value) (Spectral counts) for contrasts 5. Control 100 mM NaCl Vs Th17 + 100 mM NaCl

Fisher's Exact Test for Contrast Control Vs Th17						
	Known proteins	Accession	MW	Control	Th17	Fisher's Exact Test (P-Value)
1	RecName: Full=Glycinin G2; Contains: RecName: Full=Glycinin A2 subunit; Contains: RecName: Full=Glycinin B1a subunit; Flags: Precursor	gi 121277 (+9)	54 kDa	1,617	1,368	95% (0.015)

2	34 kDa maturing seed vacuolar thiol protease precursor	gi 1199563 (+14)	43 kDa	115	133	95% (0.036)
3	51 kDa seed maturation protein precursor	gi 351726078 (+1)	51 kDa	93	113	95% (0.024)
4	beta-conglycinin beta subunit	gi 63852207 (+1)	48 kDa	529	324	95% (0.0000000041)
5	Chain A, Crystal Structures Of Recombinant And Native Soybean Beta- Conglycinin Beta Homotrimers Complexes With N-Acetyl-D- Glucosamine	gi 21465628 (+4)	48 kDa	644	395	95% (0.00000000099)
6	glyceraldehyde-3-phosphate dehydrogenase	gi 351727206 (+1)	37 kDa	146	182	95% (0.0029)
7	glycinin A3B4 subunit	gi 10566449 (+2)	58 kDa	825	627	95% (0.00021)
8	Lea protein	gi 311698 (+1)	49 kDa	94	122	95% (0.0061)
9	RecName: Full=Bowman-Birk type proteinase inhibitor C-II; Flags: Precursor	gi 124029 (+10)	9 kDa	18	34	95% (0.0078)
10	RecName: Full=P24 oleosin isoform B; AltName: Full=P91	gi 266689 (+3)	23 kDa	116	132	95% (0.048)
	Predicted proteins					
1	PREDICTED: aldehyde dehydrogenase family 2 member B4, mitochondrial-like	gi 356567618	58 kDa	0	5	95% (0.025)
2	PREDICTED: glyceraldehyde-3-phosphate dehydrogenase	gi 356508778	37 kDa	138	172	95% (0.0037)
3	PREDICTED: glyceraldehyde-3-phosphate dehydrogenase-like	gi 356516587	37 kDa	126	143	95% (0.043)
4	PREDICTED: heat shock 70 kDa protein-like	gi 356500683	72 kDa	44	74	95% (0.00075)
5	PREDICTED: P24 oleosin isoform A	gi 356571311	24 kDa	112	133	95% (0.023)
6	PREDICTED: tripeptidyl-peptidase 2-like isoform 1	gi 356530860 (+2)	145 kDa	5	0	95% (0.039)
	Unknown proteins					
1	unknown	gi 255641166 (+2)	37 kDa	11	3	95% (0.042)
2	unknown	gi 255627023 (+24)	18 kDa	8	1	95% (0.027)
3	unknown	gi 255626103 (+1)	18 kDa	5	0	95% (0.039)

	Unnamed protein product					
1	unnamed protein product [Glycine max]	gi 227303916 (+1)	60 kDa	26	39	95% (0.032)
2	unnamed protein product [Glycine max]	gi 227307930 (+3)	52 kDa	12	23	95% (0.025)
3	unnamed protein product [Glycine max]	gi 257676113 (+2)	84 kDa	121	85	95% (0.036)
4	unnamed protein product [Glycine max]	gi 259662381 (+2)	27 kDa	32	55	95% (0.0026)

Table 5.4f: Fisher Exact test (P-value) (Spectral counts) for contrasts 6. LCO + 100 mM NaCl Vs Th17 + 100 mM NaCl

	Known proteins	Accession	MW	LCO	Th17	Fisher's Exact Test (P-Value)
1	RecName: Full=Beta-conglycinin, alpha chain; Flags: Precursor	gi 121281 (+5)	70 kDa	1,068	842	95% (0.0014)
2	34 kDa maturing seed vacuolar thiol protease precursor	gi 1199563 (+14)	43 kDa	200	133	95% (0.0034)
3	51 kDa seed maturation protein precursor	gi 351726078 (+1)	51 kDa	96	113	95% (0.032)
4	beta-conglycinin alpha prime subunit	gi 290563695 (+4)	72 kDa	801	592	95% (0.000093)
5	beta-conglycinin beta subunit	gi 63852207 (+1)	48 kDa	566	324	95% (0.000000000012)
6	Chain A, Crystal Structures Of Recombinant And Native Soybean Beta- Conglycinin Beta Homotrimers Complexes With N-Acetyl-D-Glucosamine	gi 21465628 (+4)	48 kDa	716	395	95% (0.0000000000000033)
7	dehydrin-like protein	gi 351723341 (+1)	24 kDa	157	175	95% (0.031)
8	glyceraldehyde-3-phosphate dehydrogenase	gi 351727206 (+1)	37 kDa	164	182	95% (0.030)
9	glycinin A3B4 subunit	gi 10566449 (+2)	58 kDa	912	627	95% (0.000000043)
10	glycinin A5A4B3 precursor	gi 351734402 (+2)	64 kDa	859	711	95% (0.043)
11	glycinin G4 subunit [soybeans, Peptide, 560 aa]	gi 255224	64 kDa	841	694	95% (0.039)
12	Lea protein	gi 311698 (+1)	49 kDa	106	122	95% (0.038)
11	lipoxygenase L-1	gi 161318153 (+2)	94 kDa	379	386	95% (0.050)
13	RecName: Full=Bowman-Birk type proteinase	gi 124029 (+10)	9 kDa	20	34	95% (0.016)

	inhibitor C-II; Flags: Precursor					
14	RecName: Full=Glycinin G2; Contains: RecName: Full=Glycinin A2 subunit; Contains: RecName: Full=Glycinin B1a subunit; Flags: Precursor	gi 121277 (+9)	54 kDa	1,612	1,368	95% (0.042)
	Predicted proteins					
1	PREDICTED: glyceraldehyde-3-phosphate dehydrogenase	gi 356508778	37 kDa	148	172	95% (0.014)
2	PREDICTED: glyceraldehyde-3-phosphate dehydrogenase-like	gi 356516587	37 kDa	127	143	95% (0.039)
3	PREDICTED: heat shock 70 kDa protein-like	gi 356500683	72 kDa	55	74	95% (0.015)
4	PREDICTED: PR-5 protein	gi 356513419	24 kDa	17	5	95% (0.016)
	Unknown proteins					
1	unknown	gi 255630323 (+5)	18 kDa	97	119	95% (0.014)
2	unknown	gi 255636164 (+2)	35 kDa	71	88	95% (0.028)
3	unknown	gi 255637491 (+1)	24 kDa	47	64	95% (0.020)
4	unknown	gi 255625639 (+1)	23 kDa	0	8	95% (0.0026)
	Unnamed protein product					
1	unnamed protein product	gi 219971748 (+5)	38 kDa	6	14	95% (0.036)
2	unnamed protein product	gi 259662381 (+2)	27 kDa	24	55	95% (0.000055)

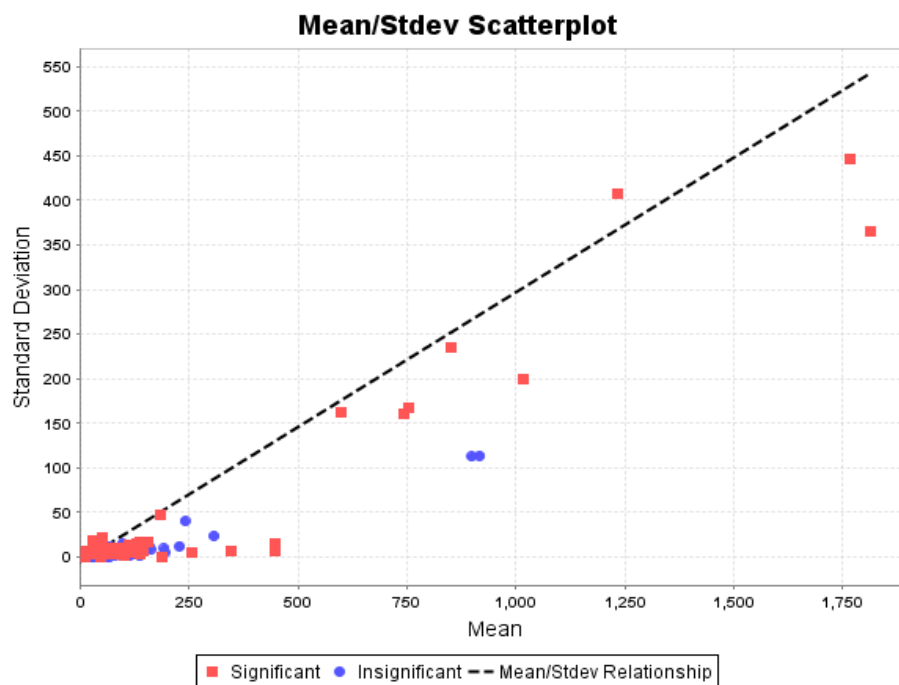


Fig. 5.4a: Mean/Standard deviation scatterplot for Soybean contrast 1. Control Vs LCO

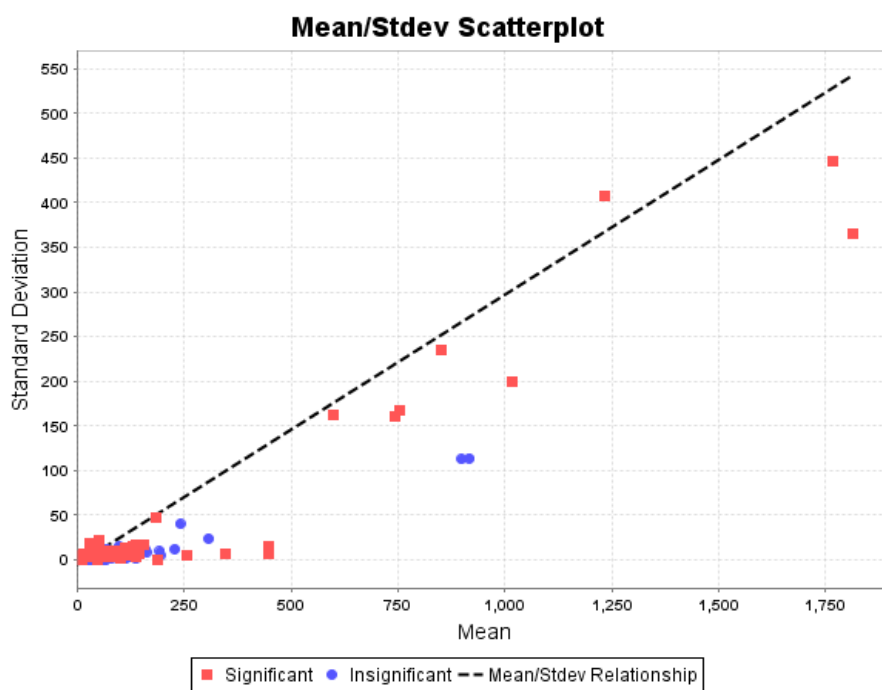


Fig. 5.4b: Mean/Standard deviation scatterplot for Soybean 2. Control Vs Th17

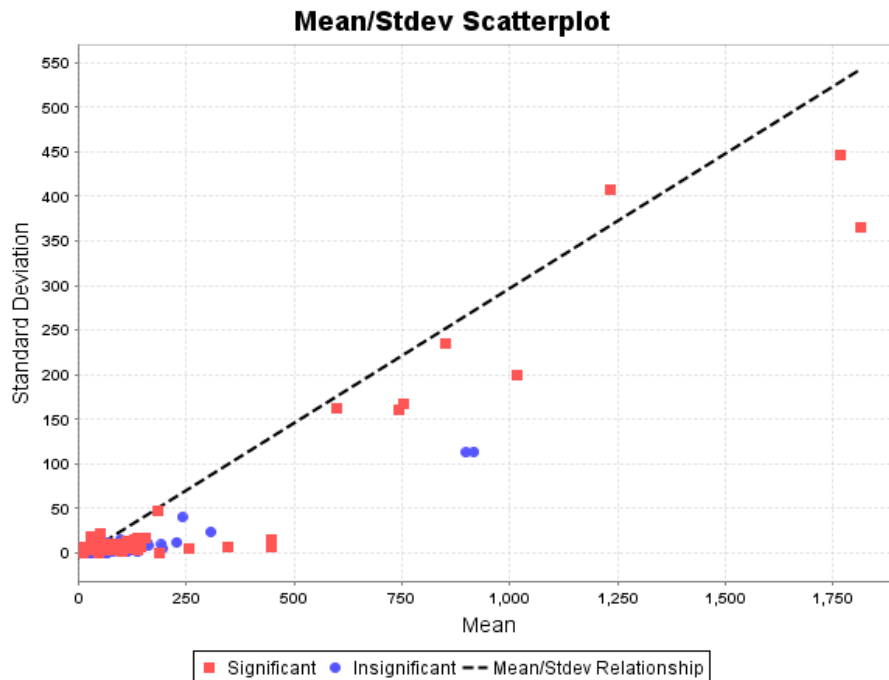


Fig. 5.4c: Mean/Standard deviation scatterplot for Soybean 3. LCO Vs Th17

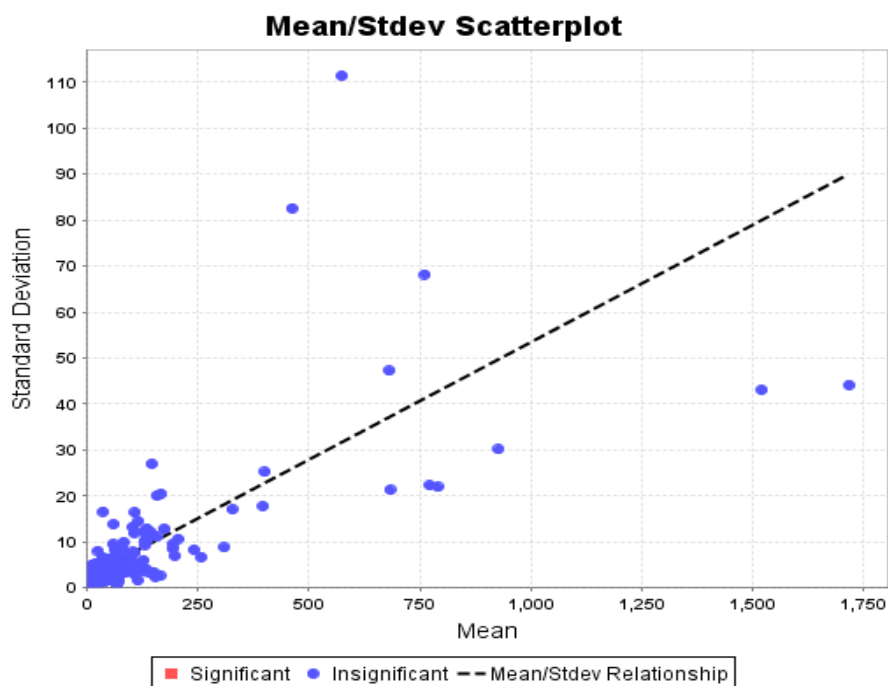


Fig. 5.4d: Mean/Standard deviation scatterplot for Soybean 4. 100 mM NaCl Vs LCO + 100 mM NaCl

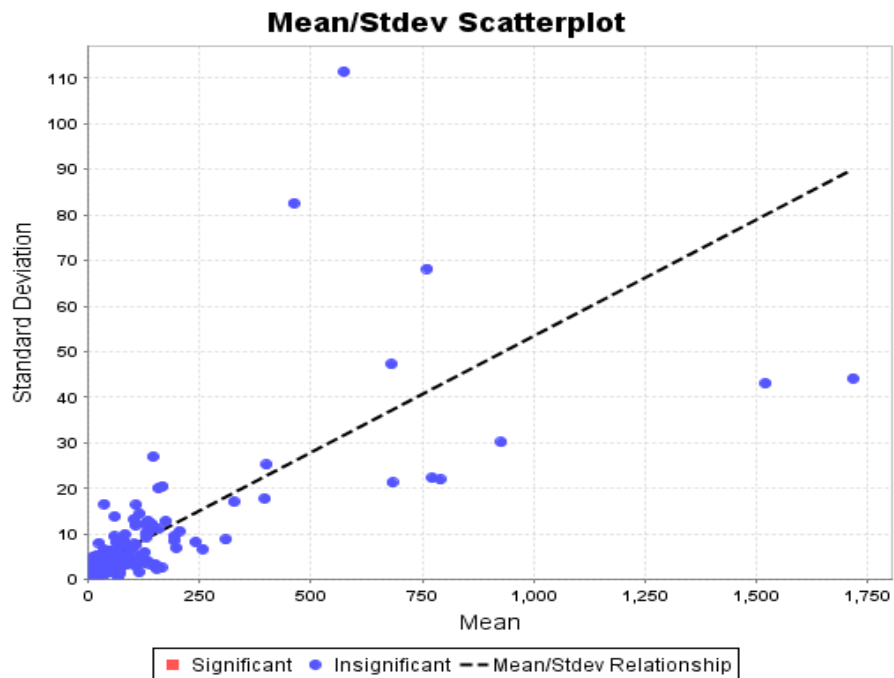


Fig. 5.4e: Mean/Standard deviation scatterplot for Soybean 5. 100 mM NaCl Vs Th17 + 100 mM NaCl

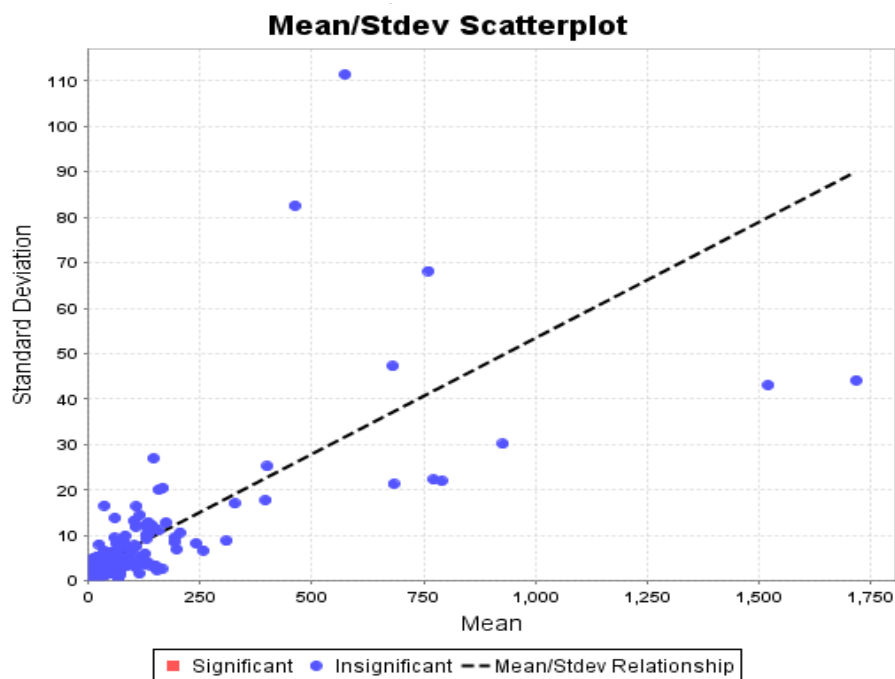


Fig. 5.4f: Mean/Standard deviation scatterplot for Soybean 6. LCO + 100 mM NaCl Vs. Th17 + 100 mM NaCl